Investigating the protective role of the natural hormone Melatonin, in reducing drug-induced cardiotoxicity in the therapy of chronic diseases

Kasi Ganeshan, T.

Investigating the protective role of the natural hormone Melatonin, in reducing drug-induced cardiotoxicity in the therapy of chronic diseases.

By

Thulangana Ganeshan

School of Life Sciences
University of Westminster, London

A thesis submitted to the University of Westminster in candidature for the award of the degree of Doctor of Philosophy

2019

Author's Declaration

I declare that the present work was carried out in accordance with the Guidelines and Regulations of the University of Westminster. The work is original except where indicated by special reference in the text.

The submission as a whole or part is not substantially the same as any that I previously or am currently making, whether in published or unpublished form, for a degree, diploma or similar qualification at any university or similar institution.
Until the outcome of the current application to the University of Westminster is known, the work will not be submitted for any such qualification at another university or similar institution.

Any views expressed in this work are those of the author and in no way represent those of the University of Westminster.

Signed: Thulangana Ganeshan Date: 22.07.19

Acknowledgments

"Thanking God for providing me this opportunity and guidance to do this Ph.D. in the most wonderful way I could have imagined. The utmost glory belongs to his name Jesus Christ".

~Amen~

Firstly, I would like to express my sincere gratitude to my supervisor Dr. Nelson Chong for the continuous support of my Ph.D. study and related research, for his patience, motivation, and immense knowledge had guided and helped me in all the time of research and writing of this thesis. I could not have imagined having a better advisor and mentor for my Ph.D. study. My sincere heartfelt appreciation to my supervisor Dr. Nelson Chong.

Besides my supervisor, I would like to thank the rest of my thesis committee, Dr. Bradley Elliott and Dr. Stipo Jurcevic for their insightful comments and encouragement which had provided me the incentive to widen my research from various perspectives.

I would love to thank my fellow colleagues Rhys, Louise and Moonisha for their help and support in my research work. A special thanks to Thakor for providing me support and help with any technical issues throughout these four years.

Last but not least, a massive gratitude to my friends Zain, Voni, Mano and my sister Joanne who had been with me in this last four years of my Ph.D. I had enjoyed working alongside them and their love and support had constantly helped me throughout this process.

Finally a very big thank you to my Mom, Dad and my brother for their ever loving support and encouragement from day one till now, without whom this would have not been possible.

Abstract

Heart failure (HF) is a highly complex disorder and a major end-point of cardiovascular diseases (CVD). The pathogenesis of HF is mostly unresolved but involves interplay between cardiac structural and electrical remodelling, metabolic alterations, cell death and altered gene expression. Mitochondrial dysfunction and HF are common complications of chronic treatment from diverse groups of drugs, in particular anticancer drugs such as doxorubicin (DOX). Treatment of animals and cardiomyocytes with cardiotoxic chemicals such as β-adrenergic receptor agonists (such as isoproterenol) induces cardiac dysfunction and HF. Previous work done by the group have identified the pineal hormone melatonin was protective against stress-induced cardiac arrhythmias and simulated heart failure in cardiomyocytes *in vitro*. Melatonin synthesis is also dramatically decreased with age and in patients with CVD.

The aim of the present project was to better understand the pathogenesis of drug-induced cardiac dysfunction and delineate the role of melatonin in cardioprotection in H9c2, a model rat cell line *in vitro*. Using the Seahorse XF analyser method, it was demonstrated that commonly used medication for chronic diseases such as amiodarone, amitriptyline, and statins all caused altered mitochondrial dysfunction. In addition, cardiotoxic chemicals (isoproterenol, hydrogen peroxide, DOX) altered oxidative phosphorylation and glycolysis in living cardiomyocyte-derived H9c2 cells; these deleterious metabolic changes were ameliorated by melatonin. Flow-cytometry and Alamar Blue staining methods demonstrated that DOX robustly induced apoptosis in H9c2 cells (~30%) which was reversed by melatonin.

Doxorubicin-induced stress in H9c2 cells dramatically altered gene expression in several key signalling pathways integral in cardiac function and disease. These included mitochondrial metabolism (UCP2, PPARɣ, Drp1, Mfn1, Parp 1, Parp2, Sirt3 and Cav3), apoptosis (Bcl2 and Bcl-xL), cardiac electrophysiology and arrhythmia (Scn5a, SERCA2a), calcium handling (SERCA2a) and cardiac remodelling (Myh7, ms1). Melatonin pre-treatment attenuated or completely blocked this DOX-induced alteration in gene expression in cardiomyocytes.

In conclusion, the present result demonstrated for the first time that melatonin is cardioprotective against drug-induced cardiotoxicity and apoptosis via modifying diverse heart failure-related signalling pathways. This provides novel insight on the

possible use of melatonin as an adjunct intervention in several therapies including anti-cancer.

Conferences attended

T.Ganeshan. J.D. Bell. N.W. Chong. (2017), “Attenuation of doxorubicin-induced-mitochondrial dysfunction and cardiotoxicity *in vitro* by the pineal hormone, melatonin” In the proceedings of British Pharmacology Society (BPS), London, UK (invited talk). 11th- 13th December 2017.

T.Ganeshan. J.D. Bell. N.W. Chong. (2018), “Mechanism of action of melatonin against doxorubicin-induced cardiotoxicity” In the proceedings of WCP 2018, Kyoto, Japan. 1st- 4th July 2018.

T.Ganeshan. J.D. Bell. N.W. Chong. (2019), “The pineal hormone melatonin inhibits doxorubicin-induced mitochondrial dysfunction and apoptosis in cardiomyocytes” In the proceedings of European Society of Cardiology (ESC), Heart Failure 2019 - 6th World Congress on Acute Heart Failure , Athens, Greece. 25th-28th May 2019.

T.Ganeshan. J.D. Bell. N.W. Chong. (2019), “The pineal hormone melatonin inhibits doxorubicin-induced mitochondrial dysfunction and apoptosis in cardiomyocytes” In the proceedings of European Society of Cardiology (ESC) Congress 2019, Paris, France. 31st- 4th September 2019.

Publications

Ganeshan TK, Bell JD and Chong NW (2019). The pineal hormone melatonin inhibits doxorubicin-induced mitochondrial dysfunction and apoptosis in cardiomyocytes. European Journal of Heart Failure. 21 (suppl.S1), P617.

Ganeshan TK, Bell JD and Chong NW (2019). The pineal hormone melatonin inhibits doxorubicin-induced mitochondrial dysfunction and apoptosis in cardiomyocytes. European Heart Journal (abstract in press).

Table of Contents

List of Figures

Abbreviations

AANAT	arylalkylamine-N-acetyltransferase
ABLIM	acting-binding LIM
ABRA	actin binding Rho activator
ANF	atrial natriuretic factor
ANG-II	angiotensin 2
Apaf-1	apoptotic protease-activating factor 1
ATRA	all-trans retinoic acid
BMP	bone morphogenic protein
BNP	b-type natriuretic peptide
CAMK	calmodulin dependant kinase
CBP	CREB binding protein
CoQ10	co enzyme Q10
DISC	death-inducing signaling complex
Drp1	dynamin-related protein 1
ECAR	Extracellular acidification rate
ERK	extracellular signal-regulated kinase
FADD	Fas-associated death domain
FasL	Fas ligand
FCCP	Carbonyl cyanide-*4*-(trifluoromethoxy) Phenylhydrazone
FITC	fluorescein isothiocyanate
GSH	Glutathione
GSK-3beta	glycogen synthase 3 beta
GSSG	glutathione disulphide
HF	Heart failure

JNK	c-Jun NH_2-terminal kinase
Keap 1	kelch-like ECH-associated protein 1
LVD	Left ventricular dysfunction
LVEF	Left ventricular ejection fraction
LVH	left ventricular hypertrophy
MAPK	mitogen activated protein kinase
MEF2	myocyte enhancer factor 2
MPTP	mitochondrial permeability transition pore
MRF	myogenic regulatory factor
MRTF	myocardin related transcription factor
MS1	myocyte stress 1
NCX	Na^+/Ca^{2+} exchanger
NFAT	nuclear factor of activated T-cells
Nrf2	nuclear factor erythroid derived 2 like 2
OCR	Oxygen consumption rate
OPA1	optic atrophy protein 1
ROCK	rho-associated kinase
RyR2	ryanodine receptor 2
SCN	superchiasmatic nuclei
Serca	sarco/endoplasmic reticulum Ca^{2+}-ATPase
SRF	serum response factor
STARS	striated muscle specific activator of Rho Signalling
TRAIL	TNF-related apoptosis inducing ligand
β-MHC	β-myosin heavy chain

Chapter 1.
Introduction

Introduction

An estimated 7 million people are living with cardiovascular disease (CVD) in the UK, with an annual spend of £11 billion on intervention and management (BHF report 2012). More than 1 in 4 deaths in the UK are caused by CVD (160,000 deaths per year), with a common end-point of sudden cardiac death. Deaths from coronary heart disease (CHD) is decreasing dramatically each year (BHF report 2012), whereas, counter-intuitively, the prevalence of cardiac arrhythmias and heart failure (HF) is dramatically on the increase. It is estimated that 17 million people will have atrial fibrillation, the most clinically observed form of arrhythmia, by the year 2030 in Europe, with 200,000 new cases per year (e.g. Rahman et al., 2014). Heart failure patients are also on the increase with an estimated 500,000 sufferers in the UK. Drug treatments for cardiac arrhythmias are limited because of poor efficacy and the drugs being pro-arrhythmogenic. Drug treatment for heart failure is also limited by long term efficacy, patient-compatibility and organ toxicity (e.g. kidney).

In United States (US) and European cohort studies, the lifetime risk of AF is 22-26% in men and 22-23% in women by age 80 years compared to men. The standard risk for a 40-year-old person was 25% (Magnani et al., 2011). In the recent years current anticancer therapies are associated with direct increased risk of cardiac damage, including left ventricular (LV) dysfunction (LVD) and heart failure (HF) (Chen et al, 2012).The Childhood Cancer Survivor Study showed that, 15 to 25 years after diagnosis, survivors of childhood cancer have an 8.2-fold higher rate of cardiac death compared with the age-matched and sex-matched national average. However, compared with controls, long-term childhood cancer survivors had 15-fold increased rates of congestive HF, 10-fold higher rates of CVD, and 9-fold higher rates of stroke (Yeh et al, 2004; Pinder et al, 2007). Cardiotoxicity induced heart failure is becoming more common and has a detrimental effect on the population (Armstrong et al, 2014).

1.1 Heart Failure

Heart failure is a major public health epidemic worldwide. Heart failure is a low cardiac output syndrome characterized by both systolic and diastolic dysfunction. The velocity and extent of ventricular contraction and the rate of pressure development are decreased in heart failure (Figure 1.1). Left ventricular ejection fraction (LVEF) measures the amount of blood being pumped out of the left ventricle during each contraction. LVEF is a common measurement used to assess heart function although heart failure with preserved left ventricular function (Hf-pEF) lies within the normal range. The heart failure with reduced left ventricular function (HF-rEF) is usually with LVEF less than 35% (Kalogeropoulos *et al*, 2016).

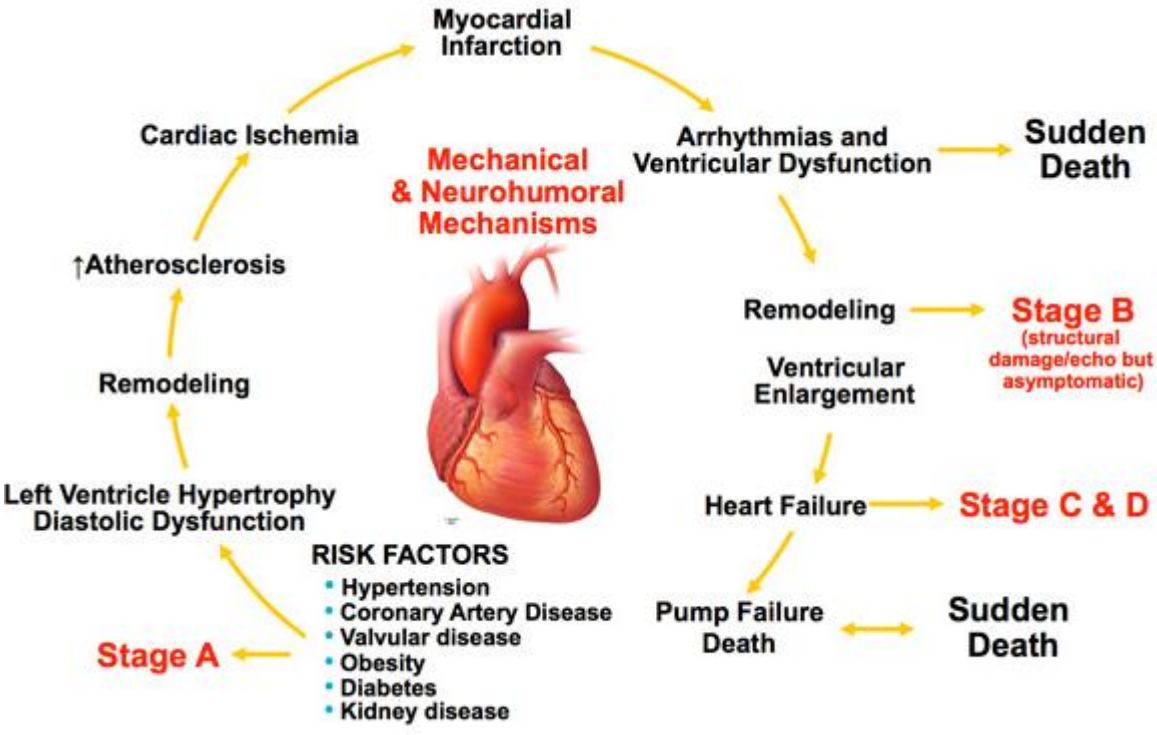

Figure 1.1 Heart failure progression. The cycle of heart failure progression involving different stages (Weintraub *et al*, 2010).

The pathophysiological changes occurring through heart failure take in three major forms such as LV dysfunction, pulmonary hypertension (PH), and right ventricular (RV) dysfunction (Figure 1.2).

During LV dysfunction there are few pathogenesis mechanisms which result in LV dysfunction. The higher volume overload of the heart results in high output state causing increased LV dilation and eccentric hypertrophy (Wilcox and Yancy, 2016). As a result of the high output it leads to the development of heart failure.

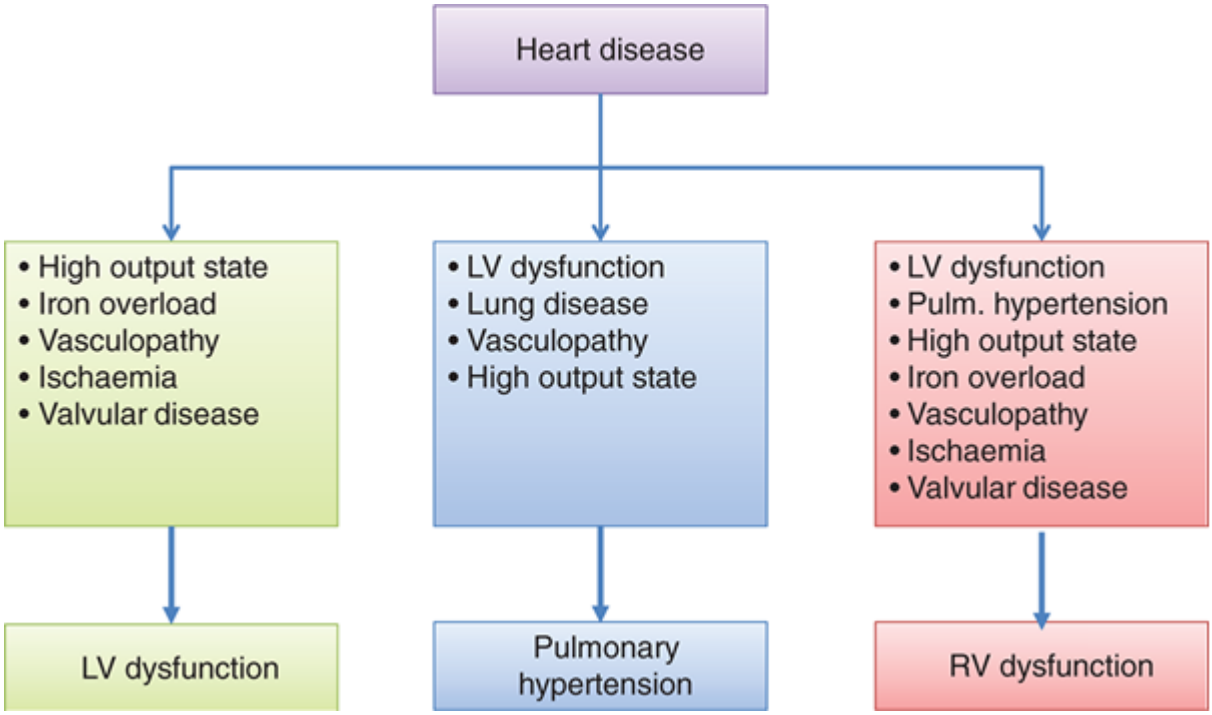

Figure 1.2: Pathophysiological forms of heart failure. LV, left ventricular; RV, right ventricular (Farmakis *et al*, 2016).

There are several contributing factors towards HF which eventually leads to cardiac-related death. Calcium cycling is crucial for both contraction and relaxation in cardiomyocytes. During the depolarisation of the cell the transverse tubules triggers the entry of small quantities of Ca2+ into the cardiomyocyte sarcoplasmic reticulum (SR) membrane (e.g. Stammers *et al*,

2015). The influx of Ca2+ triggers the opening of the nearby calcium release channels known as the type 2 ryanodine receptors (RyR2), a large tetrameric protein complex. The release of larger quantities of calcium from the sarcoplasmic reticulum via RyR2 increases the intracytoplasmic calcium which activates troponin C to stimulate the cross bridge formation between actin and myosin filaments in sarcomeres to cause cardiac contraction (e.g. Santulli *et al*, 2015).

On the other hand, sarcoplasmic- endoplasmic reticulum ATPase (SERCA2a) initiates cardiomyocyte relaxation by pumping calcium ions from the cytoplasm back into the sarcoplasmic reticulum, shutting off contraction (e.g. Stary *et al*, 2016). The SERCA2a activity is regulated by 52 amino acid peptide known as phospholamban. In the dephosphorylated state phospholamban inhibits the activity of SERCA2a but when it becomes phosphorylated by calcium dependent and calmodulin- dependent protein kinase (CaMKII),(Nakagawa et al, 2016) SERCA2a becomes activated resulting in decrease in cytoplasmic calcium and relaxation occurs. During ischaemia the ATP production is reduced which can impair the activity of SERCA2a; this was observed in animal models and heart failure patients (Gorski et al, 2015). This impairment least favours the calcium being pumped back into the SR during diastole thus interfering with both contraction and relaxation of the cardiomyocytes (Kho et al, 2015). However in heart failure, the diastolic calcium levels increase due to the reduced activity of SERCA2a and increased activity of phospholamban. Therefore, SERCA2a activity is crucial for calcium cycling handling under normal conditions. In heart failure, this process becomes disrupted and the imbalance of the calcium handling can have detrimental effects on the heart.

1.2 Functions of the mitochondria

Mitochondria is a double membrane organelle found most in eukaryotic organisms. Mitochondria comprise 25–30% of cell volume across mammalian species (Brown et al, 2017), with only the myofilaments being

more densely packed within cardiac myocytes. Mitochondria are primarily located within subsarcolemmal, perinuclear, and intrafibrillar regions of the cardiomyocyte. Mitochondrial dynamics in the form of fission, fusion, and autophagy are highly regulated processes that are essential for energy production and structural integrity of the organelles (Suliman and Piantadosi, 2016). The high mitochondrial content of cardiomyocytes is needed to meet the enormous energy requirement for contraction and relaxation (which is also an active process). About 90% of cellular ATP is utilized to support the contraction–relaxation cycle within the myocardium (Opie, 1998).

The ‘myocardial power grid’ consists of mitochondrial ATP supply that transfers energy throughout the cell along intracellular phosphotransfer buffering systems. Mitochondria utilize carbon sources from food substrates, which are catabolized and passed through the Krebs cycle and are then channelled through a series of redox reactions along the inner mitochondrial membrane. The oxidation of these substrates creates a proton electrochemical gradient, predominantly in the form of mitochondrial membrane potential (Mitchell, 1961). Protons that reenter the mitochondrial matrix through complex V (mitochondrial ATP synthase) liberate energy that phosphorylates ADP, regenerating ATP (Thomas and Gustafsson, 2013).

However, when there is a dysregulation in the mitochondria, the highly regulated processes that are essential to maintain structural integrity and energy production fails. Mitochondrial dysfunction arises partly due mutations in the mitochondrial DNA that code for mitochondrial components. They may also result from the adverse effects of drugs, infections and other environmental causes. Abnormal mitochondria are a major source of reactive oxygen species (ROS) production, which can induce cellular damage. Cellular ROS production occurs when ROS formation outpaces or exhausts compensatory signals and overwhelms endogenous scavenging systems (Aon et al, 2010; Brown et al, 2013; Murphy and Steenbergen, 2008). ROS are produced at several different sites within cells, both within and outside of mitochondria (Murphy and Steenbergen, 2008; Nabeebaccus et al, 2011). Mitochondrial ROS production occurs at various sites along the inner mitochondrial membrane as well as in the mitochondrial matrix by

components of the ETC and the Krebs cycle, respectively. ROS (and other associated reactive intermediates) can damage proteins and lipids, trigger cell-death cascades, and evoke synchronized collapses in the cellular energy grid (Zorov et al, 2006; Aon et al, 2006; Orr et al, 2013).

Abnormal mitochondria can promote programmed cell death through the release of cytochrome c into the cytosolic compartment and activation of caspases. Apoptosis occurs in two different pathways. The extrinsic pathway utilizes cell-surface death receptors and links external stimuli to intracellular apoptotic cell death machinery. The intrinsic pathway involves the mitochondria and endoplasmic reticulum, which, again, sense stimuli and transduce signals to execute apoptosis via another distinct set of molecules (Degterev et al., 2003). Therefore, mitochondria directly influence ongoing cell injury and death. Mitochondrial abnormalities have also been implicated in aberrant cellular calcium homeostasis, vascular smooth muscle pathology, myofibrillar disruption, and altered cell differentiation, all important issues in cardiovascular disease, including HF.

Drugs can have adverse effects on the mitochondrial function. Doxorubicin, Statins, Rosiglitazone, Amitriptyline and Amiodarone are among the frequently used drugs to manage a variety of diseases which have been known to cause mitochondrial dysfunction in chronic use. Doxorubicin (DOX) is an anthracycline commonly used in cancer treatment. The cardiotoxicity caused by DOX could be acute (hours to days) to intermediate (weeks and months) and late onset (>12 months) and even years after treatment has finished. However, its clinical use is greatly restricted by the development of cardiomyopathy and clinical congestive failure (Liu et al, 2008). Statins (HMG-CoA reductase inhibitors) are a class of lipid lowering drugs used in treatments for hypercholesterolemia and reduce cardiovascular diseases. Statins competitively inhibit the conversion of HMG-CoA to mevalonate, a precursor for cholesterol synthesis (Herninger and Fritz, 2017) thereby eventually reducing the cell's intrinsic cholesterol synthesis and favouring the uptake of serum LDL cholesterol. On the other hand, statins are known to promote muscle weakness during prolonged time periods. Statin therapy is associated with decreased myocardial function and increase risks of stokes

(Lim et al, 2013). Rosiglitazone is a thiazolidinedione antidiabetic drug used in treating type 2 diabetes mellitus. It works as an insulin sensitizer, by binding to the peroxisome proliferator –activated receptor in cells and making the cells more responsive to insulin. Its use has dramatically decreased over the years due to association of increased risks of heart attacks and deaths (Varga et al, 2015; Pharaon et al 2017).

Amitriptyline is tricyclic antidepressant used to treat mainly depressions and other anxiety disorders. This drug has significant adverse effects on the heart as it causes disturbances in the rhythm of the heart, QT prolongation, leading to cardiac dysfunction (Zima et al, 2008; Arici et al, 2013). Amiodarone is a potent antiarrhythmic agent that is used to treat ventricular arrhythmias and atrial fibrillation. Chronic use of amiodarone induces multiple organ toxicity via reduced phospholipid degradation which leads to its accumulation and, consequently lipid peroxidation, ROS generation, and disturbance of cellular calcium (Abuzaid et al, 2015).

1.2 Melatonin

Melatonin was initially discovered by Lerner and colleagues in late 1950s, which acted as a robust endocrine signal that can regulate the circadian time and day length. It is produced from the pineal gland located behind the third cerebral ventricle of the brain (Figure 1.3) (Johnstone and Skene, 2015). In 1950s, Lerner and his co-workers discovered melatonin as a potent lightening agent. Melatonin was isolated from beef pineal glands and was injected into the frog skin, followed by incubation in *in vitro*. The result showed the frog melanocytes were lightened when melatonin was injected (Lerner *et al*, 1959).

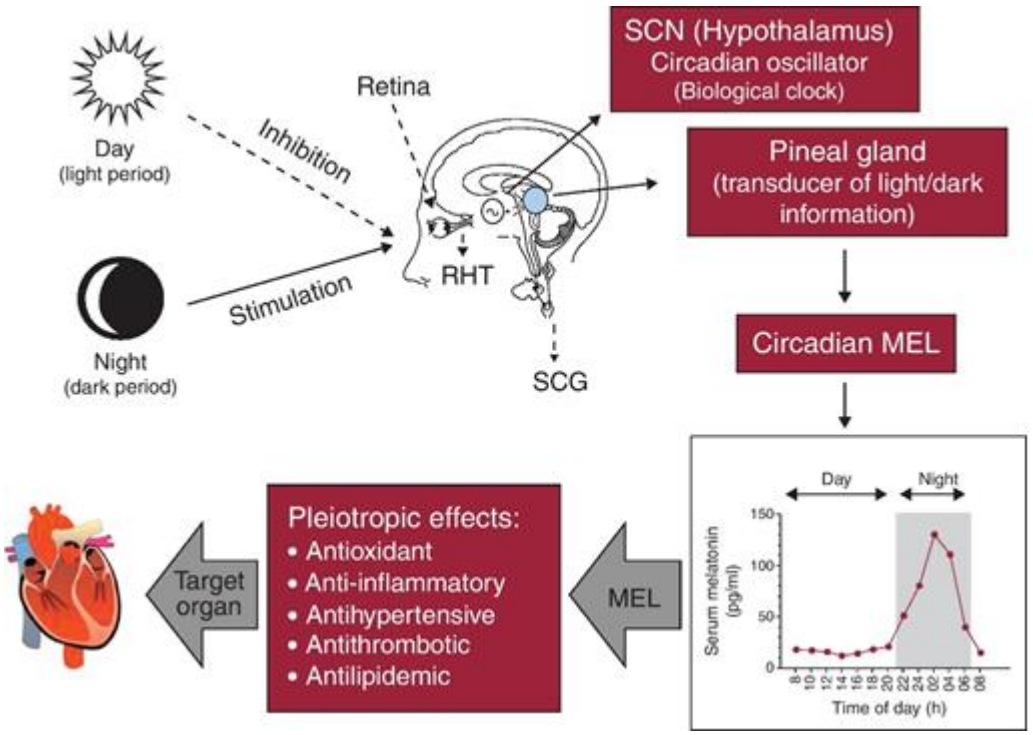

Figure 1.3. The neuroendocrine connection between the pineal gland and the brain (Dominguez-Rodriguez et al, 2012).

Melatonin can influence both daily and seasonal rhythms in many species. The daily rhythmic production of melatonin is a conserved characteristic in mammalian physiology (Figure1.4). It is present in higher levels during the

night and minute levels during the day (Ganguly *et al*, 2002). This phenomenon was understood in late 1990s, when Maywood and colleagues observed in Syrian hamsters, where melatonin mediates the seasonal response to photoperiod within the medio-basal hypothalamus (MBH), specifically via the melatonin (IMEL) binding sites found in the dorsomedial nucleus (DMN). The distributions of androgen receptors with IMEL sites have distinct regions of overlap in adult male hamsters. Together, the results indicate there are regions which are responsive to both gonadal steroids and melatonin which may regulate seasonal reproduction in GnRH release and melatonin influences the sensitivity of the steroidal feedback on cells (Maywood *et al*, 1996).

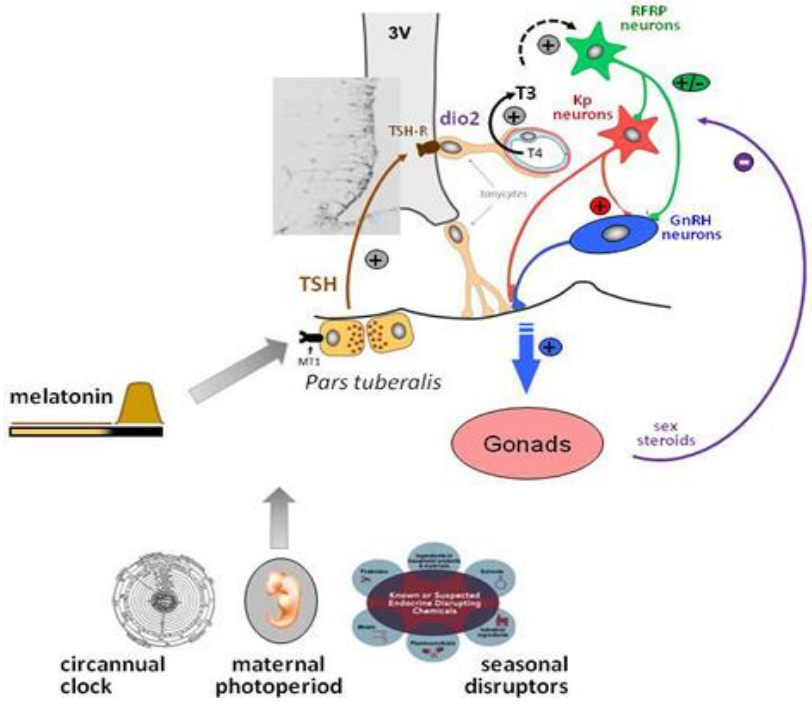

Figure 1.4: Seasonal rhythmic production of melatonin.

Light perceived through the retinal photoreceptors (PR), and transmitted through the retino-hypothalamic tract (RHT), affects mammalian reproduction via a complex pathway that involves the pineal, the suprachiasmatic nucleus (SCN) of the hypothalamus (HYP), the paraventricular nuclei, (PVN), superior cervical ganglion (SCG), and the pituitary gland. Hormones secreted include gonadotropin releasing hormone (GnRH) from the hypothalamus, luteinizing

hormone (LH), and follicle stimulating hormone (FSH) from the pituitary, which affects gonadal activity (Sengupta, 2011).

1.2.1 Melatonin Synthesis

Circulating melatonin is synthesised in the pineal gland however local levels of melatonin in the eye is synthesised by the retina. In most mammalian species the circadian rhythmic system of the pineal melatonin synthesis is due to poly-synaptic pathway linking the pineal gland to the hypothalamic SCN, which is the origin of the master mammalian circadian clock. From the SCN, the neurones pass via the paraventricular nuclei, to the upper thoracic intermediolateral cell column of the spinal cord and then sympathetic neurones of the superior cervical ganglion, innervates the pineal. As a result this activates arylalkylamine-N-acetyltransferase (AA-NAT), a key enzyme in melatonin synthesis pathway. The increase in AANAT activity results in an increase in the intracellular concentration of N-acetyl serotonin where there is a transfer of a methyl group to the 5-hydroxy group of N-acetylserotonin which is then converted to melatonin (N-acetyl 5-methoxytryptamine; MEL) by hydroxyindole-O-methyltransferase (Figure 1.5) (Pevet, 2014; Erren and Reiter, 2015; Emens and Burgess, 2015; Qian and Scheer, 2016).

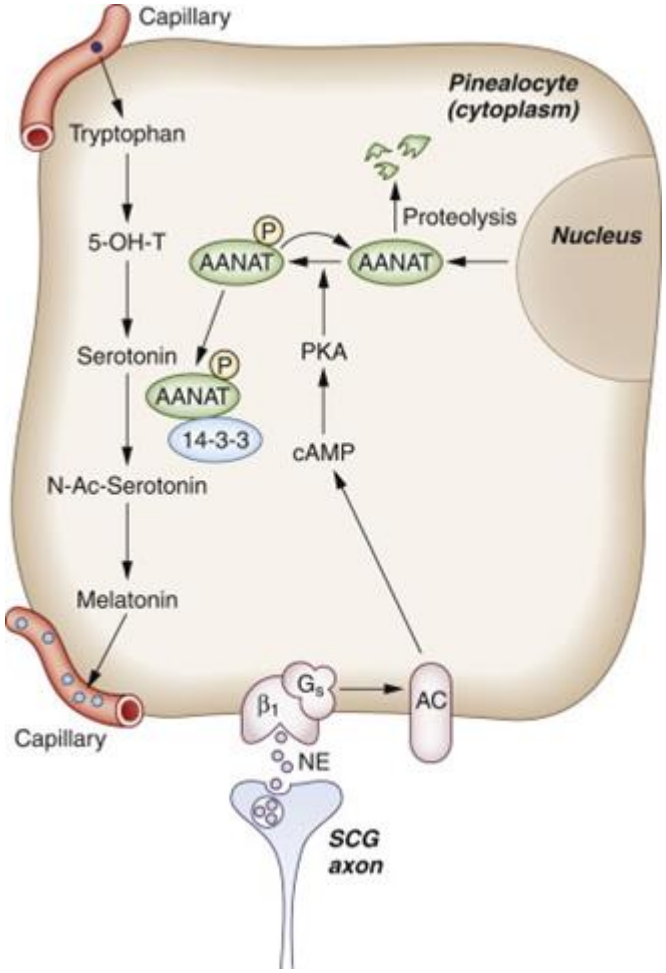

Figure 1.5: Melatonin synthesis in the pineal gland (Henry, 2015).

1.3 The circadian timing system

The human circadian system allows an organism to predict the daily environmental changes taking place. Many physiological factors such as temperature, hormones and electrolytes along with behavioural changes such as mood, sleep, performance and alertness are maintained through circadian rhythms (Skene and Arendt, 2006). Circadian rhythms are rhythms that are endogenously generated and synchronized to 24h day by the light/dark cycle, to regulate physiological factors in an organism. In the absence of light/dark cycle the circadian rhythms become desynchronized from the 24h day, resulting in dysregulated clock system, affecting many other physiological factors (Hu et al, 2016).

The circadian system involves a circadian oscillator, a photodetector and an output signal. These elements together with neural connections link to the melatonin rhythm generating system. This is important with regards to the regulation of melatonin production and functions (Johnstone and Skene, 2015). In the melatonin rhythm generating system the oscillator regulating the pineal gland function is found in the SCN which can control the stimulations of the pineal gland in 24hr basis. Light plays an important role in activating the SCN clock via the photoreceptors in the retina and the retinal hypothalamic tract (Emens and Burgess, 2015) as shown in Figure 1.6. It stimulates the pineal gland and influences AANAT activity for melatonin synthesis. Melatonin transmits the internal time information throughout the body to allow regulation and providing feedback information to the brain (Tan et al, 2015).

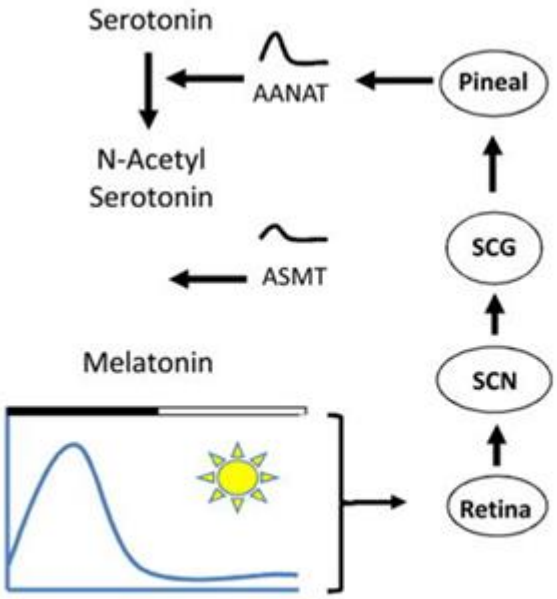

Figure 1.6: Pineal melatonin synthesis and AANAT activity is dependent on the daily light:dark cycle Arylalkylamine N-acetyltransferase (AANAT), suprachiasmatic nuclei (SCN). (Tosini et al, 2014).

The role of melatonin in synchronisation of the circadian system was first observed in rat circadian rhythms. Redman and colleagues demonstrated the daily administrations of melatonin can entrain free running circadian activity rhythms in rat. When the injections were stopped, the activity rhythms became free running again. The onset of the circadian activity coincided with the time of the daily injections (Redman *et al*, 1983). This suggests time of day is crucial for melatonin administration to synchronize the circadian rhythms. Melatonin is a potent synchronizer of rat circadian rhythms and has a direct action on the circadian pacemaker (Armstrong, 1989).

1.4 Molecular basis of the circadian clock

The molecular mechanisms underlying the circadian timing system are controlled by clock factors and clock controlled genes. The circadian-drive of clock genes are primarily expressed through self-sustaining interactive intracellular transcriptional/translational feedback loops (Figure 1.7). During the subjective day, certain key clock genes are transcribed *(e.g. Per1, Per2, Per3, Cry1, Cry2 and Reverbα)* by heterodimeric complexes of *CLOCK* and *BMAL1* (Peschke et al, 2015). This continues till subjective night until the levels of PER/CRY proteins become sufficiently high enough to suppress the activity of *CLOCK/BMAL1* activation. During early morning, the levels of *PER/CRY* starts to decline allowing the transcription of genes to take place. Specifically the gene transcription of AANAT (clock controlled gene) occurs at this time point which is crucial for the synthesis of melatonin hormone. The diurnal rhythm of AANAT activity and melatonin synthesis in the pineal gland of vertebrates is controlled by the circadian clock and synchronized by environmental photic and thermal signals. This is the negative feedback loop of the system and the cycle continues. On the other hand, there is a secondary loop which is controlled by Reverbα and Reverbβ which can supress Bmal1 transcription. At the end of the night the *REVERB* proteins starts to disappear and Bmal1 peaks, therefore this can be seen as a positive feedback loop of the system (Erren and Reiter, 2015; Peschke et al, 2015; Tan et al, 2015; Saha et al, 2018).

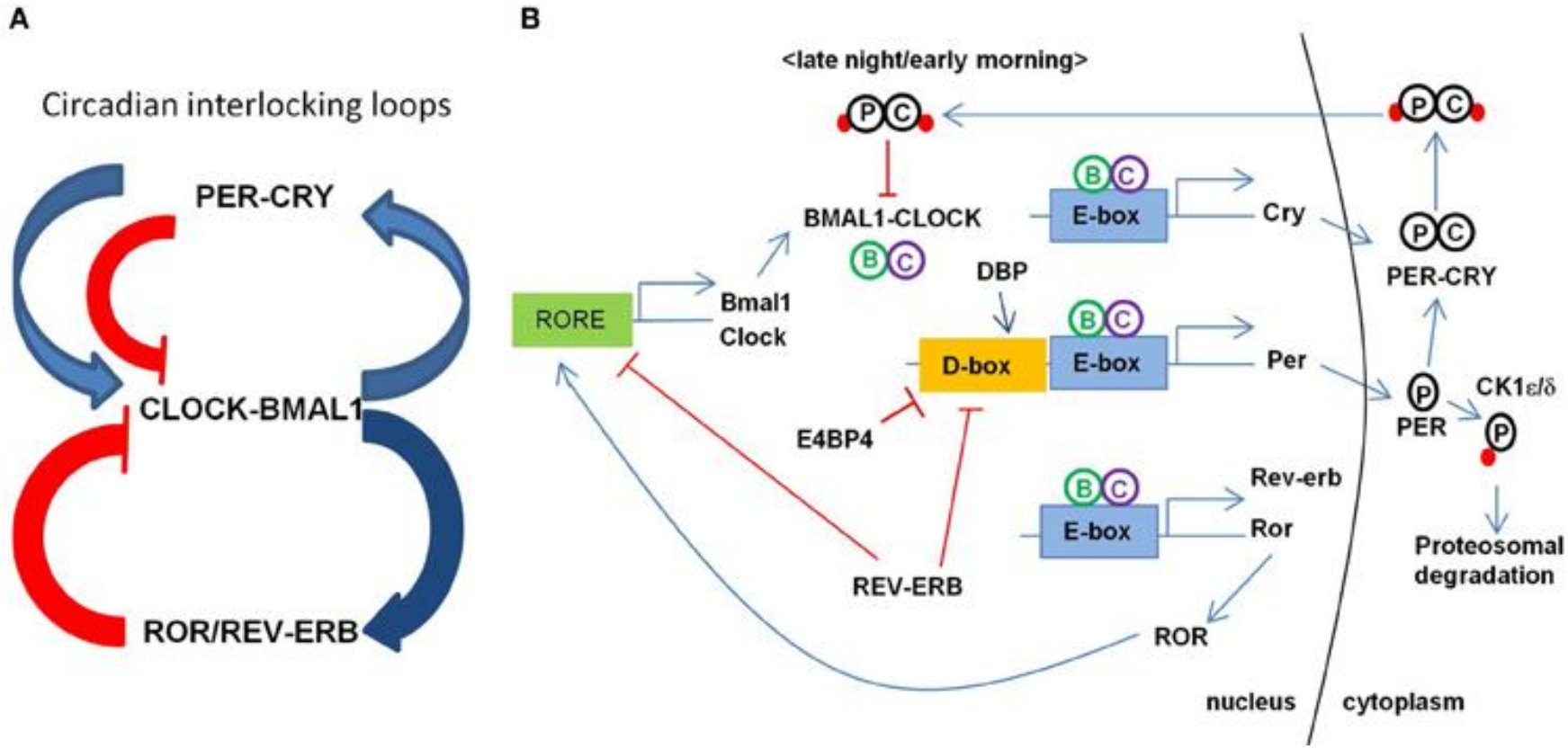

Figure 1.7: The transcriptional regulation of clock genes in mammals. (A) Circadian interlocking loops show that a primary loop of CLOCK-BMAL1 and PER-CRY complexes and an additional feedback loop of ROR/REV-ERB, conferring a tight transcriptional regulation. (B) Transcription of BMAL1 and CLOCK is regulated by ROR and REV-ERB through binding RORE elements at their promoters (Cho, 2012).

1.5 Role of melatonin in cardiomyocyte mitochondrial function

The regulatory role of melatonin in circadian and seasonal rhythms is well established (Acuna et al, 1986), and it is known as the chemical expression of darkness (Reiter, 1993). However, there is increasing evidence showing its involvement in many other functions, involving the role as a powerful anti-oxidant. Melatonin was first demonstrated to be a direct scavenger of oxidants by Tan and colleagues using an in vitro system, this group found that melatonin directly scavenged the highly toxic ·OH (Tan et al, 1993). Li and colleagues provided the first evidence that melatonin neutralized ·OH in vivo (Li et al, 1997). Furthermore, Bromme and colleagues supported the finding for administration of melatonin reduced ·OH generated during cerebral ischemia-reperfusion (Bromme et al, 2000).

In the mitochondria the electron transport chain generates ATP via the reduction of oxygen to water, however certain percentage of oxygen can be reduced by dissipating single electrons to produce free radicals. The most abundant ROS production is from superoxide anion radical (O_2^-) from the electron leakage from oxygen molecule (Erdemli et al, 2016). Multiple electron transfer leading to other ROS generation is negligible, but, secondarily, peroxynitrite anion (ONOO−, formed from O2− and nitric oxide, NO), hydroxyl radical (OH, formed via H2O2 from superoxide dismutation), carbonate radical (CO3−, formed from OH and HCO3 −, or from ONOOCO2 − decomposition), and nitrogen dioxide (NO2, formed from peroxynitrate, ONOOH or ONOOCO2 −) are generated. These other ROS and RNS (reactive nitrogen species) have a much higher reactivity than O2− (Pandi-Perumal et al, 2013; Tan et al, 2015; Manchester et al, 2015).

Generally higher concentrations of these free radicals can mediate cellular damage in components such as DNA, lipids and proteins in the mitochondria (as it is the origin of ROS production). Free radical damage can be seen as oxidative stress which can lead to cell death, senescence or tumorigenesis (Andrabi et al, 2015). On the other hand melatonin benefits the cell against oxidative damage by having direct free radical scavenging properties (Figure 1.8).

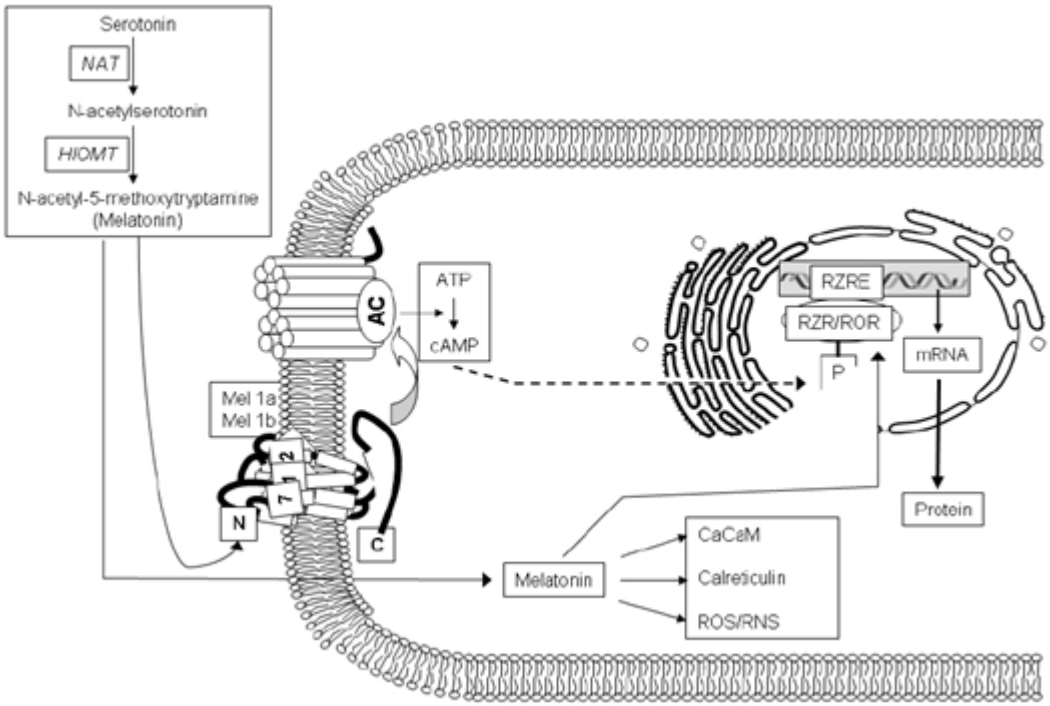

Figure1.8: Actions of melatonin exerts its effects through both membrane and nuclear receptors. At the mitochondrial level melatonin increases its efficiency as an antioxidant by reducing free radical generation and increasing ATP production (Reiter et al, 2010).

Oxidants are detoxified, antioxidants are stimulated, pro-oxidants are suppressed, and prevention of free radical formation can be seen with melatonin. Melatonin administration in cells increases respiration and the activity of the complexes I to complex IV in the ETC. The physicochemical nature of the reaction between melatonin and free radicals has been investigated. Three mechanisms have been proposed and tested, including single electron transfer, hydrogen atom transfer, and radical adduct formation (Paredes and Reiter, 2010; Galano et al, 2011) Using In vitro cell-free system in the presence of one-electron oxidants, $ONOO^-$, or alkoxyl radicals, several studies found that single electron transfer and hydrogen atom transfer were important characteristics of the antioxidant activity of melatonin (Mahal et al, 1999).In the presence of $^{\cdot}OH$, however, radical adduct formation seems to be the major mechanism by which melatonin detoxifies $^{\cdot}OH$. This property is not

observed in other antioxidants therefore melatonin can both participate in electron transport and act as an antioxidant.

Within the cell melatonin is localized in subcellular compartments such as the nucleus, cell membrane and mitochondria to scavenge free radicals (Sarihan et al, 2015). When melatonin detoxifies the OH^- (free radical), it is converted to cyclic 3-hydroxymelatonin, which is also a potent radical scavenger. Cyclic 3-hydroxymelatonin is an intermediate metabolite of melatonin and it undergoes oxidation resulting in the formation of N^1-acetyl-N^2-formyl-methoxykynuramne (AFMK). Deformation of AFMK leads to the generation of N2-acetyl-5-methoxykynuramine (AMK). These compounds are also major melatonin metabolites with a similar potency to melatonin in detoxifying ROS and reducing oxidative stress. The sequence of scavenging ROS by melatonin and its metabolites is known as melatonin's antioxidant cascade (Mukerjee et al, 2015; Giacomo and Antonio, 2007; Barthi et al, 2014).

In addition to its free radical scavenging capacity which protects mitochondria from oxidative damage, melatonin also exerts its protective effect on mitochondria by direct involvement in membrane integrity, permeability transition pore, electron transport, and ATP production. Garcia and colleagues first demonstrated that melatonin helped maintain mitochondrial membrane integrity and MPTP in vitro using a microsomal system (Garcia et al, 1999). Melatonin was further shown to interact with mitochondrial ETC. Complexes I and IV to promote electron flux under basal conditions to increase ATP production (Martin et al, 2002). The high redox potential of melatonin (−0.98 V) was postulated to facilitate the electron transfer in the ETC., by donating an electron to complex I of the ETC (Reiter, 2000).

In conclusion the potential mechanisms or approaches by which melatonin interacts with mitochondria are listed (i) Melatonin directly detoxifies ROS/RNS through its nonreceptor-mediated free radical scavenging capacity, thereby lowering damage to mitochondrial proteins and DNA (Acuna et al, 2002) (ii) Melatonin increases the activity of antioxidative enzymes while suppressing pro-oxidant enzymes in mitochondria (Acuna et al, 2005; Inarrea et al, 2011) (iii) Melatonin stabilizes the mitochondrial inner

membrane, thereby maintaining mitochondrial integrity (Garcia et al, 1999) (iv) Melatonin increases the activity of mitochondrial electron transport chain (ETC.) complexes and improves mitochondrial respiration and ATP production, thereby reducing electron leakage and ROS generation (Martin et al, 2000) (v) Melatonin may directly control the currents through the mitochondrial permeability transition pore (MPTP) (Andrabi et al, 2004; Jou, 2011).

1.6 Drug induced cardiotoxicity and heart failure

1.6.1 Introduction

Heart failure is predominantly caused by cardiovascular conditions such as hypertension, coronary heart disease and valvular heart disease, it can also be an adverse reaction induced by drug therapy. In addition, some drugs have the propensity to adversely affect haemodynamic mechanisms in patients with an already existing heart condition. Most non-cardiac drugs are known to be associated with the development or worsening of heart failure and cardiac function (Swift et al, 2006).The drug-mediated effects act on cardiac preload, cardiac afterload or myocardial contractility. Drugs that increase cardiac preload or cardiac afterload may have unfavourable effects on ventricular function, because increased cardiac preload or afterload intensifies the demand on ventricular performance. The ability of the heart to comply with this increased demand will depend on pre-existing ventricular function.

Moreover, drugs that may adversely affect heart function without precipitating overt symptoms or signs of heart failure are also evident. Example of these drugs include anticancer agents such as, mitoxantrone, cyclophosphamide, fluorouracil, capecitabine and trastuzumab; immunomodulating drugs such as interferon-alpha-2, interleukin-2, infliximab and etanercept; antidiabetic drugs such as rosiglitazone, pioglitazone and troglitazone; antimigraine drugs such as ergotamine and methysergide; appetite suppressants such as fenfulramine, dexfenfluramine and phentermine; tricyclic antidepressants; antipsychotic drugs such as clozapine; antiparkinsonian drugs such as pergolide and cabergoline; glucocorticoids; and antifungal drugs such as itraconazole and amphotericin B. NSAIDs, including selective cyclo-oxygenase (COX)-2 inhibitors (e.g. Ibuprofen), are included as a result of their ability to cause heart disease, particularly in patients with an already existing cardiorenal dysfunction (Solard and Spidsted, 2006).

Amongst these classes of drugs, a group of particular concern are the anti-cancer chemicals called Anthracyclines such as doxorubicin (DOX) (Swift et

al, 2006). Doxorubicin and its derivatives may cause cardiomyopathy in a disturbingly high number of exposed individuals, who may develop symptoms of insidious onset several years after drug therapy. The risk seems to encompass all exposed individuals, but data suggest that children are particularly vulnerable. Thus, a high degree of awareness towards this particular problem is warranted in cancer survivors subjected to anthracycline-based chemotherapy.

Cardiotoxicity is defined as occurrence of heart electrophysiology dysfunction or myocardial damage, as a result the heart weakens and is unable to pump blood around the body efficiently. Cardiotoxicity is one of the most important adverse reactions of chemotherapy, leading to a significant increase of morbidity and mortality, where 35%-43% of patients had developed clinical symptomatic heart failure after doxorubicin treatment (McGowan, 2017). Cardiotoxicity can appear early or late in the course of the disease, and since the most typical sign of chronic cardiotoxicity is a subclinical, asymptomatic systolic or diastolic cardiac dysfunction that can lead to irreversible heart failure and death (Florescu et al, 2013) (Figure 1.9).

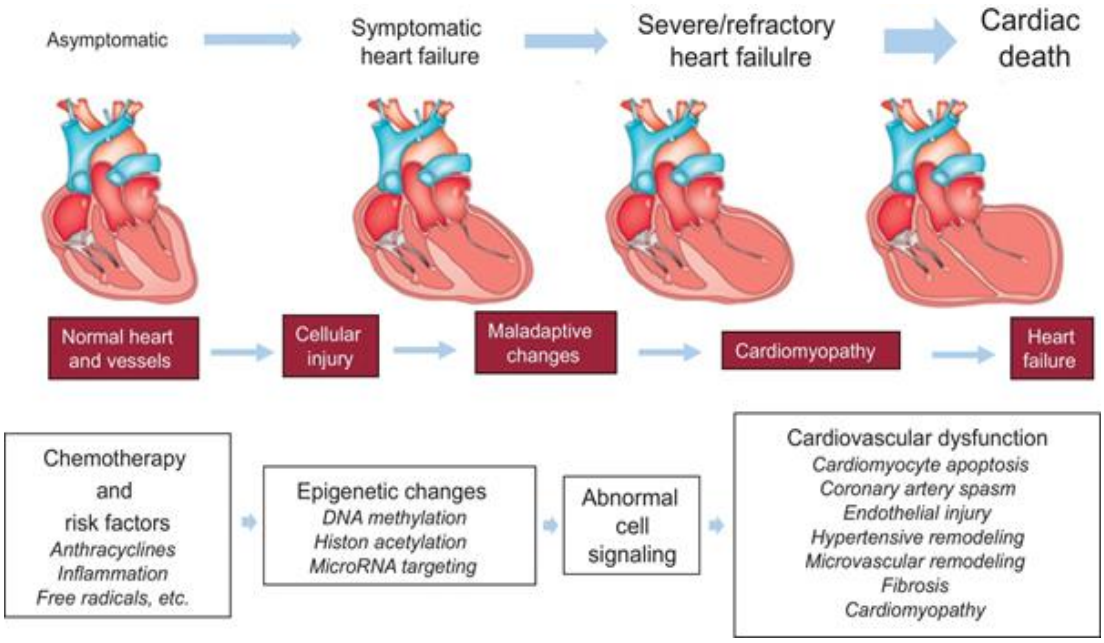

Figure 1.9: Changes occurring in the heart at different stages after induced by drugs, leading to cardiovascular dysfunction (Madonna, 2017).

Drug-induced cardiotoxicity can lead to diverse cardiac dysfunction. Cardiomyopathy is when heart muscle becomes weakened, enlarged, thickened, or stiff. This can lead to changes in disturbances in heart rhythm and ultimately to heart failure. Myocarditis is inflammation (swelling) of the heart which can also lead to changes in heart rhythm and decrease in heart performance. Pericarditis is inflammation (swelling) of the sac surrounding the heart which can cause chest pains and decreased in cardiac performance. Cardiotoxicity can also lead to acute coronary syndromes which are caused by blood vessel damage and, reduces blood flow to the heart. This can cause chest pains and in severe cases myocardial infarction. Chemotherapy can cause acute severe damage to the heart and in some cases can lead to congestive heart failure (CHF) in the first year of treatment (Taimeh et al, 2013).

1.7 Cardiotoxicity and cardiomyocyte apoptosis

Chemotherapy-induced cardiotoxicity (such as the use of DOX) can lead to cardiomyocyte cell death and irreversible heart damage. Therefore pharmacological intervention of apoptosis pathways may represent a promising therapeutic strategy for a number of cardiovascular diseases and disorders including myocardial infarction, ischemia/reperfusion injury, chemotherapy cardiotoxicity, and end-stage heart failure (Mitry et al, 2016).

Two noteworthy apoptotic pathways (i.e. pathways that in the end prompt to action of executioner caspases), the "extrinsic" and "intrinsic" cascades, transduce apoptotic signals in mammalian cells. The extrinsic pathway utilizes cell-surface death receptors and links external stimuli to intracellular apoptotic cell death machinery. The intrinsic pathway involves the mitochondria and endoplasmic reticulum, which, again, sense stimuli and transduce signals to execute apoptosis via another distinct set of molecules (Degterev *et al.*, 2003). Figure 1.10 summarizes the interlinked pathways of the extrinsic and intrinsic apoptotic cascades.

1.7.1 Intrinsic Apoptotic Pathway

The intrinsic pathway transduces extracellular and intracellular stimuli, including nutrient depletion, radiation, hypoxia, oxidative stress, ischemia-reperfusion, and DNA damage. Direct signaling from each of these is unclear, but they converge on the pivotal event of mitochondrial outer membrane permeabilization (MOMP) (Saelens *et al.*, 2004). At the mitochondria, MOMP often follows dissipation of the mitochondrial inner transmembrane potential, which may involve opening of the mitochondrial permeability transition pore. A separate mechanism for MOMP involves members of the Bcl-2 family of proteins acting at the outer mitochondrial membrane. Bcl-2 (the mammalian homologue of ced-9) is the prototype of the important family of genes in this intrinsic pathway of apoptosis, upon apoptotic stimuli, they undergo conformational change, oligomerise and

translocate to the mitochondrial outer membrane, promoting MOMP (Green and Kroemer, 2004).

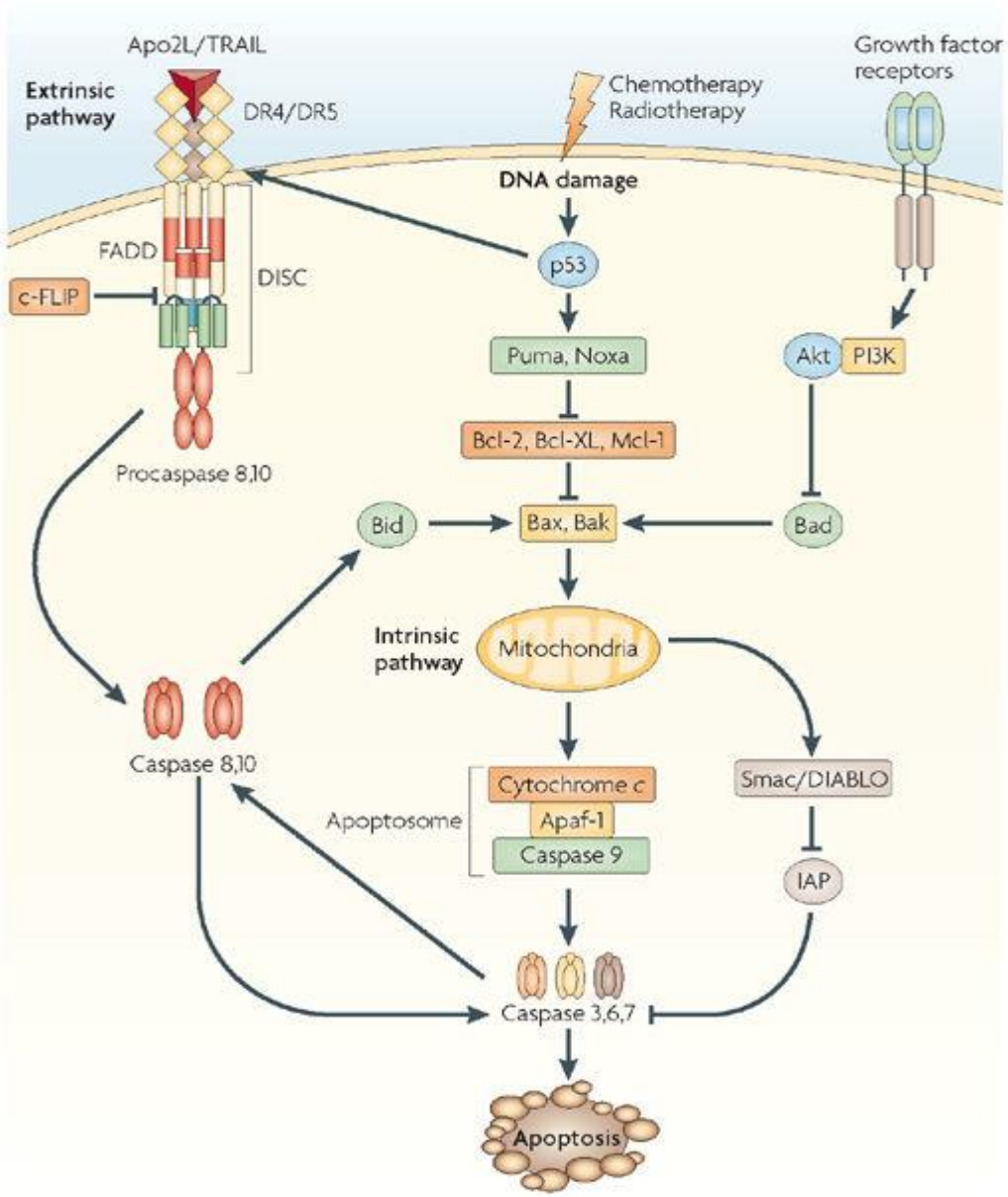

Figure 1.10: The Apoptotic Cascade exhibiting the extrinsic and intrinsic pathways. Cyt c, cytochrome c; DAG, diacylglycerol; ERK, extracellular signal-regulated kinase; FADD, Fas-associated death domain; FAK, focal adhesion kinase; PI3K, phosphoinositide 3-kinase; PIP2, phosphatidylinositol bisphosphate; PIP3, phosphatidylinositol trisphosphate; PLCβ, phospholipase C β; PKA, cyclic AMP-dependent protein kinase; PKC, protein kinase C; Bad, Bcl-2-associated death promoter; Bcl-2, B-cell lymphoma 2 (Ashkenazi, 2008).

Nuclear protein TR3 also binds Bcl-2 and promotes MOMP (Zhao *et al.*, 2006). Histone 1.2, released from the nucleus after DNA damage, triggers MOMP – again via an interaction with Bcl-2 family members. After MOMP, critical apoptogens (eg, cytochrome c) are released from the mitochondrial intermembrane space into the cytosol (Strasser, 2005). When in the cytosol, cytochrome c binds to the adaptor protein, Apaf-1. Apaf-1 oligomerizes into an apoptosome, which recruits and activates caspase-9. Like DISC in the extrinsic pathway, recruitment of caspase-9 in the apoptosome is dependent on ‘‘death domain motifs’’ on both caspase-9 and Apaf-1 (Cain *et al.*, 2000). As with caspase-8, activated caspase-9 activates downstream effector caspases and leads to the execution phase of apoptosis.

1.7.2 Extrinsic Apoptotic Pathway

In the extrinsic pathway, death ligands (such as FasL) act and bind with their various cell-surface death receptors (such as Fas ligand receptor), reorganizing the inactive receptor and stimulating the enlisting of adaptor proteins [such as Fas-associated via death domain (FADD)], that successively recruits procaspase-8 into a multiprotein complex referred to as the death inducing signalling complex (DISC) (Walczak and Krammer, 2000). Cluster of those interacting proteins inside the DISC promotes auto proteolytic process and activation of the caspase-8 by elicited proximity (Igney and Krammer, 2002). In cells, processed caspase-8 is enough to activate the opposite downstream effector caspases directly, resulting in the execution section of caspase-mediated cell death, caspase-8 mediates cleavage of the proapoptotic Bcl-2 family member, Bid, which afterwards releases mitochondrial proapoptotic factors (Fulda and Debatin, 2006), linking the extrinsic pathway to the intrinsic pathway of caspase-mediated cell death.

1.8 Doxorubicin – induced cardiotoxicity and heart failure

In pathophysiological conditions, heart failure may result from drug-mediated effects on cardiac preload, cardiac afterload or myocardial contractility. Drugs that increase cardiac preload or cardiac afterload may have unfavourable effects on ventricular function, because increased cardiac preload or afterload intensifies the demand on ventricular performance. Among the most cardio toxic drugs, doxorubicin is a well-known anti-cancer drug known or inducing cardio toxicity in heart. Many studies over the past had reported cancer survivors aged from 4 to 20 years after doxorubicin treatment > 60% observed significant decreases in fractional shortening and ejection fractions (Mitry and Edwards, 2016).

Doxorubicin, also known as Adriamycin or Rubex, is an anthracycline antibiotic that was isolated from a mutated strain of *streptomyces peucetius* bacterium (Arcamone et al, 1969). Doxorubicin operates on many levels by different molecular mechanisms as well as an interaction with iron, disconcerting calcium homeostasis, altering the activity of intracellular or intra-mitochondrial oxidant enzymes, and binding to topoisomerases promoting their dysfunction (Arcamone et al, 1969).

Doxorubicin is among the most frequently used anthracyclines included in chemotherapeutic regimens, to treat broad spectrum of cancers. The anthracyclines are antibiotic agents which antineoplastic action results from the inhibition of the nucleic acid synthesis by binding to both strands of the deoxyribonucleic acid (DNA) helix. This binding prevents normal function of the ribonucleic acid (RNA) and DNA polymerases (Takemura and Fujiwara, 2007). The introduction of the anthracyclines has contributed considerably to the improvement of survival in patients with cancer. However, anthracycline-induced cardiotoxicity is a well-known adverse effect of this category of drugs and a major limitation to the total dose that can safely be administered. (Rhoden et al, 1993.).

Based on the dose-dependency of the anthracycline-induced impairment of left ventricular function, an upper limit of the cumulative dose of 550 mg/m^{2}is

generally recommended. When this upper limit of the cumulative dose is exceeded, early heart failure may develop in about 30% of the patients receiving these high dosages (Rhoden et al, 1993). In a study among 201 children who had completed chemotherapy with anthracyclines, decreased fractional shortening on echocardiography was present in more than 60% of the patients who had received >500 mg/$m^2$and were followed up for at least 10 years (Steinhers 1991). A retrospective analysis revealed that 30-year childhood cancer survivors had a 15-fold higher rate of heart failure and 10-fold higher rate of other cardiovascular diseases when compared to estimated values in their siblings. Cardiac abnormality can be seen as asymptomatic disturbances in cardiac rhythms, changes in blood pressure, thickening of pericardium, cardiac dilation, and cardiomyopathy (Angsutararux et al, 2015; Lestuzzi, 2010).

1.8.1 Oxidative Stress: a key mechanism in doxorubicin-induced cardiotoxicity

Generally, DOX induces cardio toxicity by exerting effects on the mitochondria with increased reactive oxygen species (ROS) production. Usually, mitochondria are the site where most of ROS are synthesised as a consequence of electrons escaping from electron transport chain and captured by oxygen, rendering it to be the site of superoxide production.

Enzymes among mitochondria, as well as NADPH enzyme (also called NADPH dehydrogenase), cytochrome P-450 reductase, and xanthine oxidase (XO), will rework DOX and alternative anthracyclines within the sort of quinone to semiquinone via one electron reduction of the quinone moiety in ring C (Schimmel *et al*, 2004). In mitochondrial electron transport chain, oxygen free radical is also generated when an electron is transferred from NADH to oxygen molecule by NADH-ubiquinone oxidoreductase or complex I. Thereafter, the free radical undergoes a dismutation, a reaction that is accelerated by SOD enzyme, generating less-reactive specie hydrogen peroxide (H_2O_2), which can be detoxified by catalase or glutathione

peroxidase (GPx) in the presence of glutathione GSH (Kalivendi et al, 2001).Oxygen free radical (O_2^-) may react with H_2O_2 and form the highly reactive hydroxyl radical (OH^-) by Haber-Weiss reaction. Under stress conditions, O_2^- facilitates the release of free iron from iron-containing molecules, for example, [4Fe-4S]-containing enzymes, leading to the generation of OH^- from Fenton reaction. Moreover, O_2^- can facilitate the OH^- production in the reaction by generating ferrous iron (Fe (II) from the reduction of ferric (Fe(III) (Angsutararux et al, 2015). This reactive ·OH can oxidize membrane lipid and subsequently generates lipid radicals e.g., 4-hydroxy-2-nonenal (HNE) (Figure 1.11).

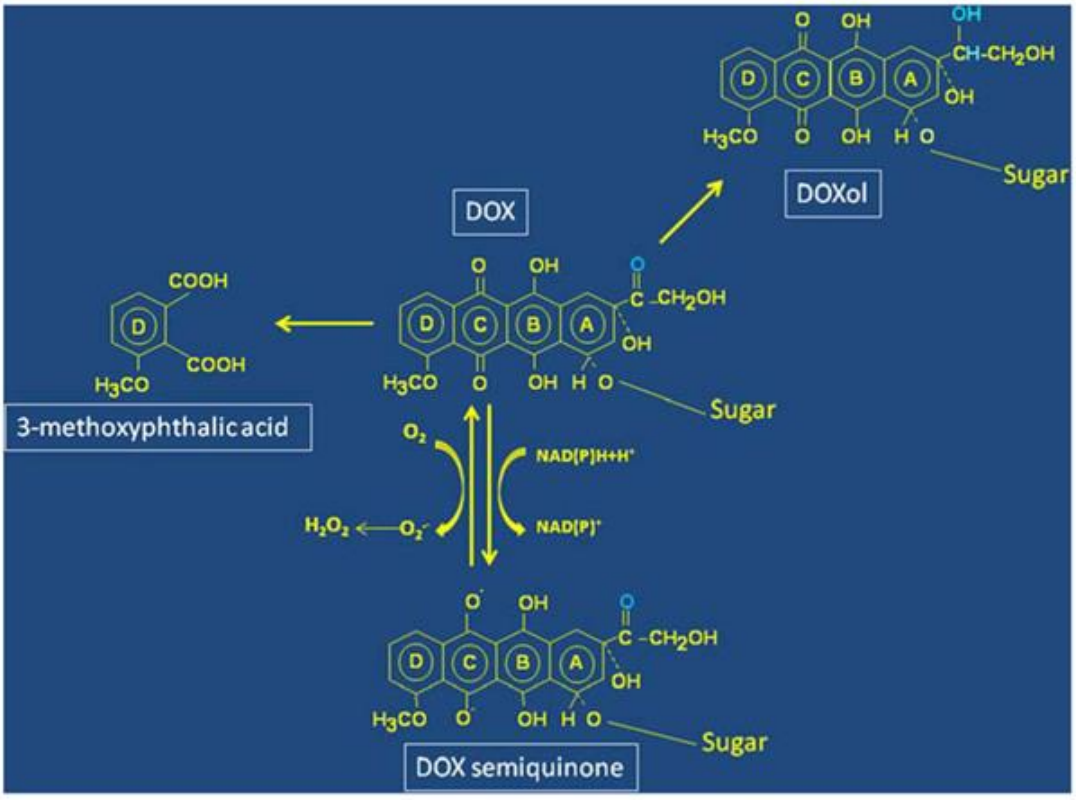

Figure 1.11: A redox cycling of Doxorubicin.

Redox cycling between the quinone and semiquinone shapes (ring C) of doxorubicin (DOX) winds up in oxygen radicals frame Cardiac myocytes, which speak to ~85% of aggregate heart mass, are the real contracting cells in the heart. In the previous decade, real advance has been made toward understanding the apoptosis instruments in cardiomyocytes. Cardiomyocyte apoptosis is an exceedingly controlled process; pharmacological intercession of apoptosis pathways may speak to a promising helpful technique for various cardiovascular illnesses and clutters including myocardial dead tissue, ischemia/reperfusion damage, chemotherapy cardiotoxicity, and end-stage heart failure (Gammella et al, 2014).

The interaction between DOX and iron have been known since 1980, when the first studies demonstrated that DOX had a strong affinity for iron (Tsai et al, 2000) and that the iron complex could cause lipid peroxidation through its interactions with the negatively-charged membranes (Chau et al, 2002). DOX reduction in the presence of free iron also sets up a cycle for free radical generation (redox recycling) and the metabolite doxorubicinol (metabolite of doxorubicin metabolised by aldoketoreductase) is known to interact with thiol groups on proteins, compounding the damages to the cell (Haghikia et al, 2014). More recent studies have suggested that the effects of DOX on iron metabolism are not mediated by doxorubicin–iron interactions, but rather via the proteins that sequester and bind intracellular iron. One such mechanism involves the doxorubicinol metabolite forming complexes with the Fe–S group the cytoplasmic aconitase/IRP-1 (iron regulatory protein), thereby enhancing the stability of transferrin mRNA and preventing translation of iron sequestration proteins (Monti et al, 2013). The subsequent decrease in IRP-1 leads to an increase in free iron, which could perpetuate the cycle of free radical generation. Interference with iron sequestration therefore remains a critical component of DOX-induced cardiotoxicity (Jungswadee, 2016).

The iron chelator dexrazoxane (DXZ) has been demonstrated, in both preclinical and clinical studies, to reduce the cardio toxic effects of DOX. DXZ is currently the only FDA-approved drug for prevention of DOX-induced cardiotoxicity (Ichikawa et al, 2014). Dexrazoxane is permeable to enter the cell, where it is metabolized into its open-ring form, ADR-925. The open-ring structure resembles the iron chelator EDTA (ethylenediaminetetra acetic acid), where it can bind free iron in the cell, decreasing intracellular concentrations or disrupt the association of iron with DOX. Thus, preventing the DOX-iron complex formation and thereby decreasing superoxide production. Dexrazoxane's protective effects appear in part to be that of protecting the cardiac mitochondria. Lebrecht and colleagues (2007) demonstrated that cardiomyocytes from rats treated with DOX and dexrazoxane for seven weeks had greater mitochondrial function than rats treated with DOX alone (Lebrecht et al, 2007). However in the recent years

the efficiency of dexrazoxane has reduced, overall it provides protection against cardiotoxicity but not adequate enough to supress against cardiotoxicity (Liesse et al, 2018).

Exposure to DOX also induces iron accumulation specifically in mitochondria, and mice with heart-specific deletion of ABCB8 that is involved in iron export out of the mitochondria were a lot of sensitive to DOX cardiotoxicity. The decrease or deletion of this gene caused retention of iron in the mitochondria (Ichikawa et al., 2014). Thus it is likely to disrupt cardiac function by generating oxidative stress and impairing the mitochondrial function.

1.8.2 Mechanism of action of DOX viaTopoisomerase II

The oxidant role of DOX was originally thought to be singular however it has become evident that doxorubicin's interaction with topoisomerases is of primary importance (Yang et al, 2014). Topoisomerases are highly conserved proteins in many organisms. DNA topoisomerases are ubiquitous enzymes that control the topology of DNA by cutting and resealing one or two strands of DNA double helices, thereby allowing DNA stands or double helices to pass through or rotate around each other (Zhang *et al*, 2007). DNA topoisomerases monitor, modify, and maintain the proper topology of DNA during replication, transcription, recombination, and repair. They have also been implicated in apoptotic DNA degradation (Lodish et al, 1995). Human cells contain six topoisomerases: 2 types IA, two types IB, and 2 types IIA; every catalyst being coded by a unique gene. Type I topoisomerases cleave and religate one strand of DNA at a time, whereas type II enzymes catalyse the cleavage-religation of 2 strands of the DNA duplex in concert. Topoisomerase type IIs differ from topoisomerase type I which induce only single DNA strand breaks to relieve torsional stress formed during biological processes such as DNA replication and transcription (Corbett and Berger, 2004; Nitiss, 2009).

Topoisomerase II is essential for decatenation of DNA- a process important for replication and transcription of DNA during mitosis, and deficiency in topoisomerase II prevents normal cytokinesis resulting in cell death. Doxorubicin has also been described as a poison of the DNA decatenating enzyme topoisomerase II whereby the drug stabilises the topoisomerase II-DNA cleavable complexes (Figure 1.12). Topoisomerase II acts to cleave one strand of duplex DNA, allowing a second duplex strand to pass through. Once it has passed through, the first strand of duplex DNA is re-sealed (Berger et al, 1996; Swift et al, 2003; Swift et al, 2007).

The interaction of topoisomerase II and doxorubicin has been described whereby the drug inserts into the minor groove of duplex DNA alongside the topoisomerase protein, resulting in stabilisation of the cleavable complex through a protein–drug interaction (Moro et al, 2004). Stabilisation of the cleavable complex results in the stalling of topoisomerase enzymatic activity and the induction of a DNA double strand breaks. This break is then thought to become a cytotoxic lesion, resulting in apoptosis. (Swift et al, 2008). It has been demonstrated by Zhang and colleagues, the cardiomyocyte specific deletion of topoisomerase IIβ in mice protects cardiomyocytes from doxorubicin-induced DNA double-strand breaks and transcriptome changes that are responsible for defective mitochondrial biogenesis and ROS formation by 70% compared to the control. In addition it blocked DOX induced decrease in cardiac ejection fraction and prevented the development of doxorubicin-induced progressive heart failure in mice, suggesting that doxorubicin-induced cardiotoxicity is mediated by topoisomerase-IIβ in cardiomyocytes (Zhang et al, 2012).

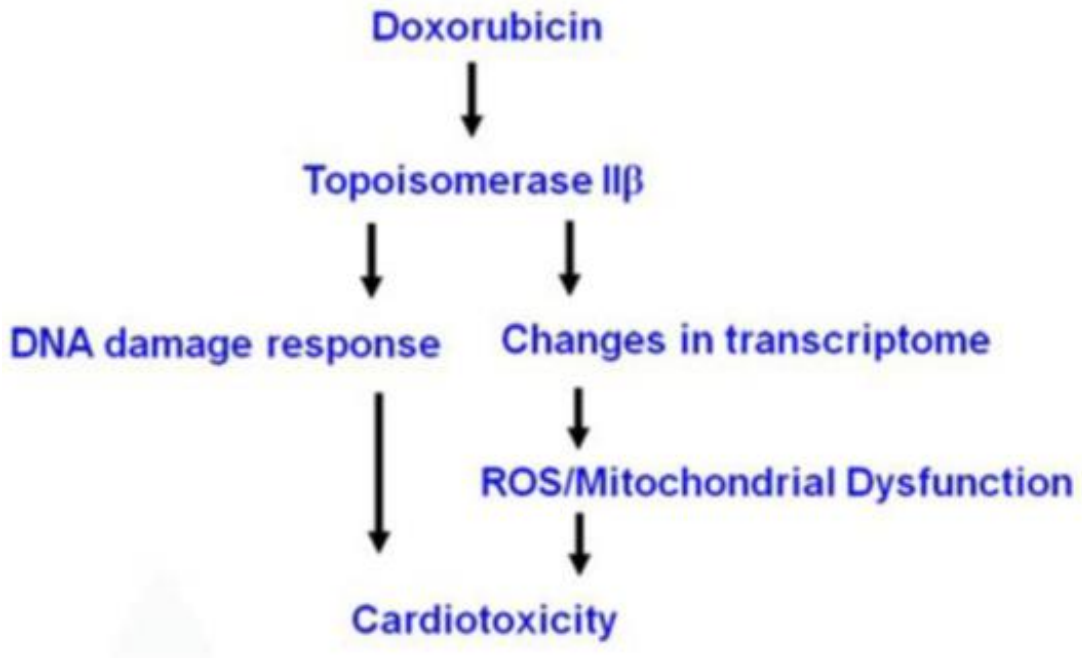

Figure 1.12: Mechanisms of Doxorubicin involved in topoisomerase IIβ pathway leading to cardiotoxicity (Zhang et al, 2012).

1.8.4 Calcium homeostasis dysregulation

Calcium imbalance is an important mechanism of toxicity of DOX. Precise temporal-spatial regulation of calcium is crucial for the correct function of the heart (Gopal, 2015). Doxorubicin directly exerts its effect on level of important component of sarcomeric reticulum calcium release or uptake channels, for example, ryanodine receptor (RYR2) and sarco-/endoplasmic reticulum Ca^{2+} ATPase (SERCA2). In cardiac excitation and contraction coupling, a small amount of Ca2+ enters through the L-type Ca2+ channel during membrane depolarization. This Ca2+ influx triggers a large scale release of Ca2+ from the Sarcoplasmic Reticulum (SR) membrane via Ryanodine Receptor (RyR). Released Ca 2+ binds to myofibirillar proteins, TnC-induce muscle contraction (Arai et al, 1992). Intracellular Ca2+ concentrations are regulated by three membrane systems; a plasma membrane system, a

sarcoplasmic reticulum (SR) membrane system and a mitochondrial membrane system.

Muscle relaxation is started by ATP-dependent Ca2+ transport into the SR by SERCA. The function of SERCA2 is regulated by the phosphorylated protein phospholamban. The majority of Ca2+ transported into the SR lumen is bound to the Ca2+, binding protein - calsequestrin. Other routes for Ca 2+ removal from the cytosol are those via the plasma membrane Ca2+-ATPase and the sodium-calcium exchanger (Na+/Ca2+ exchanger) on the plasma membrane. Ca 2+ transport through the mitochondrial membrane is thought to be a passive process (Gopal, 2015).

The endoplasmic reticulum (ER) plays an important role in multiple cellular processes such as folding of secretory and membrane proteins, lipid biosynthesis and calcium homeostasis. Various factors, such as oxidative stress and the disturbance of calcium compartmentalization, which interferes with ER function, lead to the accumulation of unfolded proteins which disrupt the membrane proteins (Rochette *et al*, 2015). Free radical generated by oxidative stress readily attack polyunsaturated fatty acids of the lipid membrane and decrease the membrane fluidity. As a result, the modifications of the lipid structure in the ER membrane suggest the activity of SERCA is inhibited (Kaplan *et al,* 2003), thereby disturbing the function of membrane-bound protein including mitochondrial calcium channel. The stress caused by this situation to the ER results in disruption of ER calcium homeostasis and accumulation of calcium concentrations inside ER.

Sustained increase in intracellular Ca2+ concentrations activates calcineurin. Calcineurin is a ubiquitously expressed serine/threonine phosphatase that exists as a heterodimer, comprised of a 59-kDa calcium-binding catalytic A subunit and a 19-kDa Ca2+-binding regulatory B subunit (Lodish et al, 1995). Activation of calcineurin is mediated by binding of Ca2+ and calmodulin to the regulatory and catalytic subunits, respectively. Calmodulin is an essential subunit of many plasma membrane Ca2+ ATPases. A rise in Ca2+ induces the binding of Ca2+ ions to calmodulin, which triggers an allosteric activation

of the Ca2+ ATPase as result the export of Ca2+ ions from the cell accelerates and the original Ca2+ is restored (Kang, 2001).

Doxorubicin can directly affect the expression level of important component of sarcomeric reticulum calcium release or uptake channels, for example, ryanodine receptor and SERCA2, leading to an impaired calcium handling and subsequent impaired cardiac contraction. It has been reported that DOX modifies the thiol group (–SH) of RYR2. This modification enhances the probability of RYR2 channel to adopt its open state, making cytosol overloaded with calcium ions. Additionally, DOX could increase the activity of voltage-sensitive L-type calcium channel on cardiac cell membrane as well as inhibiting the Na^{+}/Ca^{2+} exchanger (NCX) on sarcolemmal membrane, resulting in calcium overload (Figure 1.13).

When cytosolic calcium ions were excessive, the relaxed state after contraction would be undermined, and thus the contraction-relaxation cycle of cardiomyocytes is interrupted. DOX's major metabolite doxorubicinol was shown to have more profound effect on contraction-relaxation cycle as compared to DOX. Doxorubicinol could inhibit RYR2, Na^{+}/K^{+} pump on the cell membrane, and proton pump on mitochondria, resulting in the impairment of relaxation.

Treatment with doxorubicin will increase oxidative stress and disrupts calcium equilibrium among the cell (Zhang et al., 2009). ROS raises calcium levels by promoting its release from the sarcoplasmic reticulum. This successively creates a vicious circle where elevated Ca2+ levels then increase ROS production through Ca2+-sensitive ROS-producing enzymes (Zhang et al., 2009). Since the mitochondria are located in close proximity to the Ca2+-release site, they are exposed to massive quantities of Ca2+. The overwhelming levels of ROS, in conjunction with elevated levels of Ca2+ beyond the threshold, trigger the opening of the mitochondrial permeability transition pore (mPTP). This causes a loss in mitochondrial membrane potential and ultimately the discharge of cytochrome c (Zhang et al., 2009). Cytochrome c, situated within the inner mitochondrial membrane, (Childs et

al., 2002; Chen et al., 2007) forms a part of the intrinsic apoptotic pathway. As a result this vicious process of calcium mishandling in the cells leads to cardiomyocytes cell death.

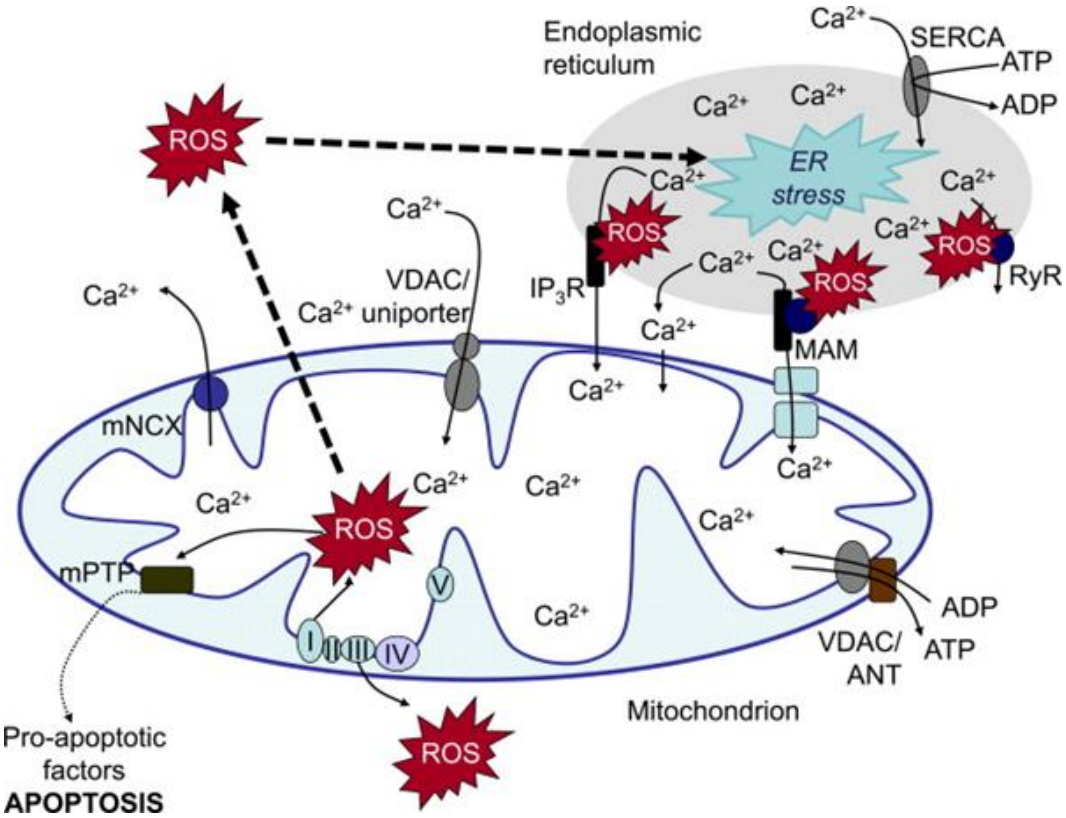

Figure 1.13: The crosstalk between calcium and ROS in mitochondria and the endoplasmic reticulum. SERCA – sarco/endoplasmic reticulum Ca2+ ATPase; RyR – ryanodine receptors; IP3R – IP3 receptor; VDAC – voltage-dependent anion channel; ANT – adenine-nucleotide transporter; mPTP – mitochondrial permeability transition pore; mNCX – mitochondrial sodium/calcium exchanger (Gorlach et al, 2015).

1.8.5 Lipid Peroxidation

DOX-induced generation of free radicals is likely to lead to lipid peroxidation of the cell membrane. When free radicals are produced close to cell membranes, OH^- radicals attack the fatty acids within the membrane, generating a carbon-cantered free radical (Horenstein et al., 2000). Carbon-cantered free radicals then react with oxygen to form peroxyl radicals which in turn form lipid hydro peroxides that increase membrane permeability. Lipid hydro peroxides can also form toxic by-products such as malondialdehyde (MDA) which can damage membrane proteins and render membrane-bound enzymes inactive (Horenstein et al., 2000). MDA is a mutagen in human and bacterial cells and carcinogenic in rats and causes large insertions and deletions of DNA at GC-rich regions (Niedernhofer et al., 2003) Studies assessing lipid peroxidation have been carried out under non-physiological conditions and at elevated concentrations of DOX, conditions which alone will promote oxidative stress and contribute towards cardiotoxicity (Gewirtz, 1999).

Glutathione (GSH) reduces harmful peroxides into less harmful alcohols in the presence of glutathione peroxidase-1 (GSH-Px1) and in doing so becomes oxidized to glutathione disulphide (GSSG). GSSG is then recycled back into GSH in the presence of glutathione reductase and NADPH (Olson et al., 1981). GSH is abundant in the cytosol, nucleus and mitochondria, highlighting the importance of this antioxidant within a cell (Valko et al., 2007). GSH protects against oxidative stress by scavenging hydroxyl radicals and detoxifying hydrogen and lipid peroxides (Masella et al., 2005). Unfortunately, treatment with DOX can deplete endogenous GSH and inhibit GSH-Px1 function which then reduces the ability to clear out harmful peroxides and leads to cell dysfunction (Mukherjee et al., 2003; Siveski-Iliskovic et al., 1994).

1.9 Doxorubicin regulated gene expression in heart failure progression

Mitochondrial Dysfunction

Mitochondrial morphology is important for maintenance of mitochondrial network and cellular physiology. Mitochondria are the primary targets of Dox resulting in mitochondrial dysfunction, oxidative stress and activating intracellular signalling pathways for apoptosis. The mitochondrial fusion and fission process is important for maintaining functional mitochondria. When cells undergo through a stress environment, the fusion process causes mitochondrial elongation and the fission process cause mitochondrial fragmentation. These events lead towards apoptosis at the end stage. Doxorubicin disrupts the mitochondrial fusion and fission process by altering the expression of genes mitofusins 1 and 2 (mfn1, mfn2) and optic atrophy protein 1 (OPA1) which are key regulatory genes involved in mitochondrial fusion and fission. Mitochondrial fission and fusion are accomplished by four GTPases in the dynamin family: (Mfn1) and (Mfn2) for outer mitochondrial membrane fusion, OPA1 for inner mitochondrial membrane fusion, and dynamin-related protein 1 (Drp1) for fission (Papanicolaou et al., 2012). Excessive or unopposed fission could lead to mitochondrial fragmentation, mitophagy, decreased anti-oxidative capacity and increased production of reactive oxygen species (ROS) and ultimately the cell death. OPA 1 and Mfn2 are down regulated in ischemic heart failure models, with OPA 1 mainly involved in mitochondrial cristae remodelling leading to increase fragmented mitochondria and greatly reduced oxygen consumption and electrochemical potential. Mfn2 down regulation greatly impairs the metabolic parameters of mitochondria along with the development of left ventricular hypertrophy observed in mouse models (Chiong et al, 2014; Tang et al, 2017).

Mitochondrial uncoupling protein 2 (UCP2) is the most popular protein in its family of mitochondrial anion carrier proteins. Mitochondrial uncoupling proteins are located in the mitochondrial inner membrane which can promote the proton leak across the mitochondrial inner membrane. It is the essential regulator of mitochondrial membrane potential, that disperse the

mitochondria proton gradient by translocating H+ across the inner membrane, following with respiratory activity, ROS and ATP generation (Yu et al, 2000). Many studies demonstrated that UCP2 has protective effect on myocardial damage, and down-regulated UCP2 is associated with failing heart (Chen et al, 2014). It has been well established that increased ROS production and a marked reduction in expression of anti-oxidant enzymes are associated with the cardiotoxicity of Dox. UCP 2 knockout studies show that down regulation of the gene causes changes in morphology, mitochondrial membrane potential loss, mitochondrial Ca2+ overload, the opening of mitochondrial permeability transition pore, and subsequent increased ROS generation as well as ATP reduction also apoptosis-associated proteins (cytochrome C and caspase-3) were decreased (Liu et al, 2014; Wang et al, 2018).

Arrythmia

Malignant arrhythmias account for a significant portion of heart failure related deaths (Sadredini et al, 2016). The heart beats with remarkable fidelity and resilience but however under certain circumstances the heart rhythm can fail. This phenomenon is referred as cardiac arrhythmia. Cardiac arrhythmia arises in three categories such as automaticity, triggered activity and re-entry. Automaticity is when there is acceleration in the spontaneous firing rate of the myocytes generated from the sinoatrial node or elsewhere. The automaticity of ventricular myocytes is at normal levels but however they are elevated in response to a cardiac disease (Mersirca et al, 2015). Irregular activation patterns arise which results in wave fronts originating from ventricular loci collide with the wave fronts from sinoatrial node disturbing the normal rhythm of the heart (Zhang et al, 2015).

The *SCN5A* gene is located in chromosome 3p21 with 28 exons and is a member of the human voltage-gated sodium channel gene family and encodes alpha subunit of the main cardiac sodium channel Na v 1.5. Na v 1.5 is known to be responsible for maintaining the normal function of inward sodium current. This current is the main component in fast depolarization

phase after which the excitation–contraction coupling cascade along with proper conduction of the electrical impulse is subsequently initiated within the heart.

Doxorubicin induced free radical formation in mitochondria and sarcoplasmic reticulum alters the membrane potential of the sodium gated ion channels and supresses the expression of the gene. Aberrant sodium channels resulting from lowly expression of *SCN5A* would potentially cause disorganization of the cardiac electrophysiological system, produce various arrhythmias and result in structural heart diseases. Inward and outward transmembrane currents are in dynamic balance physiologically, while variants in *SCN5A* could induce two states in the sodium channel: “gain-of-function state” or “loss-of-function state” (Zhang et al, 2018).

Within the subunits of the Na v 1.5 channel there are major 4 domains DI-DIV (Zhao et al, 2015). In long QT syndrome this gene becomes mutated and leads to gain of function in the intracellular domain between DIII-DIV. As a result prolongation of action potentials occur which sets up a substrate for arrhythmias (Musa et al, 2015). In ventricular fibrillation, SCN5A has loss of function that reduces the sodium current flow, shortens the action potential duration and decelerates the conduction velocity. This creates a substrate for re-entrant arrhythmias (Saffitz and Corradi, 2016).

Cardiac Remodelling

Cardiac remodelling is defined as a group of molecular, cellular and interstitial changes that manifest clinically in changes in size, mass, geometry and function of the heart after injury. Cardiac remodelling encompasses the changes at the cellular and gene expression level that occur upon after the injury. Janice Pfeffer was the first researcher to use the term remodelling in the current context, to describe the progressive increase of the left ventricular cavity in experimental model of myocardial infarction rat models. There are two types of cardiac remodelling which were recognized - physiological (adaptive) remodelling and pathological remodelling (Azevedo et al, 2016). Cardiomyocyte hypertrophy, a major consequence of pressure or volume overload, plays a central role in the progression of heart failure and lethal

cardiac arrhythmias. Cardiomyocytes become enlarged to increase muscle mass to reduce wall stress (Watkins et al, 2011).
Intermediate effect of DOX can take place from weeks to months which can lead to remodelling of the heart. Myh7 gene encodes beta (β)-myosin heavy chain (β-MHC). In cardiac muscle cells β-MHC forms part of a large protein known as type II myosin and it is responsible for the interaction with actin protein for cell movement and shape. During cardiotoxicity the gene disruption causes up-regulation of β-MHC with corresponding downregulation of α-MHC. This happens through p38 MAPK, extracellular signal regulated kinase (ERK) and c-Jun NH2-terminal kinase (JNK) signalling pathways. Cardiac remodelling could lead to the development of hypertrophy in the heart (Zhang et al, 2018).

Heart Failure

There are several contributing factors towards heart failure which eventually leads to cardiac death. Doxorubicin is a potent producer of ROS during oxidative stress which in turn affects the calcium handling in the mitochondria. Calcium cycling is crucial for both contraction and relaxation in cardiomyocytes. Mitochondrial calcium overload has also been linked to increased ROS release and reduced ATP production in heart failure. Mitochondrial calcium is mainly involved in cardiac contraction and electron transport chain to maintain cellular energy homeostasis. In heart failure, this process is disrupted, and disturbed mitochondrial Ca 2+ uptake culminates in NADPH oxidation and ROS generation and accumulation. Both defective Ca 2+ and Na + handling was proposed to initiate a vicious cycle leading to changes in NAD(P)H/NAD(P) + redox state and oxidative stress, which potentially affects excitation contraction coupling (ECC), cardiac dysfunction and heart failure (Kiyuna et al, 2018).
The process of excitation contraction coupling (ECC) in the ventricular myocyte begins with the entry of Ca2+ via the L-type Ca2+ current (ICa) (Bers, 2002). This relatively small Ca2+ influx is amplified by a larger Ca2+ release from the sarcoplasmic reticulum (SR). The resulting increase in

intracellular (cytoplasmic) Ca2+ concentration results in conformational changes in the myofilament proteins, which ultimately leads to cross bridge cycling and myocyte contraction. Cardiac sarcoplasmic reticulum Ca 2+ -ATPase 2a (Serca2a) is a fundamental protein involved in the process of removing Ca 2+ into the sarcoplasmic reticulum during diastole. SERCA2a transports the Ca2+ released during ECC back into the SR lumen against the electrochemical [Ca2+] gradient using chemical energy from ATP. However, in heart failure there is a reduction of Serca2a protein level and function. Hasenfuss and colleagues (1994) investigated the relationship between the SERCA2a levels in failing human myocardium. The finding showed that reduced SR Ca2+-ATPase protein levels in failing myocardium is consistent with measurements showing that expression of SR Ca2+-ATPase is reduced at the level of the mRNA in failing compared with non-failing human myocardium (Hasenfuss et al, 1994).

MS1 is a myofibrillar protein involved in the regulation of gene expression in both cardiac and skeletal muscle. It is also known as striated muscle activator of Rho Signalling and Serum Response Factor dependent transcription (STARS) (Arai et al, 2002) or Actin-binding Rho-activating protein (ABRA) (Troidl et al, 2009). It was initially discovered by Mhahadeva and colleagues where they identified an array of genes that were differentially expressed; acutely up-regulated post-aortic banding in a pressure-overload rat model for left ventricular hypertrophy (LVH) (Mahadeva et al, 1998). One of these differentially expressed acutely induced cDNA fragments were subsequently characterised and designated *ms1* (Mahadeva et al, 2002).

Apoptosis

The intrinsic pathway firmly controlled by the Bcl-2 protein family including anti- apoptosis Bcl-2, Bcl-xL, pro- apoptosis Bax, Bak. The counter apoptotic controls apoptosis by restraining the pro- apoptotic factors, for example, Bax, cytochrome c discharge, caspase-9 and the executioner caspase-3 that prompt apoptosis (Radogna et al., 2007; Shamas et al., 2013). In this way, the proportions between the anti and pro- apoptotic Bcl-2 family characterizes whether apoptosis would happen or not. Dong et al., (2014) proposed that In H9C2 cells DOX-intervened a lessening in the expression of Bcl-2 and Bcl-xL actuating PARP and caspase-3 resulting in cardiomyocytes apoptosis. Dox induced oxidative stress and apoptosis shows a down regulation of Bcl-2 and an up regulation of Bax, cleaved caspase 3 and cytochrome c (Zhang et al, 2018).

1.10 Aims

The overall aim of this thesis was to elucidate the protective properties of melatonin against drug - induced cardiac stress and explore its mechanisms of action *in vitro*.

Specific experimental objectives

I. To examine the beneficial effects of melatonin on the metabolic phenotype in cardiac cells during stress.

II. To deduce the effect of melatonin in the attenuation of drug induced apoptosis in cardiac cells *in vitro*.

III. To examine expression of genes, part of key cellular pathways to provide insight into mechanism of DOX-induced cardiotoxicity and protection by melatonin in cardiac cells *in vitro*.

Chapter 2.

Methods and Materials

2.1 H9c2 Cell line

The rat embryonic ventricular cardiomyoblast cell line, H9c2, has been extensively used as a cell model system in cardiac research, in particular stress-related pathways (e.g. Fothergill and Chong, 2014; Pisarenko et al., 2015; Wang et al., 2015; Watkins et al., 2014). Recently, H9c2 cells have been utilised in cardiac metabolism analysis using the Seahorse machine (e.g. Cheung et al., 2015; Porter et al., 2014; Scurtu et al., 2015; Yang et al., 2015). H9c2 cells have been demonstrated to reflect primary rat ventricular cardiomyocytes in diverse pathological conditions including hypertrophy, hypoxia-reoxygenation, IR and oxidative stress (e.g. Watkins et al., 2011; Kuznetsov et al., 2015). Collectively, this makes the H9c2 cells an ideal system to use in this project.

H9c2 cells (16-19), were cultured as monolayers in Dulbecco's modified Eagle's medium supplemented with fetal calf serum (10%) and penicillin (1%) under an atmosphere of 5% CO2 at 37°C incubator. The medium was replenished every 2 days. Once the cells reach 70% of confluence, they were washed with 0.5% of trypsin EDTA solution for cell detachment and centrifuged at 20^{o} C, 1500g for 5 minutes. H9c2 cells were then counted, seeded into appropriate plates and/or flasks and used in subsequent experiments.

2.2 Cell Counting

After trypsinisation and centrifugation (T75 flask), the cells were resuspended in 5ml of media and treated with 0.5% Trypan Blue.The number of cells were estimated using a haemocytometer (Abcam, 2016).

2.3 Seahorse XF Extracellular Analyser

The XF Analyser (Seahorse Bioscience) is a powerful tool used to measure and interrogate the major energy-producing pathways of cells - mitochondrial respiration and glycolysis. Two key measurements are Oxygen Consumption Rate (OCR) which measures mitochondrial respiration of cells and the Extracellular Acidification Rate (ECAR) which measures the glycolytic activity of cells. These measurements allows the determination of the mitochondrial function and dysfunction in living cells in real time.

The Seahorse XF Cell Energy Phenotype Test is the only single assay that can simultaneously report baseline and maximal mitochondrial respiration and glycolytic activity in live cells. The Seahorse XF Cell Energy Phenotype Test is a reagent kit and analysis method that allows you to rapidly determine the energy Phenotype of the cells, plot it on an energy map, and allows to easily compare, metabolic phenotypes across cell types and treatment conditions (Figure 2.1). The response to an induced energy demand is their metabolic potential, it is the measure of cells' ability to meet an energy demand via respiration and glycolysis. It is measured by the percentage increase of stressed OCR over baseline OCR, and stressed ECAR over baseline ECAR.

Metabolic potential equations for generating phenotype chart:

$$\text{Stressed OCR (\%)} = \frac{\text{Stressed OCR}}{\text{Baseline OCR}} \text{ x } 100$$

$$\text{Stressed ECAR (\%)} = \frac{\text{Stressed ECAR}}{\text{Baseline ECAR}} \text{ x } 100$$

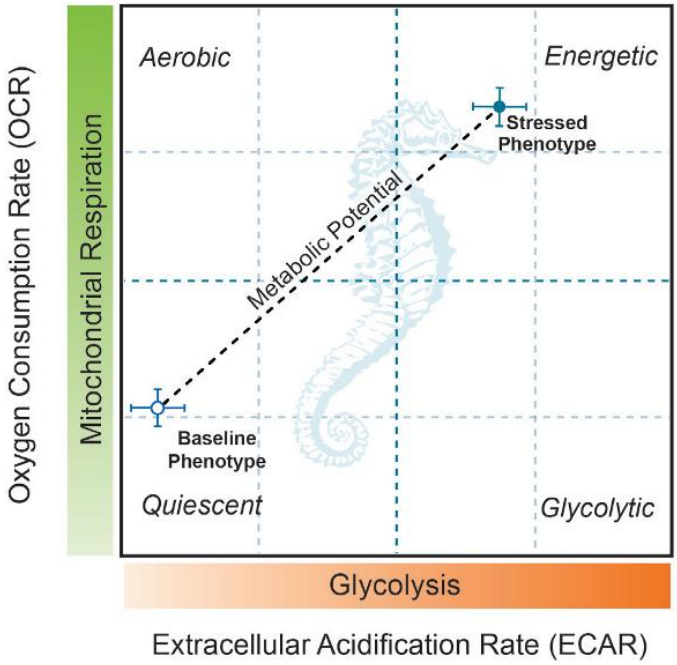

Figure 2.1: The relative utilization of the two energy pathways of a cell population is determined under both baseline (Baseline Phenotype) and stressed (Stressed Phenotype) conditions.

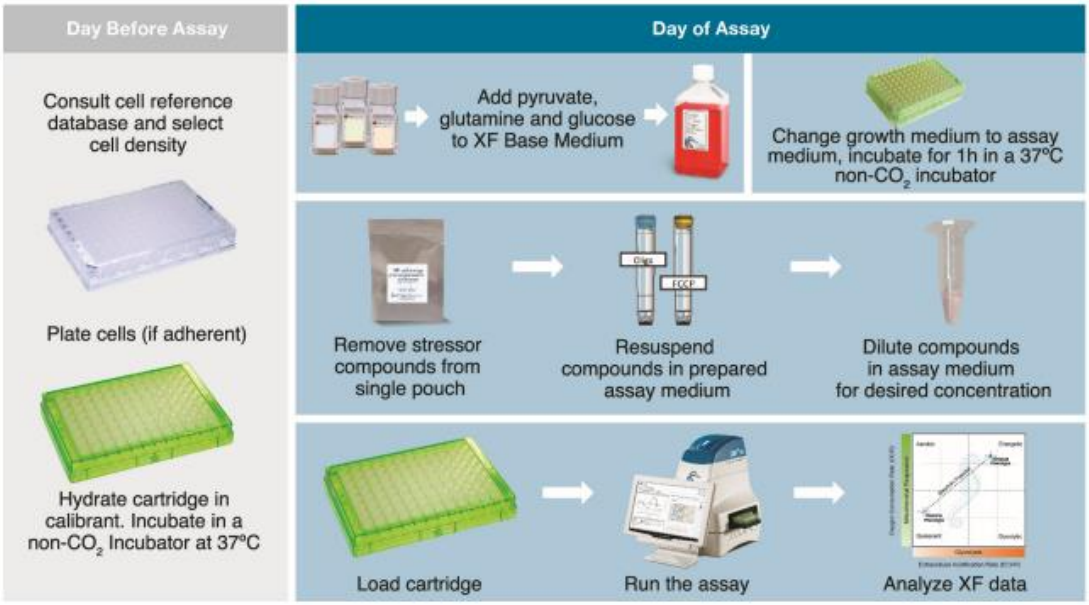

Figure 2.2: Represents the Phenotype Assay workflow in Seahorse (Seahorse Agilent, 2017).

Unbuffered media composition

Seahorse XF unbuffered media consisted of Dulbecco's Modified Eagle's Medium (CAT# 103575-100), 1mM of Pyruvate (0.5 ml; 100mM stock), 4mM Glutamine (1 ml; 200mM stock) and 25mM Glucose (1.25 ml; 1M stock). The pH was adjusted to 7.4 using 5M NaOH and 5M HCl, filter sterilised through a 0.2µM filter and stored at 4°C until required.

Experimental treatment conditions

The drugs used in this experiment were melatonin (CAT#M5250) and doxorubicin (CAT# D1515)**,** purchased from Sigma –Aldrich. Four experimental treatment conditions were used for this assay for over 24hrs.

Group A: Untreated with no drugs (control) for 24 hrs

Group B: Doxorubicin (0.1µM) for 24hrs

Group C: Melatonin + Doxorubicin, pre-incubation with melatonin (1µM) for 2hrs, thereafter addition of doxorubicin (0.1µM) for 24hrs.

Group D: Melatonin (1µM) for 24hr

2.3.1 Two-step seeding process for the Seahorse assay

H9c2 cells were seeded in a two-step seeding process in XF24 cell culture plates (CAT# 100777-004), to ensure a consistent and even monolayer. Cells were resuspended to obtain a final seeding density in 100µl of growth media per well. Background correction wells were left unseeded (A1, B4, C3 and D6) and only 100µl media was placed into these cells (Figure 2.2). After 2 hours in a 37°C incubator, cells were adhered and a further 150µl media was added to each well (including background correction wells), bringing the total volume in each well to 250µl. The cells were incubated overnight for 24 hours in a 37°C humidified incubator with 5% (v/v) CO_2.

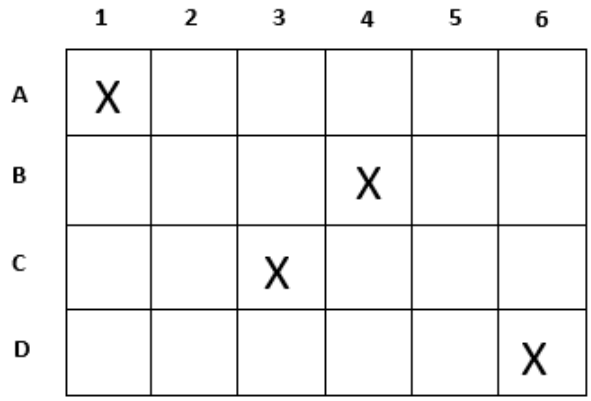

Figure 2.3: Layout of the Seahorse 24 well plate. The crossed out wells indicate blank wells (media only with no cells).

2.3.2 Preparation of the Sensor Cartridge for the XF24 assay

To hydrate the XF24 sensor cartridge, 1 ml of Seahorse Bioscience XF24 Calibrant pH 7.4 media was added to each well of the utility Seahorse Bioscience 24-well plate. The sensor cartridge was placed back on top of the utility plate and stored at 37°C without CO_2 overnight to prevent evaporation of the XF Calibrant solution.

Cell plate preparation with unbuffered media

The cell plate was removed from the incubator and checked for an even confluent monolayer. Seahorse XF media was warmed in a 37°C water bath and the cells were rinsed twice with 500µl of Seahorse XF media and replenished with 500µl of media. The cell plate was incubated at 37°C without CO_2 for 30 minutes.

Loading the XF Sensor cartridge with stressor compounds

The stressor compounds Oligomycin and carbonyl cyanide p-[trifluoromethoxy]-phenyl-hydrazone (FCCP) were obtained from the

Phenotype Kit (CAT# 103275-100). Oligomycin was suspended in 630µl of assay medium and FCCP was suspended in 720µl of assay medium to make the final concentration of each compound to 100µM. Thereafter 300µl of Oligomycin stock was combined with 600µl of FCCP (2µM) and 2100µl of assay medium to prepare a 10x stock solution. The port A of the hydrated sensor cartridge plate was added with 56 µl of the stock solution.

2.3.3 Calibrating the sensors and running a Seahorse experiment

The XF24 machine was switched ON and the instrument was stabilised to 37°C (2 hours) before the samples were measured. An experimental template was designed for each experiment using the assay wizard and the template loaded prior to running the experiment. Once the XF sensor cartridge had reached the required temperature, the assay was initiated and the plate was loaded into the machine in the correct orientation for calibration. At the end of the pre-programmed calibration procedure (30 minutes), the utility plate was replaced with the experimental cell plate and the assay was started. The mix/wait/measure cycle used for these experiments was 3 min /2 min /3 min. When the run was completed, the data was transferred onto Seahorse XF Cell Energy Phenotype Test Report Generator software analyser. The software utilises the data to calculate to produce values for OCR and ECAR at different time points with the addition of stressor compounds. The software generates line graph for both OCR and ECAR against time and used to generate bar charts along with the phenotype chart showing the metabolic pathway the cells have taken during mitochondrial respiration.

2.4 Flow - cytometric detection of apoptosis

The annexin V-fluorescein isothiocyanate (FITC)/propidium iodide (PI) apoptosis detection kit (ab14085, Abcam) was used to detect apoptosis. Annexin V is a protein, vascular anticoagulant α; bound to phospholipid bilayers in a calcium dependent manner (Andree et al, 1990).

Phospholipids of the cell membrane are asymmetrically distributed between the inner and outer leaflets of the membrane. Phosphatidylcholine and sphingomyelin are exposed on the external leaflet of the lipid bilayer, while phosphatidylserine is located on the inner surface. During apoptosis, this asymmetry is disrupted and phosphatidylserine becomes exposed on the outside surface of the plasma membrane. Propidium iodide is used together with annexin V-FITC, to differentiate dead cells from dying cells. Binding of annexin V correlated with other changes is consistent with apoptosis, including changes in nuclear morphology, DNA fragmentation and membrane leaflet symmetry. Only cells stained with both annexin V and propidium iodide demonstrated chromatin condensation, a late indicator of apoptosis.

2.4.1 Seeding process for flow - cytometry

H9c2 cells were seeded in six well culture plates, to ensure a consistent and even monolayer (near confluent). Cells were resuspended to obtain a final seeding density in 1ml of complete DMEM media per well. Thereafter, further 1ml of complete media only was added to each well, bringing the total volume in each well to 2ml. The cells were incubated overnight for 24 hours in a 37°C humidified incubator with 5% (v/v) CO_2. Thereafter the complete media was removed from each well and 2ml of 1% serum media was added into each well. The cells were incubated a further 24 hours in a 37°C humidified incubator with 5% (v/v) CO_2.

2.4.2 Preparation of the compensation controls

Compensation is required for a flow cytometry experiment because of the physics of fluorescence and these controls are used to differentiate the FITC and PI stain used in the assay. A fluorochrome is excited and emits a photon in a range of wavelengths in the emission spectrum. Some of those photons spill into a second detector, causing single stained samples to appear double positive for both stains. Therefore, an application of mathematical correction to the data addresses this spill over. This is known as compensation.

The cells were treated with 0.8µM doxorubicin to induce apoptosis of approximately 50%. The flow cytometry contains three compensation controls with induced apoptosis:

- Apoptosis induced unstained (contains no stain) control
- Apoptosis induced PI stain only
- Apoptosis induced Annexin V-FITC stain only

The remaining wells were used for experimental treatments. The cells were incubated overnight for 24 hours in a 37°C humidified incubator with 5% (v/v) CO_2.

2.4.3 Staining and processing of samples for apoptosis experiments

H9c2 cells were washed once with 1ml of phosphate- buffered saline and thereafter trypsinised with 0.5ml of Trypsin-EDTA. The cells were resuspended twice in trypsin and thereafter the cells were transferred into labelled Eppendorf tubes containing 1ml of complete media [Dulbecco's modified Eagle's medium supplemented with foetal calf serum (10%) and penicillin (1%)].

Cell count was performed to give the desired concentration of cells between 1-5x10^5/ml for each different treatment groups. Final volume of 700 µl of cell suspension (containing 1-5x10^5/ml) from each treatment group was

transferred into labelled Eppendorf tubes and centrifuged at 1000 rcf for 5 minutes at room temperature.

The supernatant was discarded and the cells were resuspended in 500 µl of 1× binding buffer containing (in mM) 10 HEPES/NaOH (pH 7.4), 140 NaCl, and 2.5 $CaCl_2$. Thereafter 5µl of Annexin V-FITC was combined with 5µl of propidium iodide and added into the relevant Eppendorf tubes. The cells were washed twice in binding buffer and transferred onto labelled LP4 tubes. The mixture was incubated for 5 min at room temperature in the dark and then analysed for the percentages of early (Annexin V-FITC positive and propidium iodide negative) and late (annexin V-FITC positive and propidium iodide positive) apoptotic cells using a Cyan ADP DakoCytomation flow cytometer.

2.4.4 Flow cytometry operation

The Summit 4.4 software and flow cytometry machine were switched ON and the instrument stabilized to 37°C at least 30 minutes before an experiment was run. The appropriate lasers were turned ON at 488nm and 635nm to warm up and stabilise to measure fluorescent emissions of FITC and PI. An experimental template was designed for the experiment using the Annexin-FITC/PI protocol assay and the template loaded prior to running the experiment. Once the assay was set up a sample clean calibration was carried out using cleaning solution, 5% bleach followed by deionized water and thereafter the assay was started. Once the run was completed the data is transferred onto Flowing software analyser to evaluate the results. The data is spread across four quadrants – live cells, early apoptosis, late apoptosis and necrosis. Cells undergoing through each different stage of apoptosis will be represented in the respective quadrants as percentages. The data then is calculated and plotted.

2.5. Alamar Blue cell viability assay

Alamar blue cell viability reagent is a resazurin based reagent. Resazurin is the active component in alarmar blue cell viability reagent is a nontoxic, cell-permeable compound that is blue in colour and non- flouroscent. Upon entering live cells, the cellular reducing environment reduces resazurin to resorufin a compound that is red and highly fluorescent (Figure 2.3). Viable cells continuously convert resazurin to resorufin increasing the overall fluorescence and colour of the media surrounding the cells. Also, the conversion of resazurin to resorufin results in a pronounced colour change, therefore cell viability can be detected using absorbance-based plate readers. Therefore this makes it an established and a reliable indicator of cell viability and death. Alamar Blue was used in this experiment to determine cell viability after 24 hr treatment with doxorubicin and melatonin.

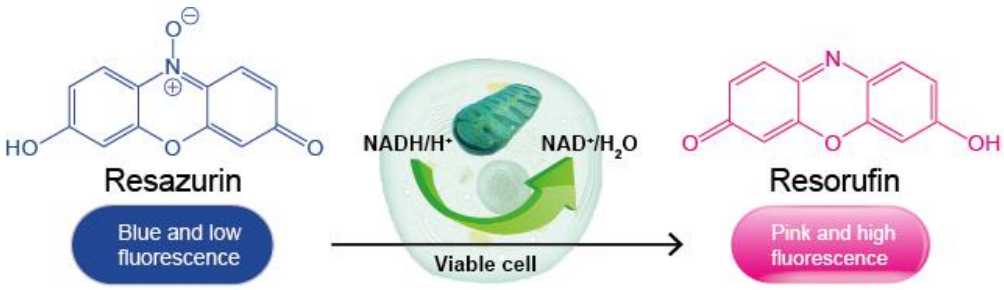

Figure 2.4: Chemical reaction taking place when resazurin is reduced to resorufin (APB Biosciences, 2018).

2.5.1 Seeding Process for Alamar stain experiments

The H9c2 cells were seeded on 96 well plate to ensure a consistent monolayer of cells were achieved. Each well contained 100µl of complete DMEM media. The cells were incubated in a 37°C humidified incubator with 5% (v/v) CO_2. The day prior to the treatment the media was removed from

each well and replaced with 100 µl of 1% serum media. The cells were incubated overnight for 24hrs in a 37°C humidified incubator with 5% (v/v) CO_2

2.5.2 Treatment Conditions for flow cytometry and Alamar staining experiments

The drugs used in this experiment were melatonin (CAT# M5250) and doxorubicin (CAT# D1515; Sigma). Four experimental treatment conditions were used for this assay for over 24hrs.

Group A: Untreated with no drugs (control) for 24 hrs

Group B: Doxorubicin (0.5µM) for 24hrs

Group C: Melatonin + Doxorubicin, pre-incubation with melatonin (1µM) for 4hrs, thereafter addition of doxorubicin (0.5µM) for 24hrs.

Group D: Melatonin (1µM) for 24hr

2.5.3 Determination of cell viability in Alamar staining experiments

After 24 hr incubation the complete media was removed from the cells and replaced with 100µl of the prepared Alamar blue reagent (10µl of Alamar Blue+ 90µl of complete media) into each of the treated wells. In addition, two blank wells (no cells) contained 100µl of Alamar blue reagent were used as negative controls. The plate was covered with foil to protect from direct light and incubated in 37°C humidified incubator with 5% (v/v) CO_2 for 2 hours, till colour change was detected. Thereafter the absorbance measurements of the media were recorded at 570nm and 600nm using SPECTROstar Nano plate reader, for the respective treatment groups.

The following equation formula was used to determine the percentage reduction of Alamar blue for each different treatment groups. Thereafter, the data value for % reduction of Alamar blue reagent for each different

treatment group was expressed as relative abundance from the total population of cells, with standard error of mean.

$$\% \text{ Reduction of Alamar blue reagent} = \frac{(E_{oxi600} \times A_{570}) - (E_{oxi570} \times A_{600})}{(E_{red570} \times C_{600}) - (E_{red600} \times C_{570})} \times 100$$

Eoxi570 = Molar extinction coefficient (E) of oxidized Alamar blue reagent at 570nm= 80586

Eoxi600 = Molar extinction coefficient (E) of oxidized Alamar blue reagent at 600nm= 117216

Ered570 = Molar extinction coefficient (E) of reduced Alamar blue reagent at 570nm= 155677

Ered600 = Molar extinction coefficient (E) of reduced Alamar blue reagent at 600nm= 14652

A570 = absorbance of treated wells at 570nm

A600 = absorbance of treated wells at 600nm

C570 = absorbance of negative control wells at 570nm

C600 = absorbance of negative control wells at 600nm

2.6. Gene expression analysis using reverse transcription-polymerase chain reaction (RT-PCR)

2.6.1 Seeding process for gene expression analysis

For each experiment, H9c2 cells were seeded at approximately 50% confluence in two six well plates and left overnight in a 37 C humidified incubator with 5% CO2. Thereafter, the cells were serum-starved (1% FCS) for an additional 24 hours.

2.6.2 Preparation of treatment conditions for gene expression analysis

Four experimental treatment conditions were used for these studies (Figure 2.4).

Group A: Untreated with no drugs (control) for 24 hrs

Group B: Doxorubicin (0.5µM) for 24hrs

Group C: Melatonin + Doxorubicin, pre-incubation with melatonin (1µM) for 4hrs, thereafter addition of doxorubicin (0.5µM) for 24hrs.

Group D: Melatonin (1µM) for 24hr

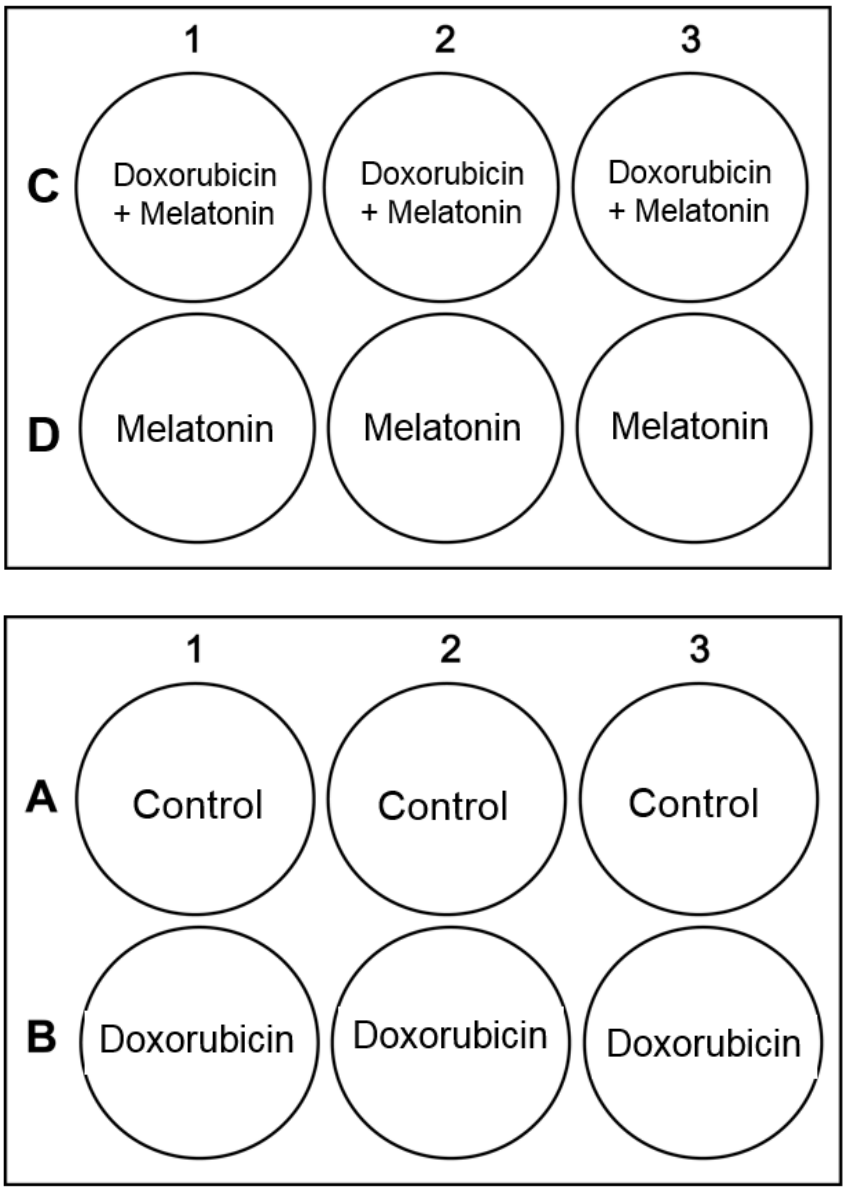

Figure 2.5: An overview of the plate map for the drug treatments in gene expression analysis.

2.6.3 Total RNA Extraction from H9c2 cells

Following each experiment, 500µl of Trizol (CAT# 15596018; Thermo Fisher Scientific) were added to the cells for 5 mins to lyse the cells and thereafter the cells were scraped off from the well surface and transferred into labelled Eppendorf tubes. Next, 100µl of chloroform was added to each tube and vortexed for 10 seconds. Samples were left for 3mins at room temperature and then centrifuged at 12000 rpm for 15 mins.

The aqueous phase (top layer) was carefully removed and transferred into a fresh set of labelled Eppendorf tubes and 250µl of isopropyl alcohol was added to each tube and samples were vortexed for few seconds. The samples were then placed in a -80°C freezer overnight. Thereafter, the samples were centrifuged at 12000 rpm for 30 mins. The supernatant was then completely removed and the RNA pellet was resuspended gently in 1ml of 70% ethanol followed by centrifugation at 7500 rpm for 5 mins. The supernatant was discarded and the RNA pellet was air dried for approximately 5-10 min. The RNA was then resuspended in 20 µL of DEPC-treated water and incubated in a hot block (55-60°C) for 10min to solubilise the RNA. The RNA yields from the samples were quantified by absorbance using the NanoDrop™ spectrophotometer from Thermo scientific (#ND-2000C). The concentration of RNA was recorded and used for dilution accordingly (Appendix A).

2.6.4 Reverse Transcription (RT) reactions

Complementary DNA (cDNA) was synthesised using the H Minus First Strand cDNA Synthesis Kit (CAT# K1631; Thermo Scientific), using the manufacturer's instructions. RNA was extracted from the cells using H Minus First Strand cDNA Synthesis Kit provided by Thermo Scientific, using the manufacturer's instructions. The volume of cDNA in each tube was diluted accordingly with RNAse free water with 11µl with the addition of 1µl oligo dT primer, bringing the final volume up to 12µl (Appendix A).

Next step involved the preparation of master mix for the RT reactions.

Master Mix	Total=8uL
10mM dNTP mix	2uL
5X Reaction buffer	4uL
Ribolock RNase Inhibitor	1uL
Revert Aid RT	1uL

RNA samples were denatured (65°C, 5 mins) and then kept on ice. Thereafter 8µl of Master Mix were added to each tube to bring up the final volume to 20µl. The mixtures will then be incubated in a PCR machine at 42°C for 1h followed by 70°C for 5mins. Finally, 80µL of RNase-free water were added to each RT reaction to make the working stock (final volume 100µL).

2.6.5 Semi-quantitative polymerase chain reaction (PCR)

The first step involved preparation of master mix (Table 1) and labelling13 PCR tubes on the ice, they were labelled from 1 to 13 and contained as follows:

Tube	Treatment	Volume of cDNA (µl)	Volume of PCR master mix (µl)
1	Untreated	2	18
2	Untreated	2	18
3	Untreated	2	18
4	Dox+Mel	2	18
5	Dox+Mel	2	18
6	Dox+Mel	2	18
7	Dox alone	2	18
8	Dox alone	2	18
9	Dox alone	2	18
10	Mel alone	2	18
11	Mel alone	2	18
12	Mel alone	2	18
13	-	-	18

Table 1. Reagents required to prepare Master Mix for 15 PCR tubes.

2x Taq mix	150uL
Water	90uL
Primer F+R	30uL

The PCR tubes were placed in the machine under the set parameters (Table 2). The numbers of cycles differ for each different gene.

Table 2. PCR parameter

Initial denaturation (95C) = 2mins (only for 1 cycle)
Denaturation (95C) = 15sec
Annealing (58C) = 15sec
Extension (72C) = 10sec
Cycle number between 22-35
Final extension (72C) = 10 mins-one cycle

2.6.6 Agarose Gel Electrophoresis

Agarose gels (1.5%) were prepared using 1.5g agarose (#10688973, Fisher Bioscience) with 100ml of 1xTBE (#10130740, Fisher Bioscience) buffer and 4µl of Gel-red (with 1-to-1 dilution with water) (#BT41003, Cambridge Bioscience). Molten agarose was poured into a casting tray and was left to set. Once set, the samples were loaded onto the gel with the 100bp molecular weight ladder (#N0467S, New England BioLabs). TBE buffer was poured on top of it until the Gel was covered with very narrow layer of TBE and the samples electrophoresed at 100V for 30 mins. Thereafter the gel documentation system was used to visualise the gel (iBright CL1500 Invitrogen).

2.6.7 Quantification of PCR using the Image J software

Image J software was used to quantify the PCR fragments of the gel image for the genes. The colour of the gel image was first inverted (PCR fragments are black in a white background) and then each PCR fragment was selected and analysed. The arbitrary numerical value for each PCR fragment was calculated and then the percentage of each peak on the plot was calculated. This gave an arbitrary value for each gene from separate experiments. The expression levels of each experimental sample (per gene) were divided by

expression levels of the internal control gene (Cyclophillin A) and these ratios plotted and analysed.

2.6.8 Primer design

Primer pairs for each gene were designed using the online software Primer3Plus (https://www.ncbi.nlm.nih.gov/tools/primer-blast/). Coding regions for primer design for each gene was preselected using ENSEMBL to identify exonic regions with large (>1500bp) introns. These cDNA sequences were then copy and pasted into the Primer3Plus software. The primers were then selected according to the following criteria; length between 19 to 21 base pairs, length of amplification product between 150 to 210bp, Tm of about 65°- 75°C, minimum of 40% and maximum of 60% GC content for temperature stability and sufficient strength of the bond between the primer and mRNA. The primers were synthesised by Fisher Bioscience. In order to determine the specificity of the primers, all sequences (Table 3) were compared with the GenBank, using the program Blast which is available at the National Centre for Biotechnology Information website.

Table 3. Primers sequences

Gene	Forward Primer	Reverse Primer	Size (bp)	Cycle
Cyclo A	5'-CCACCGTGTTCTTCGACATC-3'	5'-CTGGGAACCATTTGTGTTTG-3'	150	22
36B4	5'- CGACCTGGAAGTCCAACTAC-3'	5'- ATCTGCTGCATCTGCTTG-3'	119	22
Cav3	5'-GACCGAAGAGCACACAGATC-3'	5'-GACGGTGAAAGTGGTGTAGC-3'	196	28
Drp1	5'-CCCAAGGATATTGAGCTTC-3'	5'-CAGCTAGAGTTCTGCGCC-3'	166	28
Mfn1	5'-GTCACACAACCAACTGCTTC-3'	5'-GTCATCTCTCAAGAGGGCAC-3'	203	28
PPAR-ɣ	5'-GACATCCCGTTCACAAGAGC-3'	5'-CTTTATCCCCACAGACTCG-3'	199	28
Parp 1	5'-GTACTGGGGATGTCACTG-3'	5'-GAGGTGATCGAGACGGGAG-3'	192	30
Parp 2	5'-CCAAGGTCGGAAAGGCTC-3'	5'-CCAGAACAAGCCACCAAG-3'	205	30
Sirt 3	5´-GCACACCCAGTGGTATCC-3´	5´-GAAGTAGTGAGCGACATTG-3´	191	28
Bcl2	5'-GCCTTCTTTGAGTTCGGTG-3'	5'-GAAATCAAACAGAGGTCGC-3'	170	28
Bcl-xL	5'-GCATTGTGGCCTTCTTCTC-3'	5'-GGCTGCTGCATTGTTCCC-3'	180	28
Ucp2	5'-GCGCCAGATGAGCTTTGC-3'	5'-CCTGGAAGCGGACCTTTAC- 3'	176	28
Ms1	5'-GTGACAGCATAGACACAGAGGAC-3'	5'-CACTGCTGCCACCTGCCTT-3'	200	30
Serca2a	5'-CTTTCGTTTTGGCTTGGTTC-3'	5'-ATCCGCTGCACACTCTTTCT-3'	208	28
Scn5a	5'-GACCCATTTGCCGACCTCAC-3'	5'-GTAGTAGGGGTCAAGGGCG-3'	180	28
Myh7	5'-GAGGTCAAGGCCAAGAATG-3'	5'-CTGTATGGCGTCCGTCTCA-3'	180	28

2.7. Quantitative real-time PCR

2.7.1 Preparation of the PCR reaction

Quantitative real-time PCR was performed using PowerUp SYBR Green (CAT#A25742) purchased from Thermo Fisher Scientific. Multiple reactions were performed using the master mix. Typical 10µl reaction contained the following:

Component	Total=10uL
PowerUp SYBR green master mix	5uL
Forward and Reverse primer	1uL
cDNA (1µg)	1uL
Nuclease free water	3uL

The reaction mixture (10uL) was pipetted into each well of an Optical 96- well reaction plate (CAT#4346907). The plate was sealed and centrifuged briefly (1000rpm, 1 minute) to spin the contents down and to eliminate any air bubbles.

2.7.2 Quantitative real-time PCR

Polymerase chain reaction (PCR) was conducted on a 7500 Fast Real-Time PCR System (Applied Biosystems). Cyclophilin A and 36B4 were used as internal controls for standardisation.

Once the Optical 96- well reaction plate was placed in the instrument the following thermal cycling conditions were used for this amplification reaction.

Initial Holding Stage	50°C	2 minutes
Holding Stage	95°C	2 minutes
Denaturation Stage (40 cycles)	95°C	3 seconds
Annealing and Extension Stage	60°C	30 seconds

2.7.3 Data analysis and quantification of quantitative PCR

The threshold cycle (REF) values were obtained from the amplification curve using the comparative ΔΔCT method. This method allows the quantitative determination of fold induction of gene of interest between different samples using the following formula;

Fold induction = $2^{-\Delta\Delta CT}$

ΔCT = mean CT (gene of interest) - mean CT (reference gene)

ΔΔCT = ΔCT (unknown) - ΔCT (control)

The control sample, which is represented by the non-treated allows for corrections to be made for inter-assay variation. It is important to note that the above formula is based on the assumption that the efficient of the PCR reaction for both the reference internal control gene, and the gene of interest is identical with a doubling of product being achieved with every cycle

2.6. Statistical analysis

Data are presented as mean ± SEM. Group data were analysed using One - way ANOVA with multiple comparisons and post-hoc Tukey corrections. The analyses were performed using GraphPad Prism 7.0 software. *P* values of <0.05 were considered statistically significant.

Chapter 3.

Drug-induced oxidative stress and mitochondrial dysfunction

3.1 Introduction

Mitochondria are the primary organelle for physiological reactive oxygen species (ROS) production and is also the main target for damage caused by chronic sustained over production of ROS. Chronic pathological ROS production is extremely detrimental for cardiomyocytes (Ghao et al, 2012). This overload of free radicals includes hydroxyl radicals ($^{\cdot}OH$), superoxide ($O_2^{\cdot -}$), hydrogen peroxide (H_2O_2), nitric oxide (NO), and peroxynitrite (OONO-). These free radicals promote macromolecule damage such as DNA, lipids, proteins, and carbohydrates oxidation (Lee and Won, 2014; Lopez et al, 2017; Capetta et al, 2017). This production of ROS can act as intracellular signalling molecule for various destructive pathways which include apoptotic pathway. Once activated, it leads to release of apoptotic factors such as cytochrome c and apoptosis-inducing factor (AIF), ultimately leading to cardiac cell death (Niizuma et al, 2010). Hydrogen peroxide and Isoproterenol are potent inducers of ischemia and hypertrophy in cardiac cells. They trigger the production of ROS in mitochondria leading to mitochondrial metabolic dysfunction and eventually loss of function.

Hydrogen peroxide is a potent generator for reactive oxygen species. These ROS species are capable of generating cellular damage during myocardial ischemia and reperfusion. Hydrogen peroxide is the most stable and therefore, has the greatest potential to diffuse from its origin of production to cause tissue damage at distant sites. Several studies have examined the myocardial effects of hydrogen peroxide. It was observed that H_2O_2 can induce arrhythmias, reduce myocardial function, lipid peroxidation, enzyme activation and as well as altering intracellular calcium concentrations. Hydrogen peroxide can activate enzymes by oxidation in the downstream signalling pathway of PKC (Kumaran and Mainzen, 2010). The specific activation of PKC pathway mediates deleterious effects of myocardial ischemia and reperfusion injury. Within the narrow window of exposure to H_2O_2, the PKC dependence causes changes in the intracellular calcium ion concentrations and cell shortening of the ventricular myocytes (Nizuma et al, 2010).

Isoproterenol (ISO) is a manufactured catecholamine with the expansion of two methyl groups. It is structurally similar to adrenaline and mimics the sustained adrenergic receptor activation which represents an important hallmark of the pathogenesis of maladaptive cardiac hypertrophy (Lalitha et al, 2013). The activation of β-adrenergic signalling in turn induces many different pathological mechanisms which contribute to the hypertrophic phenotype including enhanced protein synthesis, proto-oncogene expression, elevated oxidative stress, stimulation of mitogen activated protein kinases and phosphotidyl inositol-3 kinases (Turrubiarte et al, 2015). A single high subcutaneous (SC) dose of ISO between 10 and 85 mg/kg in adult rats causes myocardial necrosis and fibrosis (Heather et al, 2009; Roy and Mainzen, 2013). Low doses of ISO (0.3 to 6 mg/kg) during the 1st, 2nd and 3rd weeks induce necrosis in areas of the myocardium (Ribeiro et al, 2009). In turn, moderate doses (35 mg/kg) administered SC for 3 days induced dilated cardiomyopathy. Chronic treatment (100 mg/kg) > 2 weeks in adult rats produces diastolic dysfunction and causes decrease of fatty acids and glucose in the myocardium (Turrubiarte et al, 2015).

To investigate the effects of oxidative stress induced by hydrogen peroxide and isoproterenol in H9c2 cells, the Seahorse XF Analyser (Seahorse Bioscience) is used. It is a powerful tool used to measure and interrogate the major energy-producing pathways of cells - mitochondrial respiration and glycolysis. Two key measurements are Oxygen Consumption Rate (OCR) which measures mitochondrial respiration of cells and the Extracellular Acidification Rate (ECAR) which measures the glycolytic activity of cells. These measurements allow the determination of the mitochondrial function and dysfunction in living cells in real time.

Aims

The studies outlined in this chapter will examine the effect of simulated oxidative stress induced by hydrogen peroxide and Isoproterenol on mitochondrial metabolism and dysfunction in H9c2 cells *in vitro*. The beneficial effect of melatonin will also be investigated.

3.2 Results

3.2.1 Seeding Density

Seeding densities of 6000, 12,000, 25,000 and 40,000 of H9c2 cells were experimented to determine the optimum seeding density for the growth of consistent monolayer of cells for the Seahorse experiments (Figure 3.1).

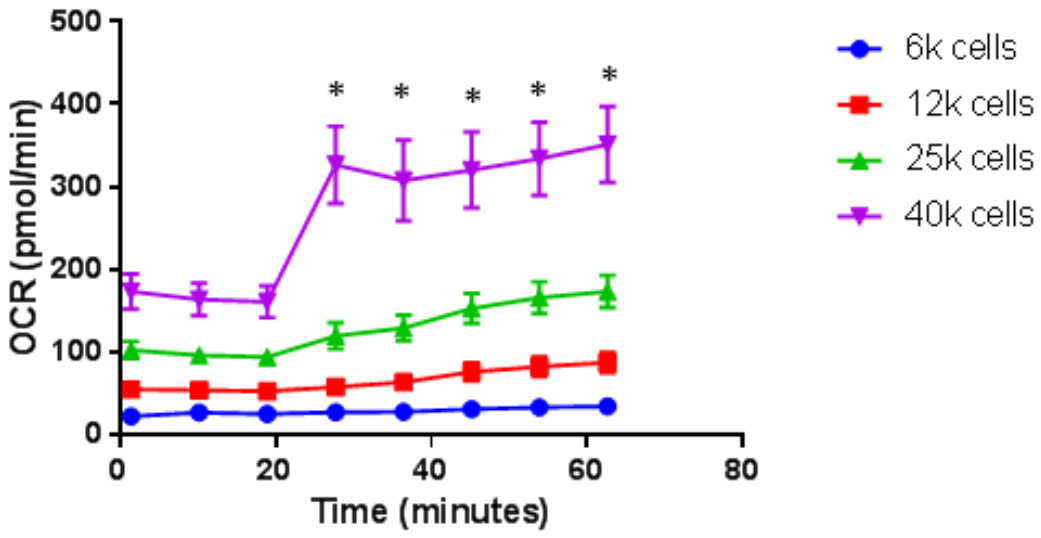

Figure 3.1**: OCR induction for different seeding density of H9c2 cells**. H9c2 cells were seeded at different densities of 6k, 12k, 25k and 40k per well in Seahorse Bioscience culture plates for 24 hrs. Initially the baseline measurements of Oxygen consumption rate (OCR) were made. Oligomycin/FCCP mix (1µM/2µM) was injected to determine the maximum oxygen consumption in these cells. The experiment was repeated and produced similar results. Data shown are mean± SEM, n=6 per group. One Way Anova: F (3, 28) = 41.87, *P<0.0001.

The results indicate a seeding density of approximately 40,000 cells where there is a good FCCP induction in the cells and the baseline OCR measurement lie within the range (100-200 pmol/min) (Seahorse Bioscience, 2016). At 6k and 12k, the cells have not reached a consistent monolayer, indicated by the low OCR values. At 25k the cells produced OCR induction at baseline of 100 pmol/min, however it was low compared to the OCR induction given by cells seeded at 40,000. At 40k the cells produced a good response towards FCCP and gave a consistent OCR induction.

3.2.2 FCCP Optimisation

The optimisation of FCCP was determined on H9c2 cells pre-treated with H_2O_2 (200µM) for 24hrs, using 0.1µM, 0.5µM, and 1µM (Figure 3.2).

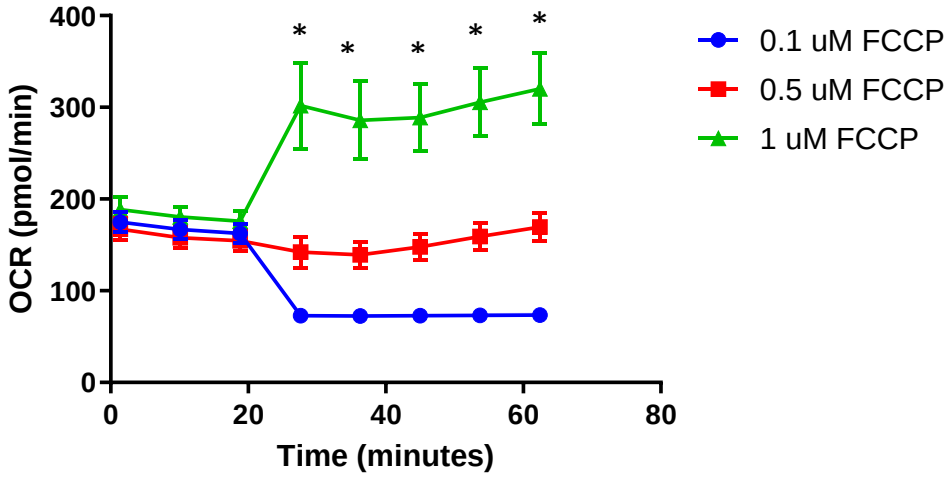

Figure 3.2: **FCCP dose response (optimisation) for H9c2 cells pre-treated with H_2O_2**. H9c2 cells were seeded at 40k and treated with H_2O_2 (200µM) for 24hrs. The initial OCR measurements were made. Then different concentrations of FCCP (0.1 µM, 0.5 µM and 1 µM) were injected to determine maximum OCR of the cells. The experiment was repeated and produced similar results. Data shown is mean± SEM, n=6 per group. One Way Anova: F (2, 21) = 21.12, *P<0.0001.

In the current study, the optimum FCCP concentration used on H9c2 cells was 1μM (Figure 3.2). FCCP at 1 μM provided consistent induction with the maximum OCR for these experiments (Figure 3.3).

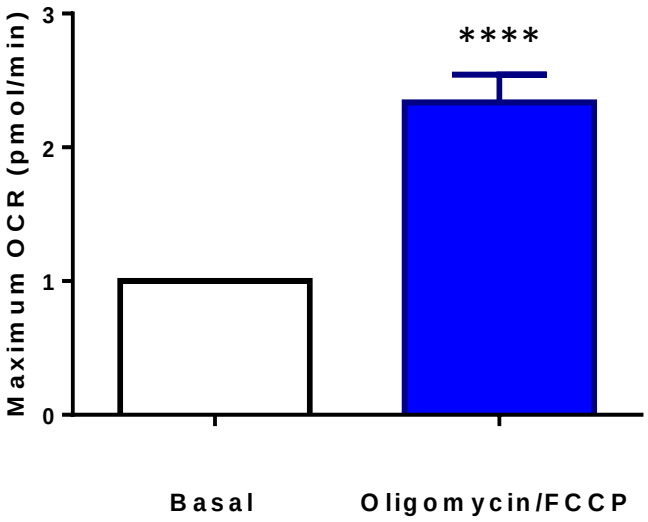

Figure 3.3: Maximum OCR in H9c2 cells induced by mitochondrial stressors (oligomycin and FCCP). The induction was 2.3±0.2 fold [n=12 separate experiments (6-7 wells per experiment), ****p<0.0001]. The experiment was repeated and produced similar results.

3.2.3 The effect of hydrogen peroxide on metabolic phenotype in H9c2 cells

The effect of melatonin alone on mitochondrial function was examined using the Seahorse assay and this showed no change in oxygen consumption rate (Figure 3.4).

Hydrogen peroxide (H_2O_2) is a stress inducer in H9c2 cardiomyocytes by generating oxidative stress and inducing cellular hypertrophy *in vitro* (Petrosillo et al, 2010).

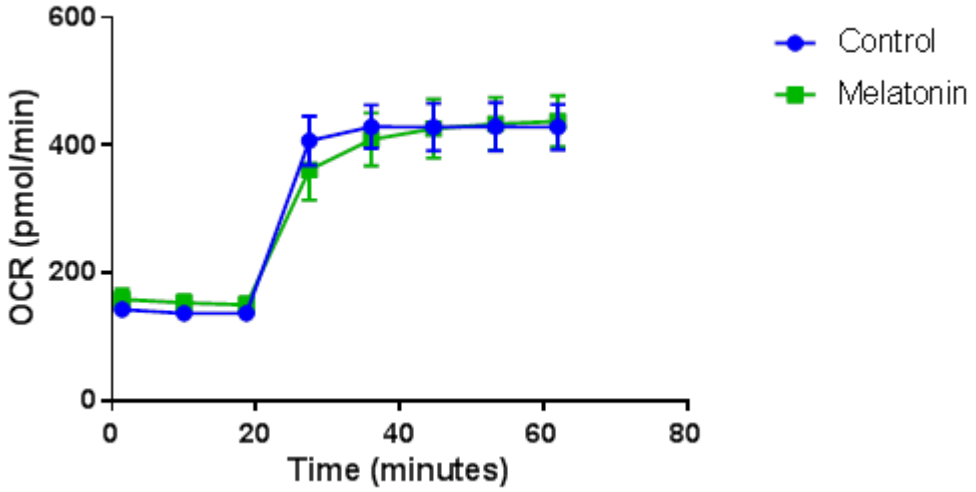

Figure 3.4**. Effect of melatonin alone on oxygen consumption rate (OCR).** Control (untreated) had no drugs. Melatonin (1µM) was used for 24hrs. Melatonin had no effect on OCR when compared with the control. The experiment was repeated 5 times and produced similar results. Data shown is mean± SEM, statistically no significant difference, n=4-6 wells per group.

(A)

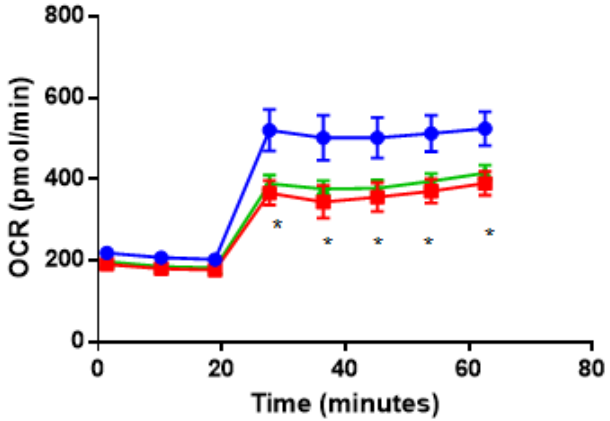

(B)

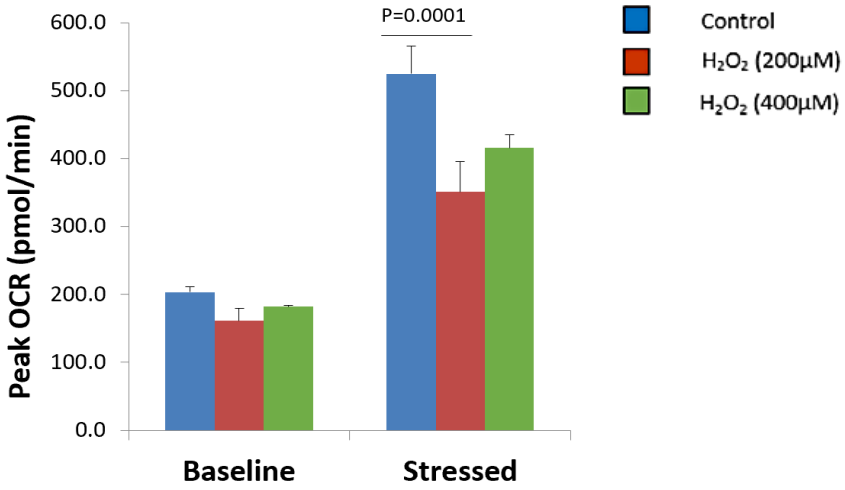

(C)

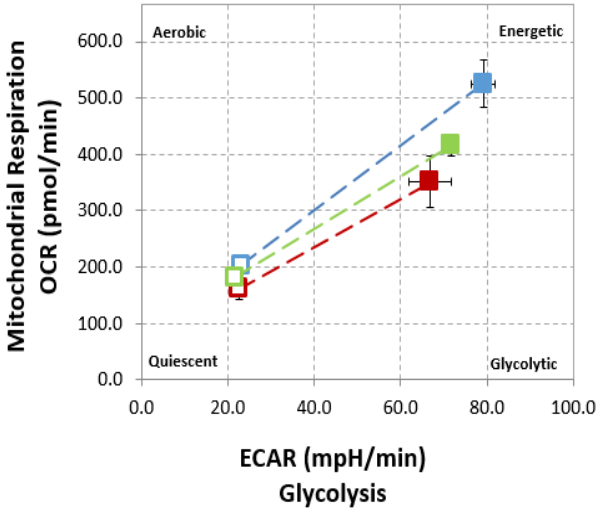

Figure 3.5: **Hydrogen peroxide decreases maximum OCR in H9c2 cells.**H9c2 cells were seeded and treated with H_2O_2 (200uM and 400uM) for 24hrs. The FCCP concentration of 1uM was injected to determine the maximum OCR. **(A)** OCR changes for 200uM and 400uM H_2O_2. **(B)** Peak OCR changes during baseline and stressed for 200uM and 400uM H_2O_2. **(C)** Cell energy phenotype of the cells under pre-treatment of H_2O_2 shifts towards energetic. The experiment was repeated and produced similar results. Data shown is mean± SEM, n=6 per group. One Way Anova: F (3, 12) = 331.1, *P< 0.0001.

Hydrogen peroxide treatment decreased maximum OCR by ~45% (Figure 3.5A & B) at both 200 and 400 µM. The phenotype chart indicates the metabolic phenotype of the cells. Hydrogen peroxide decreased the energetic of the cells and lowered glycolysis capacity (Figure 3.5C).

In order to test the beneficial effect of melatonin, H9c2 cells were pre-treated with melatonin and then treated with hydrogen peroxide (200 µM) for 24 hrs. Pre-treatment of H9c2 cells with melatonin blocked the decrease in maximum OCR induced by hydrogen peroxide (Figure 3.6).

(A)

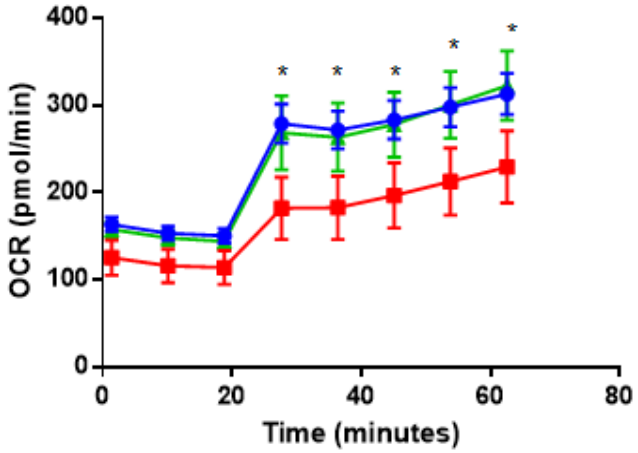

(B)

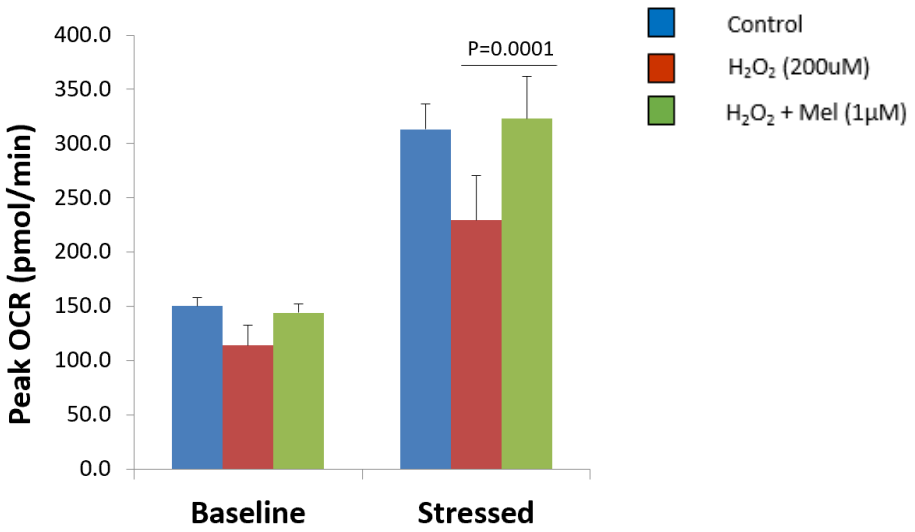

(C)

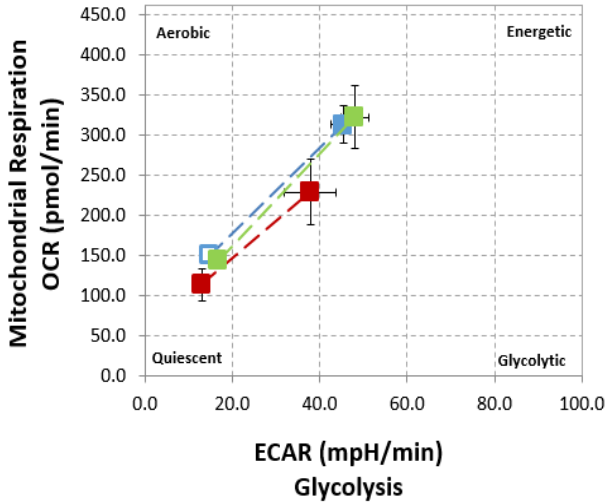

Figure 3.6**: Melatonin attenuated hydrogen peroxide reduction of maximum OCR in H9c2 cells.** The cells are pre-treated with 200µM of H_2O_2 with pre-incubation of melatonin (1µM), for 24hrs. **(A)** OCR changes with 200µM H_2O_2 and melatonin. **(B)** Peak OCR changes during baseline and stressed conditions. **(C)** Cell energetic changes for 200µm H_2O_2 and melatonin. The experiment was repeated and produced similar results. Data shown is mean± SEM, n=6 per group. One Way Anova: F (2, 12) = 26.29, *P<0.0001.

3.2.4 Isoproterenol decreased maximum oxygen consumption rate in H9c2 cells

Isoproterenol (ISO) treatment induces oxidative stress in H9c2 cells and initiate cellular hypertrophy. The current study examined the effect of ISO on mitochondrial function in H9c2 cells. At both 10 and 50 µM, ISO decreased ~40% in maximum OCR (Figure 3.7), with a decrease in cell energetics (Figure 3.8B). Interestingly, melatonin pre-treatment (1µM, 1 hr) blocked ISO reduction of peak OCR and reversed cell energetics (Figure 3.8)

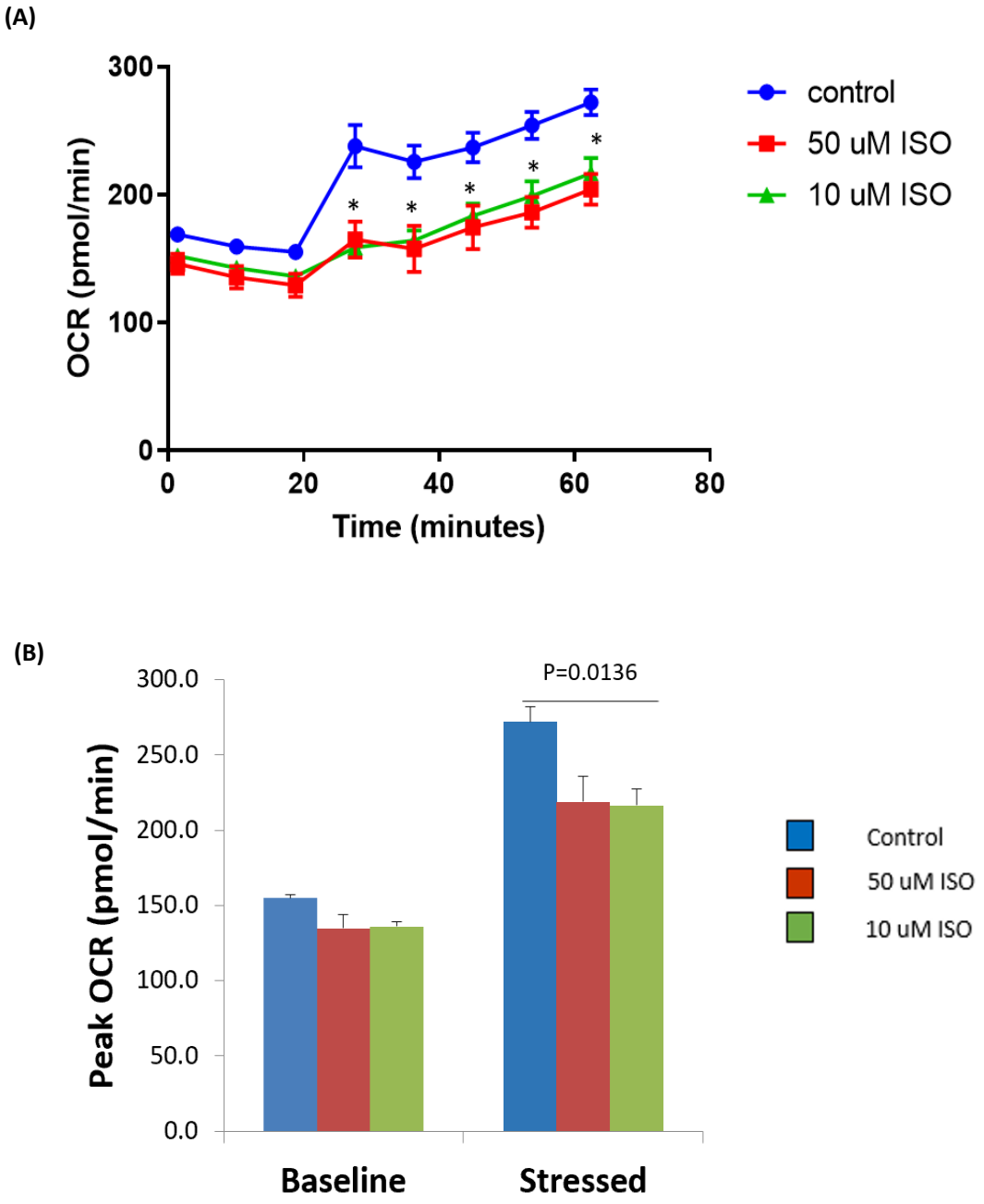

Figure 3.7**: Isoproterenol decreased maximum OCR in H9c2 cells.** The cells were treated with 10µM or 50µM of isoproterenol for 24hrs. (A) OCR changes for 10µM and 50µM of isoproterenol. (B) Peak OCR changes during baseline and stressed conditions. The experiment was repeated and produced similar results. Data shown is mean± SEM, n=6 per group. One Way Anova: F (2, 21) = 5.307, *P= 0.0136.

(A)

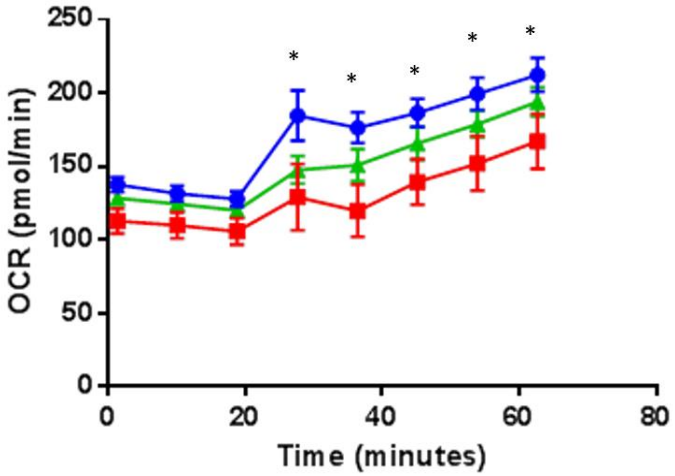

(B)

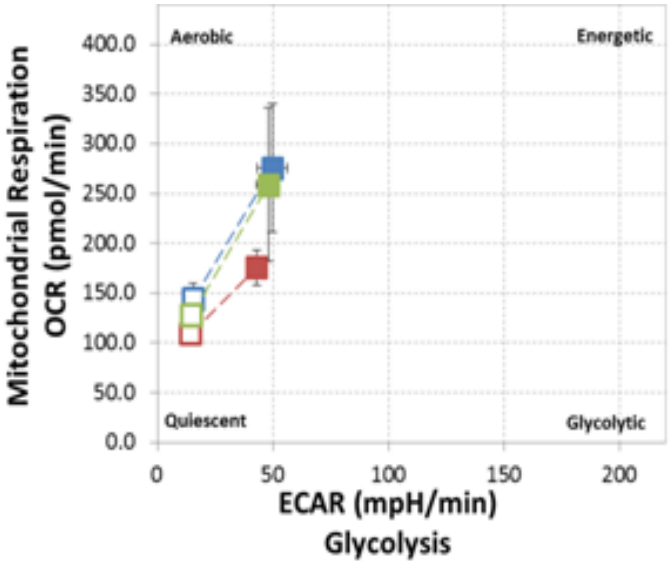

(C)

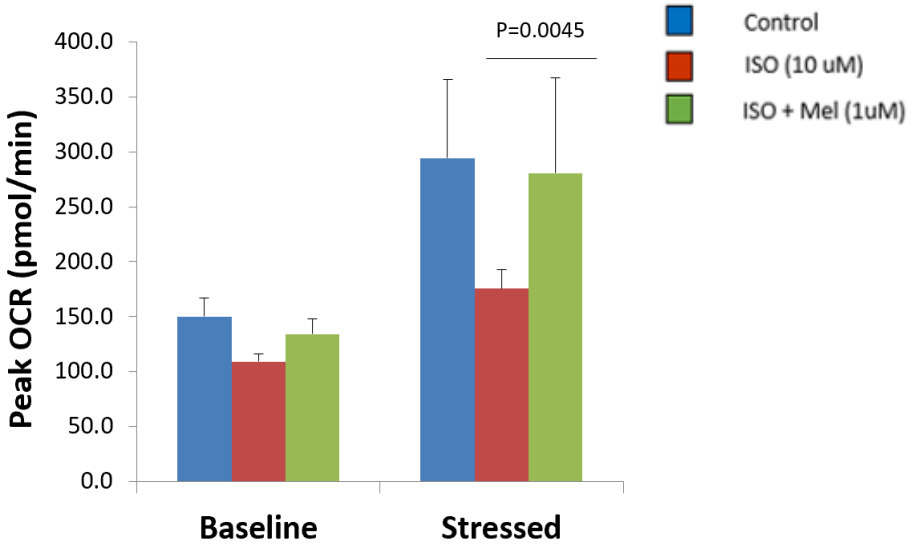

Figure 3.8: **Melatonin attenuates Isoproterenol reduction of maximum OCR in H9c2 cells.** The cells were treated with 10µM isoproterenol (ISO) with melatonin (1µM) pre-incubation for 24hrs. **(A)** OCR changes in cells treated with isoproterenol and melatonin. **(B)** Peak OCR changes during baseline and stressed conditions. **(C)** Phenotype chart shows the shift towards aerobic in the three groups. The experiment was repeated and produced similar results. Data shown is mean± SEM, n=6 per group. One Way Anova: F (2, 21) = 7.062, *P= 0.0045.

3.3 Discussion

Cardiac disease such as heart failure and cardiac arrhythmias are complex disorders with multifactorial aetiology that are largely unresolved, however one common trigger in cardiac disease states is chronic oxidative stress. In the current study, the effect of well-established triggers of cardiac phenotypes (hydrogen peroxide and isoproterenol) were used to test if these compounds can alter the metabolic profile in a model cell line and examine if melatonin can attenuate this alteration in cardiac function *in vitro*.

The main important findings of this study were:

1. Both hydrogen peroxide and isoproterenol, at a dose that causes cardiac dysfunction and hypertrophy *in vitro*, decreased the basal and peak OCR in cardiac cells.
2. A low pharmacological dose of melatonin, typically used in *in vitro* studies, attenuated or even blocked the decrease in OCR in stressed-induced cardiac cells.

In this study, H9c2 cells were under stress caused by hydrogen peroxide and isoproterenol. Both chemical agents are potent stress inducers in cardiomyocytes (Ojha, 2010) and mimic ischemic conditions in cells by inducing oxidative stress. In H9c2 cells oxidative stress affects mitochondria and functionality (Wu and Cederbaum, 2013; Shin et al, 2016; Dai et al, 2018).

Mitochondria are considered the main intracellular source of ROS production and paradoxically, the major target of a free radical attack. During normal physiological conditions, ROS are generated at very low levels, but can increase dramatically in pathophysiological conditions such as myocardial ischaemia/reperfusion (I/R) injury and inflammation (Paradies *et al*, 2010). These pathological changes can lead to a loss in the phospholipid cardiolipin, which in turn, is responsible for the loss of activity of the respiratory chain

complexes I, III and IV and mitochondrial dysfunction (Paradies *et al*, 1999; Lochner *et al*, 2015).

Melatonin has beneficial effects in a number of pathophysiological conditions associated with increased oxidative stress such as hypertension, myocardial hypertrophy and I/R. Melatonin can exert its cardio protective actions via its free radical scavenging activities as well as the induction of anti-oxidant enzymes (Hardeland, 2005; Cardinali *et al*, 2006). Interestingly, Petrosillo and co-workers (2003) demonstrated that, at pharmacological concentrations (50µM), melatonin effectively protects against I/R damage: it caused a reduction in lipid peroxidation and counteracted the reduction in State 3 respiration and the respiratory control ratio in rat heart mitochondria, isolated after exposure of the heart to I/R. This study showed that the protection by melatonin against mitochondrial dysfunction was associated with improvement in functional recovery during reperfusion (Petrosillo *et al*, 2003). One mechanism of action of melatonin in cardioprotection against I/R induced damage in cardiomyocytes is by inhibiting MPTP opening in the mitochondria (Petrosillo *et al*, 2009), which will stabilise membrane potential and inhibit cytochrome c leakage and apoptosis.

In the current study, treatment of H9c2 cells with H_2O_2 and ISO for 24 hrs mimicked the ischemic situation in H9c2 cells *in vitro* (Ohjia, 2010). During ischemia, cardiomyocytes lose their ability to respire efficiently due to the failing mitochondria. Treatment of cells with hydrogen peroxide for 24 hours stimulates large amounts of ROS production. Ultimately this uncouples mitochondrial function and the complexes within the ETC chain (I, III, IV) leading to reduced activity (Paradies *et al*, 1999). The ATP synthase becomes the target of the free radicals which results in decreased activity to carry out oxidative phosphorylation. The cells starve due to the mitochondria dysfunctionality to carry out aerobic respiration to meet the energy demands. The decrease in ATP could lead to cell death caused by apoptosis or necrosis.

The current Seahorse data demonstrated that treatment of H9c2 cells with either H_2O_2 (200µM) or ISO (10µM) resulted in lower OCR values due to the effect of free radicals on the mitochondria respiratory chain, which decreased the ability of the cells to respire efficiently (Figures 3.5 and 3.7). Of interest, melatonin pre-treatment blocked this decrease in OCR caused by oxidative stress.

At present, the mechanism of action of melatonin is unclear. Melatonin and its metabolites have free radical scavenging abilities and acts as a robust anti-oxidant for the cells (Favero et al, 2017). It is conceivable that this property of melatonin directly protected against ROS-induced damage to the mitochondria and the ETC function, thus improving OCR (Ahmad et al, 2016; Favero et al, 2017).

Chapter 4.

Cardio toxicity induced by diverse groups of drugs

4.1 Introduction

Cardiotoxicity is emerging as a critical issue drug intervention in many treatments in particular anti-cancer therapy. Over the decades, numerous studies sought to identify the intracellular targets and elucidating the molecular mechanisms involved in drug-induced cardiotoxicity (Minotti et al, 2004; Bassareo et al, 2016; Li et al, 2018). Majority of studies have contributed to the theory that it is in fact a multifactorial process that leads to cardiomyocyte death as the terminal downstream event (Kalyanaraman et al, 2002; Fukazawa et al, 2003; Minotti et al, 2004). Mitochondrial dysfunction has become an apparent hallmark of drug-induced cardiotoxicity (Torkarska et al, 2006).

Abnormalities in mitochondrial functions such as defects in the respiratory chain/oxidative phosphorylation (OXPHOS) system, decreased adenosine tri-phosphate (ATP) production, a switch in metabolic substrate utilisation, mitochondrial deoxyribonucleic acid (DNA) damage, modulation of mitochondrial sirtuin activity, and a vicious cycle of free radical formation have all been suggested as the primary causative factors in the pathogenesis of drug-induced cardiotoxicity (Verma et al, 2013). These defects act synergistically to create a bioenergetics crisis, which culminates in cardiomyocytes death. Melatonin is a potent antioxidant, and has been shown to influence mitochondrial homeostasis and function. Although accumulating studies support the mitochondrial protective role of melatonin, the exact mechanisms by which melatonin confers mitochondrial protection in the context of drug-induced cardiotoxicity remain to be elucidated. The accumulation of drugs can impose a direct threat on the mitochondria. They have a high affinity for cardiolipin, an integral component of the inner mitochondrial membrane. The binding of these drugs to cardiolipin does not allow for cardiolipin interaction with key respiratory complexes (Goormaghtighe, 1980). Thus, hindering the mitochondrial respiratory complex functions.

Drugs for chronic disorders such as cardiovascular diseases, diabetes, depression and anxiety and cancer, conveys severe adverse effects, in chronic use (Vigneri et al, 2009; Nguyen et al, 2012). This chapter focuses on evaluating some of the most commonly used drugs in diverse disorders, imposing cardiotoxicity. Doxorubicin, Statins, Rosiglitazone, Amitriptyline and Amiodarone are among the frequently used drugs to manage a variety of diseases which have been known to cause mitochondrial dysfunction in chronic use.

Doxorubicin (DOX) is an anthracycline commonly used in cancer treatment. The cardiotoxicity caused by DOX could be acute (hours to days) to intermediate (weeks and months) and late onset (>12 months) and even years after treatment has finished. However, its clinical use is greatly restricted by the development of cardiomyopathy and clinical congestive failure (Liu et al, 2008).

Statins (HMG-CoA reductase inhibitors) are a class of lipid lowering drugs used in treatments for hypercholesterolemia and reduce cardiovascular diseases. Statins competitively inhibit the conversion of HMG-CoA to mevalonate, a precursor for cholesterol synthesis (Herninger and Fritz, 2017) thereby eventually reducing the cell's intrinsic cholesterol synthesis and favouring the uptake of serum LDL cholesterol. On the other hand, statins are known to promote muscle weakness during prolonged time periods. Statin therapy is associated with decreased myocardial function and increase risks of stokes (Lim et al, 2013).

Rosiglitazone is a thiazolidinedione antidiabetic drug used in treating type 2 diabetes mellitus. It works as an insulin sensitizer, by binding to the peroxisome proliferator –activated receptor in cells and making the cells more responsive to insulin. Its use has dramatically decreased over the years due to association of increased risks of heart attacks and deaths (Varga et al, 2015; Pharaon et al 2017).

Amitriptyline is tricyclic antidepressant used to treat mainly depressions and other anxiety disorders. This drug has significant adverse effects on the heart

as it causes disturbances in the rhythm of the heart, QT prolongation, leading to cardiac dysfunction (Zima et al, 2008; Arici et al, 2013).

Amiodarone is a potent antiarrhythmic agent that is used to treat ventricular arrhythmias and atrial fibrillation. Chronic use of amiodarone induces multiple organ toxicity via reduced phospholipid degradation which leads to its accumulation and, consequently lipid peroxidation, ROS generation, and disturbance of cellular calcium levels (Abuzaid et al, 2015).

The XF Analyser (Seahorse Bioscience) is a powerful tool used to measure and interrogate the major energy-producing pathways of cells - mitochondrial respiration and glycolysis. Two key measurements are Oxygen Consumption Rate (OCR) which measures mitochondrial respiration of cells and the Extracellular Acidification Rate (ECAR) which measures the glycolytic activity of cells. These measurements allow the determination of the mitochondrial function and dysfunction in living cells in real time. The drugs will be tested to evaluate mitochondrial function in H9c2 cells and the XF analyser allows to measure this effect.

Aim

The aim of this study is to critically evaluate mitochondrial dysfunction in cardiomyocytes under diverse drug treatments. The beneficial effect of melatonin is tested alongside these drugs to support the protective mechanism of melatonin against cardio toxicity.

4.2 Results

4.2.1 Doxorubicin treatment of H9c2 cells

Doxorubicin (DOX) is an anthracycline commonly used in cancer treatment. The cardiotoxicity caused by DOX could be acute (hours to days) to intermediate (weeks and months) and late onset (>12 months) and even years after treatment has finished. However, its clinical use is greatly restricted by the development of cardiomyopathy and clinical congestive failure (Liu et al, 2008). It is therefore vital to understand the mitochondrial function of cardiomyocytes after chronic exposure to DOX-treatment. Measurements of OCR and ECAR thus provide excellent parameters to convey the toxic effects of DOX in cardiomyocytes.

H9c2 cells were treated with two concentrations of DOX (0.1µM and 0.01µM) for 24 hours. The lower concentration of DOX had no significant effect on the OCR of H9c2 cells whereas the higher concentration (0.1µM) produced a consistent robust decrease in peak OCR (~40%; Figure 4.1 & 4.2). This concentration (0.1µM or 100 nM) was used in subsequent studies. Of interest, DOX-treatment decreased OCR was attenuated by melatonin. Data is represented as OCR values with SEM [CON, 934±30; DOX, 554±30; DOX+MEL, 858±30 pmol/min] (Figure 4.2). Equally important, melatonin improved cell energetics of H9c2 cells treated with DOX (Figure 4.2C).

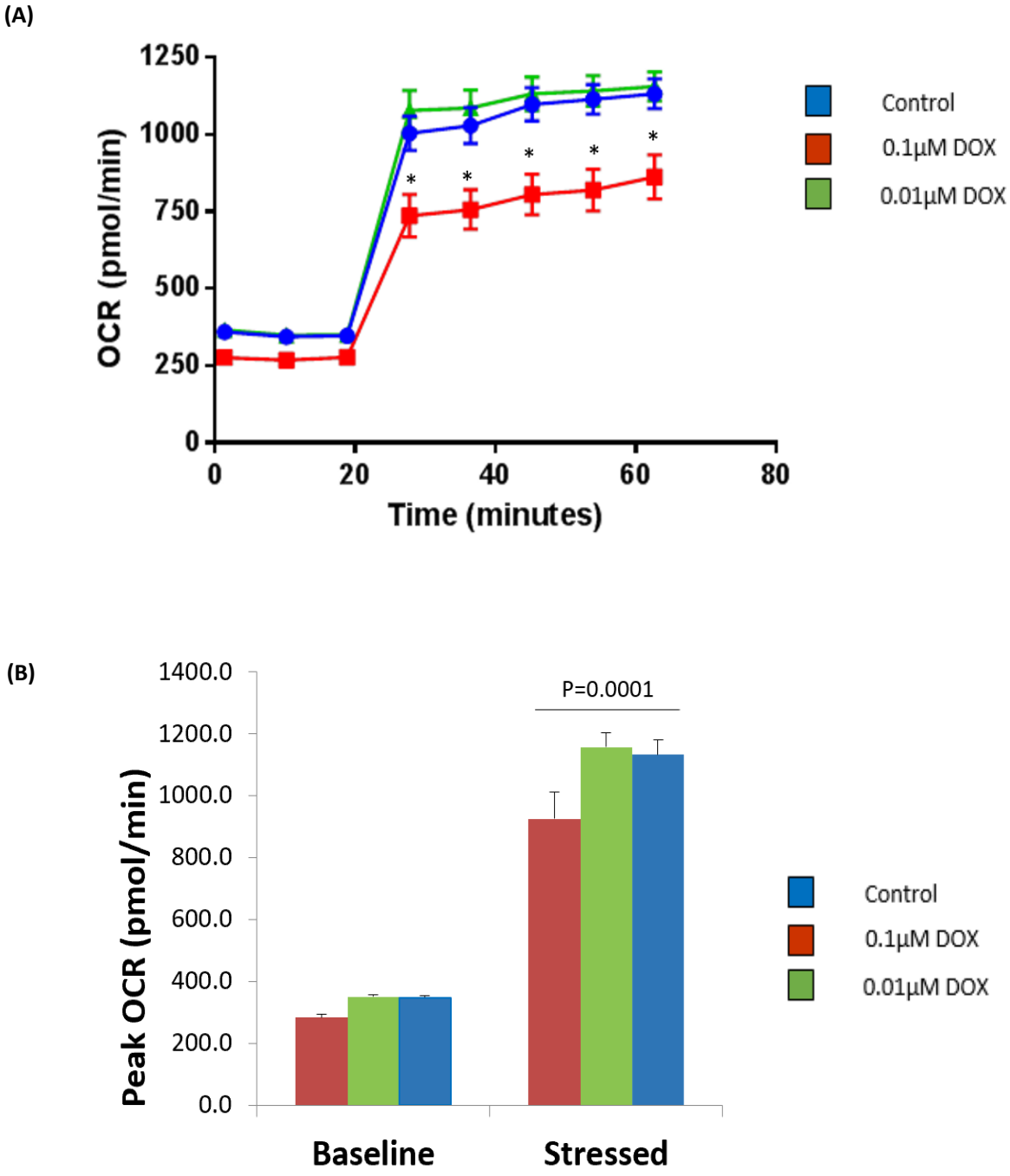

Figure 4.1: **Doxorubicin decreased peak OCR in H9c2 cells.** H9c2 cells were treated with doxorubicin (0.1µM and 0.01µM) for 24hrs. (A) OCR changes with 0.1µM and 0.01µM DOX. (B) Peak OCR changes during baseline and stressed conditions. The experiment was repeated and produced similar results. Data shown is mean± SEM, n=6 per group. One Way Anova: $F(2, 12) = 43.14$, $P<0.0001$.

(A)

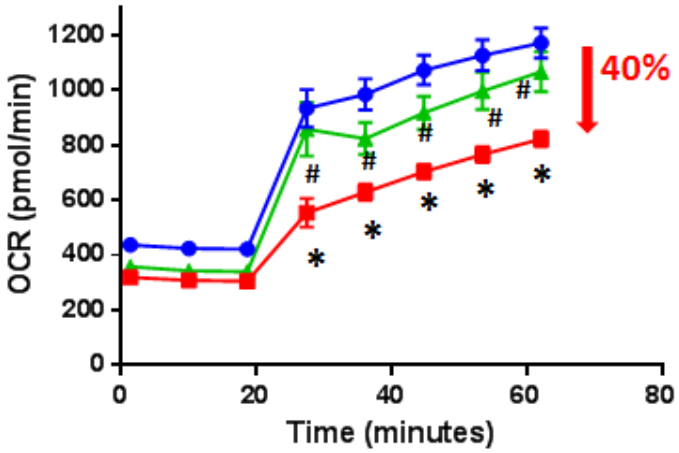

(B)

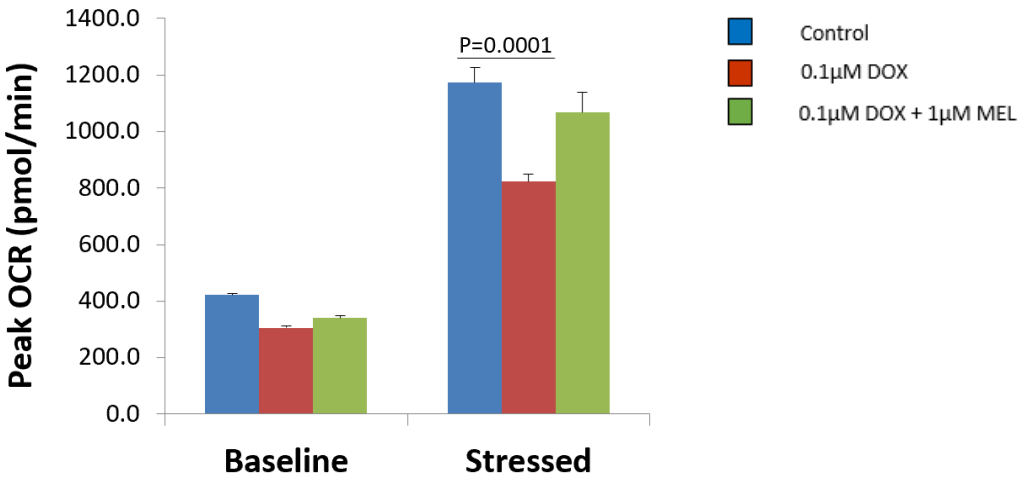

(C)

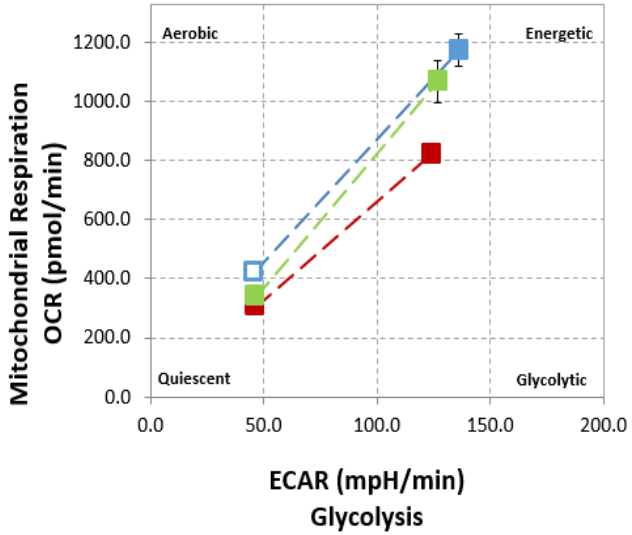

Figure 4.2: **Melatonin attenuates DOX-induced mitochondrial dysfunction in H9c2 cells.** H9c2 were treated with 0.1µM DOX with melatonin (1µM) pre-incubation for 24hrs. **(A)** OCR changes in cells with DOX (0.1 µM) with and without MEL (1 µM). **(B)** Peak OCR changes during baseline and stressed conditions. **(C)** Metabolic phenotype changes with DOX (0.1 µM) with and without MEL (1 µM). Data shown are mean± SEM, n=2 (six replicates). One Way Anova: F (3, 28) = 10.65, P< 0.0001.

4.2.2 Statin treatment of H9c2 cells

Statins (HMG-CoA reductase inhibitors) are a class of lipid lowering drugs used in treatments for hypercholesterolemia and reduce cardiovascular diseases. Statins competitively inhibit the conversion of HMG-CoA to mevalonate, a precursor for cholesterol synthesis (Herninger and Fritz, 2017) thereby eventually reducing the cell's intrinsic cholesterol synthesis and favouring the uptake of serum LDL cholesterol. On the other hand, statins are known to promote muscle weakness during prolonged time periods. Statin therapy is associated with decreased myocardial function and increase risks of stokes (Lim et al, 2013).

Two commonly prescribed statins, Simvastatin and Pravastatin (at intervention concentration of 10 µM) both significantly decreased the peak OCR to a similar extent (~50%) (Figure 4.3). Both statins modestly decreased the basal OCR in H9c2 cells. The concentration of this drug was chosen according to previous work done on H9 c2 cells (Gan Guo et al, 2009; Bonafacio et al, 2016). The cells were seeded at 40k and used for the Seahorse experiment. H9c2 cells were pre-treated with 10µM of simvastatin or pravastatin for 24hrs, thereafter they were treated according to the Seahorse experimental protocol.

ECAR is a measure of the rate of glycolysis during mitochondrial respiration which was reduced by both statins (~50%) during when compared with the control (no statin). Of note, Pravastatin have a slightly improved ECAR than simvastatin and induces less adverse effects compared to simvastatin.

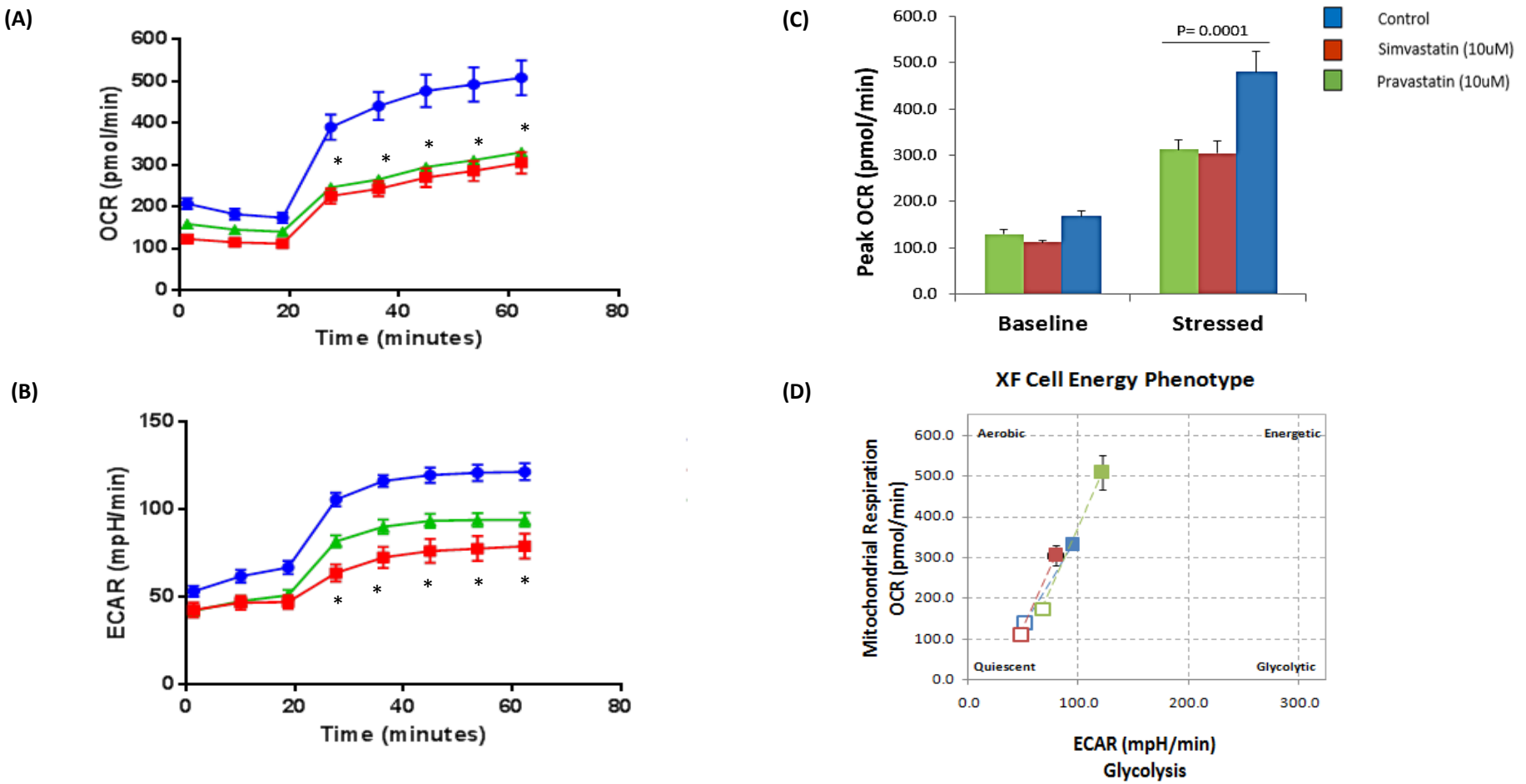

Figure 4.3: **Effects of simvastatin and pravastatin on mitochondrial function in H9c2 cells.** H9c2 cells were pre-treated with 10µM of simvastatin or pravastatin for 24hrs. **(A)** The OCR changes in cells treated with simvastatin and pravastatin. **(B)** The measure of extracellular acidification rate (ECAR) showing changes in glycolysis. **(C)** Peak OCR changes during baseline and stressed conditions. **(D)** The metabolic phenotypic changes in cells simvastatin and pravastatin. Data shown is mean± SEM, n=6 per group. One Way Anova: F (2,12) = 32.42, P<0.0001.

4.2.3 Rosiglitazone and Amitriptyline treatment

Rosiglitazone is a thiazolidinedione antidiabetic drug used in treating type 2 diabetes mellitus. It works as an insulin sensitizer, by binding to the peroxisome proliferator –activated receptor in cells and making the cells more responsive to insulin. Its use has dramatically decreased over the years due to association of increased risks of heart attacks and deaths (Varga et al, 2015; Pharaon et al 2017).

Amitriptyline is tricyclic antidepressant used to treat mainly depressions and other anxiety disorders. This drug has significant adverse effects on the heart as it causes disturbances in the rhythm of the heart, QT prolongation, leading to cardiac dysfunction (Zima et al, 2008; Arici et al, 2013).

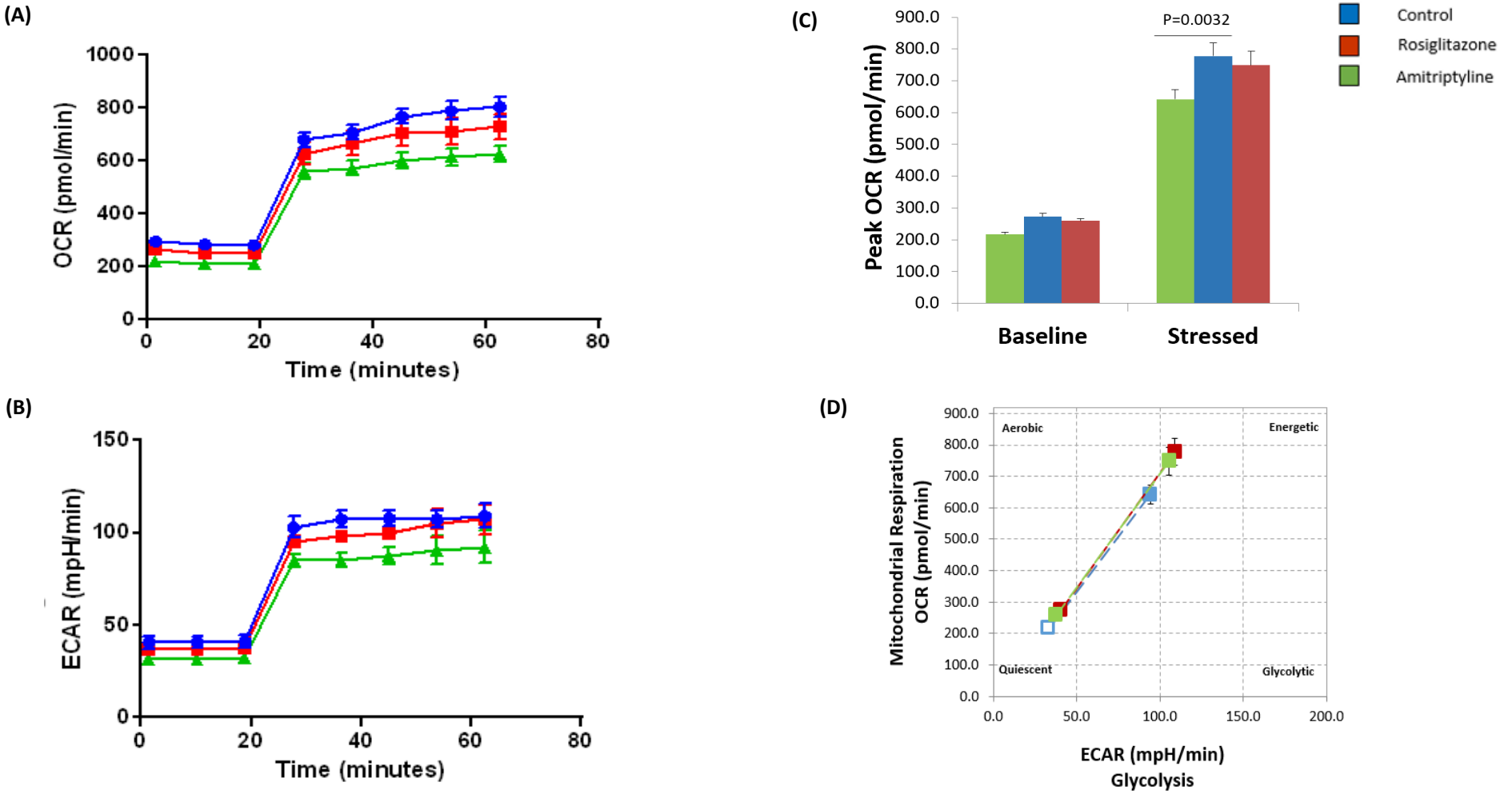

Figure 4.4: **Effects of Rosiglitazone and Amitriptyline on mitochondrial function in H9c2 cells**. H9c2 cells were treated with Rosiglitazone (10µM) and Amitriptyline (10µM) for 24hrs. **(A)** The OCR changes in cells treated with rosiglitazone and amitriptyline. **(B)** The measure of extracellular acidification rate (ECAR) showing changes in glycolysis in cells. **(C)** Peak OCR changes during baseline and stressed conditions. **(D)** The metabolic phenotypic changes in cells. Data shown is mean± SEM, n=6 per group. One-way Anova: F (2,12) = 9.633, P= 0.0032.

Rosiglitazone slightly decreased the OCR in cardiomyocytes but this was not significant (Figure 4.4), not even at higher concentration of 50µM (Figure 4.5) However, amitriptyline (at 10 µM) significantly reduced the OCR and ECAR (~ 20%) in H9c2 cells when compared with control (Figure 4.4).

4.2.5 Amiodarone treatment

Amiodarone is a potent antiarrhythmic agent that is used to treat ventricular arrhythmias and atrial fibrillation. Chronic use of amiodarone induces multiple organ toxicity via reduced phospholipid degradation which leads to its accumulation and, consequently lipid peroxidation, ROS generation, and disturbance of cellular calcium (Abuzaid et al, 2015).

Unlike any other drugs that were examined in this study, amiodarone-treatment (10µM) increased peak OCR by ~ 30% (with no change in basal OCR) compared to control (Figure 4.5). In addition, amiodarone increased basal ECAR by ~ 50% with no increase in ECAR with the stressors (FCCP) indicating that amiodarone-treated H9c2 cells are at maximum ECAR at basal level (Figure 4.5B). This increased demand for glycolysis, mitochondrial respiration and ATP production induced by amiodarone will increase risk of cardiomyocytes mitochondrial respiration failure. Consequently, these events can lead to the progression of heart failure in the long-term usage of amiodarone.

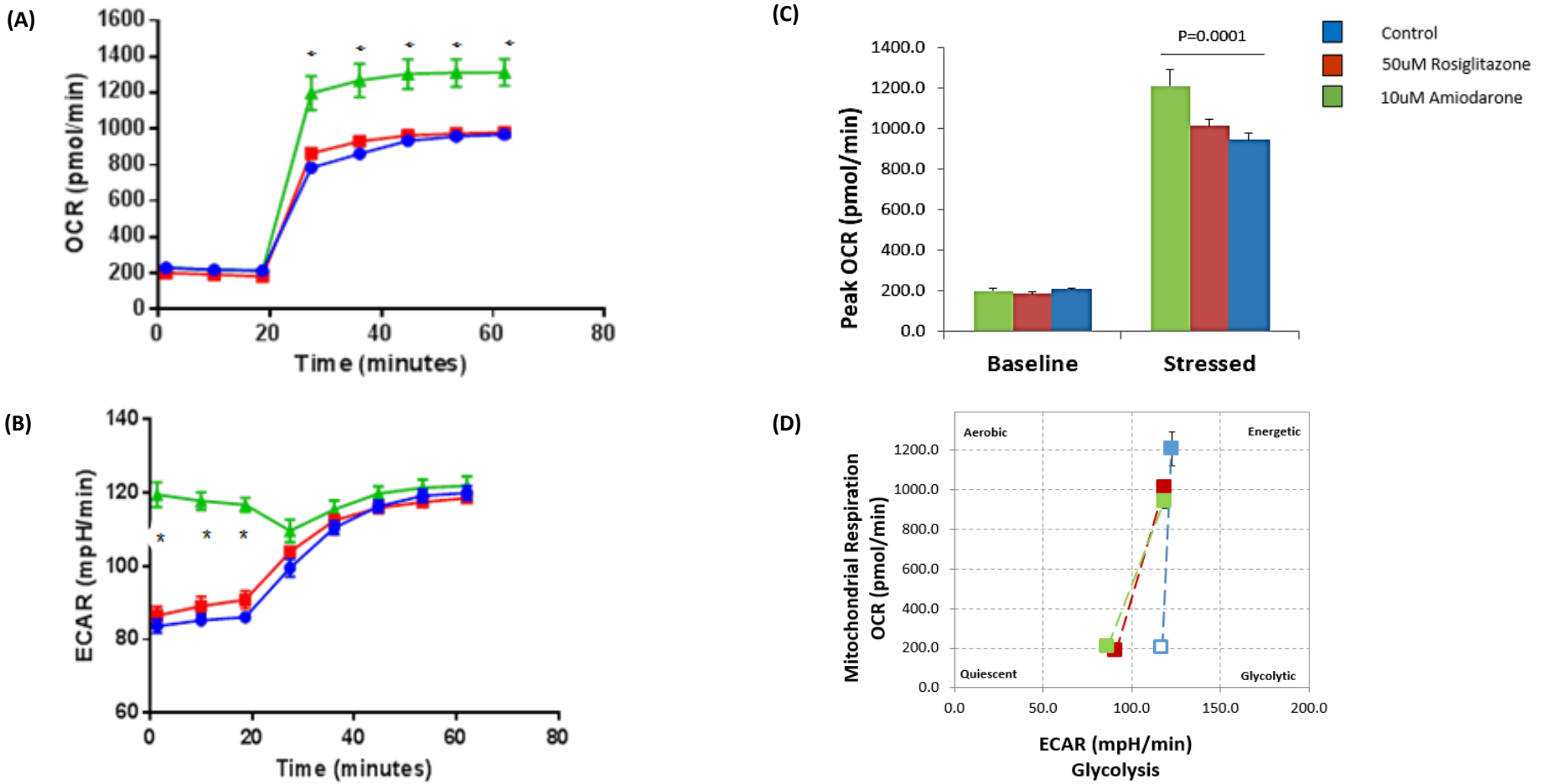

Figure 4.5: **Effects of Rosiglitazone and Amiodarone on mitochondrial function in H9c2 cells.** H9c2 cells were treated with rosiglitazone (50µM) and amiodarone (10µM) for 24hrs. **(A)** The OCR changes in cells treated with rosiglitazone and amiodarone. **(B)** The measure of extracellular acidification rate (ECAR) showing changes in glycolysis in cells. **(C)** Peak OCR changes during baseline and stressed conditions. **(D)** The metabolic phenotypic changes in cells. Data shown is mean± SEM, n=6 per group. One Way Anova: F (2,12) = 31.80, P<0.0001.

4.3 Discussion

The heart is a vital organ demanding vast amounts of energy to sustain its contractile function. Mitochondrial respiration is responsible for generating 90% of this energy in the form of ATP via the ETC (Li et al, 2002). The ETC located in the inner mitochondrial membrane consists of a series of electron carriers grouped into four enzyme complexes: complex I (NADH dehydrogenase); complex II (succinate dehydrogenase); complex III (cytochrome c reductase); and complex IV (cytochrome c oxidase). The synthesis of ATP via this respiratory chain involves two coupled processes: electron transport and oxidative phosphorylation (OXPHOS) (Wallace, 2003). Disruption of cardiac energy homeostasis is a critical feature of DOX-induced cardiotoxicity.

In the current study, diverse drugs groups were examined for cardiotoxicity in H9c2 cells *in vitro*.

The main important findings of this study were:

1. All drugs tested (except rosiglitazone) altered metabolic function in cardiomyocytes by decreasing peak OCR.
2. An exception was amiodarone which increased peak OCR and raised basal ECAR to peak levels.
3. Doxorubicin robustly decreased peak OCR which was significantly attenuated by melatonin.

Diverse drugs used for many chronic diseases have limited usage because of adverse effects caused by toxicity, in particular to the heart. However, the mechanism of cardiotoxicity of these drugs are unclear. The current study provided evidence to suggest that one main mechanism of cardiotoxicity is via mitochondrial dysfunction. The OCR data for DOX and other cardio toxic drugs attenuated the mitochondrial respiration functionality. Oxygen consumption rate is lowered most of the drug treatments when compared with the control group. The accumulation of drugs in the cardiomyocytes directly imposes threat on the mitochondria. In addition, as mentioned

previously, these drugs have a high affinity for cardiolipin (Goormaghtighe, 1980), an integral component of the inner mitochondrial membrane. The binding of these drugs to cardiolipin does not allow for cardiolipin interaction with key respiratory complexes (Goormaghtighe, 1980) and this could be one key mechanism of cardiotoxicity.

As the inner mitochondrial membrane represents a critical site for drug accumulation, the respiratory chain can be considered a potential target for drug-induced toxicity. Accumulating studies have demonstrated that cardio toxic drugs disrupts mitochondrial respiration at multiple levels, by inhibiting complexes of the respiratory chain or inhibiting phosphorylation steps and inducing partial uncoupling (Syed-Ahmed et al, 2000). In particular, studies aimed at determining the sensitivity of respiratory complexes to cardio toxic drugs were found mainly located in complex I, III, and IV, with a specific vulnerability for complexes I (NADH dehydrogenase) and IV (cytochrome c oxidase) (Marcillat et al, 1989). Additional findings indicate inactivation of complex II (Muraoka et al, 2003).The effect of cardiotoxic drugs on mitochondrial respiration results in a bioenergetics decline (shown by decrease in peak OCR), and is a hallmark of impaired cardiac function in the onset and progression of drug-induced cardiotoxicity and heart failure

Amiodarone is antiarrhythmic drug and chronic usage of the drug leads to adverse side effects of sinus rhythm and left ventricular dysfunction (Grosu et al, 2018). Rosiglitazone is an anti-diabetic drug but however chronic use imposes cardiotoxic effects on the heart causing congestive heart failure, chronic hypertension and left ventricular hypertrophy (Chinnam et al, 2012). Interestingly, rosiglitazone (50µM) and amiodarone increased the peak OCR in H9c2 cells. These results can relate to the long-term usage of the drug where the cardiac cells are potentially at a risk of being damaged due to the over workload demand. Cardiac tissue requires an uninterrupted supply of respiratory substrates to meet the very high ATP demand imposed by continuous beating. Over 90% of this ATP is generated by OXPHOS with the necessary mitochondrial network taking up approximately one third of cardiomyocytes cell volume.

Amiodarone and rosiglitazone exert main effects to counteract the effects of endogenous catecholamines on myocardial metabolism. They decrease cardiac afterload, and increase blood supply to the myocardium which compensates for the increase in myocardial oxygen consumption due to the increase in myocardial contractility. As a result, there is elevated ROS production and mitochondrial membrane potential depolarization. This oxygen demand is represented in the OCR data from the Seahorse analyses. (Petrosillo et al, 2003; Petrosillo et al, 2009; Nyguen et al, 2012)

A drug of particular interest is amiodarone which exhibited extremely high basal ECAR in H9c2 cells. The high basal ECAR represents high production of lactate in the cells through glycolysis. During ATP demand, the cells are deprived of oxygen supply and therefore they shift from aerobic to anaerobic respiration to meet the ATP demand. Consequently, the limited anaerobic metabolism of cardiomyocytes results in a build-up of lactic acid and reduced pH in affected areas of the heart. This process of lacto acidosis can induce damage to the cardiac cells, which weaken overtime, resulting in impaired myocardium contractility and loss of function.

The common adverse effects of statins are related with muscle soreness, fatigue and myopathy. This leads to muscle damage and affects mitochondrial function at cellular level (Auer et al, 2014). Amitriptyline is an anti-depressant drug and adverse side effects causes muscle fatigue and weakness. Both these drugs have decreased OCR and ECAR. The present data provide evidence to support these muscle-related adverse effects may be related to the decreased oxygen supply to the cells thus causing muscle weakness and damage.

In conclusion, the present study indicated that a key mechanism of cardiotoxicity for diverse drug groups involves altered mitochondrial metabolic function. The decreased or increased cellular oxygen consumption hinders the efficient respiratory capacity of the cardiomyocytes. It is likely that abnormal mitochondrial function, decreased respiratory complex activity, increased ROS production, and augmented electron leakage and mPTP

opening have all been the main reasons for failing mitochondrial function in the pathophysiology of drug-induced cardiotoxicity.

Chapter 5.

Melatonin attenuates doxorubicin-induced apoptosis in H9c2 cells

5.1 Introduction

Doxorubicin induces cardiac toxicity and cell death in cardiomyocytes during acute and long-term treatment which limits its usage. Doxorubicin greatly enhance ROS production leading to oxidative stress and subsequent cell dysfunction and apoptosis in cardiomyocytes.

Generally, doxorubicin induces cardio toxicity by exerting effects on the mitochondria with increased reactive oxygen species (ROS) production. Usually, mitochondria is the site of ROS production and are synthesised as a consequence of electrons escaping from electron transport chain and captured by oxygen, rendering it to be the home of superoxide production. A one-electron reduction of the C ring of DOX results in the formation of a semiquinone free radical which, following a reaction with oxygen, produces superoxides, peroxides and hydroxyl radicals (Montaigne et al., 2012; Olson et al., 1981; Sinha, 1989).

As a consequence of increased ROS production causes increased oxidative stress has a detrimental effect on calcium equilibrium in the cells (Zhang et al., 2009). ROS raises calcium levels by promoting its release from the sarcoplasmic reticulum. This successively creates a vicious circle where elevated Ca2+ levels then increase ROS production through Ca2+-sensitive ROS-producing enzymes (Zhang et al., 2009). Since the mitochondria are in close proximity to the Ca2+-release site, they are exposed to massive quantities of Ca2+ influx. The overwhelming levels of ROS, in conjunction with elevated levels of Ca2+ beyond the threshold, trigger the opening of the mitochondrial permeability transition pore (mPTP). This causes a loss in mitochondrial membrane potential and ultimately the discharge of cytochrome c (Zhang et al., 2009). Cytochrome c, situated within the inner mitochondrial membrane, (Childs et al., 2002; Chen et al., 2007) forms a part of the intrinsic apoptotic pathway. As a result this vicious process of calcium mishandling in the cells due to oxidative stress induced by doxorubicin, leads to cardiomyocytes cell death.

The Seahorse studies presented in Chapter 4 demonstrated that DOX-treatment in H9c2 cells resulted in mitochondrial dysfunction in terms of

OXPHOS and glycolysis. Of great interest and clinical relevance, melatonin pre-treatment attenuated DOX-induced mitochondrial dysfunction. Melatonin has well known function to detoxify ROS and reduce oxidative stress. It acts as a powerful anti-oxidant to bring out this effect as a free radical scavenger. This powerful feature of melatonin is used to investigate against DOX-induced apoptosis in cells. However, the protective role of melatonin on DOX-induced cell death is unknown using the current H9c2 cell model.

Aim

The aim of this study was to utilise DOX to induce cardiotoxicity and apoptosis in H9c2 cells. The potential beneficial effect of melatonin will be assessed in attenuating DOX-induced apoptosis in H9c2 cells.

5.2 Flow Cytometry results

5.2.1 The Compensation assay

Phospholipids of the cell membrane are asymmetrically distributed between the inner and outer leaflets of the membrane. Phosphatidylcholine and sphingomyelin are exposed on the external leaflet of the lipid bilayer, while phosphatidylserine is located on the inner surface. During apoptosis, this asymmetry is disrupted, and phosphatidylserine becomes exposed on the outside surface of the plasma membrane. Propidium iodide is used together with annexin V-FITC, to differentiate dead cells from dying cells. Binding of annexin V correlated with other changes is consistent with apoptosis, including changes in nuclear morphology, DNA fragmentation and membrane leaflet symmetry. Only cells stained with both annexin V and propidium iodide demonstrated chromatin condensation, a late indicator of apoptosis.

The compensation control assay (carried out for each flow cytometry experiment) calibrates the stains which are being used. Compensation is required for a flow cytometry experiment because of the physics of fluorescence and these controls are used to differentiate the FITC and PI stain used in the assay. For each different stain, the compensation works by removing the overlap between each stain at a wavelength between 480nm-675nm in the emission spectrum. A fluorochrome is excited and emits a photon in a range of wavelengths in the emission spectrum. Some of those photons spill into a second detector, causing single stained samples to appear double positive for both stains. Therefore, an application of mathematical correction to the data addresses this spill over. This is known as compensation. Consequently, this allows distinguishing the different types of apoptotic population of cells stained by FITC and PI (Figure 5.1).

According to manufacturers' instruction, a DOX concentration that produced ~50% apoptosis was used for the compensation assay to work. This done to make sure the distinguished apoptotic cell population is stained by the FITC and PI well enough in order to obtain a reliable reading. Ideally, 0.8µM DOX produced ~ 50% apoptosis in H9c2 cells for the compensation controls to

work efficiently. The compensation assay was done every time prior a new experiment and One- way Anova was used for statistical analysis.

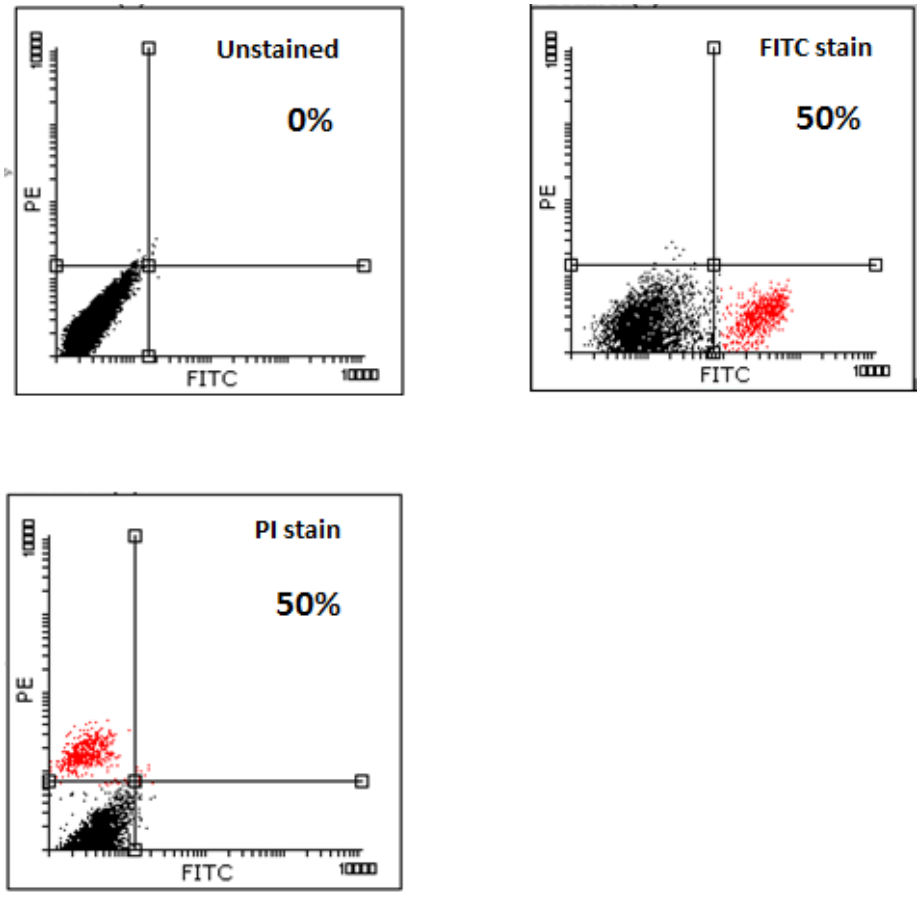

Figure 5.1. **Compensation controls for DOX-induced apoptosis in H9c2 cells.** Cells were treated with DOX (0.8µM) for 24hrs. Each different stain represents the distinguished apoptotic population of cells. Representative flow cytometry images are shown. Black (Live cells), Red (Apoptotic cells). Similar compensation controls was obtained in each experiment.

From the compensation data, at 0.8µM Dox, maximum of 50% of apoptosis was induced in H9c2 cells over 24hr time period (Figure 5.1). Each quadrant represents the population of apoptotic cells stained by each respective dye.

5.2.2 Doxorubicin-induced apoptosis in H9c2 cells

Cardiomyocyte apoptosis precedes cardiac dysfunction and heart failure in ageing, myocardial infarction, and drug-induced cardiotoxicity. In order to examine the beneficial role of melatonin in attenuating DOX-induced cell death, the gold standard method of flow cytometry was utilised. The H9c2 cells were treated with 0.3µM DOX, this concentration was chosen to induce 20~30% apoptosis in the total viable cell population. Melatonin was used alongside to attenuate the effect of doxorubicin.

The data obtained from the Flowing software, represents apoptotic and viable cells in respective quadrants- live cells, early apoptosis, late apoptosis and necrosis as percentage from the total cell population.
Doxorubicin (0.3µM, 24 hrs) significantly induced apoptosis (~20%) in H9c2 cells which was inhibited by melatonin (Figure 5.2, 5.3 and 5.4).

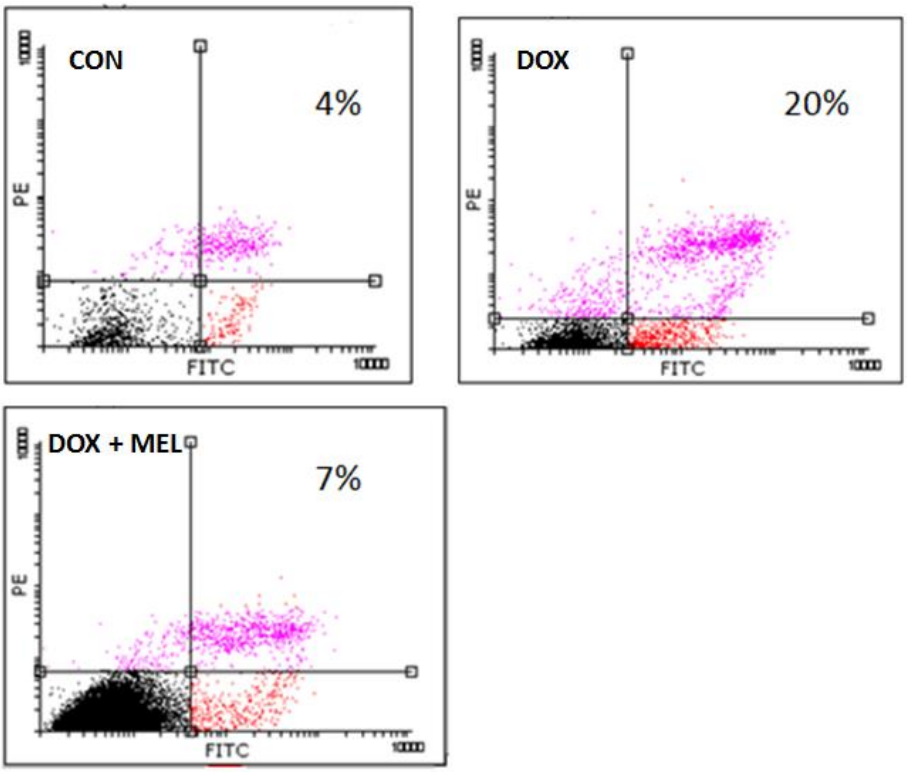

Figure 5.2: **Melatonin attenuates DOX-induced apoptosis in H9c2 cells in flow cytometry assay.** Cells were treated with DOX (0.3 µM) with and without MEL (1 µM) for 24 hr. Representative data are shown (in duplicate wells). Percentages represent total apoptotic cells. Black (Live cells), Red (Apoptotic cells) and Pink (Necrotic cells).

The above data is used to replot into bar chart showing the percentage apoptosis for each different treatment group.

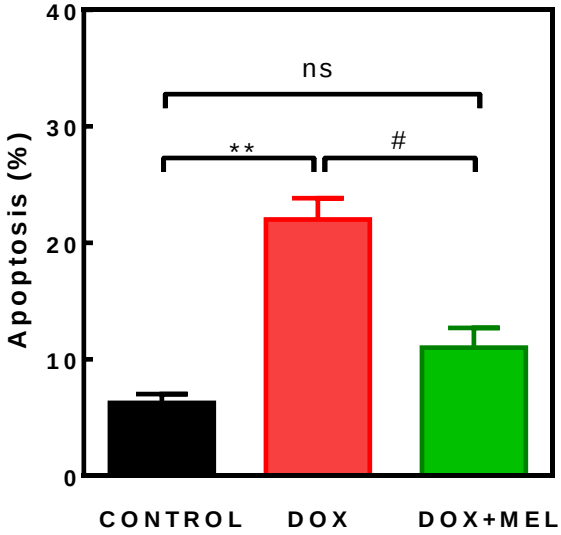

Figure 5.3. **Melatonin attenuated doxorubicin-induced cell death in H9c2 cells in flow cytometry assays.** Cells were treated with DOX (0.3 µM) with and without MEL (1 µM) for 24 hr. Con: 6.3±0.8%; DOX: 22±1.8%; DOX+MEL: 11±1.7%. (n=4 separate experiments in duplicate wells). ANOVA p=0.0001, F (2, 9) = 29.1; **p = 0.001, #p=0.004.

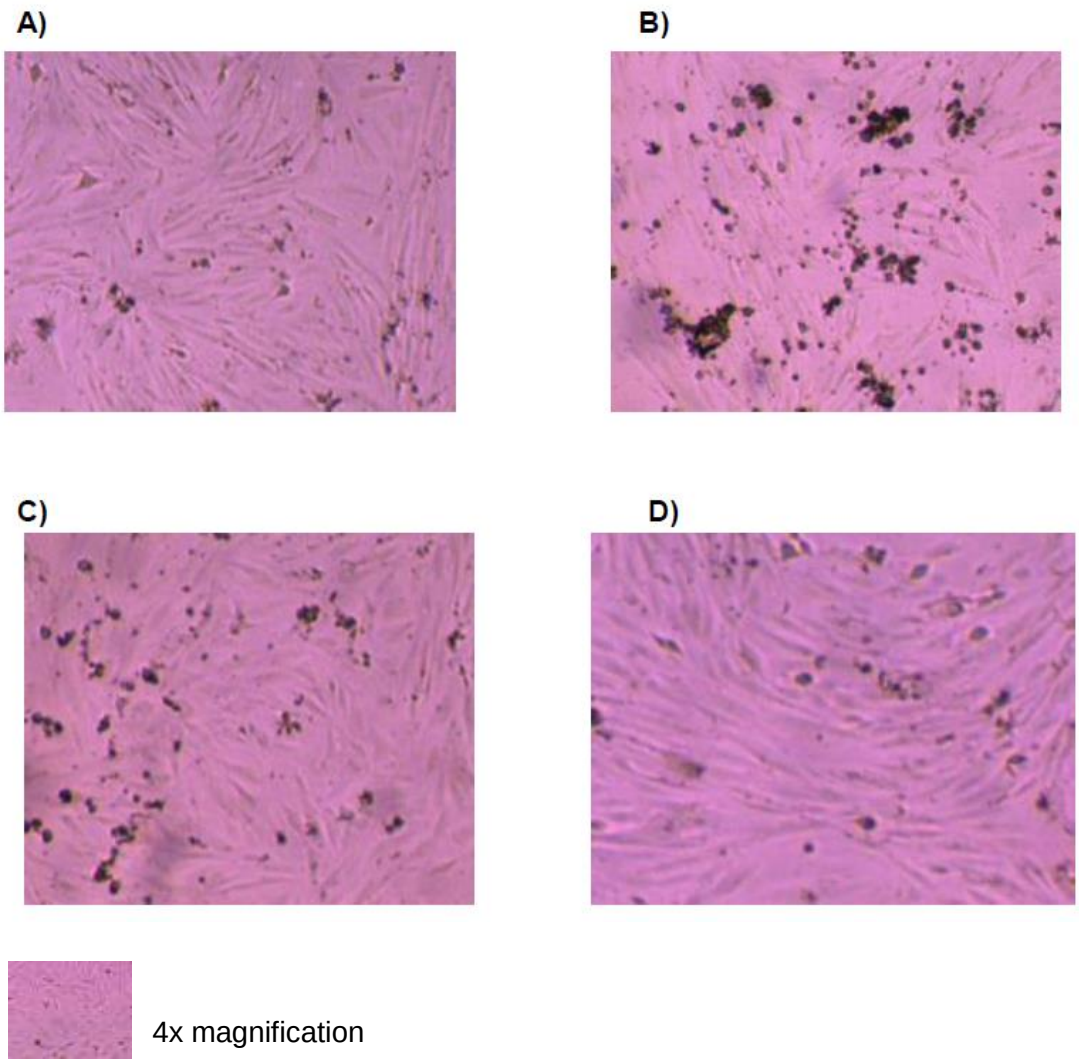

Figure 5.4. Doxorubicin and melatonin morphology in H9C2 cardiomyocytes. The image above represents the cell viability in each treatment groups. Cell viability is reduced in group B, treated with dox (0.5 μM) for 24hrs. In presence of melatonin (group c) the cell viability is increased. Groups A and D display similar pattern in terms of cell viability.

5.3 Alamar Blue stain cell viability assay

Alamar blue cell viability reagent is a resazurin based reagent. Resazurin is the active component in Alamar blue cell viability reagent is a nontoxic, cell permeable compound that is blue in colour and fluorescent. Upon entering live cells, the cellular reducing environment reduces resazurin to resorufin a compound that is red and highly fluorescent. The colour change can be detected by absorbance-based plate readers, to deduce cell viability. Alamar Blue was used in this experiment to determine cell viability after 24 hr treatment with doxorubicin and melatonin.

Alamar Blue staining was used to determine cell viability after 24 hr treatment with DOX and melatonin (summarised in Figure 5.5 and Table 5.1; see Appendix C). H9c2 cells treated with DOX (0.5µM, 24 hrs) consistently produced reduction in cell viability (~30%). This concentration of the drug was chosen to produce similar level of apoptosis as of flow cytometry. Flow cytometry assay is relatively more sensitive to measure apoptosis compared to Alamar blue cell viability assay. The data is represented as relative abundance of the group to the total number of cells with standard error of mean.

Thus, low concentration of Dox (0.3µM) can be used in Flow Cytometry to produce the same level of apoptosis at ~ 30%. This effect this was completely blocked by melatonin preincubation (1µM, 2hrs) (Figure 5.5). Melatonin alone had no effect on cell viability.

Table 5.1: **Melatonin blocked doxorubicin-induced cell death in H9c2 cells** (measured using the Alamar Blue stain method). Data are presented as mean±SEM (n=5 separate experiments; each experiment had 3 to 10 samples). See Appendix C for additional results.

Control	Dox	Dox + Mel	Mel
100.3 ± 0.3	71.11 ± 3.3	97.28 ± 2.7	98.04 ± 2.8

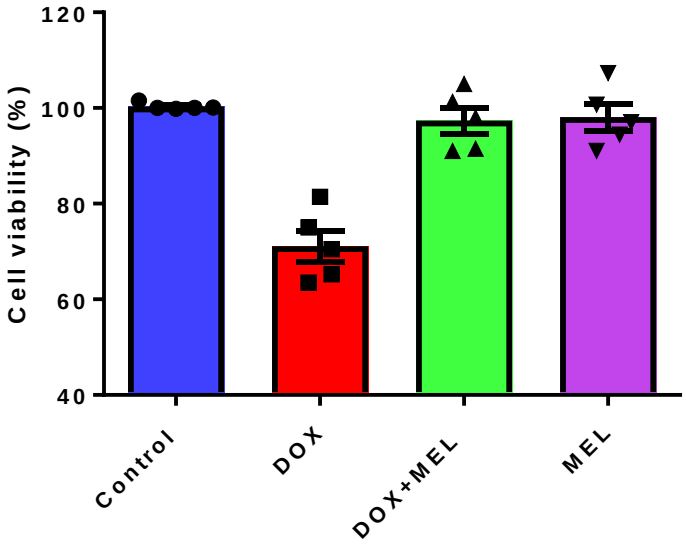

Figure 5.5: **Melatonin blocked doxorubicin-induced cell death in H9c2 cells.** Cells were treated with DOX (0.5µM) with and without MEL (1µM) for 24hr. Data are presented as mean ± SEM (n=5 separate experiments; each experiment had 3 to 10 samples). One Way Anova: F (3, 16) = 29.12, P< 0.0001. Data considered statistically significant.

5.4 Discussion

Doxorubicin induced cardiotoxicity involves the dysfunction of mitochondrial function via disruption of OXPHOS and glycolysis. In the present study, the effect of melatonin on DOX-induced cell death was measured using flow cytometry and Alamar Blue staining methods.

The main important findings of this study were:

1. Doxorubicin treatment for 24 hours significantly induced H9c2 cell death.
2. Melatonin blocked DOX-induced apoptosis and necrosis as measured by two robust measurements of cell viability and apoptosis.

While toxicity induced by DOX involves multiple factors, the primary mechanism of cardiomyocyte cell death is widely believed to be due to DOX-induced generation of ROS and concomitant destructive effects of these free radicals (Singal *et al*., 2000). Doxorubicin undergoes redox cycling by dehydrogenases like the NADH dehydrogenase enzyme, which is part of the mitochondrial complex I. Since cardiomyocytes have an abundance of mitochondria, they are especially susceptible to DOX-induced ROS generation (Govender *et al*., 2014).

Accumulating data have demonstrated that treatment of cardiomyocytes with antioxidant compounds prevent ROS formation and toxicity induced by DOX (Chularojmontri *et al*., 2005; Lou *et al*., 2015; Quiles *et al*., 2002; Spallarossa *et al*., 2004). One of the key events in induction of apoptosis is the loss of mitochondrial membrane integrity. The intrinsic apoptotic pathway, stimulated by ROS causes a loss of mitochondrial membrane potential, leading to the opening of pores in the membrane and the leakage of cytochrome c into the cytoplasm. This starts a cascade leading to activation of executioner caspases like Caspase-3 and ultimately cellular apoptosis (Kalyanaraman *et al*., 2002). The loss of mitochondrial membrane potential gradient is recognized as the point of no return in the

apoptotic pathway (Zamzami *et al*., 1995), underlining the importance of this event. One of the ways DOX is thought to mediate cardiac cell apoptosis is through the intrinsic pathway, initiated in the mitochondria (Hsu *et al*, 2014).

It is well documented that melatonin acts as an effective antioxidant in various *in vitro* and *in vivo* models of cardiac diseases not only by scavenging free radicals but also by increasing the gene expression of antioxidative enzymes like GPx, GR, and SOD (Wang, 2009). Melatonin exerts its antiapoptotic activity by its known ability to inhibit release of cytochrome c from Ca^{2+} mediated mitochondria (Rhao et al, 2014). Mitochondria membrane potential is crucial factor for the maintenance of cellular bioenergetics homeostasis and its dissipation leads to formation of mitochondrial permeability transition pore (mPTP) in cardiotoxicity. Melatonin increased the expression of antiapoptotic proteins like bcl-2 through SIRT1 pathways and also decreased the expression of apoptotic factor Bax (Wang et al, 2009; Sims and Muyderman, 2010; Li et al, 2014; Yang et al, 2015). Therefore melatonin maintains the mitochondrial membrane potential in cardiomyocytes and indirectly inhibits the opening of the mPTP (Gouriou et al, 2013). It will be of interest to examine the possible mechanisms of action of melatonin in protecting H9c2 cells from DOX-induced cell death (see Chapter 6).

In conclusion the beneficial effects of melatonin administration against these conditions are in part due to its direct free radical scavenger activity and its indirect antioxidant properties. The data obtained from the current study (chapters 4 and 5) provide evidence demonstrating the effect of melatonin on mitochondrial bioenergetics and its role in anti-apoptosis. This will undoubtedly provide novel insight that will deepen our understanding of melatonin's protective mechanisms during DOX-induced cardiotoxicity. It is recommended that in the future, the therapeutic value of melatonin in the treatment of DOX-induced cardiotoxicity will be useful to assess mitochondrial function in cardiomyocytes.

Chapter 6.

Doxorubicin-induced gene alteration in H9c2 cells: beneficial role of melatonin

6.1 Introduction

Doxorubicin is a potent drug used to treat several cancers including carcinomas and sarcomas (Thorn et al., 2011). Although effective, the adverse effect of DOX limits its clinical use. Patients are affected by DOX-induced cardiotoxicity in a dose-dependent manner and may present to the clinic with a serial decline in ventricular ejection fraction and reduced contractile function with associated diastolic dysfunction (Chatterjee et al., 2010; Thorn et al., 2011). The DOX-induced morphological and functional abnormalities of the cardiac tissue results in irreversible dilated cardiomyopathy which once established, may progress into biventricular congestive heart failure; carrying a poor prognosis of approximately 50% mortality (Chatterjee et al., 2010).

The acute effect of DOX can occur within few hours to days. This results in the early stages of arrhythmia and apoptosis. Malignant arrhythmias account for a significant portion of heart failure related deaths (Sadredini et al, 2016). The exact mechanisms of DOX-induced cardiotoxicity is unclear but it will involve disruptions in multiple diverse signalling pathways such as apoptosis, cardiac hypertrophy and cardiomyopathy, mitochondrial dysfunction and cardiac electrical remodelling (Troidl et al, 2009; Cheung et al, 2015; Tarradas et al, 2017; Haque and Wang, 2017).

Apoptosis is initiated and executed through two major signalling pathways: the intrinsic and extrinsic pathways. Intrinsic apoptosis pathway (also named as mitochondrial apoptosis pathway) is triggered by intracellular stress such as oxidative stress, calcium overload, and DNA damage, leading to Bax/Bak-dependent mitochondrial outer membrane permeabilization and release of cytochrome *c* from mitochondria into cytosol. Cytosolic cytochrome *c* and apoptotic protease-activating factor 1 (Apaf-1) then form apoptosome and result in activation of caspase 9. The intrinsic pathway firmly controlled by the Bcl-2 protein family including anti- apoptosis Bcl-2, Bcl-xL, pro- apoptosis Bax, Bak. Mitochondrial uncoupling protein 2 (UCP2) is the most studied protein in its family of mitochondrial anion carrier proteins. Mitochondrial

uncoupling proteins are located in the mitochondrial inner membrane which can promote the proton leak across the mitochondrial inner membrane and provide protection via p38 signalling pathway (Dong et al, 2014; Zhang et al, 2018).

Intermediate effect of DOX can take place from weeks to months which can lead to remodelling of the heart. Myh7 gene encodes beta (β)-myosin heavy chain (β-MHC). In cardiac muscle cells β-MHC forms part of a large protein known as type II myosin and it is responsible for the interaction with actin protein for cell movement and shape. During cardiotoxicity the gene disruption causes up-regulation of β-MHC with corresponding down-regulation of α-MHC. This happens through p38 MAPK, extracellular signal-regulated kinase (ERK) and c-Jun NH_2-terminal kinase (JNK) signalling pathways. Cardiac remodelling could lead to the development of hypertrophy in the heart.

The chronic effect of DOX takes months to years progressing towards heart failure. In heart failure, an excessive preload overwhelms the contractility of the heart, resulting in decreased cardiac output characterized by both systolic and diastolic function. Serca2a is a fundamental protein involved in the process of removing Ca^{2+} into the sarcoplasmic reticulum during diastole. Serca2a transports the Ca2+ released during ECC back into the SR lumen against the electrochemical [Ca2+] gradient using chemical energy from ATP. However, in heart failure there is a reduction of Serca2a protein level and function. It seems to act via the Serca2a attenuating calcium overload via ERK1 pathway (Tarradas et al, 2017).

MS1 is a myofibrillar protein involved in the regulation of gene expression in both cardiac and skeletal muscle. It is also known as striated muscle activator of Rho Signalling and Serum Response Factor dependent transcription (STARS) (Arai et al, 2002) or Actin-binding Rho-activating protein (ABRA) (Troidl et al, 2009).

The signalling pathway of JNK and MAPKs are disrupted and the changes affect the transcription of the MS1 gene leading to the down regulation of the

gene and whereby melatonin may interfere with this pathway to attenuate the gene expression.

Aim

The aim of the present study was to delineate the mechanisms of action of doxorubicin-induced cardiotoxicity and melatonin action by examining altered gene expression in doxorubicin-treated H9c2 cells with or without melatonin.

6.2 Results - Semi quantitative PCR analysis

In the present study, gene expression was analysed under four conditions in H9c2 cells: control group (no drugs added); DOX group; DOX+MEL group (cells pre-treated with melatonin and then DOX); Melatonin alone. The concentration of DOX used is 0.5 μM, this concentration was used similar to previous experiments used for apoptosis studies.

Image J software was used to quantify the PCR fragments of the gel image for the genes. The colour of the gel image was first inverted (PCR fragments are black in a white background) and then each PCR fragment was selected and analysed. The arbitrary numerical value for each PCR fragment was calculated and then the percentage of each peak on the plot was calculated. This gave an arbitrary value for each gene from separate experiments. The expression levels of each experimental sample (per gene) were divided by expression levels of the internal control gene (Cyclophillin A) and these ratios plotted and analysed. See Appendix B, for results.

In order to identify putative mechanisms of action of DOX-induced cardiotoxicity and melatonin action, candidate genes that are involved in the progression of heart failure will be measured. These genes are categorised here in five main groups with overlapping functions: cardiac conductivity, mitochondrial function, cardiac remodelling, apoptosis and heart failure.

6.2.1 CAV3

DOX-treatment of H9c2 cells significantly decreased CAV3 gene expression which was modestly attenuated by melatonin but it was not statistically significant (Figure 6.1).

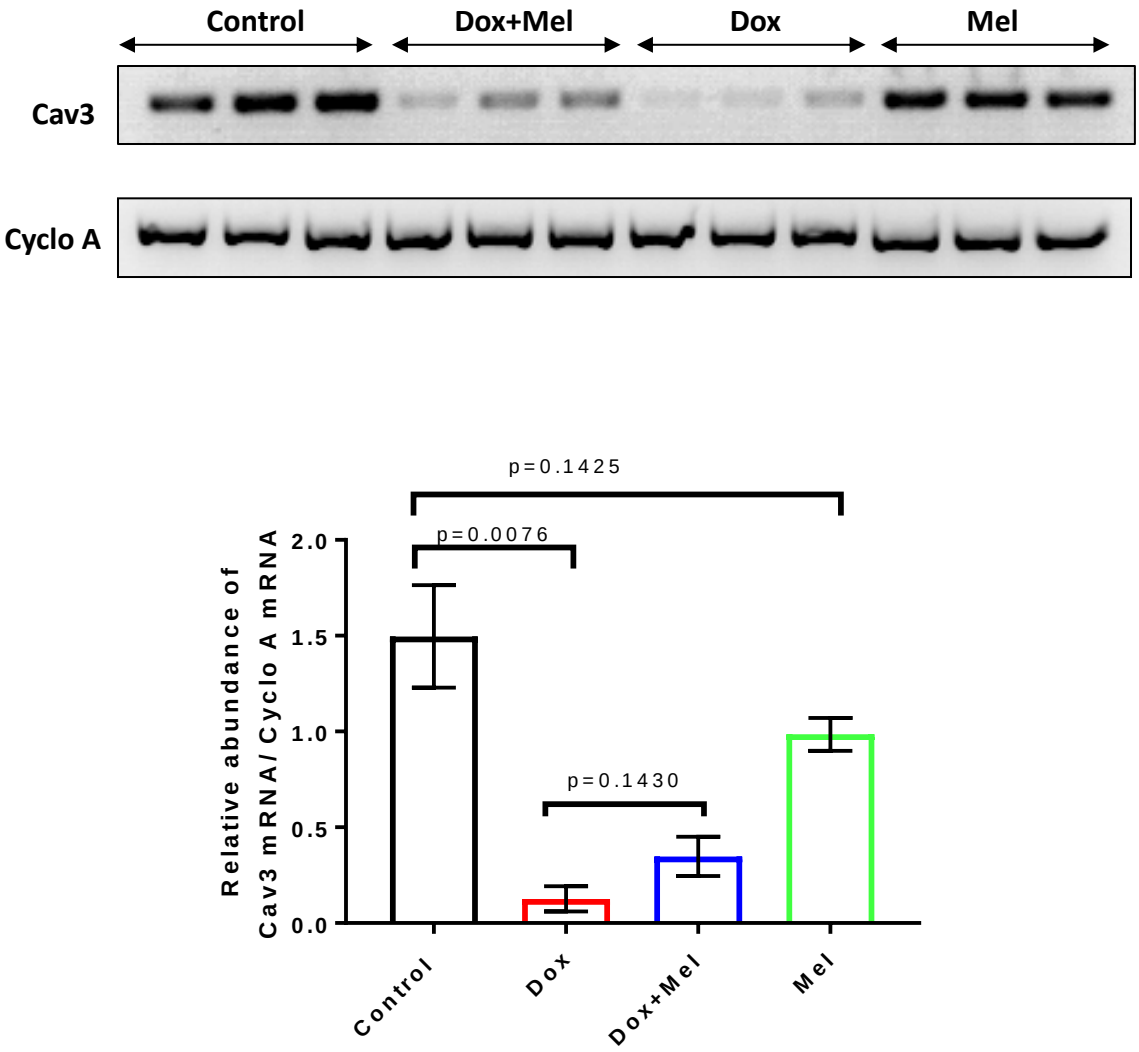

Figure 6.1. Melatonin attenuates doxorubicin downregulation of *CAV3* gene expression in H9c2 cells. Cells were DOX - treated (0.5 µM, 24 hrs) with and without melatonin (1µM). The results presented are mean ± SEM, n= 3. One-Way ANOVA: F (3, 8) = 16.57, P=0.0009. Data considered statistically significant at p≤0.05.

6.2.2 Drp1

Doxorubicin robustly decreased Drp1 mRNA expression in H9c2 cells which was attenuated by melatonin (Figure 6.2).

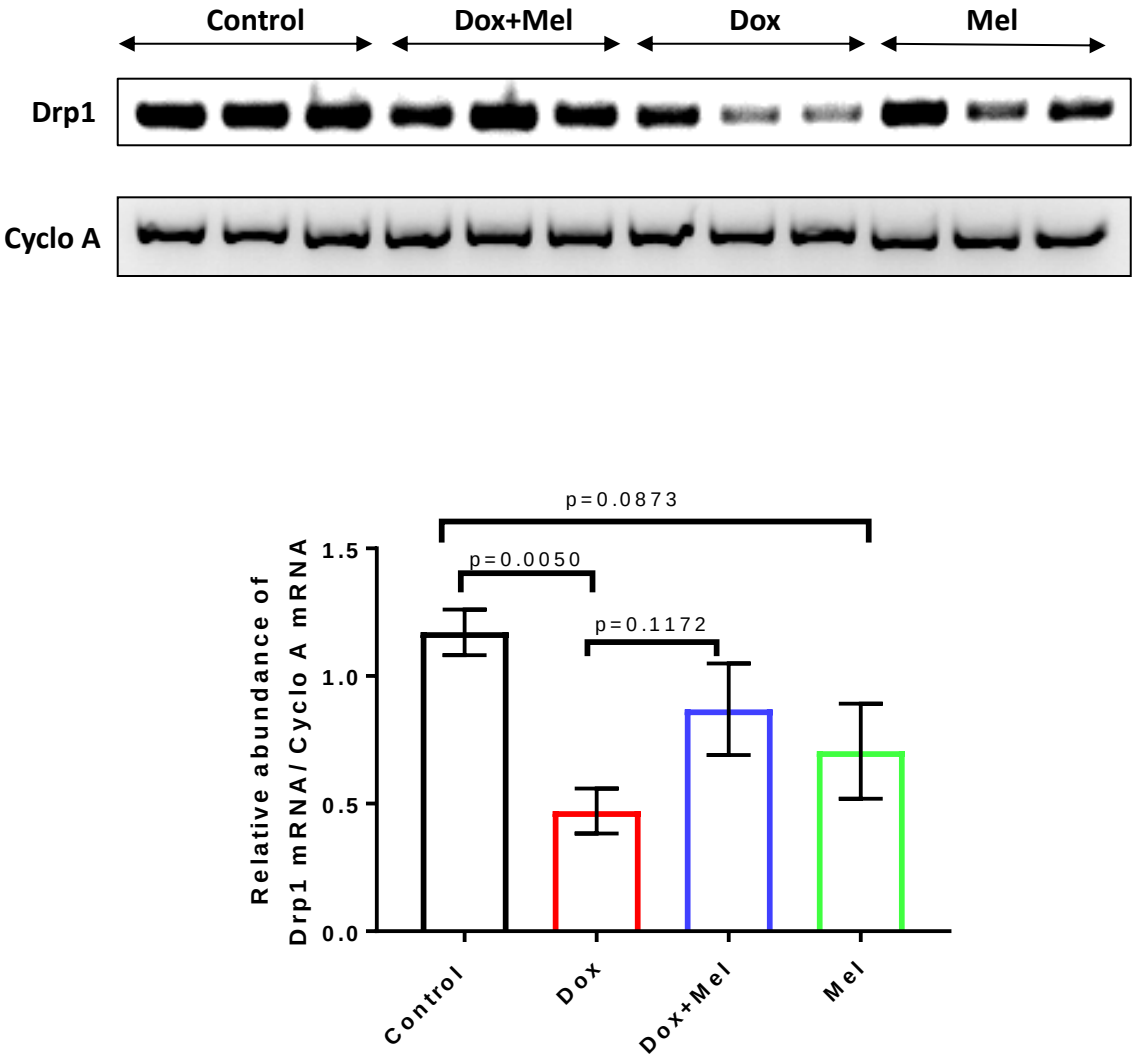

Figure 6.2. Melatonin attenuates doxorubicin downregulation of *Drp1* gene expression in H9c2 cells. Cells were DOX - treated (0.5 µM, 24 hrs) with and without melatonin (1µM). The results presented are mean ± SEM, n= 3. One-Way ANOVA: F (3, 8) = 4.19, p=0.0467. Data considered statistically significant at p≤0.05.

6.2.3 Mfn1

Mfn1 gene expression was significantly decreased by DOX-treatment in H9c2 cells and this was reversed by melatonin (Figure 6.3).

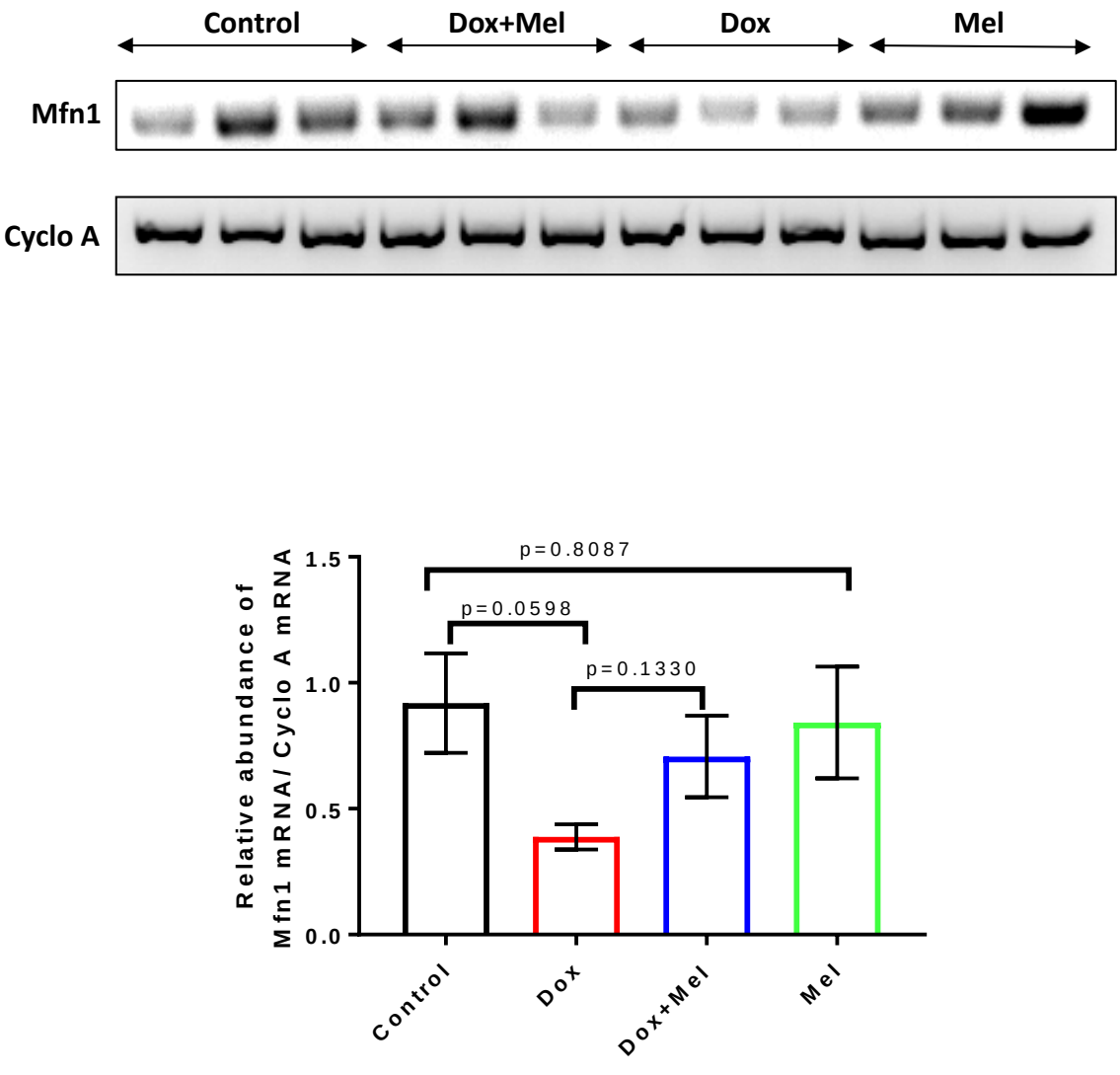

Figure 6.3. Melatonin attenuates doxorubicin downregulation of *Mfn1* gene expression in H9c2 cells. Cells were DOX - treated (0.5 µM, 24 hrs) with and without melatonin (1µM). The results presented are mean ± SEM, n= 3. One-Way ANOVA: F (3, 8) = 1.88, p=0.2112. Data considered statistically significant at p≤0.05.

6.2.4 PPAR-γ

Dox-treatment deceased PPAR-γ gene expression in H9c2 cells which was significantly attenuated by melatonin (Figure 6.4).

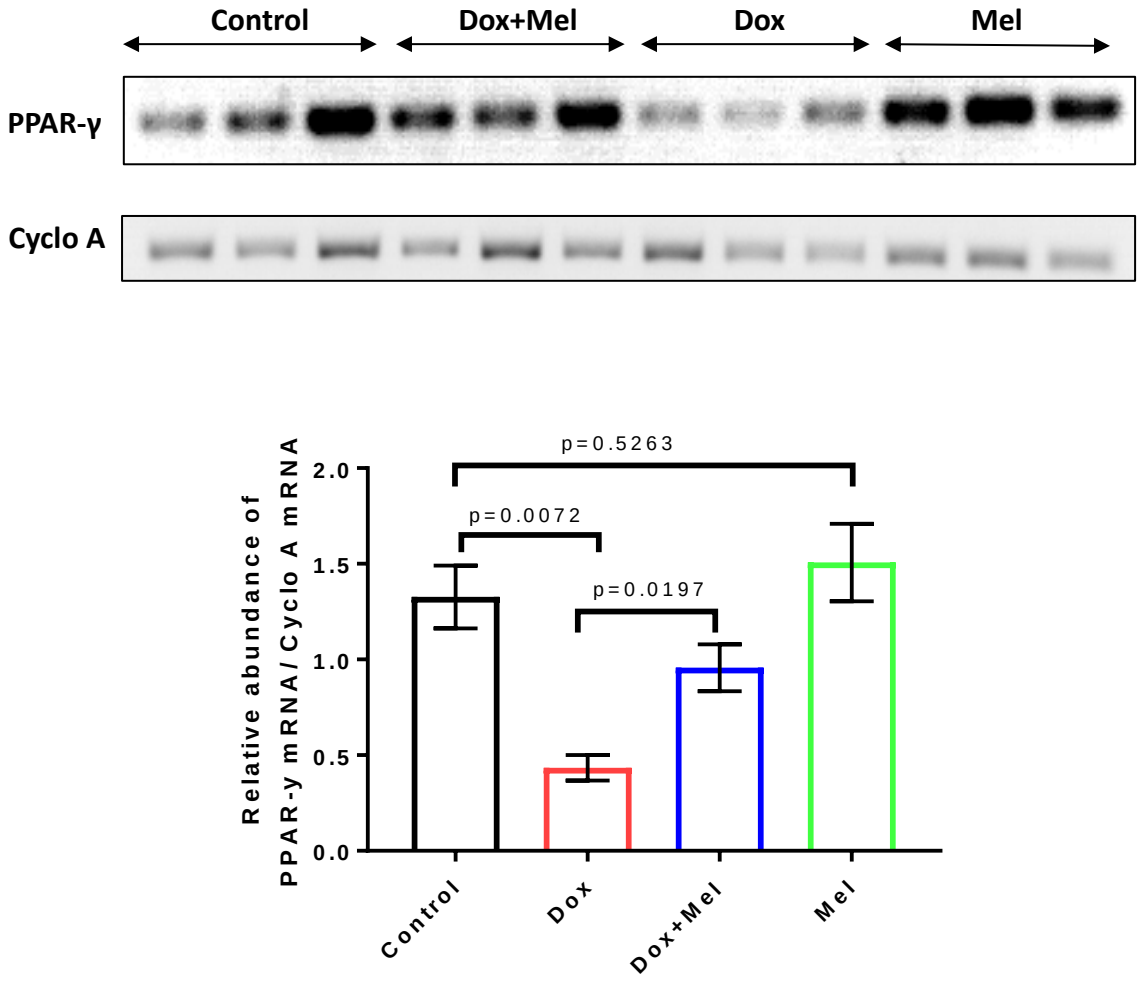

Figure 6.4. Melatonin attenuates doxorubicin downregulation of *PPAR-γ* gene expression in H9c2 cells. Cells were DOX - treated (0.5 µM, 24 hrs) with and without melatonin (1µM). The results presented are mean ± SEM, n= 3. One-Way ANOVA: F (3, 8) = 10.36, p=0.0040. Data considered statistically significant at p≤0.05.

6.2.5 Sirt3

Doxorubicin alone (0.5µM, 24 hrs) had no significant effect on Sirt3 gene expression in H9c2 cells (Figure 6.5). However under DOX-induced stress, melatonin modestly increased Sirt3 gene expression. Melatonin alone also significantly increased Sirt3 mRNA expression compared to the untreated control (Figure 6.5).

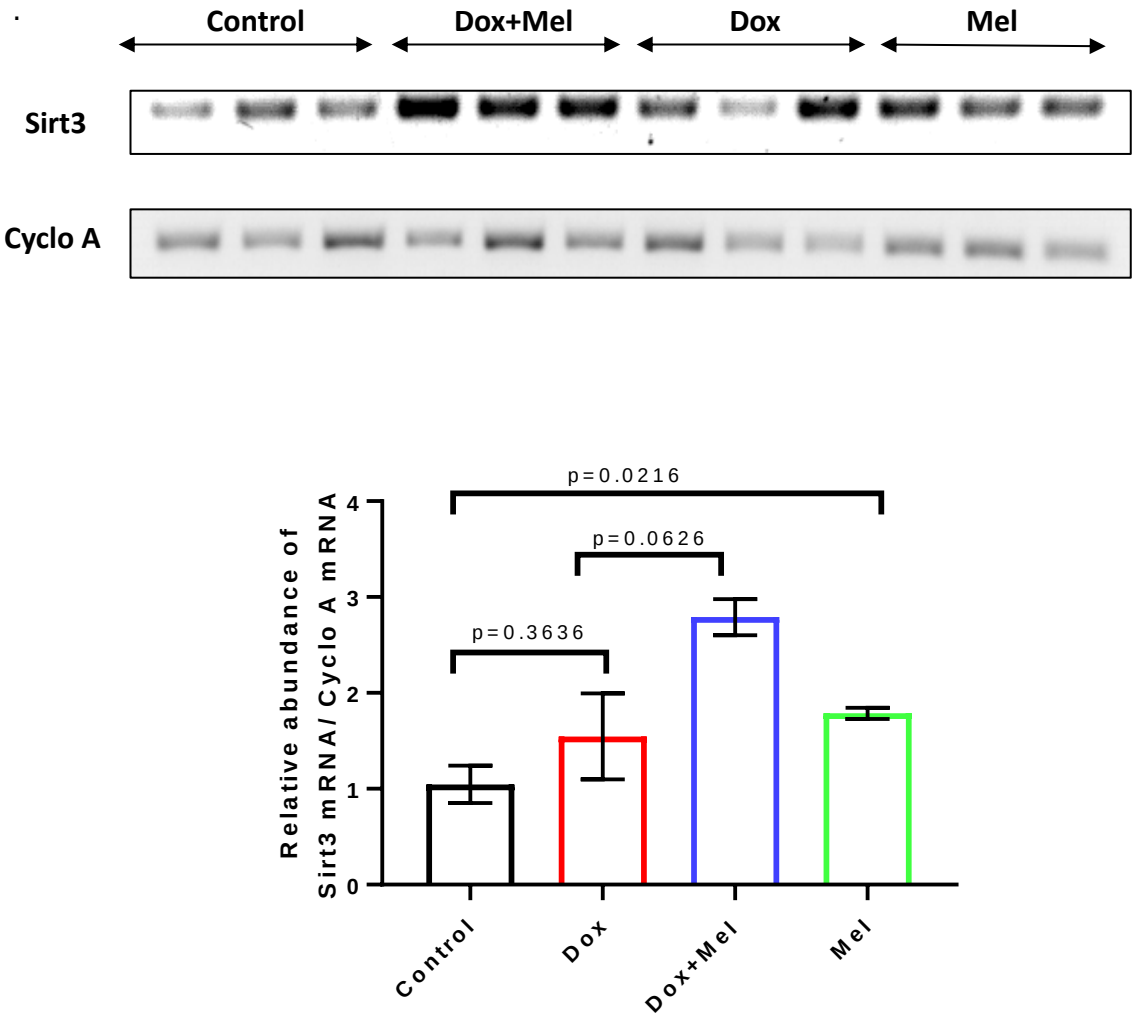

Figure 6.5. Melatonin enhanced *Sirt3* gene expression under doxorubicin-induced stress in H9c2 cells. Cells were DOX -treated (0.5 µM, 24 hrs) with and without melatonin (1µM). The results presented are mean ± SEM, n= 3. One-Way ANOVA: F (3, 8) = 7.77, p=0.0094. Data considered statistically significant at p≤0.05.

6.2.6. Parp 1

Melatonin attenuates Dox-induced downregulation of Parp 1 mRNA in H9c2 cells (Figure 6.6).

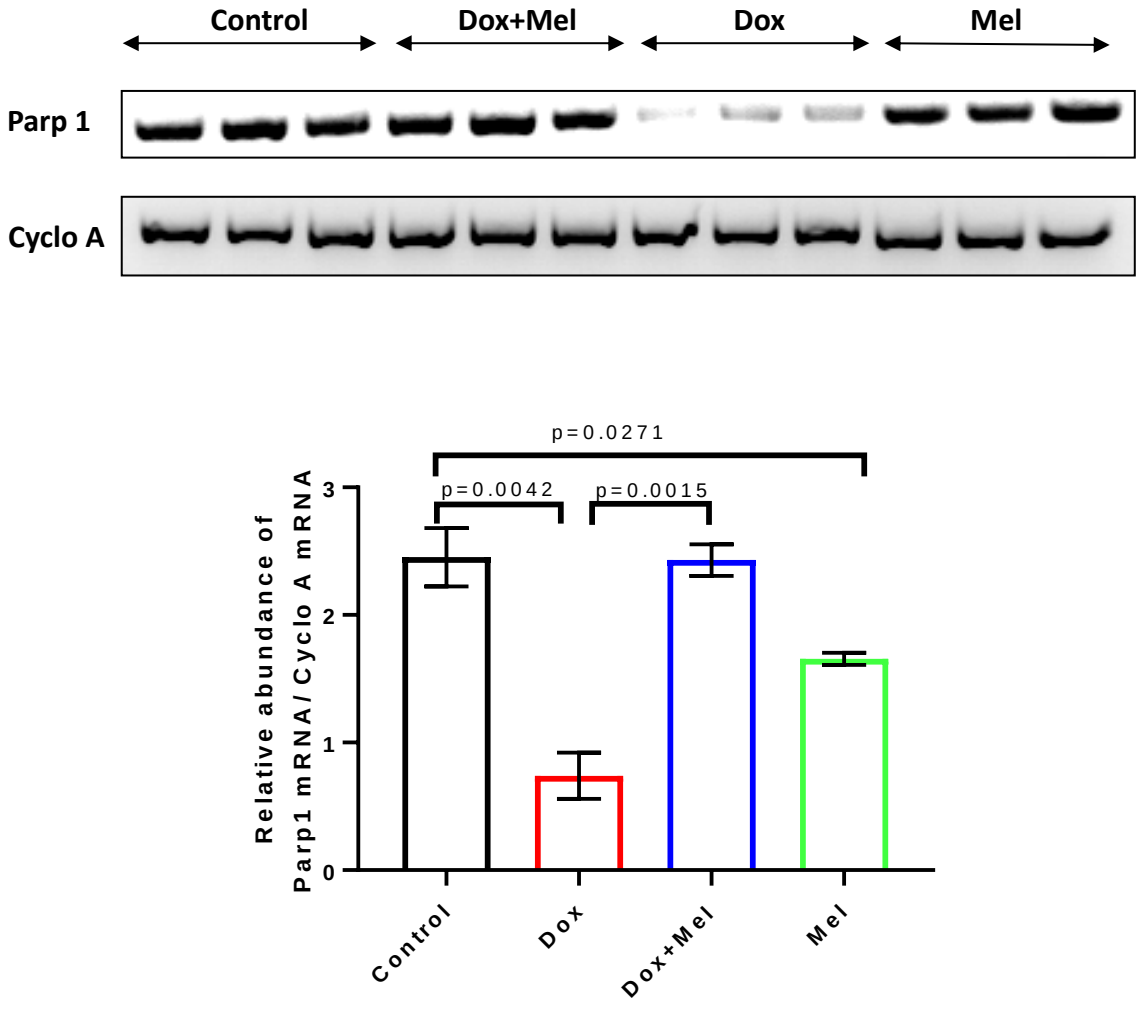

Figure 6.6. Melatonin attenuates doxorubicin downregulation of *Parp 1* gene expression in H9c2 cells. Cells were DOX - treated (0.5 µM, 24 hrs) with and without melatonin (1µM). The results presented are mean ± SEM, n= 3. One-Way ANOVA: F (3, 8) = 25.51, p=0.0002. Data considered statistically significant at p≤0.05.

6.2.7. Parp 2

Melatonin attenuates DOX-induced downregulation of Parp 2 mRNA in H9c2 cells (Figure 6.7).

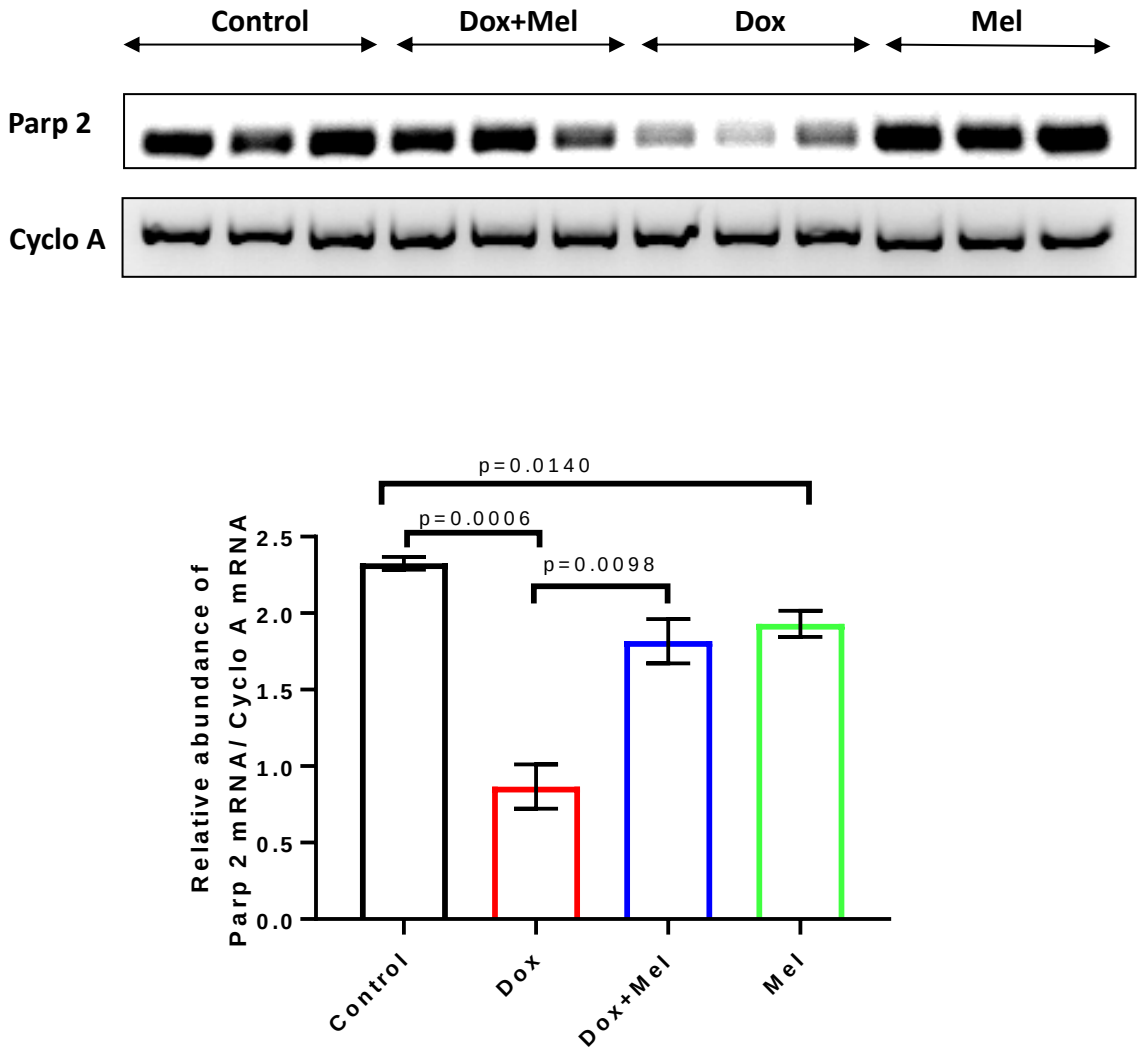

Figure 6.7. Melatonin attenuates doxorubicin downregulation of *Parp 2* gene expression in H9c2 cells. Cells were DOX - treated (0.5 µM, 24 hrs) with and without melatonin (1µM). The results presented are mean ± SEM, n= 3. One-Way ANOVA: F (3, 8) = 29.95, p=0.0001. Data considered statistically significant at p≤0.05.

6.2.8 Ms1

Doxorubicin robustly decreased ms1 mRNA expression in H9c2 cells (Figure 6.8). Melatonin pre-treatment partially reversed this inhibition in ms1 gene expression,

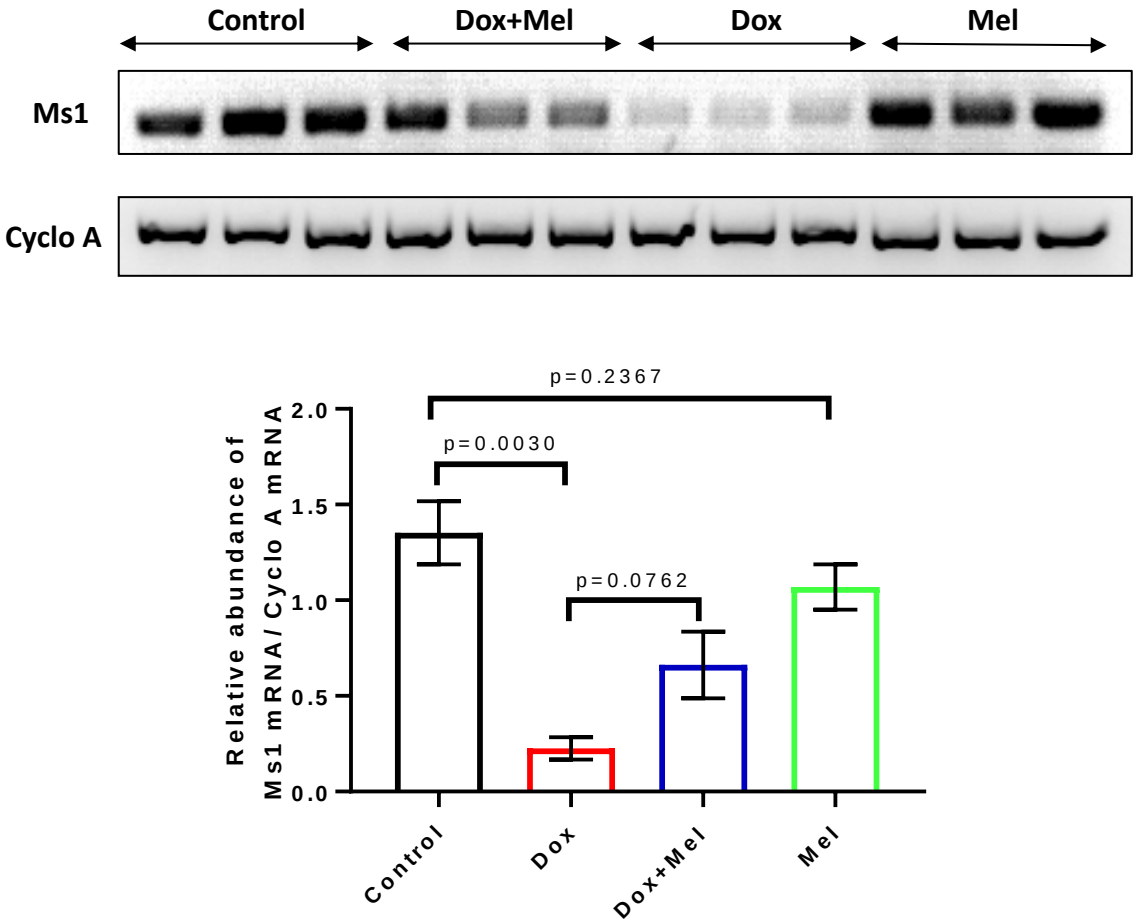

Figure 6.8. Melatonin attenuates doxorubicin downregulation of *Ms1* gene expression in H9c2 cells. Cells were DOX - treated (0.5 µM, 24 hrs) with and without melatonin (1µM). The results presented are mean ± SEM, n= 3. One-Way ANOVA: F (3, 8) = 12.86, p=0.0020. Data considered statistically significant at p≤0.05.

In order to confirm the authenticity of the semi-quantitative gene analysis study, *Ms1* was measured using real-time qPCR (Figure 6.9).

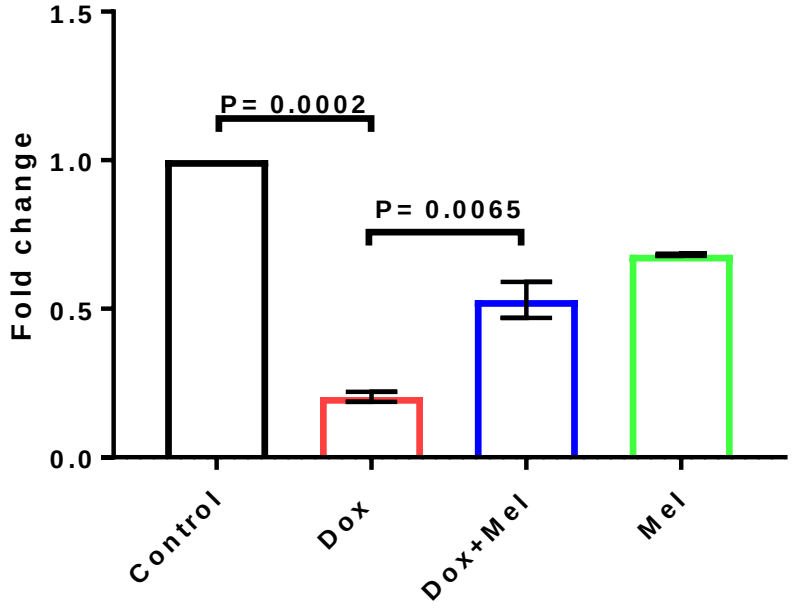

Figure 6.9: Melatonin attenuates doxorubicin-induced downregulation of *Ms1* gene expression in H9c2 cells measured using quantitative PCR. . Cells were DOX -treated (0.5 µM, 24 hrs) with and without melatonin (1µM). The results presented are mean ± SEM, n= 3. One-Way ANOVA: F (3, 4) = 109.5, p=0.0003. Data considered statistically significant at p≤0.05.

6.2.9 Serca2a

Doxorubicin treatment decreased the expression of Serca2a mRNA in H9c2 cells (Figure 6.10), which was partially reversed by melatonin.

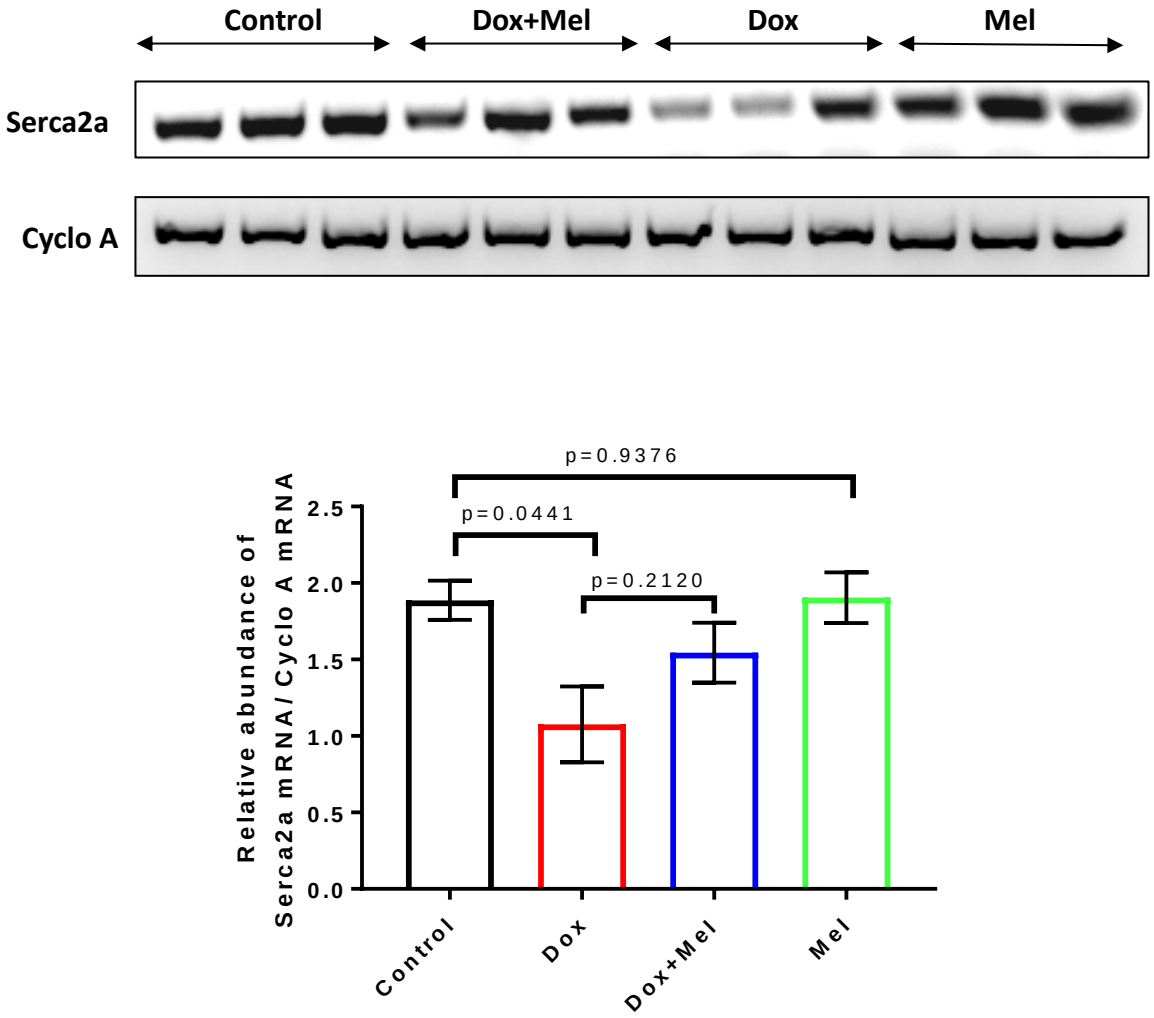

Figure 6.10. Melatonin attenuates doxorubicin downregulation of *Serca2a* gene expression in H9c2 cells. Cells were DOX - treated (0.5 µM, 24 hrs) with and without melatonin (1µM). The results presented are mean ± SEM, n= 3. One-Way ANOVA: F (3, 8) = 4.20, p=0.0464. Data considered statistically significant at p≤0.05.

In order to confirm the authenticity of the semi-quantitative gene analysis study, *Serca2a* was measured using real-time qPCR (Figure 6.11).

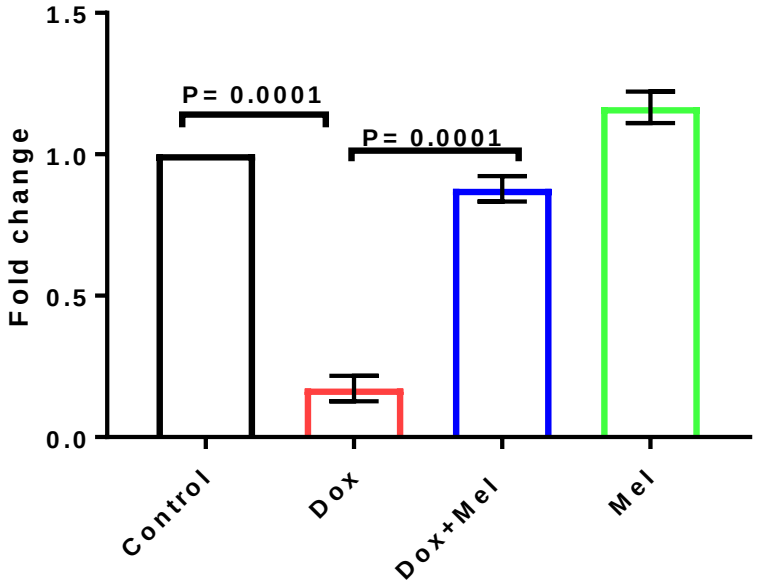

Figure 6.11: Melatonin blocks doxorubicin-induced downregulation of *Serca2a* gene expression in H9c2 cells measured using quantitative PCR. Cells were DOX -treated (0.5 µM, 24 hrs) with and without melatonin (1µM). The results presented are mean ± SEM, n= 3. One-Way ANOVA: F (3, 8) = 12.26, p=0.0023. Data considered statistically significant at p≤0.05.

6.2.10 Scn5a

Doxorubicin-induced stress dramatically increased Scn5a gene expression in H9c2 cells, which was blocked by melatonin (Figure 6.12).

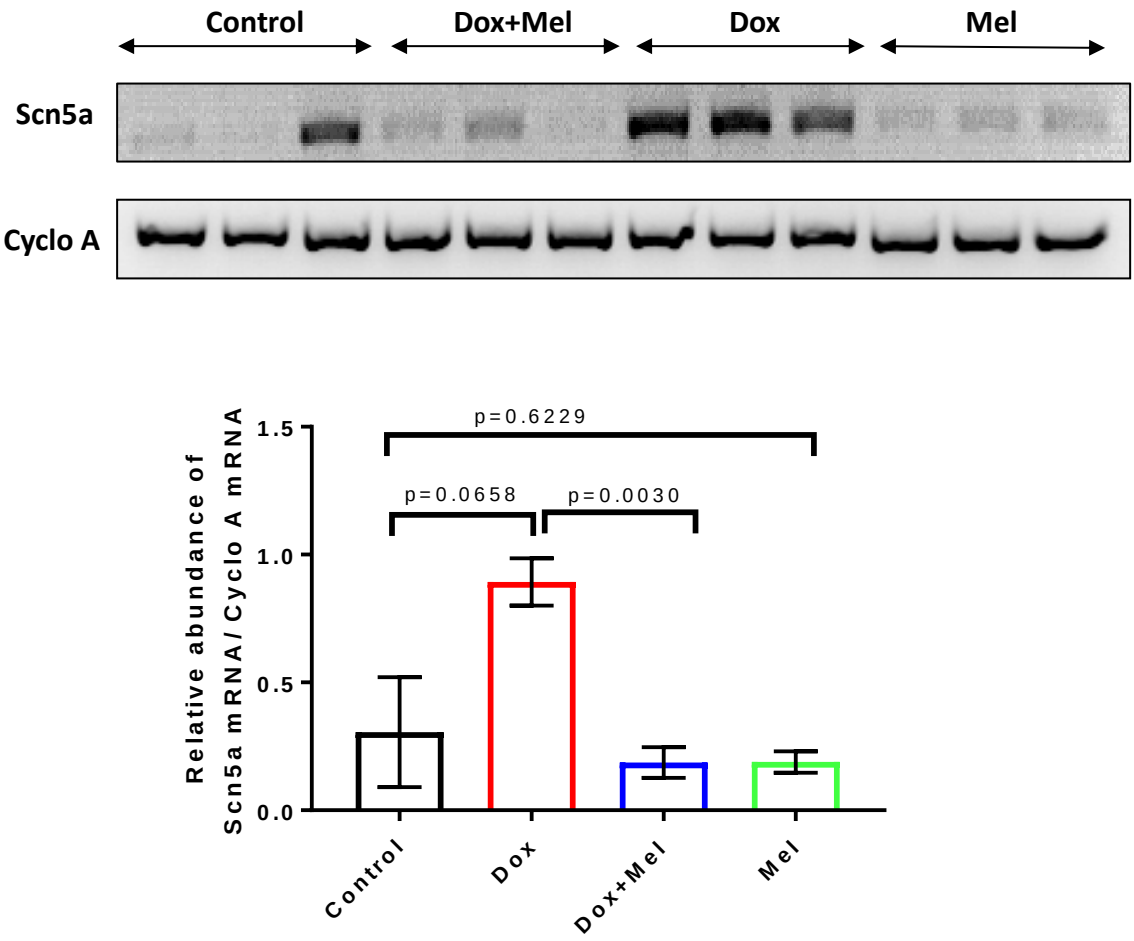

Figure 6.12. Doxorubicin-induced stress increased *Scn5a* gene expression which was blocked by melatonin in H9c2 cells. Cells were DOX - treated (0.5 µM, 24 hrs) with and without melatonin (1µM). The results presented are mean ± SEM, n= 3. One-Way ANOVA: F (3, 8) = 7.60, p=0.0100. Data considered statistically significant at p≤0.05

In order to confirm the authenticity of the semi-quantitative gene analysis study, *Scn5a* was measured using real-time qPCR (Figure 6.13).

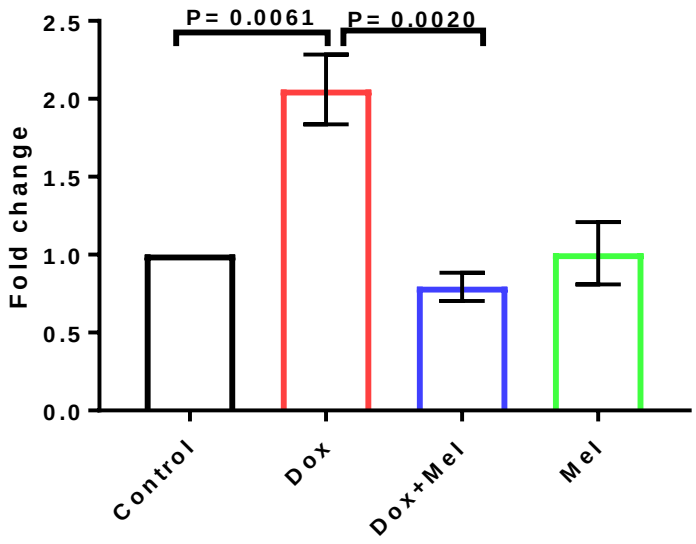

Figure 6.13: Melatonin blocked Dox-induced upregulation of *Scn5a* gene expression in H9c2 cells using quantitative PCR. Cells were DOX - treated (0.5 µM, 24 hrs) with and without melatonin (1µM). The results presented are mean ± SEM, n= 3. One-Way ANOVA: F (3, 8) = 13.3, p=0.0018. Data considered statistically significant at p≤0.05

6.2.11 Myh7

Doxorubicin-induced stress dramatically increased Myh7 gene expression in H9c2 cells, which was partially reversed by melatonin (Figure 6.14).

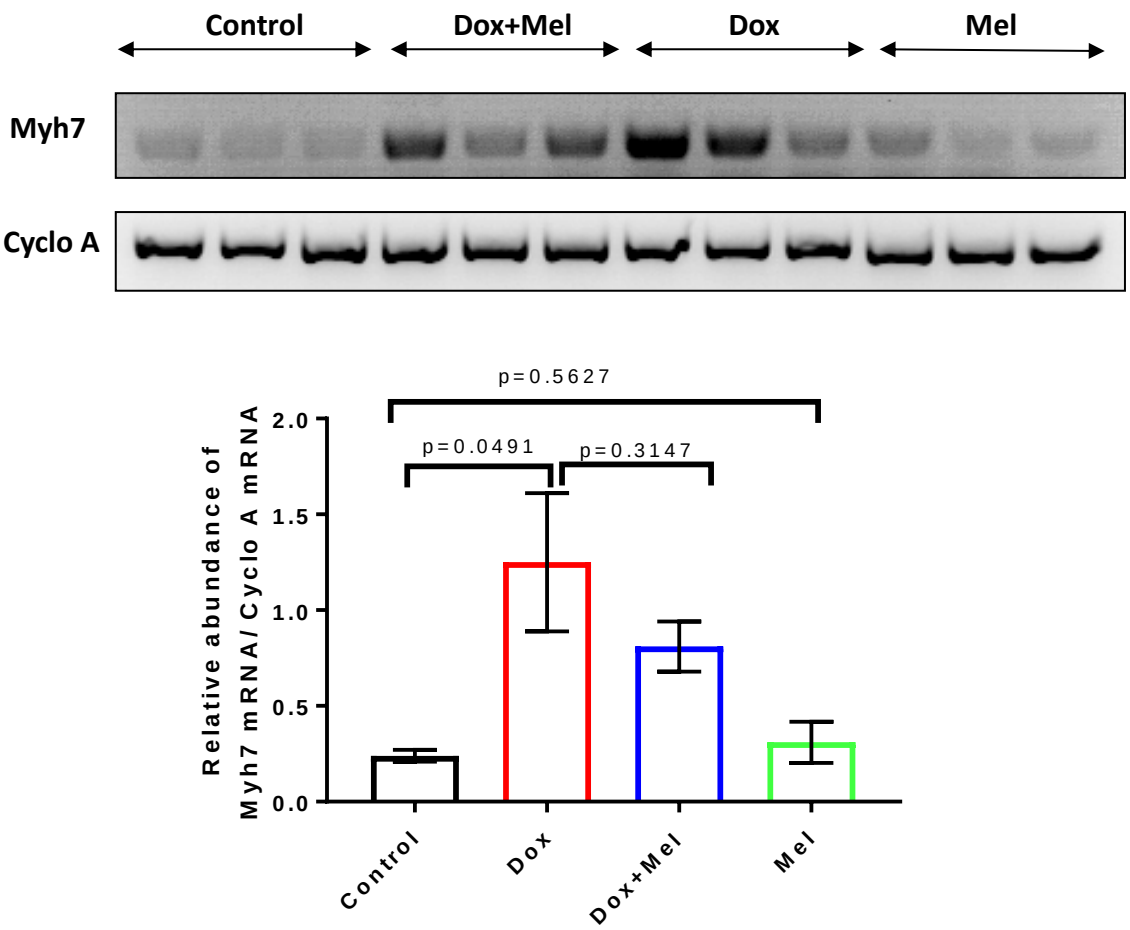

Figure 6.14. Doxorubicin increased *Myh7* gene expression which was partially reversed by melatonin in H9c2 cells. Cells were DOX - treated (0.5 µM, 24 hrs) with and without melatonin (1µM). The results presented are mean ± SEM, n= 3. One-Way ANOVA: F (3, 8) = 5.61 and p=0.0228. Data considered statistically significant at p≤0.05

6.2.12. UCP 2

Doxorubicin decreased UCP2 gene expression in H9c2 cells which was attenuated by melatonin. Of interest, melatonin alone significantly increased UCP2 gene expression (Figure 6.15).

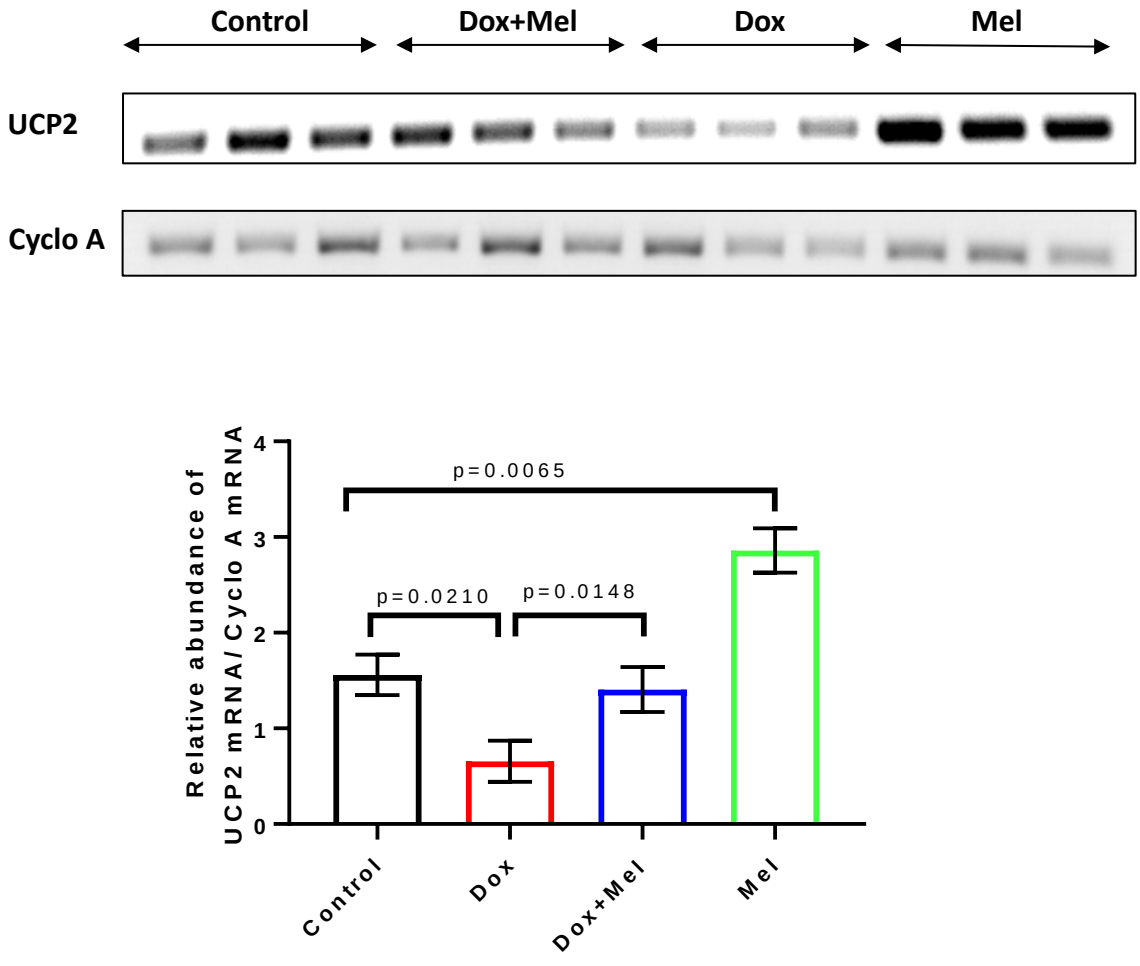

Figure 6.15. Melatonin attenuates doxorubicin downregulation of *UCP2* gene expression in H9c2 cells. Cells were DOX - treated (0.5 µM, 24 hrs) with and without melatonin (1µM). The results presented are mean ± SEM, n= 3. One-Way ANOVA: F (3, 8) = 35.02 and p=0.0001. Data considered statistically significant at p≤0.05.

In order to confirm the authenticity of the semi-quantitative gene analysis study, *UCP2* was measured using real-time qPCR (Figure 6.16).

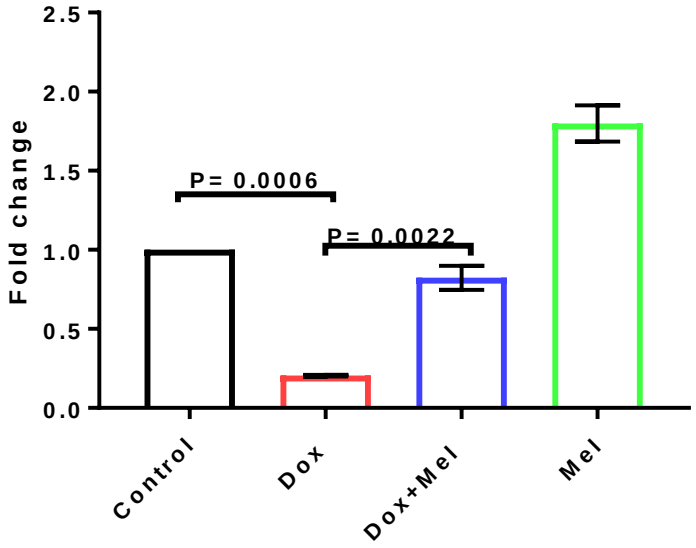

Figure 6.16: Melatonin blocks doxorubicin-induced downregulation of *UCP2* gene expression in H9c2 cells. Cells were DOX -treated (0.5 µM, 24 hrs) with and without melatonin (1µM). The results presented are mean ± SEM, n= 3. One-Way ANOVA: F (3, 8) = 10.38 and p=0.0039. Data considered statistically significant at p≤0.05

6.2.13 Bcl2

Doxorubicin-induced stress increased Bcl2 gene expression in H9c2 cells which was partially reversed by melatonin (Figure 6.17).

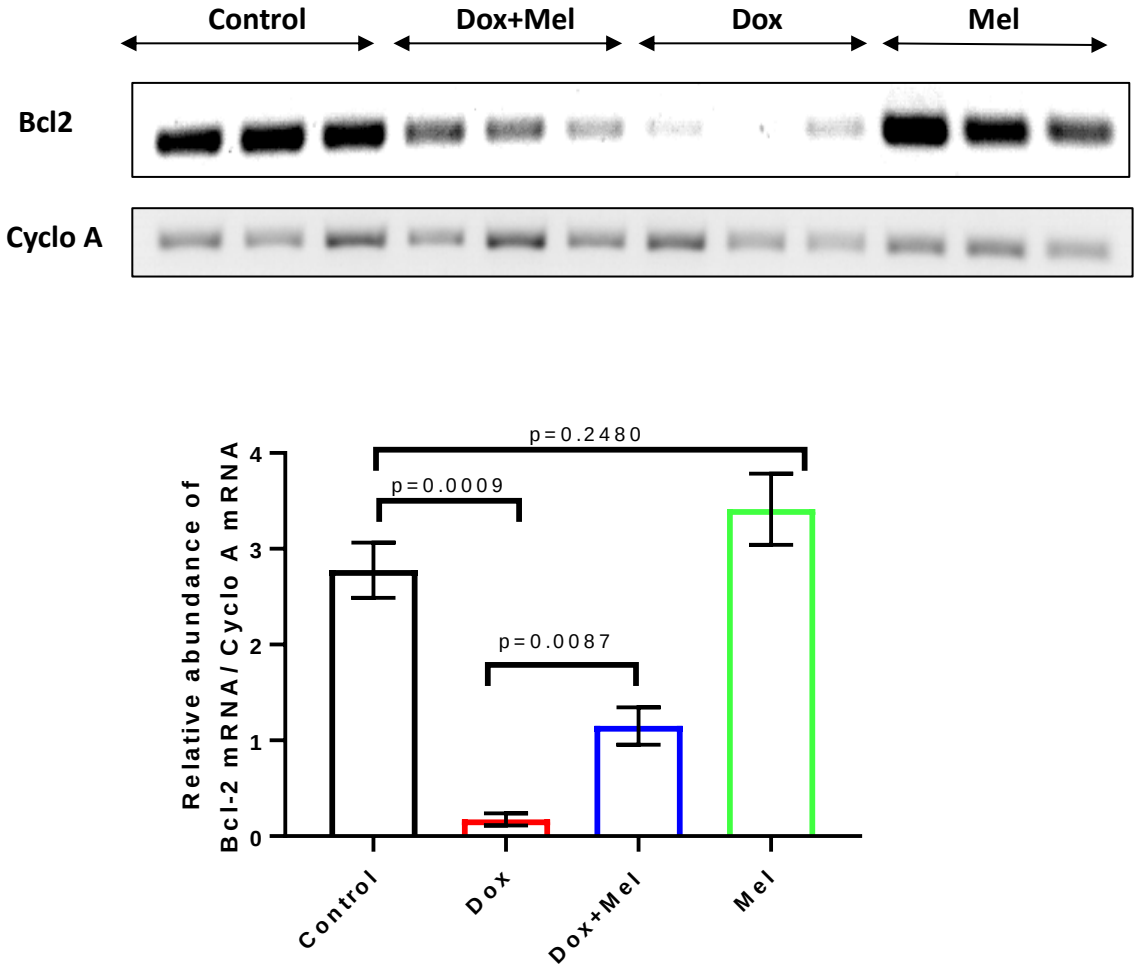

Figure 6.17. Melatonin attenuates doxorubicin downregulation of *Bcl2* gene expression in H9c2 cells. Cells were DOX - treated (0.5 µM, 24 hrs) with and without melatonin (1µM). The results presented are mean ± SEM, n= 3. One-Way ANOVA: F (3, 8) = 33.38 and p=0.0001. Data considered statistically significant at p≤0.05.

6.2.14. Bcl-xL

Melatonin enhanced Bcl-xL gene expression in H9c2 cells under DOX-induced stress (Figure 6.18).

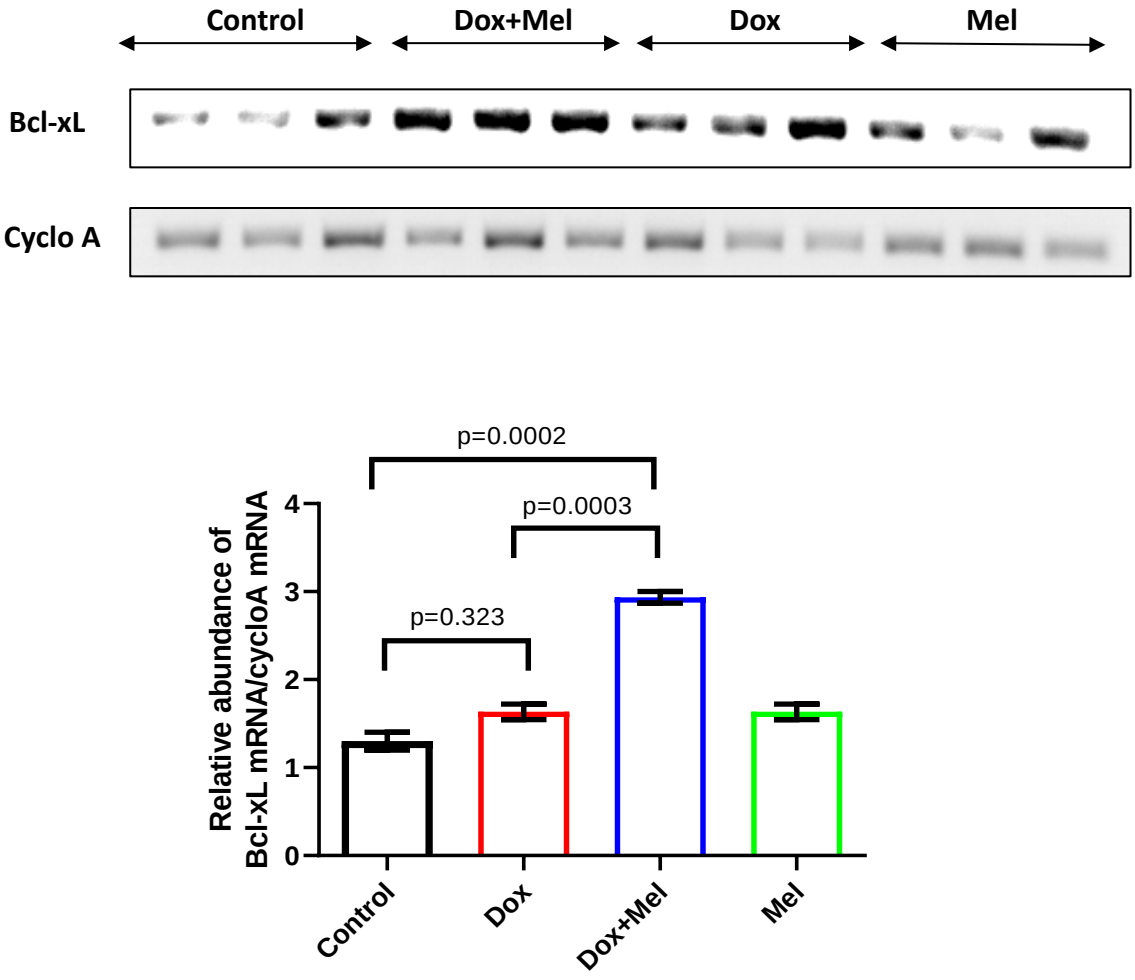

Figure 6.18. Melatonin enhanced Bcl-xL gene expression in H9c2 cells under doxorubicin-induced stress. Cells were DOX -treated (0.5 µM, 24 hrs) with and without melatonin (1µM). The results presented are mean ± SEM, n= 3. One-Way ANOVA: F (3, 8) = 69.67 and p=0.0001. Data considered statistically significant at p≤0.05.

6.3. Discussion

The global use of some anti-cancer drugs (in particular DOX) has been limited because of their common adverse effect of cardiotoxicity including heart failure. In the current project, DOX has been shown to cause acute mitochondrial dysfunction in OXPHOS and glycolysis (Chapter 4). Cell viability assays have demonstrated that DOX-treatment significantly induced apoptosis in H9c2 cells (Chapter 5). Interestingly, melatonin pre-treatment dramatically inhibited the deleterious effect of DOX on cardiac cell function and survival. However, the putative mechanisms of action of melatonin in these processes are unknown. In the current chapter, altered gene expression profiles were examined in DOX-treated cells.

The main important finding of this study was:

1. Doxorubicin treatment altered gene expression in fundamental biological processes such as mitochondrial function, cardiac electrical coupling, cell survival, cardiac remodelling and heart failure.
2. Melatonin treatment has mainly attenuated or blocked the negative effect of DOX-treatment.

H9c2 cells were treated with doxorubicin (0.5µM) and melatonin (1µM) for 24hrs. The semi-quantitative PCR technique screened for several genes involved in mitochondrial dysfunction, apoptosis, arrhythmias, cardiac remodelling and heart failure. Gene expression was studied among the genes of interest to determine if doxorubicin can alter gene expression and if melatonin was able to attenuate this effect.

ROS production from mitochondrial respiration is triggered by doxorubicin, affecting the ATP production in the cells and leading to mitochondrial dysfunction. During this process certain mitochondrial related genes becomes affected and starts to express differently (Kiyuna et al, 2018). The genes of interest in mitochondrial dysfunction were *Cav3, Mfn1, Drp1, Parp1, Parp2 and Sirt3.* The data represented that doxorubicin treatment

downregulated the expression of all these genes when compared with the control group. In the presence of melatonin, the genes were upregulated and restored back to functionality.

Cardiac arrhythmias account for a significant portion of heart failure related deaths (Sadredini et al, 2016). Arrhythmias are mostly caused by calcium mediated premature action potentials that arise from so called early or delayed after depolarisations. These heart beats cause premature ventricle contractions or short runs of ventricular tachycardia, such as long QT syndrome (Tse, 2016). The target gene involved in arrhythmia is *Scn5a* which is upregulated by doxorubicin induced cardiotoxicity to attain gain of function state which causes ventricular arrhythmias. In the presence of melatonin, the gene is downregulated and the functionality is restored.

Cardiomyocytes apoptosis is one of the latter stages in heart failure. Myocardial impairment induced by doxorubicin may involve myocyte apoptosis mediated by oxidative free radical formation (Kotamraju et al, 2000). Anti-apoptotic genes, *Bcl2, Bcl-xL* and *UCP2* were downregulated by doxorubicin when compared with control and melatonin attenuates this effect.

The myocardial injury after arrhythmias and apoptosis (triggered by doxorubicin) leads to the development of cardiac remodelling involving the increase of the left ventricular cavity. The cardiac structure changes influencing the left ventricular function. Cardiomyocytes become enlarged to increase muscle mass to reduce wall stress (Watkins et al, 2011). Mutations in β-Myosin heavy chain encoded by the gene *Myh7* which is upregulated and can be seen in left ventricular hypertrophy. Nuclear receptor transcription factors regulate cardiac metabolism, among them *PPAR-*□ is downregulated in the remodelling of the heart. In addition *Ms1* is a myofibrillar protein in cardiac muscle and involved in cardiac remodelling and the hypertrophic response. The gene is downregulated in response towards cardiac remodelling.

Following cardiac remodelling the final stage ends in heart failure. An excessive preload overwhelms the contractility of the heart, resulting in decreased cardiac output characterized by both systolic and diastolic

function. In heart failure there is a disturbed mitochondrial calcium cycling, which involves *Serca2a* gene involved in removing Ca^{2+} into the sarcoplasmic reticulum during diastole. This gene is downregulated in heart failure with loss of function.

A newly identified protein that is essential for cardiac development and stress response is ms1. MS1 is a myofibrillar protein involved in the regulation of gene expression in both cardiac and skeletal muscle. It is also known as striated muscle activator of Rho Signalling and Serum Response Factor dependent transcription (STARS) (Arai et al, 2002) or Actin-binding Rho-activating protein (ABRA) (Troidl et al, 2009). It is highly involved in cardiac remodelling and the hypertrophic response. Cardiomyocytes under physiological stress take adaptive responses via activation of Mitogen-Activated Protein Kinase (MAPK) pathways. These pathways mediate changes in gene expression by targeting transcription factors, including those that activate the SRE (Kyriakis et al, 2012). The stress-activated MAPKs, c-Jun N-terminal Kinase (JNK) and p38-MAPK, are activated strongly by cardiac ischaemia/reperfusion injury.

Both the JNK and p38 pathway are involved in mediating diverse adaptive responses in myocytes, including protection from redox stresses, ischaemic preconditioning and the induction of muscle hypertrophy. MS1 induction by mechanical loading activates downstream stress-responsive pathways converging on ternary complex factors (TCF)/SRF, which are a known target of stress-activated MAPKs such as JNK (Whitmarsh et al, 1997; Kuwahara et al, 2005). MS1 had shown reduced expression in H9c2 cells under doxorubicin treatment. It is known that MS1 promoter may be a downstream target for the JNK signalling pathway.The MS1 promoter has been characterised in some detail with binding sites for several transcription factors having been identified and some of these may be JNK targets (Chong et al, 2012; Ounzain et al, 2012). Of particular interest is an SRF binding site at an SRE located 305 base pairs upstream of the transcription start site (Chong et al, 2012). SRF is known to interact with a family of TCFs which are directly phosphorylated by JNK and other MAPKs, thus providing a possible mechanism for JNK mediated regulation of the MS1 promoter. In the

presence of DOX-induced stress it is conceivable that the signalling pathway of JNK and MAPKs are disrupted and the changes affect the transcription of the ms1 gene leading to downregulation and whereby melatonin may interfere with this pathway to attenuate the downregulation of ms1.

Calcium mishandling is a critical hallmark of cardiac dysfunction and heart failure; one key factor essential for calcium homeostasis in cardiomyocytes is SERCA2a. SERCA2a is thought to have physiologically strategic and intricate roles in cardiac electrophysiological and mechanical function. Its diastolic translocation of released Ca^{2+} from cytosol to SR minimizes cytosolic [Ca^{2+}]. This ensures full myocardial relaxation, a normal ventricular diastolic compliance and filling, and minimizes delayed after-potentials that would otherwise compromise membrane electrophysiological stability. These functions thus prevent the diastolic dysfunction and arrhythmic tendency characteristic of cardiac failure (Huang, 2013).

Doxorubicin is a major contributory factor for the death of cardiomyocytes, including oxidative stress, calcium overload and mitochondrial permeability transition pore (mPTP) opening. Calcium overload results in part from excessive sarco/endoplasmic reticulum (SR/ER) Ca^{2+} release and Ca^{2+} influx through the plasma membrane. Impaired calcium reuptake resulting from decreased expression and activity of SERCA2a is a hallmark of HF.

Doxorubicin is known to modulate the PI3K/Akt and the MAPK/ERK1/2 signalling pathways itself and may contribute to its cardiotoxicity. PI3K/Akt is known to reduce oxidative stress and decrease mPTP opening (Maulik et al, 2018). Hu and colleagues (2018) have shown that H9C2 cells undergoing simulative hypoxia/reoxygenation (H/R) induction and they observed melatonin treatment promoted phosphorylation of ERK1 in cardiomyocytes against H/R. To further elucidate the underlying mechanism for protective effect of melatonin cardiomyocytes against H/R, Hu et al (2018) observed the effects of melatonin on expression of SERCA2a. Their results showed SERCA2a expression is decreased during H/R and melatonin inhibited the downregulation of SERCA2a due to H/Rin cardiomyocytes. *In vivo* studies further confirmed that melatonin regulates the expression of SERCA2a via

ERK1 (Gomez et al, 2016; Hu et al, 2018). Therefore, one of the mechanism by which melatonin protect cardiomyocytes against reperfusion injury and oxidative stress maybe through modulation of SERCA2a, attenuating calcium overload via ERK1 pathway.

An immediate adverse effect of DOX-treatment in humans is cardiac arrhythmias, which can be lethal. A key factor that regulates the correct electrical firing and coupling of the cardiac action potential (AP) is a protein called Scn5a. Scn5a gene is member of the human voltage-gated sodium channel gene family and encodes alpha subunit of the main cardiac sodium channel $Na_v1.5$. $Na_v1.5$ is known to be responsible for maintaining the normal function of inward sodium current. *Scn5A* −/− mice are not viable, while *Scn5A* +/− knockout mice display cardiac conduction defects and ventricular tachycardia (Papadatos et al, 2002).

Doxorubicin induced free radical formation in mitochondria and sarcoplasmic reticulum alters the membrane potential of the sodium gated ion channels *(*Nordgren et al., 2017). Sodium current participates in phase 0 and 2 of the AP, which is an important determinant on the production of heart rhythms, normal conduction, and maintenance of excitement. As a result, the *SCN5A* variants would potentially cause disorganisation of the cardiac electrophysiological system, produce various arrhythmias and result in structural heart diseases due the loss of function and gain of function states (Onwuli et al, 2017). The gain of function state of Scn5a increase intracellular sodium concentration thereby causing a secondary increase in intracellular calcium that, in turn, leads to cellular remodelling, arrhythmia and heart failure (Zhang et al, 2018).

Recently a study has shown that *SCN5A* expression is regulated by the GATA4 transcription factor in the human heart. GATA4 synergises with GATA5 in the activation of the *SCN5A* gene via binding to GATA-BS within the *SCN5A* proximal promoter and intron 1 regions. GATA4 is considered a master regulator of cardiac transcriptional networks and plays a key role in cardio genesis and in adult cardiac cells (Tarradas et al, 2017). Of

interest, Ouzain and colleagues (2012) have demonstrated that GATA4 negatively regulates MS1 expression in striated muscle cells.

Genetic variants in *GATA4* (or *GATA5*) genes could be related to arrhythmogenic diseases via dysregulation of *SCN5A* expression. The effect of mutations on GATA4 (and GATA5) function could determine the levels of $Na_V1.5$ channel expression, which could explain the variability of phenotypes associated with *SCN5A*-related arrhythmias. At present the mechanism whereby DOX induced Scn5a expression in cardiomyocytes is unknown. However, it is reasonable to suggest that it can affect the transcription factors GATA 4 and GATA 5 which in turn can regulate SCN5a gene expression. Melatonin provides protection against DOX-induced cardiac electrophysiology uncoupling via balancing gene alteration such as changes in Scn5a expression.

Metabolic dysfunction in the heart is a key disorder and contributing factor to progressive heart failure. Uncoupling proteins, such as UCP2, are cationic carrier protein which plays an important role in regulation of metabolism, for example ROS production, glucose control and immunity and implicated pathologies such as heart failure, diabetes, and cancer (Harper et al, 2004). Uncoupling proteins are located in the mitochondrial inner membrane which can promote the proton leak across the mitochondrial inner membrane. It is an essential regulator of mitochondrial membrane potential, that disperse the mitochondria proton gradient by translocating H+ across the inner membrane, following with respiratory activity, ROS and ATP generation (Yu et al, 2000). A study on the mechanism of melatonin on DOX-induced cardiotoxicity in relation to UCP2 expression is unknown. The current study indicated that DOX dramatically reduced UCP2 expression which was blocked by melatonin. Indeed, melatonin alone significantly increased basal UCP2 mRNA levels compared to untreated control cells.

The precise mechanism whereby UCP dysfunction may lead to heart failure is unclear. Wang *et al.* (2018) recently demonstrated that DOX interacts with general control nonderepressible 2 (GCN2), a protein kinase that modulates amino acid metabolism in response to nutrient deprivation caused by cellular

stress (Anda et al., *2017*). This interaction leads to decreased expression of UCP2 as well as Bcl-2 and subsequently initiated cell death and heart failure (Figure 6.19). Data from the current project supports the notion that the presence of enough melatonin may reduce oxidative stress in the mitochondria by inhibiting the activation of GCN2 by DOX. This may be through its antioxidant mechanism through ROS scavenging and MPTP inhibition as well as UCP2 gene activation (Tan et al., *2016)*. In turn, the activated UCP2 prevents cardiomyocytes damage by inducing proton leak in inner mitochondrial membrane to reduce mitochondrial membrane potential to increase oxygen consumption as demonstrated in previous studies (Pecquer et al., 2002; Moon et al., 2015).

Chen and colleagues (2018) provided additional data to support the role that UCP2 is an anti-apoptotic factor in H9c2 cells. UCP2 knockdown induced apoptosis whereas a drug which induced UCP2 expression (ursolic acid) attenuated hypoxia-reoxygenation induced apoptosis via a protective p38 signalling pathway.

Thus, UCP2 homeostasis is modulated by melatonin to decrease DOX-induced oxidative stress due to melatonin's mitochondrial targeted antioxidants initiating mitochondrial protection via UCP2 activation, to reduce cardiomyocytes oxidative stress. Of interest, the present project has also demonstrated that DOX reduced Bcl2 expression in H9c2 cells which was attenuated by melatonin.

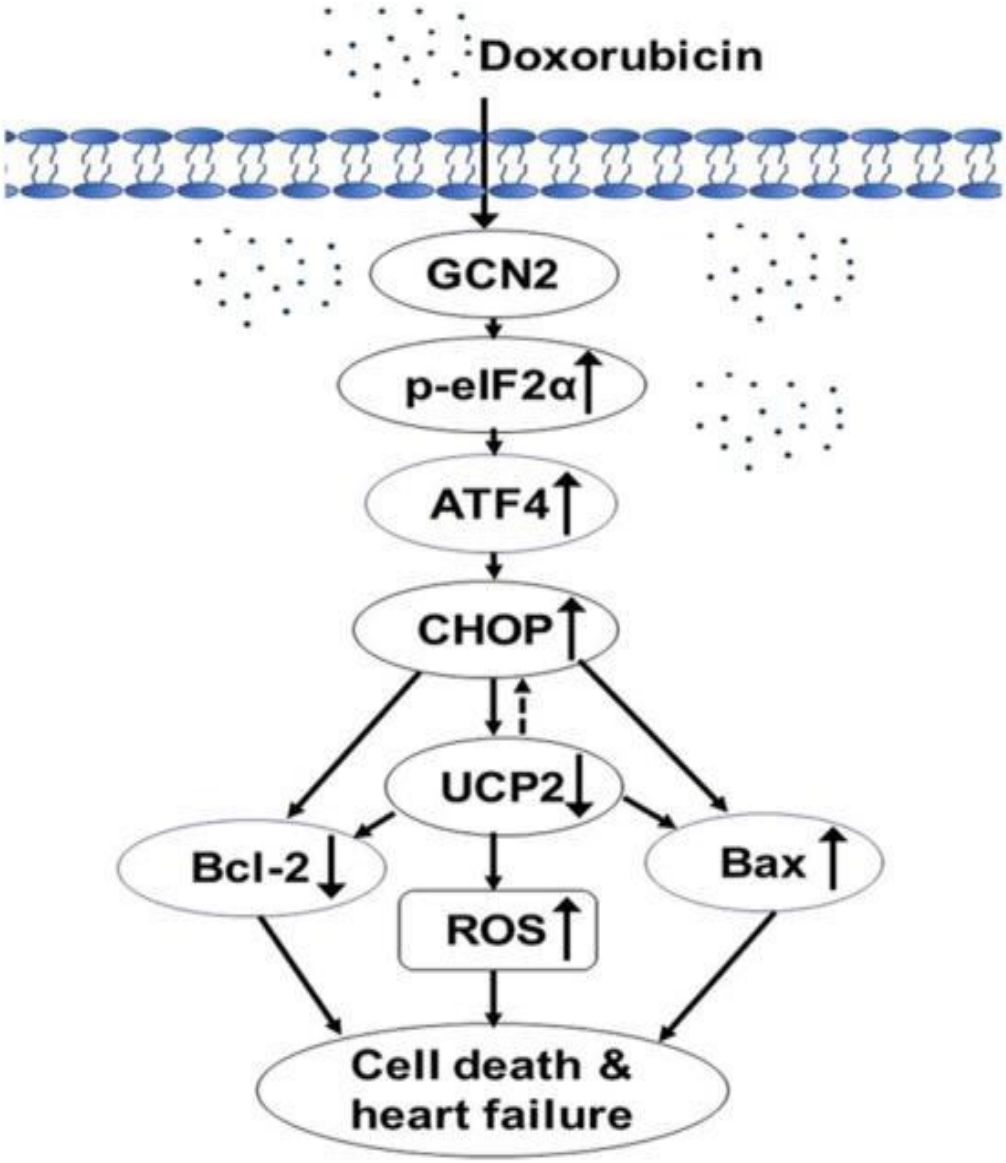

Figure 6.19. A putative mechanism of the cardio protective role of melatonin involving UCP2. Doxorubicin interacts with GCN2 and activates to cellular stress response which initiates decrease in UCP2. Melatonin may reduce cellular stress by inhibiting the activation of GCN2 by doxorubicin via ROS scavenging and inhibiting mPTP opening, reducing cellular stress, which in turn may increase UCP2 and reduce cell death and heart failure (adapted from Wang et al, 2018).

Chapter 7.

General Discussion

7.1 Discussion

A major global limitation of drug intervention in chronic diseases is organ damage such as cardiotoxicity. More than 30% of new drug candidates do not progress beyond phase I clinical trials because of cardiac complications. Indeed, more medicine are being identified as cardio toxic with the use of sensitive assays such as utilisation of human induced pluripotent stem cells derived cardiomyocytes and high-throughput electrophysiology screening techniques. However, the molecular and cellular mechanisms of drug-induced cardiotoxicity, in particular anti-cancer drugs, are unclear and mostly unknown.

In the present project, the metabolic dysfunctions in cardiomyocytes caused by groups of commonly used drugs were examined using the Seahorse assay. Using flow-cytometry and Alamar Blue staining methods, cardiomyocyte cell death caused drug-treatment was investigated. Finally, a putative gene pathway that may be central in drug-induced cardiotoxicity was delineated using PCR. Accumulative evidence demonstrated that the pineal hormone melatonin may play a beneficial role in cardio-protection and this was examined in the current project.

The main important findings of the current study were:

1. Diverse drugs including anti-depressants, anti-cancer, anti-cardiac arrhythmia, and statins, altered mitochondrial activity (OXPHOS, glycolysis) and compromised cardiomyocyte function.
2. Mitochondrial dysfunction caused by cardio toxic chemicals which induce oxidative stress (Isoproterenol, hydrogen peroxide) which was attenuated by melatonin treatment.
3. Doxorubicin, a commonly used anti-cancer drug robustly caused mitochondrial dysfunction and apoptosis in cardiomyocytes, was robustly blocked by melatonin.
4. Doxorubicin-treated cardiomyocytes dramatically altered gene expression in diverse regulatory pathways in apoptosis, metabolism,

cardiac conductivity, cardiac remodelling and heart failure. Melatonin pre-treatment attenuated these changes in gene expression.

In this study, H9c2 cells were examined under a diverse range of drugs. Hydrogen peroxide (200µM) and isoproterenol (10µM) are potent stress inducers in cardiomyocytes. They mimic ischemic conditions in cells by inducing oxidative stress (Ojha, 2010). Cardiotoxic drugs such as statins (10µM), doxorubicin (0.1µM), amiodarone (10µM), amitriptyline (10µM) and rosiglitazone (50µM) exert their toxic characteristics in cells to disrupt the metabolic function of the mitochondria and hinder the ATP production of the cells.

Cardiac cell function and metabolism is hindered by cardiotoxicity. The accumulation of drugs in the cardiomyocytes directly imposes threat on the mitochondria. As mentioned previously in above chapters, these drugs have a high affinity for cardiolipin (Goormaghtigh, 1980), an integral component of the inner mitochondrial membrane. The binding of these drugs to cardiolipin does not allow for cardiolipin interaction with key respiratory complexes (Goormaghtigh, 1980). During normal physiological conditions, ROS are generated at very low levels, but can increase dramatically in pathophysiological conditions such as myocardial ischaemia/reperfusion (I/R) injury and cardiotoxicity (Paradies *et al*, 2010), causing a loss in the phospholipid cardiolipin, which in turn, is responsible for the loss of activity of the respiratory chain complexes I, III and IV (Paradies *et al*, 1999; Lochner *et al*, 2015). In particular, studies aimed at determining the sensitivity of respiratory complexes to cardio toxic drugs were found mainly located in complex I, III, and IV, with a specific vulnerability for complexes I (NADH dehydrogenase) and IV (cytochrome c oxidase), where there is an increased production of ROS (Marcillat et al, 1989). In addition mPTP opening is crucial in mitochondria where under normal circumstances, mPTP opening is closed preventing the loss of electrons and cytochrome c, however, cardiotoxic drugs have the ability to cause the opening of mPTP and disrupting the mitochondrial function.

Melatonin and its metabolites have the free radical scavenging abilities and acts as a robust anti-oxidant for the cells (Favero et al, 2017). The major target of melatonin is to inhibit the opening of the mitochondrial transition pore opening (MPTP). The opening of the MPTP is crucial for the apoptosis and necrosis of the cells with the release of cytochrome c. Melatonin effectively inhibits the opening of the MPTP and prevents the cells undergoing apoptosis during ischemia (Reiter et al, 2016).

Petrosillo and co-workers have demonstrated convincingly that melatonin effectively protects against I/R damage and the protection afforded by melatonin against mitochondrial dysfunction was associated with improvement in functional recovery during reperfusion (Petrosillo *et al*, 2003). The follow up work done in 2009, by the same group, found melatonin protects cardiomyocytes by inhibiting MPTP opening in the mitochondria (Petrosillo *et al*, 2009). It is generally accepted that melatonin exerts its cardio protective actions via its free radical scavenging activities as well as the induction of anti-oxidant enzymes (Hardeland, 2005; Cardinali *et al*, 2006). It is likely that abnormal mitochondrial function, decreased respiratory complex activity, increased ROS production, and augmented electron leakage and mPTP opening have all been the main reasons for failing mitochondrial function in the pathophysiology of drug-induced cardiotoxicity, however, melatonin has shown the potential to attenuate these effects and improve the functionality of the mitochondria much more efficiently within this acute time period.

Therefore, the drugs examined in the present thesis imposed direct metabolic dysfunction in cardiac cells affecting OXPHOS and glycolysis in cardiomyocytes by having an impact on the mitochondrial respiratory complexes. On the other hand, melatonin and its metabolites have the free radical scavenging abilities and acts as a robust anti-oxidant for the cells against cardiotoxicity (Favero et al, 2017). It improves the metabolic functions of the cell and inhibits the opening of mPTP which is crucial for maintaining mitochondrial metabolism functionality and prevents cell death (Reiter et al, 2016).

Futhermore, H9c2 cells were treated with doxorubicin (0.5µM) and melatonin (1µM) for 24hrs. The semi-quantitative PCR technique screened for several genes involved in mitochondrial dysfunction, apoptosis, arrhythmias, cardiac remodelling and heart failure. Gene expression was studied among the genes of interest to determine if doxorubicin can alter gene expression and if melatonin was able to attenuate this effect.

ROS production from mitochondrial respiration is triggered by doxorubicin, affecting the ATP production in the cells and leading to mitochondrial dysfunction. During this process certain mitochondrial related genes becomes affected and starts to express differently (Kiyuna et al, 2018). The genes of interest in mitochondrial dysfunction were *Cav3, Mfn1, Drp1, Parp1, Parp2 and Sirt3.* The data represented that doxorubicin treatment downregulated the expression of all these genes when compared with the control group. In the presence of melatonin the genes were upregulated and restored back to functionality. The target gene involved in arrhythmia is *Scn5a* which is upregulated by doxorubicin induced cardiotoxicity to attain gain of function state which causes ventricular arrhythmias. In the presence of melatonin, the gene is downregulated and the functionality is restored.

Cardiomyocytes apoptosis is one of the latter stages in heart failure. Myocardial impairment induced by doxorubicin may involve myocyte apoptosis mediated by oxidative free radical formation (Kotamraju et al, 2000). Anti-apoptotic genes, *Bcl2, Bcl-xL* and *UCP2* were downregulated by doxorubicin when compared with control and melatonin attenuates this effect.

The myocardial injury after arrhythmias and apoptosis (triggered by doxorubicin) leads to the development of cardiac remodelling involving the increase of the left ventricular cavity (Watkins et al, 2011). Mutations in β-Myosin heavy chain encoded by the gene *Myh7* which is upregulated and can be seen in left ventricular hypertrophy. Nuclear receptor transcription factors regulate cardiac metabolism, among them *PPAR-*□ is downregulated in the remodelling of the heart. In addition, *Ms1* is a myofibrillar protein in cardiac muscle and involved in cardiac remodelling and the hypertrophic

response. The gene is downregulated in response towards cardiac remodelling.

Following cardiac remodelling the final stage ends in heart failure. In heart failure there is a disturbed mitochondrial calcium cycling, which involves *Serca2a* gene involved in removing Ca^{2+} into the sarcoplasmic reticulum during diastole. This gene is downregulated in heart failure with loss of function.

To elucidate further, *Ms1, Serca2a, Scn5a* and *UCP2* genes were chosen after confirming with Semi-quantitative analysis to evaluate and quantify the changes in the gene expression among the different treatment groups. Quantitative real-time PCR was done on these genes involved in different stages of progressive heart failure. Doxorubicin downregulated the expression of *Ms1, Serca2a* and *UCP2* and upregulated the expression of *Scn5a* when compared with control. Melatonin attenuated this effect and restored the functionality of the genes. The data is confirmed previously by the Semi-quant PCR technique. The results from both these techniques are similar and display similar trend in gene expression in each different treatment groups.

Melatonin production declines with age in rodents and humans. Lower circulating levels of melatonin can give arise to metabolic dysfunction in cells and affecting other organ systems (Reiter et al, 2017). Melatonin in the systemic circulation of mammals quickly disappears from the blood presumably due to its uptake by cells, particularly when they are under high oxidative stress conditions. The measurement of the subcellular distribution of melatonin has shown that the concentration of this indole in the mitochondria greatly exceeds that in the blood. Melatonin presumably enters mitochondria through oligopeptide transporters. Thus, melatonin is specifically targeted to the mitochondria where it seems to function as an apex antioxidant (Reiter et al, 2017).

In the course of aging, the nocturnal melatonin peak is usually decreased, though with considerable inter-individual variability. Age-related reductions of melatonin can have different causes, a progressive deterioration of the SCN

in hypothalamus or of the neuronal transmission to the pineal gland (Skene and Swaab, 2003; Srinivasan et al, 2005). As a result, diseases and disorders associated with reduced melatonin secretion in humans can occur with age. Neurodegenerative disease (e.g. Alzheimer and Parkinson disease) patients have merely abolished melatonin rhythms. Amongst these myocardial infarction and coronary heart diseases are highly likely to occur with reduced levels of circulating melatonin in individuals and the most vulnerable are the elderly generation (Srinivasan et al, 2005; Wu and Swaab, 2007; Hardeland, 2012).

In such a case, melatonin may be re-considered as an adjunctive therapy to improve the treatment available for the diseases. In a study related with chronic insomnia, it was discovered that patients had associated with an increased risk of hypertension and elevated blood pressure. These individuals were treated with prolonged beta-blocker treatment, along with melatonin and discovered the sleep and behaviour patterns have improved with decreased hypertension in patients (Scheer et al, 2012; Li et al, 2015; Opie and Lecour, 2016). Thus, suggesting that melatonin is implicated in cardio protection and the molecular mechanism of such benefits may include decreased formation of free radicals during oxidative stress and reduced superoxide generation during cardiac injury.

The effect of calcium channel blockers were investigated in primary hypertensive patients to observe the blood pressure profiles. However, it did not greatly change the blood pressure profile, being, however, less effective at night (Lemmer, 2007). On the other hand, calcium channel blockers (e.g. Verapmil) have also shown to work better at night time along with melatonin infusion, stimulating melatonin production and improve the efficacy/ function the drug by lowering blood pressure against hypertensive conditions (Zhao et al, 2012).

Diez and colleagues (2013) provided evidence to suggest that melatonin reduced ischemia reperfusion-induced arrhythmias in rats. This work determined whether acute melatonin administration starting at the moment of reperfusion protects against ventricular arrhythmias in

Langendorff-perfused hearts isolated from fructose-fed rats, a dietary model of metabolic syndrome, and from spontaneous hypertensive rats. In both experimental models, there was metabolic alterations, a reduction in myocardial total antioxidant capacity and an increase in arterial pressure and NADPH oxidase activity. Melatonin initiated at reperfusion reduced the incidence of ventricular fibrillation from 83% to 33%. The severity of the arrhythmias progressively declined in melatonin-treated hearts. Melatonin induced a shortening of the action potential duration at the beginning of reperfusion and also a faster recovery of action potential amplitude (Diez et al, 2013). Therefore melatonin protects against ventricular fibrillation when administered at reperfusion, and these effects are maintained in hearts from rats exposed to major cardiovascular risk factors.

MPTP opening is an important event in cardiomyocyte cell death occurring during ischemia-reperfusion and therefore a possible target for cardio protection. A study group explored whether melatonin protects heart from reperfusion injury by inhibiting MPTP opening, probably via prevention of cardiolipin peroxidation. Isolated perfused rat hearts were subjected to global ischemia and reperfusion in the presence or absence of melatonin in a Langerdoff apparatus. Melatonin treatment significantly improves the functional recovery of Langerdoff hearts on reperfusion, reduces the infarct size, and decreases necrotic damage by the reduced release of lactate dehydrogenase. Also, mitochondria isolated from melatonin-treated hearts are less sensitive than mitochondria from reperfused hearts to MPTP opening demonstrated by their higher resistance to Ca^{2+}. Similar results were also obtained following treatment of ischemic-reperfused rat heart with cyclosporine A, a known inhibitor of MPTP opening. It demonstrated that melatonin prevents mitochondrial NAD(+) release and mitochondrial cytochrome c release and cardiolipin oxidation associated with ischemia-reperfusion (Petrosillo et al, 2009).

Early pinealectomy studies have shown that removal of the pineal gland reduces the mortality in animals and affects their seasonal growth in response to the circadian rhythms when compared to blinded study. Golden hamsters, especially males, blinded at 42 days of age respond with a rapid

increase in growth rate which varied seasonally. Seasonal response appears to be endogenous and not a consequence of photoperiod, temperature, age, sex or sexual activity. However, this response was modified by pinealectomy. Mortality over the 11 1/2 months of the study was increased in the blinded animals but was reversed by pinealectomy, where removal of the pineal gland had a direct effect on the mortality rate (Hoffman, 1983). Endogenous circulating melatonin from the pineal gland plays a vital role in the seasonal growth in animals and the removal of the pineal gland affects the circulating levels of melatonin which can decrease mortality and affect circadian rhythms and growth.

Pierpaoli and Bulian (2005) investigated the relationship between developmental role of the pineal complex during growth, fertility, and aging versus time. Transplantation of a very old pineal gland (with reduced melatonin secretion) into the thymus or under the kidney capsule of a young mouse produced acceleration of aging and early death. Groups of BALB/c male or female mice were surgically pinealectomized at the age of 3, 5, 7, 9, 14, and 18 months, and their life span was evaluated. Results showed that mice pinealectomized at younger age promoted acceleration of aging compared to older ages. The dominant role of the pineal in the initiation and progression of aging, as a death signal is clear. The evolutionary development role of the pineal gland had demonstrated its control over aging and its importance in regulating growth (Pierpaoli and Bulian, 2005). Older age stimulates lower production of melatonin secreted from the pineal gland.

Collectively, these data demonstrate the importance of melatonin in biological processes, health and well-being. Melatonin has shown multiple regulatory functions in organisms from increasing mortality to be a powerful antioxidant against ROS induced oxidative stress. It protects cardiomyocytes against cardiotoxicity induced by drugs and regulates gene expression of some key genes involved in the regulatory pathways of heart failure.

In conclusion, the present thesis provided novel insight into the mechanisms of drug-induced mitochondrial dysfunction and apoptosis in cardiomyocytes, which are hallmarks of heart failure. Doxorubicin altered gene expression in

numerous signalling pathways associated with cardiac disease and heart failure. Collectively, the current results provide evidence to suggest that the alteration in cardiac phenotype may be caused, at least in part, by the changes in gene expression and these were robustly inhibited by melatonin.

Chronopharmacology is one novel approach in the treatment of heart disease and cancer and the use of melatonin may confer benefits of cardio protection alongside drug treatments in humans. It is conceivable that melatonin may be used in conjunction with cardiotoxic drugs (like doxorubicin) to improve drug efficacy and safety. Delivering drug treatment during the night-time when melatonin is at its peak level may reduce the severity of early-onset cardiac dysfunction and future development of heart failure. Thus, co-treatment with melatonin may provide a new platform for intervention for cancers and heart-related diseases.

References

Abuzaid, A., et al. (2015). Acute Amiodarone Pulmonary Toxicity after Drug Holiday: A Case Report and Review of the Literature. *Case reports in cardiology*. **2015**, 927-438.

Acuna D., et al. (2005). Melatonin and nitric oxide: two required antagonists for mitochondrial homeostasis. *Endocrine*. **27**, 159–168.

Acuna D., et al. (2002). Melatonin, mitochondrial homeostasis and mitochondrial-related diseases. *Current Topics in Medicinal Chemistry*. **2**, 133–151.

Acuña., et al. (1986). Diurnal variations of benzodiapine binding in rat cerebral cortex: disruption by pinealectomy. *Journal of Pineal Research*. **3**, 101–109.

Acuna-Castroviejo, D., et al. (2017). Melatonin, clock genes and mitochondria in sepsis. *Cellular and Molecular Life Sciences*. **74**, 3965–3987.

Ahmad, T., et al. (2014a). Clinical Implications of Chronic Heart Failure Phenotypes Defined by Cluster Analysis. *Journal of the American College of Cardiology*. **64** (17), 1765–1774.

Ahn B. H., et al. (2008). A role for the mitochondrial deacetylase Sirt3 in regulating energy homeostasis. *Proceedings of the National Academy of Sciences of the United States of America*. **105**, 14447–14452.

Andrabi SA., et al. (2004). Direct inhibition of the mitochondrial permeability transition pore: a possible mechanism responsible for anti-apoptotic effects of melatonin. *FASEB Journal*. **18**, 869–871.

Angsutararux, P., Luanpitpong, S. and Issaragrisil, S. (2015). Chemotherapy-Induced Cardiotoxicity: Overview of the Roles of Oxidative Stress. *Oxidative Medicine and Cellular Longevity*. **2015**, 1–13.

Aon MA., et al. (2006). Mitochondrial criticality: a new concept at the turning point of life or death. *Biochimica et Biophysica Acta.* **12**, 675-681.

Aon MA., et al. (2010). Redox-optimized ROS balance: a unifying hypothesis. *Biochimica et Biophysica Acta*. **6**, 865–877.

Arai, A., et al. (2002). STARS, a Striated Muscle Activator of Rho Signaling and Serum Response Factor-dependent Transcription. *Journal of Biological Chemistry*. **277**(27), 24453–24459.

Arai, M., et al. (1998). Sarcoplasmic Reticulum Genes are Selectively Down-regulated in Cardiomyopathy Produced by Doxorubicin in Rabbits. *Journal of Molecular and Cellular Cardiology*. **30** (2), 243–254.

Arany Z., et al. (2005). Transcriptional coactivator PGC-1α controls the energy state and contractile function of cardiac muscle. *Cell Metabolism*.**1**, 259–271.

Arıcı, M., et al. (2013). Effects of BQ-788 on amitriptyline-induced cardiovascular toxicity. *Human & Experimental Toxicology*. **32**(3), 316–322.

Armstrong, G.T., et al. (2014). Aging and Risk of Severe, Disabling, Life-Threatening, and Fatal Events in the Childhood Cancer Survivor Study. *Journal of Clinical Oncology*. **32**(12), 1218–1227.

Auer, J., et al. (2016). Muscle- and skeletal-related side-effects of statins: tip of the iceberg? *European Journal of Preventive Cardiology*. **23**(1), 88–110.

Bajaj M., et al. (2007). Effects of peroxisome proliferator activated receptor (PPAR) α and PPAR γ agonists on glucose and lipid metabolism in patients with type 2 diabetes mellitus. *Diabetologia.* **50**, 1723–1731.

Balijepalli, R.C. and Kamp, T.J., (2008). Caveolae, ion channels and cardiac arrhythmias. *Progress in Biophysics and Molecular Biology*. **98**(2–3), 149–160.

Barger PM, Leone TC, Weinheimer CJ, Kelly DP. (2000). Deactivation of peroxisome proliferator activated receptor α during cardiac hypertrophic growth. *Journal of Clinical Investigation*. **105**, 1723–1730.

Barth, A.S. and Tomaselli, G.F. (2009). Cardiac metabolism and arrhythmias. *Circulation: Arrhythmia and Electrophysiology*. **2** (3), 327–35.

Bassareo, P.P., et al. (2016). Cardiotoxicity from anthracycline and cardioprotection in paediatric cancer patients. *Journal of Cardiovascular Medicine*. **17**, 55–63.

Beard, N.A., Wei, L. and Dulhunty, A.F., (2009). Control of muscle ryanodine receptor calcium release channels by proteins in the sarcoplasmic reticulum lumen. *Clinical and Experimental Pharmacology and Physiology*. **36**(3), 340–345.

Bengal, E., et al. (1992). Functional antagonism between c-Jun and MyoD proteins: a direct physical association*. Cell*. **68**(3), 507–19.

Benton CR., et al. (2010). Increased levels of peroxisome proliferator-activated receptor gamma, coactivator 1 alpha (PGC-1α) improve lipid utilization, insulin signalling and glucose transport in skeletal muscle of lean and insulin-resistant obese Zucker rats. *Diabetologia.* **53**, 2008–2019.

Berger JM, (1996). Structure and mechanism of DNA topoisomerase II. *Nature* **379**, 225–232.

Bernardi, P., et al. (2015). The Mitochondrial Permeability Transition Pore: Channel Formation by F-ATP Synthase, Integration in Signal Transduction, and Role in Pathophysiology. *Physiological reviews- American Journal of Physiology*. **95** (4), 1111–55.

Bers, D.M. (2000). Calcium Fluxes Involved in Control of Cardiac Myocyte Contraction. *Circulation Research*. **87** (4), 275–281.

Bhattacharya P., Pandey A. K., Paul S., Patnaik R., (2014). Melatonin renders neuroprotection by protein kinase C mediated aquaporin-4 inhibition in animal model of focal cerebral ischemia. *Life Sciences*. **100**(2), 97–109.

Bi, Y.M., et al. (2018). 3,5-Dicaffeoylquinic acid protects H9C2 cells against oxidative stress-induced apoptosis via activation of the PI3K/Akt signaling pathway*. Food & nutrition research*. **62**. 345-50.

Bonay, M. and Deramaudt, T.B., (2015). Nrf2: new insight in cell apoptosis. *Cell death & disease*. **6**(10), 1897-1905.

Bonifacio A., et al. (2016). Simvastatin induces mitochondrial dysfunction and increased atrogin-1 expression in H9c2 cardiomyocytes and mice in vivo. *Archives of Toxicology*. **90** (1), 203-15.

Bootman, M.D., et al. (2011). Atrial cardiomyocyte calcium signalling. *Biochimica et Biophysica Acta (BBA) - Molecular Cell Research*. **1813** (5), 922–934.

Borlaug, B.A. and Redfield, M.M. (2011). Diastolic and systolic heart failure are distinct phenotypes within the heart failure spectrum. *Circulation*. **123** (18), 2006-2014.

Borutaite, V., et al. (2009). Nitric oxide protects the heart from ischemia-induced apoptosis and mitochondrial damage via protein kinase G mediated blockage of permeability transition and cytochrome c release. *Journal of Biomedical Science*. **16** (1), 70.

Bratton SB., *et al*. (2001). Apoptosis in mitochondria. *The EMBO Journal*. **20**, 998–1009.

Brenner, C. and Moulin, M. (2012). Physiological Roles of the Permeability Transition Pore. *Circulation Research*. **111** (9), 1237–1247.

Bromme HJ., et al. (2000). Scavenging effect of melatonin on hydroxyl radicals generated by alloxan. *Journal of Pineal Research*. **29**, 201–208.

Brown DA., et al. (2013). Mitochondrial inner membrane lipids and proteins as targets for decreasing cardiac ischemia/reperfusion injury. *Pharmacology and Therapeutics*. **140**, 258–266.

Brown JM, Attardi LD., (2005). The role of apoptosis in cancer development and treatment response. *Nature Reviews Cancer.* **5**, 231–237.

Brown JM, Wilson G. (2003). Apoptosis genes and resistance to cancer therapy: what does the experimental and clinical data tell us. *Cancer Biology Therapy.* **2**, 477–490.

Brown, E.M. (2013). Role of the calcium-sensing receptor in extracellular calcium homeostasis. *Best Practice & Research Clinical Endocrinology & Metabolism*. **27** (3), 333–343.

C. Lestuzzi, (2010). Neoplastic pericardial disease: old and current strategies for diagnosis and management. *World Journal of Cardiology*. **2** (9), 270.

Cain K., et al (2000). Apaf-1 oligomerizes into biologically active approximately 700-kDa and inactive approximately 1.4-MDa apoptosome complexes. *Journal of Biological Chemistry.* **275**, 6067–6070.

Carnicer, R., et al. (2013). Nitric oxide synthases in heart failure. *Antioxidants & redox signaling* **18** (9), 1078–99.

Catterall, W.A., (2014). Sodium Channels, Inherited Epilepsy, and Antiepileptic Drugs. *Annual Review of Pharmacology and Toxicology*. **54**(1), 317–338.

Chatterjee, K., et al. (2010). Doxorubicin cardiomyopathy. *Cardiology*. **115** (2), 155–62.

Chau et al. (2002). Coordinating Etk/Bmx activation and VEGF upregulation to promote cell survival and proliferation. *Oncogene*. **21**, 8817-29.

Chen, H.-H., et al. (2016). Melatonin pretreatment enhances the therapeutic effects of exogenous mitochondria against hepatic ischemia-reperfusion injury in rats through suppression of mitochondrial permeability transition. *Journal of Pineal Research*. **61** (1), 52-68.

Chen, J., et al. (2012). Incidence of Heart Failure or Cardiomyopathy After Adjuvant Trastuzumab Therapy for Breast Cancer. *Journal of the American College of Cardiology*. **60**(24), 2504–2512.

Chen, Z.J., et al. (2014). Effect of ucp2-sirna on inflammatory response of cardiomyocytes induced by septic serum*. Chinese journal of contemporary paediatrics*.**16**, 851–855.

Chen. M., et al. (2018). Ursolic acid stimulates UCP2 expression and protects H9c2 cells from hypoxia-reoxygenation injury via p38 signalling. *Journal of Biosciences*. **43** (5), 857-865.

Chen-Izu, Y., et al. (2015). Na + channel function, regulation, structure, trafficking and sequestration. *The Journal of Physiology*. **593**(6), 1347–1360.

Chinnam, P., et al. (2012). Evaluation of acute toxicity of pioglitazone in mice. *Toxicology International*. **19**(3), 250.

Cho, C.H., (2012). Molecular mechanism of circadian rhythmicity of seizures in temporal lobe epilepsy. *Frontiers in cellular neuroscience*. **6**, 55-63.

Chong, N.W., et al. (2012). STARS Is Essential to Maintain Cardiac Development and Function In Vivo via a SRF Pathway R. Kukreja. *PLoS ONE.* **7**(7), 40966-40970.

Chopra, N. and Knollmann, B.C., (2009). Cardiac Calsequestrin: The New Kid on the Block in Arrhythmias. *Journal of Cardiovascular Electrophysiology*. **20**(10), 1179–1185.

Chouchani, E.T., et al. (2014). Ischaemic accumulation of succinate controls reperfusion injury through mitochondrial ROS. *Nature*. **515** (7527), 431–5.

Chowdhury, D. et al. (2013). A proteomic view of isoproterenol induced cardiac hypertrophy: prohibitin identified as a potential biomarker in rats. *Journal of translational medicine*. **11**,130.

Cimen H., et al. (2010). Regulation of succinate dehydrogenase activity by SIRT3 in mammalian mitochondria. *Biochemistry* **49**, 304–311.

Clark, B.C. and Berul, C.I. (2016). Arrhythmia diagnosis and management throughout life in congenital heart disease. *Expert review of cardiovascular therapy*. **14** (3), 301–20.

Corbett and J.M. Berger., (2004). Structure, molecular mechanisms, and evolutionary relationships in DNA topoisomerases, *Annual review of biophysics and biomolecular structure.* **33** (95), 118.

Cullinane C., (2000). Interstrand cross-linking by Adriamycin in nuclear and mitochondrial DNA of MCF-7 cells. *Nucleic Acids Research*. **28**, 1019–1025.

Daviess, K.J.A. and Doroshowot, J.H. (1986). Redox Cycling of Anthracyclines by Cardiac Mitochondria I. Anthracycline radical formation by NADH Dehydrogenase. *The Journal of Biological Chemistry*. **261** (7), 3060–3067.

Dávila-Román VG., et al. (2002). Altered Myocardial Fatty Acid and Glucose Metabolism in Idiopathic Dilated Cardiomyopathy. *The Journal of the American College of Cardiology.* **40**, 271–277.

Debatin KM, Poncet D, Kroemer G., (2002). Chemotherapy: targeting the mitochondrial cell death pathway.*Oncogene* **21**, 8786–8803.

Debatin KM, Stahnke K, Fulda S. (2003). Apoptosis in hematological disorders. *Seminars in Cancer Biology.* **13**, 149–158.

Del Olmo-Turrubiarte, A., et al. (2015). Mouse models for the study of postnatal cardiac hypertrophy. *IJC Heart & Vasculature*. **7**, 131–140.

Deng, F., et al. (2017). Propofol Through Upregulating Caveolin-3 Attenuates Post-Hypoxic Mitochondrial Damage and Cell Death in H9C2 Cardiomyocytes During Hyperglycemia. *Cellular Physiology and Biochemistry*. **44**(1), 279–292.

Di Stasi, S.L. et al., (2010). Effects of statins on skeletal muscle: a perspective for physical therapists. *Physical therapy APTA*. **90** (10),1530–42.

Díaz-Casado, M.E., et al. (2016). Melatonin rescues zebrafish embryos from the parkinsonian phenotype restoring the Parkin/PINK1/DJ-1/MUL1 network. *Journal of Pineal Research*. **61** (1), 96-107.

Dolinsky, V.W., et al. (2016). Cardiac mitochondrial energy metabolism in heart failure: Role of cardiolipin and sirtuins. *Biochimica et Biophysica Acta (BBA) - Molecular and Cell Biology of Lipids*. **1861** (10), 1544-54.

Dongó, E., et al. (2011). The cardioprotective potential of hydrogen sulfide in myocardial ischemia/reperfusion injury. *Budapest Acta Physiologica Hungarica*. **98** (4), 369–381.

Dranka, B.P., et al. (2011). Assessing bioenergetic function in response to oxidative stress by metabolic profiling. *Free radical biology & medicine*. **51** (9), 1621–35.

Duygu*et al*., (2013).Genetics and epigenetics of arrhythmia and heart failure. *Frontier in Genetics.* **4** (219), 1-15.

Elrod, J.W., et al. (2010). Cyclophilin D controls mitochondrial pore–dependent Ca2+ exchange, metabolic flexibility, and propensity for heart failure in mice. *Journal of Clinical Investigation ASCI*. **120** (10), 3680–3687.

Fan, M., Chambers, T.C., (2001). Role of mitogen-activated protein kinases in the response of tumor cells to chemotherapy. *Drug resistance updates: reviews and commentaries in antimicrobial and anticancer chemotherapy.* **4** (4), 253–267.

Farah, C. and Reboul, C., (2015). NO Better Way to Protect the Heart during Ischemia-Reperfusion: To be in the Right Place at the Right Time. *Frontiers in pediatrics*. **3**, 6.

Farhadi, N., Oryan, S. and Nabiuni, M., (2014). Serum levels of melatonin and cytokines in multiple sclerosis. *Biomedical Journal*. **37** (2), 90.

Farmakis, D. et al., (2017). Heart failure in haemoglobinopathies: pathophysiology, clinical phenotypes, and management. *European Journal of Heart Failure*. **19** (4), 479–489.

Favero et al. (2017). Melatonin as an Anti-Inflammatory Agent Modulating Inflammasome Activation. *International Journal of Endocrinology*. **2017**, 183-195.

Fearnley, C.J., Roderick, H.L. and Bootman, M.D., (2011). Calcium Signaling in Cardiac Myocytes. *Cold Spring Harbor Perspectives in Biology*. **3** (11), 004242–a004242.

Feenstra, J. et al,. (1999). Drug-induced heart failure. *Journal of the American College of Cardiology*. **33** (5), 1152–1162.

Feiner, E.C., et al. (2011). Left Ventricular Dysfunction in Murine Models of Heart Failure and in Failing Human Heart is Associated With a Selective Decrease in the Expression of Caveolin-3. *Journal of Cardiac Failure*. **17**(3), 253–263.

Fenick DJ., (1997). Doxoform and daunoform: anthracycline-formaldehyde conjugates toxic to resistant tumor cells. *The Journal of Medicinal Chemistry* **40**, 2452–2461.

Ferrari, R., (1999). The role of TNF in cardiovascular disease. *Pharmacological Research*. **40**, 97–105.

Frias, M.A., et al. (2008). The PGE2- Stat3 interaction in doxorubicin-induced myocardial apoptosis. *Cardiovascular Research*. **80**, 69–77.

Frias, M.A., et al. (2010). Native and reconstituted HDL protect cardiomyocytes from doxorubicin-induced apoptosis. *Cardiovascular Research*. **85**, 118–126.

Fukazawa R., et al. (2003). Neuregulin- 1 protects ventricular myocytes from anthracycline- induced apoptosis via erbB4-dependent activation of PI3-kinase/ Akt. *The Journal of Molecular and Cellular Cardiology*. **35**, 1473–1479.

Fulda S, Debatin KM., (2004). Targeting apoptosis pathways in cancer therapy. *Current Cancer Drug Targets.* **4**, 569–576.

Fulda, S. and Debatin, K.-M., (2006). Extrinsic versus intrinsic apoptosis pathways in anticancer chemotherapy. *Oncogene*. **25** (34), 4798–4811.

G. Takemura and H. Fujiwara., (2007). Doxorubicin-induced cardiomyopathy from the cardiotoxic mechanisms to management. *Progress in Cardiovascular Diseases*. **49** (5), 330–352.

Galano A., et al. (2011). Melatonin as a natural ally against oxidative stress: a physicochemical examination. *Journal of Pineal Research*. **51**, 1–16.

Galati, F., Galati, A. and Massari, S., (2016). RyR2 QQ2958 Genotype and Risk of Malignant Ventricular Arrhythmias. *Cardiology research and practice*. **2016**, 8-11.

Galbiati, F., et al. (2001). Caveolin-3 Null Mice Show a Loss of Caveolae, Changes in the Microdomain Distribution of the Dystrophin-Glycoprotein Complex, and T-tubule Abnormalities. *Journal of Biological Chemistry*. **276**(24), 21425–21433.

Galley, H.F., et al. (2014). Melatonin as a potential therapy for sepsis: A phase in dose escalation study and an ex vivo whole blood model under conditions of sepsis. *Journal of Pineal Research.* **56**, 427–438.

Gao H., (2012). NADPH oxidases: novel therapeutic targets for neurodegenerative diseases. *Trends in Pharmacological Sciences*. **33** (6), 295–303.

Garcia JJ., et al. (1999). Role of pinoline and melatonin in stabilizing hepatic microsomal membranes against oxidative stress. *Journal of Bioenergetics and Biomembranes*. **31**, 609–616.

Gautier, C.A., et al. (2012). Regulation of mitochondrial permeability transition poreby PINK1. *Molecular Neurodegeneration*. **7** (1), 22.

Geng, X., Liu, S. and Chen, Y., (2014). Involvement of ERK5 and JNK in the BMP9-induced differentiation of C3H10T1/2 cells into cardiomyocyte-like cells. Chinese journal of cellular and molecular immunology. 30(8), 829–32.

George, A.L., (2013). Genetic and molecular basis of sudden cardiac death. *Journal of Clinical Investigation*.**123** (1), 75-83.

George, Jr., et al. (1995). Assignment of the human heart tetrodotoxin-resistant voltage-gated Na⁺ channel α-subunit gene (SCN5A) to band 3p21. *Cytogenetic and Genome Research.* **68**(1–2), 67–70.

Gewirtz, D.A., (1999). A critical evaluation of the mechanisms of action proposed for the antitumor effects of the anthracycline antibiotics adriamycin and daunorubicin. *Biochemical Pharmacology*. **57**, 727–741.

Goormaghtigh E., Pollakis G., Ruysschaert J. M., (1983). Mitochondrial membrane modifications induced by Adriamycin-mediated electron transport. *Biochemical Pharmacology*. **32**, 889–893.

Goormatighe E, Chatelain P, Caspers J., et al. (1980). Evidence of a complex between adriamycin derivatives and cardiolipin: possible role in cardiotoxicity. *Biochemical Pharmacology*. **29** (21), 3003–3010.

Gorski, P.A., Ceholski, D.K. and Hajjar, R.J., (2015). Altered myocardial calcium cycling and energetics in heart failure--a rational approach for disease treatment. *Cell metabolism*. **21** (2), 183–94.

Gouriou Y., Bijlenga P., Demaurex N., (2013). Mitochondrial Ca^{2+} uptake from plasma membrane Cav3.2 protein channels contributes to ischemic toxicity in PC12 cells. *The Journal of Biological Chemistry*. **288** (18), 12459–12468.

Guan K. L., Xiong Y., (2011). Regulation of intermediary metabolism by protein acetylation. *Trends Biochemical Sciences*. **36**, 108–116.

Gwathmey et al., (1987). Abnormal intracellular calcium handling in myocardium from patients with end-stage heart failure. *Circulation Research*. **61**(1), 70-76.

Györke, S., Stevens, S.C.W. and Terentyev, D., (2009). Cardiac calsequestrin: quest inside the SR. *The Journal of Physiology*. **587**(13), 3091–3094.

Haghikia A., et al. (2014). STAT3, a key regulator of cell-to-cell communication in the heart. *Cardiovascular Research*. **102**, 281-9.

Halestrap, A.P. and Pasdois, P., (2009). The role of the mitochondrial permeability transition pore in heart disease. *Biochimica et Biophysica Acta (BBA) – Bioenergetics*. **1787** (11), 1402–1415.

Hamid, T., et al. (2009). Divergent tumor necrosis factor receptor-related remodeling responses in heart failure: role of nuclear factor-kappaB and inflammatory activation. *Circulation*.**119**, 1386–1397.

Hammann, F., et al. (2017). Pharmacokinetic interaction between taxanes and amiodarone leading to severe toxicity. *British Journal of Clinical Pharmacology*. **83** (4), 927–930.

Han, S.N., et al. (2014). Identification and functional characterization of the human ether-a-go-go-related gene Q738X mutant associated with hereditary long QT syndrome type 2. *International journal of molecular medicine*. **34** (3), 810–5.

Handschin C., (2011). Peroxisome proliferator activated receptor γ coactivator 1β (PGC-1β) improves skeletal muscle mitochondrial function and insulin sensitivity. *Diabetologia*. **54** (6), 1270–1272.

Hanninen, S.L., et al. (2010). Mitochondrial uncoupling downregulates calsequestrin expression and reduces SR Ca2+ stores in cardiomyocytes. *Cardiovascular Research***. 88**(1), 75–82.

Hao Z., et al. (2005). Specific ablation of the apoptotic functions of cytochrome C reveals a differential requirement for cytochrome C and Apaf-1 in apoptosis. *Cell* .**121** (4), 579–591.

Hardeland, R. (2012). Melatonin in Aging and Disease —Multiple Consequences of Reduced Secretion, Options and Limits of Treatment. *Aging and Disease*. **3** (2), 194-255.

Hardeland. (2005). Melatonin. *The International Journal of Biochemistry & Cell Biology.* **38**(3), 313-6.

Harding, S.J., et al. (2010). Activation of ASK1, downstream MAPKK and MAPK isoforms during cardiac ischaemia. *Biochimica et Biophysica Acta (BBA) - Molecular Basis of Disease***. 1802**(9), 733–740.

Harper, M.E. and Gerrits, M.F., (2004). Mitochondrial uncoupling proteins as potential targets for pharmacological agents. *Current Opinion in Pharmacol*ogy. **4**, 603–607.

Hasenfuss et al., (1994). Relation between myocardial function and expression of sarcoplasmic reticulum Ca (2+)-ATPase in failing and nonfailing human myocardium. *Circulation Research.* **75** (3), 434-442.

Hausenloy, D. and Yellon, D., (2006). Survival kinases in ischemic preconditioning and postconditioning. *Cardiovascular Research*. **70**(2), 240–253.

Hausenloy, D.J., (2009). Signalling pathways in ischaemic post conditioning. *Thrombosis and Haemostasis*. **101**, 626–634.

Hausenloy, D.J., Mocanu, M.M., Yellon, D.M., (2004). Cross-talk between the survival kinases during early reperfusion: its contribution to ischemic preconditioning. *Cardiovascular Research*. **63**, 305–312.

Hausenloy, D.J., Yellon, D.M., (2004). New directions for protecting the heart against ischaemia reperfusion injury: targeting the Reperfusion Injury Salvage Kinase (RISK)-pathway. *Cardiovascular Research*. **61**, 448–460.

Hay, J.M., et al. (2017). Transcriptional and Post-Translational Targeting of Myocyte Stress Protein 1 (MS1) by the JNK Pathway in Cardiac Myocytes. *Journal of molecular signalling*. **12**, 3-12.

Heather, L.C., et al. (2009). Isoproterenol induces in vivo functional and metabolic abnormalities: similar to those found in the infarcted rat heart. *Journal of physiology and pharmacology : an official journal of the Polish Physiological Society*. **60** (3), 31–9.

Hemann M., et al. (2004). Suppression of tumorigenesis by the p53 target PUMA. *Proceedings of the National Academy of Sciences of the United States of America*. **101**, 9333–9338.

Henninger, C. and Fritz, G., (2017). Statins in anthracycline-induced cardiotoxicity: Rac and Rho, and the heartbreakers. *Cell Death and Disease*. **8** (1), 2564.

Henry, A.W.N., (2015). Pineal gland. *Clinical Neurology*. **3**, 54-63.

Hernández, J.S., et al. (2014). Crosstalk between AMPK activation and angiotensin II-induced hypertrophy in cardiomyocytes: the role of mitochondria. *Journal of cellular and molecular medicine*. **18** (4), 709–20.

Herron, T.J. and McDonald, K.S., (2002). Small Amounts of α-Myosin Heavy Chain Isoform Expression Significantly Increase Power Output of Rat Cardiac Myocyte Fragments. *Circulation Research*. **90**(11), 1150–1152.

Hoffman, R.A. (1983). Seasonal growth and development and the influence of the eyes and pineal gland on body weight of golden hamsters (M. auratus). *Growth*. **47** (2), 109-121.

Horenstein, M.S., Vander Heide, R.S., L'Ecuyer, T.J., (2000). Molecular basis of anthracycline induced cardiotoxicity and its prevention. *Molecular Genetics and Metabolism*. **71**, 436–444.

Hsieh, H.J., et al. (2014). Shear-induced endothelial mechanotransduction: the interplay between reactive oxygen species (ROS) and nitric oxide (NO) and the pathophysiological implications. *Journal of Biomedical Science*. **21** (1), 3.

Hydock, D.S., et al. (2009). Voluntary wheel running in rats receiving doxorubicin: effects on running activity and cardiac myosin heavy chain. *Anticancer research*. **29**(11), 4401–7.

Ichikawa, Y., et al. (2014). Cardiotoxicity of doxorubicin is mediated through mitochondrial iron accumulation. *The Journal of clinical investigation ASCI*. **124** (2), 617–30.

Ikeda, G., et al. (2016). Nanoparticle-Mediated Targeting of Cyclosporine A Enhances Cardioprotection Against Ischemia-Reperfusion Injury Through Inhibition of Mitochondrial Permeability Transition Pore Opening. *Scientific reports*. **6**, 204-67.

Inarrea P., et al. (2011). Melatonin and steroid hormones activate intermembrane Cu,Zn-superoxide dismutase by means of mitochondrial cytochrome P450. *Free Radical Biology and Medicine*. **50**, 1575–1581.

Jiang, L., et al. (2014). ZNF667/Mipu1 is a novel anti-apoptotic factor that directly regulates the expression of the rat Bax gene in H9c2 cells. *PloS one.* **9**(11), 111-120.

Jou MJ. (2011). Melatonin preserves the transient mitochondrial permeability transition for protection during mitochondrial Ca2+ stress in astrocyte. *Journal of Pineal Research*. **50**, 427–435.

Juan W.S., Huang S.Y., Chang C.C., et al. (2014). Melatonin improves neuroplasticity by upregulating the growth-associated protein-43 (GAP-43) and NMDAR postsynaptic density-95 (PSD-95) proteins in cultured neurons exposed to glutamate excitotoxicity and in rats subjected to transient focal cerebral ischemia even during a long-term recovery period. *Journal of Pineal Research*. **56** (2), 213–223.

K. J. M. Schimmel., et al. (2004). Complications of treatment: cardiotoxicity of cytotoxic drugs. *Cancer Treatment Reviews*. **30**, 181–191.

Kalayanaraman B, Joseph J, Kalivendi S., et al. (2002). Doxorubicin-induced apoptosis: implications in cardiotoxicity. *Molecular and Cellular Biochemistry*. **234–235** (1-2), 119–124.

Kalivendi, S. V., et al. (2001). Doxorubicin-induced apoptosis is associated with increased transcription of endothelial nitric-oxide synthase. Effect of antiapoptotic antioxidants and calcium. *The Journal of biological chemistry*. **276** (50), 47266–76.

Kalogeropoulos, A.P., et al. (2016). Characteristics and Outcomes of Adult Outpatients With Heart Failure and Improved or Recovered Ejection Fraction. *JAMA Cardiology*. **1** (5), 510.

Kang, J., et al. (2006). Mechanisms Underlying the QT Interval–prolonging Effects of Sevoflurane and Its Interactions with Other QT-prolonging Drugs.

The Journal of the American Society of Anesthesiologists. **104** (5),1015–1022.

Kaplan, P., et al. (2003). Free radical-induced protein modification and inhibition of Ca2+-ATPase of cardiac sarcoplasmic reticulum. *Molecular and Cellular Biochemistry*. **248** (1-2), 41–47.

Keating, M.T. and Sanguinetti, M.C., (2001). Molecular and Cellular Mechanisms of Cardiac Arrhythmias. *Cell*. **104** (4), 569–580.

Kerkelä, R., et al. (2011). Key roles of endothelin-1 and p38 MAPK in the regulation of atrial stretch response. American Journal of Physiology-Regulatory, Integrative and Comparative Physiology. 300(1), 140–149.

Kho, C., et al. (2015). Small-molecule activation of SERCA2a SUMOylation for the treatment of heart failure. *Nature communications*. **6**, 7229.

Kim H. S., et al. (2010). SIRT3 is a mitochondria-localized tumour suppressor required for maintenance of mitochondrial integrity and metabolism during stress. *Cancer Cell*. **17**, 41–52.

Kim, J.B., et al. (2007). Polony Multiplex Analysis of Gene Expression (PMAGE) in Mouse Hypertrophic Cardiomyopathy. *Science*. **316** (5830), 1481–1484.

Kingma Jr, J.G., Simard, D. and Rouleau, J.R., (2011). Modulation of nitric oxide affects myocardial perfusion-contraction matching in anaesthetized dogs with recurrent no-flow ischaemia. *Experimental Physiology*. **96** (12), 1293–1301.

Knollmann, B.C., (2009). New roles of calsequestrin and triadin in cardiac muscle. *The Journal of Physiology*. **587**(13), 3081–3087.

Koekemoer, A.L., et al. (2009). Myocyte stress 1 plays an important role in cellular hypertrophy and protection against apoptosis. *FEBS Letters*. **583**(17), 2964–2967.

Koh P.O., (2008). Melatonin prevents ischemic brain injury through activation of the mTOR/p70S6 kinase signaling pathway. *Neuroscience Letters*.**444** (1), 74–78.

Krenz, M. and Robbins, J., (2004). Impact of beta-myosin heavy chain expression on cardiac function during stress. *Journal of the American College of Cardiology.* **44**(12), 2390–2397.

Krenz, M., et al. (2003). Analysis of myosin heavy chain functionality in the heart. *The Journal of biological chemistry*. **278**(19), 17466–74.

Krumerman, A., et al. (2004). An LQT mutant minK alters KvLQT1 trafficking. *American journal of physiology- Cell physiology*. **286** (6), 1453–63.

Kumaran, K.S. and Prince, P.S.M., (2010). Caffeic acid protects rat heart mitochondria against isoproterenol-induced oxidative damage. *Cell stress & chaperones*. **15** (6), 791–806.

Kurabayashi, M., Jeyaseelan, R. and Kedes, L., (1994). Doxorubicin represses the function of the myogenic helix-loop-helix transcription factor MyoD. Involvement of Id gene induction. *The Journal of biological chemistry*. **269**(8), 6031–9.

Kuwahara, K., et al. (2007). Modulation of adverse cardiac remodeling by STARS, a mediator of MEF2 signaling and SRF activity. *Journal of Clinical Investigation.* **117**(5), 1324–1334.

Kwong, J.Q. and Molkentin, J.D., (2015). Physiological and Pathological Roles of the Mitochondrial Permeability Transition Pore in the Heart. *Cell Metabolism*. **21** (2), 206–214.

Kwong, J.Q. et al. (2014). Genetic deletion of the mitochondrial phosphate carrier desensitizes the mitochondrial permeability transition pore and causes cardiomyopathy. *Cell death and differentiation*. **21** (8), 1209–17.

Kyriakis, J.M. and Avruch, J., (2012). Mammalian MAPK Signal Transduction Pathways Activated by Stress and Inflammation: A 10-Year Update. *Physiological Reviews*. **92**(2), 689–737.

Lagouge M., et al. (2006). Resveratrol Improves Mitochondrial Function and Protects against Metabolic Disease by Activating SIRT1 and PGC 1α. *Cell*. **127**, 1109–1122.

Lalitha, G., et al. (2013). Protective Effect of Neferine Against Isoproterenol-Induced Cardiac Toxicity. *Cardiovascular Toxicology*. **13** (2), 168–179.

Lançon, J.P., et al. (1990). Changes in myocardial metabolism induced by drugs used during intensive care. *Annales francaises d'anesthesie et de reanimation*. **9** (1), 31–41.

Larsen, L.A., et al. (1999). A single strand conformation polymorphism/heteroduplex (SSCP/HD) method for detection of mutations in 15 exons of the KVLQT1 gene, associated with long QT syndrome. *Clinica chimica acta; international journal of clinical chemistry*. **280** (1-2), 113–25.

Law I. K., et al. (2009). Identification and characterization of proteins interacting with SIRT1 and SIRT3: implications in the anti-aging and metabolic effects of sirtuins. *Proteomics.* **9**, 2444–2456.

Le Minh, K., et al. (2009). Uncoupling protein-2 deficiency provides protection in a murine model of endotoxemic acute liver failure. *Critical Care Medicine.* **37**, 215–222.

Lecour, S., (2009). Activation of the protective Survivor Activating Factor Enhancement (SAFE) pathway against reperfusion injury: Does it go beyond the RISK pathway? *The Journal of Molecular and Cellular Cardiology*. **47**, 32–40.

Lecour, S., (2009). Multiple protective pathways against reperfusion injury: a SAFE path without Aktion? *The Journal of Molecular and Cellular Cardiology* **46**, 607–609.

Lecour, S., James, R.W., (2011). When are pro-inflammatory cytokines SAFE in heart failure? *The European Heart Journal*. **32**, 680–685.

Lee J. C. and Won M. H., (2014). Neuroprotection of antioxidant enzymes against transient global cerebral ischemia in gerbils. *Anatomy & Cell Biology*. **47**(3), 149–156.

Lee, K.W., et al. (2012). Role of Junctin Protein Interactions in Cellular Dynamics of Calsequestrin Polymer upon Calcium Perturbation. *The Journal of Biological Chemistry*. **287**(3), 1679.

Leenen, F.H.H., White, R. and Yuan, B., (2001). Isoproterenol-induced cardiac hypertrophy: role of circulatory versus cardiac renin-angiotensin system. *American Journal of Physiology - Heart and Circulatory Physiology*. **281** (6), 2410-6.

Lei, S., et al. (2013). Hyperglycemia-Induced Protein Kinase C 2 Activation Induces Diastolic Cardiac Dysfunction in Diabetic Rats by Impairing Caveolin-3 Expression and Akt/eNOS Signaling. *Diabetes*. **62**(7), 2318–2328.

Lei, X.G., et al. (2016). Paradoxical Roles of Antioxidant Enzymes: Basic Mechanisms and Health Implications. *Physiological reviews*. **96** (1), 307–64.

Lejay, A., et al. (2016). Ischemia reperfusion injury, ischemic conditioning and diabetes mellitus. *Journal of Molecular and Cellular Cardiology*. **91**, 11–22.

Lemasters, J.J,. et al. (2009). Mitochondrial calcium and the permeability transition in cell death. *Biochimica et biophysica acta*. **1787** (11), 1395–401.

Li H., Wang Y., Feng D., et al. (2014). Alterations in the time course of expression of the Nox family in the brain in a rat experimental cerebral ischemia and reperfusion model: effects of melatonin. *Journal of Pineal Research*. **57** (1), 110–119.

Li T, Danelisen I, Singal PK., (2002). Early changes in myocardial antioxidant enzymes in rats treated with Adriamycin. *Molecular and Cellular Biochemistry.* **232**, 19–26.

Li X., et al. (1997). Melatonin decreases production of hydroxyl radical during cerebral ischemia-reperfusion. *Zhongguo Yao Li Xue Bao*. **18**, 394–396.

Li, H., et al. (2015). Cardiac Resynchronization Therapy Reduces Subcellular Heterogeneity of Ryanodine Receptors, T-Tubules and Ca $^{2+}$ Sparks Produced by Dyssynchronous Heart Failure. *Circulation: Heart Failure*. **8** (6), 23-52.

Li, W., et al. (2018). SCN5A Variants: Association With Cardiac Disorders. *Frontiers in physiology***. 9**, 1372-1380.

Liang H, Ward WF. (2006). PGC-1α: a key regulator of energy metabolism. *Advances in physiology education*. **30**, 145–151.

Lilly, L.S., (2007).*Pathophysiology of heart disease: a collaborative project of medical students and faculty.*4th ed. United States of America: Lippincott Williams & Wilkins, pp. 269-287.

Lim, S.Y., (2013). Role of statins in coronary artery disease. *Chonnam medical journal*. **49** (1), 1–6.

Lips, D.J., et al. (2004). MEK1-ERK2 signaling pathway protects myocardium from ischemic injury in vivo*. Circulation*. **109**, 1938–1941.

Liu, D., et al. (2014). 14–3-3gamma protein attenuates lipopolysaccharide-induced cardiomyocytes injury through the bcl-2 family/mitochondria pathway*. International Immunopharmacolology.* **21**, 509–515.

Liu, G., et al. (2016). Caspase-Dependent and Caspase-Independent Pathways Are Involved in Cadmium-Induced Apoptosis in Primary Rat Proximal Tubular Cell Culture S. Ghavami*. PLOS ONE*. **11**(11), 2345-2352.

Liu, J., et al. (2008). ERKs/p53 signal transduction pathway is involved in doxorubicin-induced apoptosis in H9c2 cells and cardiomyocytes. *American journal of physiology- Heart and circulatory physiology.* **295**, 1956–1965.

Lou, H., Danelisen, I., Singal, P.K., (2005). Involvement of mitogen-activated protein kinases in adriamycin-induced cardiomyopathy. *American journal of physiology- Heart and circulatory physiology.* **288**, 1925– 1930.

Luis, J., et al. (2007). Transcriptional analysis of the human cardiac calsequestrin gene in cardiac and skeletal myocytes. *Journal of biological chemistry*. **282**(49), 35554-63.

Ma, Y., et al. (2017). Rutin attenuates doxorubicin-induced cardiotoxicity via regulating autophagy and apoptosis*. Biochimica et Biophysica Acta (BBA) - Molecular Basis of Disease*. **1863**(8), 1904–1911.

MacLennan, D.H. and Chen, S.R.W., (2009). Store overload-induced Ca 2+ release as a triggering mechanism for CPVT and MH episodes caused by mutations in RYR and CASQ genes. *The Journal of Physiology*. **587**(13), 3113–3115.

Madonna, R., (2017). Early Diagnosis and Prediction of Anticancer Drug-induced Cardiotoxicity: From Cardiac Imaging to 'Omics' Technologies. *Revista Española de Cardiología.* **70** (7), 576-582.

Magnani *et al*., (2011). Atrial fibrillation: Current knowledge and future directions in epidemiology and genomics.*Circulation*.**124** (18), 1982-1993.

Mahal HS., et al. (1999). Antioxidant properties of melatonin: a pulse radiolysis study. *Free Radical Biology and Medicine.* **26**, 557–565.

Marcillato O, Zhang Y, Davies KJ., (1989). Oxidative and nonoxidative mechanisms in the inactivation of cardiac mitochondrial electron transport chain components by doxorubicin. *The Biochemical Journal*. **259**,181–189.

Markandeya, Y.S., et al. (2015). Caveolin-3 Overexpression Attenuates Cardiac Hypertrophy via Inhibition of T-type Ca2+ Current Modulated by Protein Kinase Cα in Cardiomyocytes. *The Journal of biological chemistry*. **290** (36), 22085–100.

Martin M., et al. (2000). Melatonin-induced increased activity of the respiratory chain complexes I and IV can prevent mitochondrial damage induced by ruthenium red in vivo. *Journal of Pineal Research*. **28**, 242–248.

Martin M., et al. (2002). Melatonin increases the activity of the oxidative phosphorylation enzymes and the production of ATP in rat brain and liver mitochondria. *The International Journal of Biochemistry & Cell Biology.* **34**, 348–357.

Masella, R., et al. (2005). Novel mechanisms of natural antioxidant compounds in biological systems: involvement of glutathione and glutathione-related enzymes. *The Journal of Nutritional Biochemistry*.**16**, 577–586.

Maulik, A., et al. (2018). Ischaemic Preconditioning Protects Cardiomyocytes from Anthracycline-Induced Toxicity via the PI3K Pathway. *Cardiovascular drugs and therapy*. **32**(3), 245–253.

Maulik, S.K., et al. (2012). Genistein prevents isoproterenol-induced cardiac hypertrophy in rats. *Canadian Journal of Physiology and Pharmacology*. **90** (8), 1117–1125.

Maywood, E.S., Bittman, E.L. and Hastings, M.H., (1996). Lesions of the melatonin- and androgen-responsive tissue of the dorsomedial nucleus of the hypothalamus block the gonadal response of male Syrian hamsters to programmed infusions of melatonin. *Biology of reproduction*. **54** (2), 470–7.

Mazzaccara, C., et al. (2018). A common polymorphism in the SCN5A gene is associated with dilated cardiomyopathy. *Journal of Cardiovascular Medicine*. **19**(7), 344-356.

Mdaki, K.S., et al. (2016). Age Related Bioenergetics Profiles in Isolated Rat Cardiomyocytes Using Extracellular Flux Analyses. *PloS one*. **11** (2), e0149002.

Mesirca, P., Torrente, A.G. and Mangoni, M.E., (2015). Functional role of voltage gated Ca(2+) channels in heart automaticity. *Frontiers in physiology*. **6**, 19.

Minotti G., et al. (2004). Anthracyclines: molecular advances and pharmacologic developments in antitumor activity and cardiotoxicity. *Pharmacological Reviews.* **56**, 185–229.

Mitchell P. (1961). Coupling of phosphorylation to electron and hydrogen transfer by a chemi-osmotic type of mechanism. *Nature*. **191**, 144–148.

Mitra, M.S., et al. (2007). Mechanism of protection of moderately diet restricted rats against doxorubicin-induced acute cardiotoxicity. *Toxicology and Applied Pharmacology*. **225**, 90–101.

Mitry, M.A. and Edwards, J.G., (2016). Doxorubicin induced heart failure: Phenotype and molecular mechanisms. *IJC Heart & Vasculature*. **10**, 17–24.

Montaigne, D., Hurt, C. and Neviere, R., (2012). Mitochondria Death/Survival Signaling Pathways in Cardiotoxicity Induced by Anthracyclines and Anticancer-Targeted Therapies. *Biochemistry Research International*. **2012**, 1–12.

Monti M., et al. (2013). The sulphydryl containing ACE inhibitor Zofenoprilat protects coronary endothelium from Doxorubicin-induced apoptosis. *Pharmacological Research*. **76**, 171-81.

Moro S., (2004). Interaction model for anthracycline activity against DNA topoisomerase II. *Biochemistry.* **43**, 7503–7513.

Mukherjee, S., et al. (2003). Protection against acute adriamycin-induced cardiotoxicity by garlic: Role of endogenous antioxidants and inhibition of TNF-α expression. *BMC Pharmacology*. **3**, 1–9.

Muraoka S, and Miura T., (2003). Inactivation of mitochondrial succinate dehydrogenase by adriamycin activated by horseradish peroxidase and hydrogen peroxide. *Chemico- Biological Interactions.* **145**, 67–75.

Murphy E., and Steenbergen C. (2008). Mechanisms underlying acute protection from cardiac ischemia reperfusion injury. *Physiological Reviews*. **88**, 581–609.

Musa, H., et al. (2015). SCN5A variant that blocks fibroblast growth factor homologous factor regulation causes human arrhythmia. *Proceedings of the National Academy of Sciences of the United States of America*. **112** (40), 12528–33.

Nabeebaccus A., et al. (2011). NADPH oxidases and cardiac remodelling. *Heart Failure Reviews.* **16**, 5–12.

Nakagawa, T., Yokoe, S. and Asahi, M., (2016). Phospholamban degradation is induced by phosphorylation-mediated ubiquitination and inhibited by interaction with cardiac type Sarco(endo)plasmic reticulum Ca(2+)-ATPase. *Biochemical and biophysical research communications*. **472** (3), 523–30.

Nakagawa, Y., (2013). Metabolism and biological function of cardiolipin. *Yakugaku zasshi : Journal of the Pharmaceutical Society of Japan*. **133** (5), 561–74.

Negoro, S., et al. (2001). Glycoprotein 130 regulates cardiac myocyte survival in Doxorubicin induced apoptosis through phosphatidylinositol 3-kinase/Akt phosphorylation and BclxL/Caspase-3 interaction. *Circulation*. **103**, 555–561.

Němec, J., Kim, J.J. and Salama, G,. (2016). The link between abnormal calcium handling and electrical instability in acquired long QT syndrome – Does calcium precipitate arrhythmic storms? *Progress in Biophysics and Molecular Biology*. **120** (1), 210–221.

Neri, M., et al. (2015). Cardiac Oxidative Stress and Inflammatory Cytokines Response After Myocardial Infarction. *Current vascular pharmacology*. **13** (1), 26-36.

Nguyen, Q.T., et al. (2012). Diabetes medications and cancer risk: review of the literature. *American health & drug benefits*. **5**(4), 221–9.

Niedernhofer, L.J., et al. (2003). Malondialdehyde, a product of lipid peroxidation, is mutagenic in human cells. *The Journal of Biological Chemistry.* **278**, 31426–31433.

Niizuma K., et al. (2010). Mitochondrial and apoptotic neuronal death signaling pathways in cerebral ischemia. *Biochimica et Biophysica Acta—Molecular Basis of Disease*. **1802** (1), 92–99.

Nordgren, K.K.S., Hampton, M. and Wallace, K.B., (2017). Editor's Highlight: The Altered DNA Methylome of Chronic Doxorubicin Exposure in Sprague Dawley Rats. *Toxicological Sciences*. **159**(2), 470–479.

Octavia, Y., et al. (2012). Doxorubicin-induced cardiomyopathy: From molecular mechanisms to therapeutic strategies. *Journal of Molecular and Cellular Cardiology*. **52** (6), 1213–1225.

Ohyama, H., et al. (2001). Inhibition of cardiac delayed rectifier K+ currents by an antisense oligodeoxynucleotide against IsK (minK) and over-expression of IsK mutant D77N in neonatal mouse hearts. *Pflügers Archiv : European journal of physiology*. **442** (3), 329–35.

Olson RD and Mushlin PS., (1990). Doxorubicin cardiotoxicity: analysis of prevailing hypotheses. *FASEB J*. **4**, 3076–3086.

Olson, R.D., et al. (1981). Mechanism of Adriamycin cardiotoxicity: evidence for oxidative stress. *Life Sciences*. **29**, 1393–1401.

Onwuli, D.O., et al. (2017). Do sodium channel proteolytic fragments regulate sodium channel expression? *Channels*. **11**(5), 476-485.

Opie L. (1998). The Heart: Physiology, from Cell to Circulation. 3rd. Lipincott-Raven.

Opie, L. and Lecour, S. (2016). Melatonin has multiorgan effects. *European Heart Journal - Cardiovascular Pharmacotherapy.* **2** (4), 258-265.

Orr AL, et al. (2013). Inhibitors of ROS production by the ubiquinone-binding site of mitochondrial complex I identified by chemical screening. *Free Radical Biology and Medicine*. **65**, 1047–1059.

Ortiz, F., et al. (2014). The beneficial effects of melatonin against heart mitochondrial impairment during sepsis: inhibition of iNOS and preservation of nNOS. *Journal of Pineal Research*. **56** (1), 71–81.

Ounzain, S., et al. (2008). Comparative in silico analysis identifies bona fide MyoD binding sites within the Myocyte Stress 1 gene promoter. *BMC Molecular Biology*. **9**(1), 50-59.

Ounzain, S., et al. (2012). Cardiac Expression of ms1/STARS, a Novel Gene Involved in Cardiac Development and Disease, Is Regulated by GATA4. *Molecular and Cellular Biology***. 32**(10), 1830–1843.

Paradies, G., et al. (2010). Melatonin, cardiolipin and mitochondrial bioenergetics in health and disease. *Journal of Pineal Research*. **48** (4), 297–310.

Paradies, G., et al. (2014). Functional role of cardiolipin in mitochondrial bioenergetics. *Biochimica et Biophysica Acta (BBA) – Bioenergetics*. **1837** (4), 408–417.

Paredes SD., and Reiter RJ. (2010). Melatonin: helping cells cope with oxidative disaster. *Cell Membrane Free Radical Research*. **2**, 99–111.

Patel, H.H., Murray, F. and Insel, P.A., (2008). Caveolae as organizers of pharmacologically relevant signal transduction molecules. *Annual review of pharmacology and toxicology*. **48**, 359–91.

Pechánová, O., et al. (2015). Cardiac NO signalling in the metabolic syndrome. *British Journal of Pharmacology*. **172** (6), 1415–1433.

Peng, K., et al. (2016). Novel EGFR inhibitors attenuate cardiac hypertrophy induced by angiotensin II. *Journal of cellular and molecular medicine*. **20** (3), 482–94.

Pereira G. C., et al. (2011). Drug-induced cardiac mitochondrial toxicity and protection: from doxorubicin to carvedilol. *Current Pharmaceutical Design***.** **17**, 2113–2129.

Petrosillo et al. (2003). Role of reactive oxygen species and cardiolipin in the release of cytochrome c from mitochondria. FASEB Journal.**17**(15), 2202-8.

Petrosillo J., et al. (2010). Increased susceptibility to Ca^{2+}-induced permeability transition and to cytochrome c release in rat heart mitochondria with aging: effect of melatonin. *Journal of Pineal Research*. **48** (4), 340-346.

Petrosillo, G., et al. (2009). Melatonin protects against heart ischemia-reperfusion injury by inhibiting mitochondrial permeability transition pore opening. *American journal of physiology- Heart and circulatory physiology*. **297** (4), 487-493.

Pharaon, L.F., et al. (2017). Rosiglitazone promotes cardiac hypertrophy and alters chromatin remodeling in isolated cardiomyocytes. *Toxicology Letters*. **280**, 151–158.

Pierpaoli, W. and Bulian, D. (2005). The pineal aging and death program: life prolongation in pre-aging pinealectomized mice. *Annals of the New York Academy of Sciences*. **1057**, 133-144.

Prystowsky E. N., et al. (2010). The Impact of New and Emerging Clinical Data on Treatment Strategies for Atrial Fibrillation. *Journal of Cardiovascular Electrophysiology*. **21**, 946-958.

Rao V. K., Carlson E. A and Yan S. S., (2014). Mitochondrial permeability transition pore is a potential drug target for neurodegeneration. *Biochimica et Biophysica Acta—Molecular Basis of Disease*.**1842** (8), 1267–1272.

Redman, J., Armstrong, S. and Ng, K.T., (1983). Free-running activity rhythms in the rat: entrainment by melatonin. *Science (New York, N.Y.)*. **219** (4588), 1089–91.

Reiter RJ. (2000). Melatonin: lowering the high price of free radicals. *News in Physiological Sciences*. **15**, 246–250.

Reiter RJ. (1993). The melatonin rhythm: both a clock and a calendar. *Experientia*. **49**, 654–664.

Reiter, R.J., Tan, D.X. and Galano, A., (2014). Melatonin: Exceeding Expectations. *Physiology*, **29** (5), 325-33.

Ren, M., Phoon, C.K.L. and Schlame, M., (2014). Metabolism and function of mitochondrial cardiolipin. *Progress in Lipid Research*. **55**, 1–16.

Rezazadeh, S. and Duff, H., (2016). Dissociative States: hERG Channel (Kv11.1) Modulators That Enhance Dissociation of Drugs From Their Blocking Receptor. *Circulation: Arrhythmia and Electrophysiology*. **9** (4), e004003.

Ribeiro, D.A., et al. (2009). Ascorbic acid prevents acute myocardial infarction induced by isoproterenol in rats: role of inducible nitric oxide synthase production. *Journal of Molecular Histology*. **40** (2), 99–105.

Riquelme, J.A., et al. (2016). Dexmedetomidine protects the heart against ischemia-reperfusion injury by an endothelial eNOS/NO dependent mechanism. *Pharmacological Research*. **103**, 318–327.

Rochette, L., et al. (2015). Anthracyclines/trastuzumab: new aspects of cardiotoxicity and molecular mechanisms. *Trends in Pharmacological Sciences*. **36** (6), 326–348.

Root, K.T., Plucinsky, S.M. and Glover, K.J., (2015). Recent Progress in the Topology, Structure, and Oligomerization of Caveolin: A Building Block of Caveolae. *Current Topics in Membranes*. **75**, 305–336.

Roy, S.J. and Mainzen Prince, P.S., (2013). Protective effects of sinapic acid on cardiac hypertrophy, dyslipidaemia and altered electrocardiogram in

isoproterenol-induced myocardial infarcted rats. *European Journal of Pharmacology*. **699** (1-3), 213–218.

Ruan, Y., et al. (2015). SIRT1 suppresses doxorubicin-induced cardiotoxicity by regulating the oxidative stress and p38MAPK pathways. *Cellular Physiology and Biochemistry*. **35**(3), 1116–1124.

Sack M. N., (2011). Emerging characterization of the role of SIRT3-mediated mitochondrial protein deacetylation in the heart. *American Journal of Physiology and Heart Circulation*. **301**, 2191–2197.

Sadredini, M., et al. (2016). Beta-Adrenoceptor Stimulation Reveals Ca2+ Waves and Sarcoplasmic Reticulum Ca2+ Depletion in Left Ventricular Cardiomyocytes from Post-Infarction Rats with and without Heart Failure. *PLOS ONE*. **11** (4), e0153887.

Saffitz, J.E. and Corradi, D., (2016). The electrical heart: 25 years of discovery in cardiac electrophysiology, arrhythmias and sudden death. *Cardiovascular Pathology*. **25** (2), 149–157.

Saha, S., Singh, K.M. and Gupta, B.B.P., (2018). Melatonin synthesis and clock gene regulation in the pineal organ of teleost fish compared to mammals: Similarities and differences. *General and Comparative Endocrinology*. **6480**(18), 30213-2.

Samant S. A., et al. (2014) SIRT3 deacetylates and activates OPA1 to regulate mitochondrial dynamics during stress. *Molecular Cell Biology.* **34**, 807–819.

Sayed-Ahmed MM, Shouman SA, Rezk BM., et al. (2000). Propionyl-L-carnitine as potential protective agent against adriamycin-induced impairment of fatty acid beta-oxidation in isolated heart mitochondria. *Pharmacological Research.* **41**, 143– 150.

Schlegel, A., et al. (2001). Ligand-independent activation of oestrogen receptor α by caveolin-1. *Biochemical Journal*. **359**(1), 203-210.

Shen, Z., et al. (2015). The Role of Cardiolipin in Cardiovascular Health. *BioMed Research International*. **2015**, 1–12.

Siddoway, L.A., (2003). Amiodarone: Guidelines for Use and Monitoring - American Family Physician. *American Family Physician*. **68** (11), 2189–2197.

Sims N. R., and Muyderman H., (2010). Mitochondria, oxidative metabolism and cell death in stroke. *Biochimica et Biophysica Acta—Molecular Basis of Disease*. **1802** (1), 80–91.

Singal PK, Iliskovic N, Li T., et al. (1997). Adriamycin cardiomyopathy: pathophysiology and prevention. *FASEB J*. **11**, 931–936.

Sivagangabalan, G., et al. (2014). Regional ion channel gene expression heterogeneity and ventricular fibrillation dynamics in human hearts. *PloS one*. **9** (1), e82179.

Siveski-Iliskovic, N., Kaul, N., Singal, P.K., (1994). Probucol promotes endogenous antioxidants and provides protection against adriamycin-induced cardiomyopathy in rats. *Circulation.* **89**, 2829–2835.

Slørdal, L. and Spigset, O., (2006). Heart failure induced by non-cardiac drugs. *Drug safety*. **29** (7), 567–86.

Smiljić, S., Nestorović, V. and Savić, S., (2014). Modulatory role of nitric oxide in cardiac performance. *Medicinski pregled.* **67** (9-10), 345-52.

Solem, L., (1993). Selective Activation of the Sodium-Independent, Cyclosporine A-Sensitive Calcium Pore of Cardiac Mitochondria by Doxorubicin. *Toxicology and Applied Pharmacology*. **121** (1), 50–57.

Sommese, L., et al. (2016). Ryanodine receptor phosphorylation by CaMKII promotes spontaneous Ca2+ release events in a rodent model of early stage diabetes: The arrhythmogenic substrate. *International Journal of Cardiology*. **202**, 394–406.

Sordet O., (2003). Apoptosis induced by topoisomerase inhibitors. *Current medicinal chemistry. Anti-cancer agents*. **3**, 271–290.

Srinivasan, V., et al. (2005). Melatonin, immune function and aging. *Immunity & Ageing*. **2** (1), 17.

Stammers, A.N., et al. (2015). The regulation of sarco(endo)plasmic reticulum calcium-ATPases (SERCA). *Canadian journal of physiology and pharmacology*. **93** (10), 843–54.

Stary, V., et al. (2016). SERCA2a upregulation ameliorates cellular alternans induced by metabolic inhibition. *Journal of applied physiology*. **120** (8), 865–75.

Stuck, B.J., et al. (2008). Metabolic Switch and Hypertrophy of Cardiomyocytes following Treatment with Angiotensin II Are Prevented by AMP-activated Protein Kinase. *Journal of Biological Chemistry*. **283** (47), 32562–32569.

Suliman, HB., and Piantadosi CA. (2016). Mitochondrial quality control as a therapeutic target. *Pharmacology Reviews*. **68**, 20–48.

Sunitha, M.C., et al. (2018). p-Coumaric acid mediated protection of H9c2 cells from Doxorubicin-induced cardiotoxicity: Involvement of augmented Nrf2 and autophagy. *Biomedicine & Pharmacotherapy*. **102,** 823–832.

Swift LP., (2003). Activation of adriamycin by the pH-dependent Formaldehyde-releasing prodrug hexamethylenetetramine. *Molecular Cancer Therapy.* **2**, 189–198.

Swift LP., (2006). Doxorubicin-DNA adducts induce a non-topoisomerase II-mediated form of cell death. *Cancer Research.* **66**, 4863–4871.

Szczepanik, M., (2007). Melatonin and its influence on immune system. *Journal of physiology and pharmacology : an official journal of the Polish Physiological Society*. **58** (6) 115–24.

Tan DX., et al. (1993). Melatonin: a potent endogenous hydroxyl radical scavenger. *Endocrine Journal*. **1**, 57–60.

Tang, D., et al. (2002). ERK activation mediates cell cycle arrest and apoptosis after DNA damage independently of p53. *The Journal of Biological Chemistry*. **277**, 12710–12717.

Tang, W., et al. (2015). Caveolin-1 Confers Resistance of Hepatoma Cells to Anoikis by Activating IGF-1 Pathway. *Cellular Physiology and Biochemistry*. **36**(3), 1223–1236.

Thomas RL., and Gustafsson AB. (2013). Mitochondrial autophagy — an essential quality control mechanism for myocardial homeostasis*. Circulation Journal*. **77**, 2449–2454.

Tokarska-Schlattner M, Zaugg M, Zuppinger C., et al. (2006). New insights into doxorubicin-induced cardiotoxicity: the critical role of cellular energetics. *The Journal of Molecular and Cellular Cardiology*. **41**, 389–405.

Torkarska et al. (2006). Insights into doxorubicin-induced cardiotoxicity: the critical role of cellular energetics. *The Journal of Molecular and Cellular Cardiology.* **41**(3), 389-405.

Torti, F.M., et al. (1983). Reduced cardiotoxicity of Doxorubicin delivered on a weekly schedule. *Annals of Internal Medicine*. **99**, 745–749.

Troidl, K., et al. (2009). Actin-Binding Rho Activating Protein (Abra) Is Essential for Fluid Shear Stress-Induced Arteriogenesis. *Arteriosclerosis, Thrombosis, and Vascular Biology*. **29**(12), 2093–2101.

Tsai Y., et al. (2000). Etk, a Btk family tyrosine kinase, mediates cellular transformation by linking Src to STAT3 activation. *Molecular and cellular biology*. **20**, 2043-54.

Tse, G., (2016). Mechanisms of cardiac arrhythmias. *Journal of Arrhythmia*. **32** (2), 75–81.

Tsujimoto, Y., et al. (1985). Involvement of the bcl-2 gene in human follicular lymphoma. *Science (New York, N.Y.).* **228**(4706), 1440–3.

Turer, A.T. and Hill, J.A., (2010). Pathogenesis of myocardial ischemia-reperfusion injury and rationale for therapy. *The American journal of cardiology*. **106** (3), 360–8.

Valko, M., et al. (2007). Free radicals and antioxidants in normal physiological functions and human disease. *The International Journal of Biochemistry & Cell Biology*. **39**, 44–84.

Van der Harst, P., et al. (2006). Statins in the Treatment of Chronic Heart Failure. *PLoS Medicine*. **3** (8), 333.

Varga, Z. V., et al. (2015). Drug-induced mitochondrial dysfunction and cardiotoxicity. *American Journal of Physiology-Heart and Circulatory Physiology*. **309**(9), 1453–1467.

Verma M, Shulgna N, Pastorino JG., (2013). Sirtuin-4 modulates sensitivity to induction of the mitochondrial transition pore. *Biochim Biophys Acta.* **1827**, 38–49.

Volonte, D., et al. (2008). Caveolin-1 and caveolin-3 form heterooligomeric complexes in atrial cardiac myocytes that are required for doxorubicin-induced apoptosis. *American Journal of Physiology-Heart and Circulatory Physiology*. **294**(1), 392–401.

Wallace KB., (2003). Doxorubicin-induced cardiac mitochondrionopathy. *BMC Pharmacology and Toxicology*. **93**, 105–115.

Wallace, K.B., (2007). Adriamycin-induced interference with cardiac mitochondrial calcium homeostasis. *Cardiovascular Toxicology*. **7** (2), 101–107.

Wang J., (1991). Formaldehyde cross-links daunorubicin and DNA efficiently: HPLC and X-ray diffraction studies. *Biochemistry.* **30**, 3812–3815.

Wang X., (2009). The antiapoptotic activity of melatonin in neurodegenerative diseases. *CNS Neuroscience and Therapeutics*. **15** (4), 345–357.

Wang X., Figueroa B. E., Stavrovskaya I. G., et al. (2009). Methazolamide and melatonin inhibit mitochondrial cytochrome C release and are neuroprotective in experimental models of ischemic injury. *Stroke*. **40** (5), 1877–1885.

Wang Y., et al. (2018). GCN2 deficiency ameliorates doxorubicin-induced cardiotoxicity by decreasing cardiomyocyte apoptosis and myocardial oxidative stress. *Redox Biology*. **17**, 25-34.

Wang, J., et al. (2014). Cardioprotective trafficking of caveolin to mitochondria is Gi-protein dependent. *Anaesthesiology*. **121**(3), 538-546.

Wang, M., et al. (2015). Elatoside C protects the heart from ischaemia/reperfusion injury through the modulation of oxidative stress and intracellular Ca2+ homeostasis. *International Journal of Cardiology*. **185**, 167–176.

Wan-Gan G., et al. (2010). Simvastatin inhibits angiotensin II-induced cardiac cell hypertrophy: Role of Homer 1a. *Clinical and Experimental Pharmacology and Physiology*. **37** (1), 40-45.

Wardyn, J.D., Ponsford, A.H. and Sanderson, C.M., (2015). Dissecting molecular cross-talk between Nrf2 and NF-κB response pathways. *Biochemical Society Transactions*. **43**(4), 621–626.

Watkins, S.J., Borthwick, G.M. and Arthur, H.M., (2011). The H9C2 cell line and primary neonatal cardiomyocyte cells show similar hypertrophic responses in vitro. *In Vitro Cellular & Developmental Biology – Animal*. **47** (2), 125–131.

Whitmarsh, A.J., Shore, P., Sharrocks, A.D. and Davis, R.J., (1995). Integration of MAP kinase signal transduction pathways at the serum response element. *Science (New York, N.Y.)*. **269**(5222), 403–7.

Wilcox, J.E., et al. (2016). Heart Failure—A New Phenotype Emerges. *JAMA Cardiology*. **1** (5), 507.

Williams, T.M. and Lisanti, M.P., (2004). The caveolin proteins. *Genome biology*. **5**(3), 214-223.

Xiang, P., et al. (2009). Dexrazoxane protects against doxorubicin-induced cardiomyopathy: upregulation of Akt and Erk phosphorylation in a rat model. *Cancer Chemotherapy and Pharmacology.* **63**, 343–349.

Yan, L., et al. (2013). Quercetin inhibits left ventricular hypertrophy in spontaneously hypertensive rats and inhibits angiotensin II-induced H9C2 cells hypertrophy by enhancing PPAR-γ expression and suppressing AP-1 activity. *PloS one*. **8** (9), e72548.

Yancy, C.W., et al. (2013). ACCF/AHA Guideline for the Management of Heart Failure: Executive Summary: A Report of the American College of Cardiology Foundation/American Heart Association Task Force on Practice Guidelines. *Circulation*. **128** (16), 1810–1852.

Yang Y., Jiang S., Dong Y., et al. (2015). Melatonin prevents cell death and mitochondrial dysfunction via a SIRT1-dependent mechanism during ischemic-stroke in mice. *Journal of Pineal Research*. **58** (1), 61–70.

Yang, Q., et al. (2016). Cellular and molecular mechanisms of endothelial ischemia/reperfusion injury: perspectives and implications for postischemic myocardial protection*. American journal of translational research.* **8** (2), 765–777.

Yeh, E.T.H., et al. (2004). Cardiovascular Complications of Cancer Therapy. *Circulation*. **109**(25), 3122–3131.

Yellon, D.M. and Hausenloy, D.J., (2007). Myocardial reperfusion injury. The *New England Journal of Medicine*. **357**, 1121–1135.

Ying, H., et al. (2014). Pressure overload-induced cardiac hypertrophy response requires janus kinase 2-histone deacetylase 2 signaling. *International journal of molecular sciences*. **15** (11), 20240–53.

Youle, R.J. and Strasser, A., (2008). The BCL-2 protein family: opposing activities that mediate cell death. *Nature Reviews Molecular Cell Biology*. **9**(1), 47–59.

Yu, X.X., et al. (2000). Impact of endotoxin on ucp homolog mrna abundance, thermoregulation, and mitochondrial proton leak kinetics. *American Journal of Physiology for Endocrinology and Metabolism.* **279**, 433–446.

Yusuf, J., et al. (2012). Disturbances in calcium metabolism and cardiomyocyte necrosis: the role of calcitropic hormones. *Progress in cardiovascular diseases*. **55** (1), 77–86.

Zhang, H., Li, R.J. and Huang, X., (2015). Role of atrium in automaticity of the sinus node. *Conference proceedings : Annual International Conference of the IEEE Engineering in Medicine and Biology Society.* **2015**, 47–50.

Zhang, X., et al. (2018). A common variant alters SCN5A-miR-24 interaction and associates with heart failure mortality. *The Journal of clinical investigation*. **128**(3), 1154–1163.

Zhang, Y.W., et al. (2009). Cardiomyocyte death in doxorubicin-induced cardiotoxicity*. Archivum immunologiae et therapiae experimentalis*. **57**, 435–445.

Zhao, Y., et al. (2015). Post-transcriptional regulation of cardiac sodium channel gene SCN5A expression and function by miR-192-5p. *Biochimica et biophysica acta*. **1852** (10), 2024–34.

Zhen, J., et al. (2008). Upregulation of Endothelial and Inducible Nitric Oxide Synthase Expression by Reactive Oxygen Species. *American Journal of Hypertension*. **21** (1), 28–34.

Zheng Y., Hou J., Liu J., et al. (2014). Inhibition of autophagy contributes to melatonin-mediated neuroprotection against transient focal cerebral ischemia in rats. *Journal of Pharmacological Sciences*.**124** (3), 354–364.

Zhou, H., et al. (2014). Icariin attenuates angiotensin II-induced hypertrophy and apoptosis in H9c2 cardiomyocytes by inhibiting reactive oxygen species-dependent JNK and p38 pathways. *Experimental and therapeutic medicine*. **7** (5), 1116–1122.

Zhou, L.L., et al. (2010). Regulatory effect of melatonin on cytokine disturbances in the pristane-induced lupus mice. *Mediators of inflammation*. **2010**, 951- 210.

Zhou, S., et al. (2001). Cumulative and Irreversible Cardiac Mitochondrial Dysfunction Induced by Doxorubicin. *Cancer Research*. **61** (2), 113-118.

Zima, A. V., et al. (2008). Tricyclic antidepressant amitriptyline alters sarcoplasmic reticulum calcium handling in ventricular myocytes. *American Journal of Physiology-Heart and Circulatory Physiology*. **295**(5), 2008–2016.

Zorov DB., et al. (2006). Mitochondrial ROS-induced ROS release: an update and review. *Biochimica et Biophysica Acta.* **1757**, 509–517.

Appendix

Appendix A

Table 1: RNA concentrations used for cDNA synthesis

Samples	Concentration (ng/µl)	260/280 ratio	RNA amount (µg/20µl)	µl of each sample containing 1µg of RNA	Amount of oligo dT primer (µl)	Amount of water (µl) to make 12µl sample for cDNA
Control	267.4	1.94	5.35	3.74	1	7.26
Control	283.2	1.95	5.66	3.53	1	7.47
Control	251.3	1.96	5.03	4.00	1	7.00
Dox	196.3	1.88	3.93	5.10	1	5.90
Dox	231.3	1.85	4.63	4.33	1	6.67
Dox	120.3	1.82	2.41	8.30	1	2.70
Dox+Mel	128	1.83	2.56	7.80	1	20.8
Dox+Mel	187	1.88	3.74	5.35	1	5.65
Dox+Mel	156	1.84	3.12	6.41	1	4.59
Mel	190	1.90	3.80	5.26	1	5.74
Mel	265.4	1.92	5.30	3.80	1	7.20
Mel	267.7	1.93	5.35	3.73	1	7.27

Appendix B

Table 2: Image J quantification of Cav3 gene expression and the ratio of Cav3 expression standardised by Cyclo A.

Sample	Cav3 mRNA abundance	Cyclo A mRNA abundance	Cav3 mRNA /Cyclo A mRNA ratio
Control	4665.983	4846.36	0.96
Control	7277.882	4060.94	1.79
Control	8356.418	4819.60	1.73
Dox+Mel	712.527	4889.31	0.15
Dox+Mel	1968.497	4654.59	0.42
Dox+Mel	2201.548	4634.18	0.48
Dox	266.092	4863.31	0.05
Dox	291.678	4387.06	0.07
Dox	1223.255	4732.89	0.26
Mel	5702.397	5108.13	1.12
Mel	5161.619	5092.01	1.01
Mel	4174.154	5059.31	0.83

Table 3: Image J quantification of Drp1 gene expression and the ratio of Drp1 expression standardised by Cyclo A.

Sample	Drp1 mRNA abundance	Cyclo A mRNA abundance	Drp1 mRNA /Cyclo A mRNA ratio
Control	6023.45	4846.36	1.24
Control	5185.98	4060.94	1.28
Control	4791.35	4819.60	0.99
Dox+Mel	3081.74	4889.31	0.63
Dox+Mel	5685.10	4654.59	1.22
Dox+Mel	3511.45	4634.18	0.76
Dox	3139.86	4863.31	0.65
Dox	1783.96	4387.06	0.41
Dox	1710.55	4732.89	0.36
Mel	5482.62	5108.13	1.07
Mel	2387.62	5092.01	0.47
Mel	2913.08	5059.31	0.58

Table 4: Image J quantification of Mfn1 gene expression and the ratio of Mfn1 expression standardised by Cyclo A.

Sample	Mfn1 mRNA abundance	Cyclo A mRNA abundance	Mfn1 mRNA /Cyclo A mRNA ratio
Control	2793.81	4846.36	0.58
Control	5124.18	4060.94	1.26
Control	4431.64	4819.60	0.92
Dox+Mel	3296.74	4889.31	0.67
Dox+Mel	4666.69	4654.59	1.00
Dox+Mel	2059.28	4634.18	0.44
Dox	2302.45	4863.31	0.47
Dox	1317.01	4387.06	0.30
Dox	1848.13	4732.89	0.39
Mel	2937.50	5108.13	0.58
Mel	3413.28	5092.01	0.67
Mel	6485.86	5059.31	1.28

Table 5. Image J quantification of PPAR-γ gene expression and the ratio of PPAR-γ expression standardised by Cyclo A.

Sample	PPAR-γ mRNA abundance	Cyclo A mRNA abundance	PPAR-γ mRNA /Cyclo A mRNA ratio
Control	4045	4056	1.00
Control	4495	3029	1.48
Control	6484	4204	1.50
Dox+Mel	3085	3632	0.85
Dox+Mel	3050	3726	0.82
Dox+Mel	3755	3102	1.20
Dox	1472	4820	0.30
Dox	1587	2863	0.50
Dox	1491	2955	0.50
Mel	4530	4030	1.12
Mel	5047	3085	1.60
Mel	5102	2821	1.80

Table 6: Image J quantification of Parp 1 and Parp 2 gene expression and the ratio of the gene expressions standardised by Cyclo A.

Sample	Parp1 mRNA abundance	Parp2 mRNA abundance	Cyclo A mRNA abundance	Parp1 mRNA /Cyclo A mRNA ratio	Parp2 mRNA /Cyclo A mRNA ratio
Control	10646.96	11698.28	4846.36	2.20	2.41
Control	11835.96	9242.69	4060.94	2.91	2.28
Control	10849.50	11017.98	4819.60	2.25	2.29
Dox+Mel	11579.84	9392.28	4889.31	2.37	1.92
Dox+Mel	12442.21	9327.05	4654.59	2.67	2.00
Dox+Mel	10421.67	7093.15	4634.18	2.25	1.53
Dox	1852.70	4065.98	4863.31	0.38	0.84
Dox	4145.01	2768.52	4387.06	0.94	0.63
Dox	4260.18	5365.88	4732.89	0.90	1.13
Mel	8338.18	9517.61	5108.13	1.63	1.86
Mel	8914.15	9307.73	5092.01	1.75	1.83
Mel	8034.32	10612.78	5059.31	1.59	2.10

Table 7: Image J quantification of Sirt3 gene expression and the ratio of Sirt3 expression standardised by Cyclo A.

Sample	Sirt3 mRNA abundance	Cyclo A mRNA abundance	Sirt3 mRNA /Cyclo A mRNA ratio
Control	3120	4056	0.77
Control	4288	3029	1.42
Control	3964	4204	0.95
Dox+Mel	11174	3632	3.08
Dox+Mel	9071	3726	2.44
Dox+Mel	8825	3102	2.85
Dox	5628	4820	1.16
Dox	2979	2863	1.04
Dox	7218	2955	2.44
Mel	7413	4030	1.84
Mel	5157	3085	1.67
Mel	5204	3075	1.85

Table 8: Image J quantification of Bcl-2 gene expression and the ratio of Bcl-2 expression standardised by Cyclo A.

Sample	Bcl-2 mRNA abundance	Cyclo A mRNA abundance	Bcl-2 mRNA /Cyclo A mRNA ratio
Control	9202	4056	2.3
Control	10181	3029	3.3
Control	11466	4204	2.73
Dox+Mel	541	4820	1.5
Dox+Mel	323	2863	1.12
Dox+Mel	892	2955	0.83
Dox	5121	3632	0.11
Dox	4185	3726	0.11
Dox	2566	3102	0.30
Mel	15228	4030	3.78
Mel	11703	3085	3.79
Mel	7530	2821	2.67

Table 9: Image J quantification of Bcl-xL gene expression and the ratio of Bcl-xL expression standardised by Cyclo A.

Sample	Bcl-xL mRNA abundance	Cyclo A mRNA abundance	Bcl-xL mRNA /Cyclo A mRNA ratio
Control	4867	4056	1.2
Control	3635	3029	1.2
Control	6306	4204	1.5
Dox+Mel	14339	4820	1.5
Dox+Mel	11178	2863	1.8
Dox+Mel	9306	2955	1.6
Dox	7230	3632	2.8
Dox	5153	3726	3
Dox	4728	3102	3
Mel	7254	4030	1.8
Mel	4936	3085	1.6
Mel	4232	2821	1.5

Table 10: Image J quantification of Ucp2 gene expression and the ratio of Ucp2 expression standardised by Cyclo A.

Sample	Ucp2 mRNA abundance	Cyclo A mRNA abundance	Ucp2 mRNA /Cyclo A mRNA ratio
Control	5320	4056	1.31
Control	6023	3029	1.98
Control	5768	4204	1.39
Dox+Mel	6033	3632	1.66
Dox+Mel	5051	3726	1.36
Dox+Mel	3703	3102	1.2
Dox	2442	4820	0.5
Dox	1632	2863	0.57
Dox	2633	2955	0.9
Mel	10560	4030	2.62
Mel	8886	3085	2.88
Mel	8684	2821	3.08

Table 11: Image J quantification of Ms1 gene expression and the ratio of Ms1 expression standardised by Cyclo A.

Sample	Ms1 mRNA abundance	Cyclo A mRNA abundance	Ms1 mRNA /Cyclo A mRNA ratio
Control	4957.08	4846.36	1.02
Control	6249.10	4060.94	1.54
Control	7204.59	4819.60	1.49
Dox+Mel	2665.84	4889.31	0.55
Dox+Mel	4671.91	4654.59	1.00
Dox+Mel	2023.48	4634.18	0.44
Dox	647.53	4863.31	0.13
Dox	920.94	4387.06	0.21
Dox	1582.94	4732.89	0.33
Mel	6585.98	5108.13	1.29
Mel	5279.03	5092.01	1.04
Mel	4462.67	5059.31	0.88

Table 12: Image J quantification of Scn5a gene expression and the ratio of Scn5a expression standardised by Cyclo A.

Sample	Scn5a mRNA abundance	Cyclo A mRNA abundance	Scn5a mRNA /Cyclo A mRNA ratio
Control	506.46	4846.36	0.10
Control	313.87	4060.94	0.08
Control	3540.72	4819.60	0.73
Dox+Mel	796.11	4889.31	0.16
Dox+Mel	1399.94	4654.59	0.30
Dox+Mel	448.82	4634.18	0.10
Dox	4596.31	4863.31	0.95
Dox	4476.38	4387.06	1.02
Dox	3377.79	4732.89	0.71
Mel	772.48	5108.13	0.15
Mel	732.04	5092.01	0.14
Mel	1378.01	5059.31	0.27

Table 13: Image J quantification of Serca2a gene expression and the ratio of Serca2a expression standardised by Cyclo A.

Sample	Serca2a mRNA abundance	Cyclo A mRNA abundance	Serca2a mRNA /Cyclo A mRNA ratio
Control	8249.52	4846.36	1.70
Control	8666.64	4060.94	2.13
Control	8792.71	4819.60	1.82
Dox+Mel	5973.64	4889.31	1.22
Dox+Mel	8826.59	4654.59	1.90
Dox+Mel	7024.74	4634.18	1.52
Dox	3854.33	4863.31	0.79
Dox	3794.15	4387.06	0.86
Dox	7433.98	4732.89	1.57
Mel	8044.40	5108.13	1.57
Mel	10416.76	5092.01	2.05
Mel	10586.59	5059.31	2.09

Table 14: Image J quantification of Myh7 gene expression and the ratio of Myh7 expression standardised by Cyclo A.

Sample	Myh7 mRNA abundance	Cyclo A mRNA abundance	Myh7 mRNA /Cyclo A mRNA ratio
Control	1931.74	6393.4	0.30
Control	1115.38	5409.38	0.21
Control	1312.74	6213 .18	0.21
Dox+Mel	6452.88	6460.93	1.00
Dox+Mel	3341.64	6002 .91	0.56
Dox+Mel	5243.88	6039 .86	0.87
Dox	9602.73	5608 .33	1.71
Dox	7755.73	5158.62	1.50
Dox	3156.933	5812.79	0.54
Mel	2769.81	5317.86	0.52
Mel	977 .79	5770 .03	0.17
Mel	1362.44	5615.79	0.24

Appendix C

Alamar Blue cell viability assay

Table 15: Experiment 1 representing % cell viability for doxorubicin and melatonin.

	Control	Dox	Dox+Mel	Mel
	101	70.5	100	82
	103	70	99	81
	103	71.1	98.2	84.4
	95	71.1	104	116
	102	73.4	104	116.6
	98.2	72.6	101	85.1
	99	76	100	
	100		104	
Mean ± SEM	**100 ± 0.96**	**70.5 ± 0.79**	**101.3 ± 0.85**	**94.4 ± 7.02**

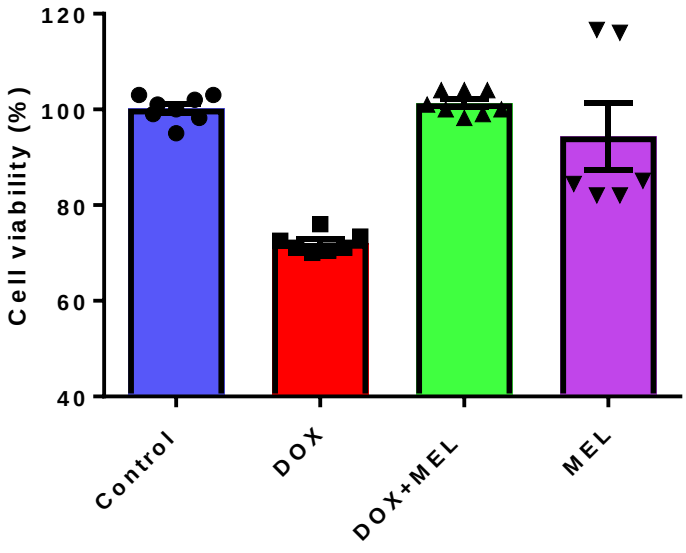

Figure 1: Experiment 1: Melatonin blocked doxorubicin-induced cell death in H9c2 cells. Cells were treated with DOX (0.5µM) with and without MEL (1µM) for 24hr. Data are presented as mean ± SEM (n=5 separate experiments; each experiment had 3 to 10 samples). One Way Anova: F (3, 25) = 21.3, P< 0.0001. Data considered statistically significant.

Table 16**:** Experiment 2 representing % cell viability for doxorubicin and melatonin.

	Control	Dox	Dox+Mel	Mel
	83.5	59	102	113
	86	57	100	113
	87	57	100	118
	143	61.3	107	98.7
	98	57.5	108	100
	100	57	103	101
	103	76.8	108	
		73	114	
		74.7		
		78.1		
Mean ± SEM	**100.1 ± 7.71**	**65.2 ± 2.92**	**105 ± 1.72**	**107.3 ± 3.40**

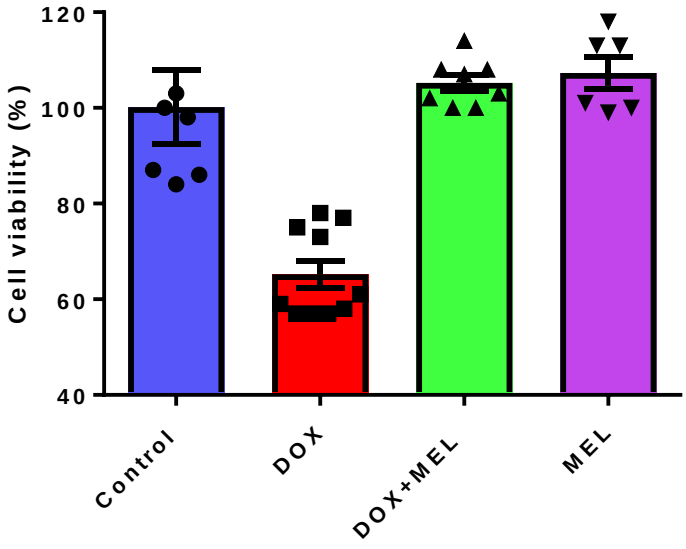

Figure 2: Experiment 2: Melatonin blocked doxorubicin-induced cell death in H9c2 cells. Cells were treated with DOX (0.5µM) with and without MEL (1µM) for 24hr. Data are presented as mean ± SEM (n=5 separate experiments; each experiment had 3 to 10 samples). One Way Anova: F (3, 27) = 25.03, P< 0.0001. Data considered statistically significant.

Table 17**:** Experiment 3 representing % cell viability for doxorubicin and melatonin.

	Control	Dox	Dox+Mel	Mel
	95	81.8	92.5	87.3
	105.4	84	93.7	89.2
	107	82.6	94.3	100
	107.8	83.7	92.8	102.8
	93	75	92	104.8
			91	
			91.5	
			91.8	
Mean ± SEM	**101.6 ± 3.16**	**81.4 ± 1.65**	**91.5 ±0.40**	**96.8 ± 3.59**

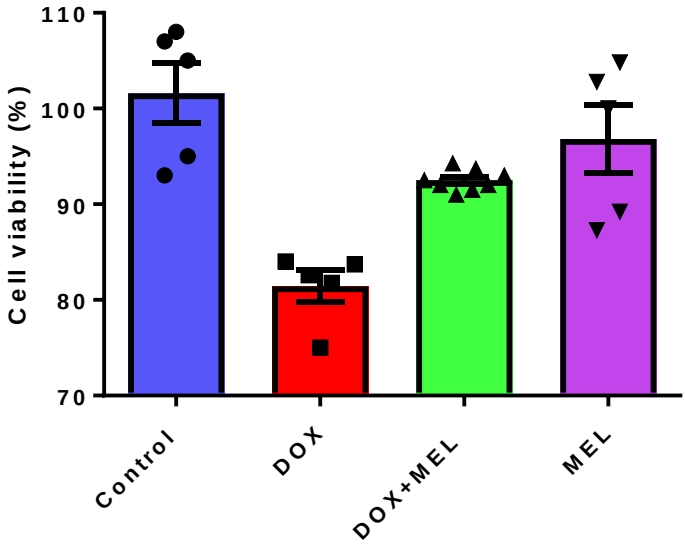

Figure 3: Experiment 3: Melatonin blocked doxorubicin-induced cell death in H9c2 cells. Cells were treated with DOX (0.5µM) with and without MEL (1µM) for 24hr. Data are presented as mean ± SEM (n=5 separate experiments; each experiment had 3 to 10 samples). One Way Anova: F (3, 19) = 13.56, P< 0.0001. Data considered statistically significant.

Table 18**:** Experiment 4 representing % cell viability for doxorubicin and melatonin.

	Control	Dox	Dox+Mel	Mel
	98	71.4	92.4	90
	92.3	76	95.2	93
	109	77.6	100	90
		74.8	102.6	92.3
				86.7
Mean ± SEM	**99.8 ± 4.90**	**74.95 ± 1.31**	**97.6 ± 2.30**	**91 ± 1.10**

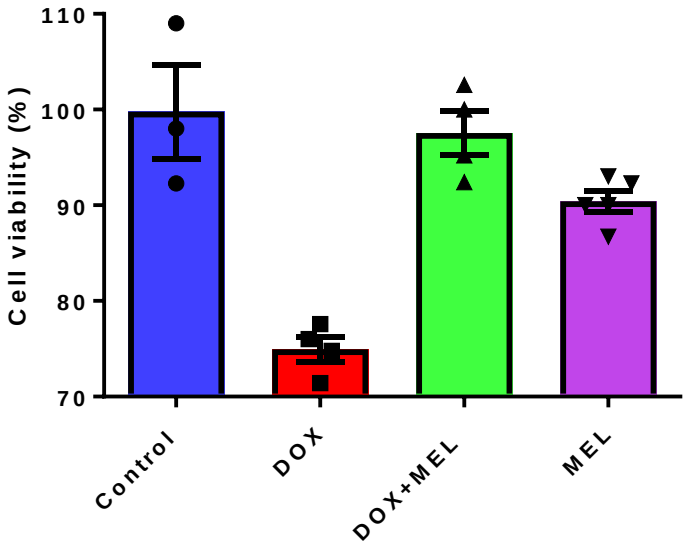

Figure 4: Experiment 4: Melatonin blocked doxorubicin-induced cell death in H9c2 cells. Cells were treated with DOX (0.5µM) with and without MEL (1µM) for 24hr. Data are presented as mean ± SEM (n=5 separate experiments; each experiment had 3 to 10 samples). One Way Anova: F (3, 12) = 22.48, P< 0.0001. Data considered statistically significant.

Table 19**:** Experiment 5 representing % cell viability for doxorubicin and melatonin.

	Control	Dox	Dox+Mel	Mel
	99	61.7	96.2	107
	101	61.3	88	98.6
	100	64.6	95	96
		64.6	92.3	96.2
		65.3	81.6	105.7
		64.4		
		62.4		
Mean ± SEM	**100 ± 0.58**	**63.5 ± 0.61**	**91 ± 2.66**	**100.7 ± 2.36**

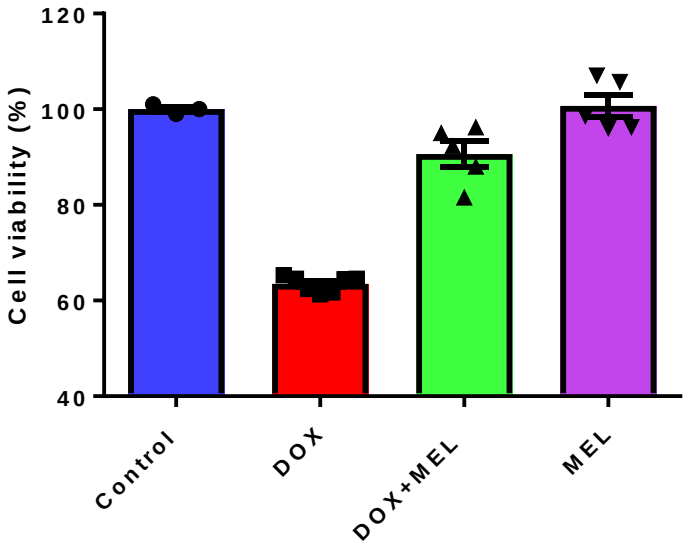

Figure 5: Experiment 5: Melatonin blocked doxorubicin-induced cell death in H9c2 cells. Cells were treated with DOX (0.5µM) with and without MEL (1µM) for 24hr. Data are presented as mean ± SEM (n=5 separate experiments; each experiment had 3 to 10 samples). One Way Anova: F (3, 16) = 104.7, P<0.0001. Data considered statistically significant.